



KINGDOM OF SAUDI ARABIA
MINISTRY OF EDUCATION
ISLAMIC UNIVERSITY OF MADINAH

Islamic University Journal of Applied Sciences (JESC)

Refereed periodical scientific journal

Volume: V

Issue: II

Year: 2023

بِسْمِ اللَّهِ الرَّحْمَنِ الرَّحِيمِ

Paper version

Filed at the King Fahd National Library No. 8742/1439 on 17/09/1439
AHInternational serial number of periodicals (ISSN) 1658-7936

Online version

Filed at the King Fahd National Library No. 8742/1439 on 17/09/1439
AHInternational Serial Number of Periodicals (e-ISSN) 1658-7944

The Journal's Website

<https://jesc.iu.edu.sa>

The papers are sent in the name of the Editor-in-Chief of the
Journal to this E-mail address

jesc@iu.edu.sa

(The views expressed in the published papers reflect the views of the
researcher only, and do not necessarily reflect the opinion of the journal)

Publication Rules at the Journal (*)

❖ General rules:

- Report original scientific research (the main results and conclusions must not have been published or submitted elsewhere).
- Fit with the topics of the journal.
- Report novel results, innovative work and show a new scientific contribution.
- Not to bear similarity of more than 25% of a previously published work of the same author(s).
- Follow the rules, regulation and authentic research methodologies.
- Fulfill the required items and the format of the journal provided in appendix below related to the guide for author.
- Opinions expressed in published articles commit the authors themselves only and not necessarily the opinion of the journal.

❖ For all articles:

- The exclusive right to publish and distribute an article, and to grant rights to others, including commercial purposes.
- For open access articles, IU will apply the relevant third-party user license where IU publishes the article on its online platforms.
- The right to provide the article in all forms and media so the article can be used on the latest technology even after publication.
- The authority to enforce the rights in the article, on behalf of an author, against third parties, for example in the case of plagiarism or copyright infringement.

The Editorial Board

Ahmad B. Alkhodre

Editor-in-Chief
Professor, Computer Science,
Islamic University of Madinah, Saudi
Arabia.

Fazal Noor

Managing Editor
Professor, Computer science and
engineering, Islamic University of
Madinah. Saudi Arabia

Tomita Kentaro

Associate Professor, Division of
Quantum Science and Engineering,
Graduate School of Engineering,
Hokkaido University, Japan

Fayez Gebali

Professor, Electrical and Computer
Engineering, University of Victoria,
Victoria, B.C., Canada

Saad Talal Alharbi

Professor in Computer Science,
Human Computer Interaction,
Faculty of Computers, Taibah
University, Saudi Arabia

Abdul Qadir Bhatti

Professor, Civil Engineering, Faculty
of Engineering, Islamic University of
Madinah.
Saudi Arabia

Essam Ramadan Shaaban

Professor, Physics, Al-Azhar University,
Assiut Branch, Egypt

Yazed Alsaawy

Associate Professor, Computer and
information systems, Islamic
University of Madinah. Saudi Arabia

M. M. Khader

Professor, Numerical Analysis,
Alimam University, Riyadh. Saudi
Arabia

**Reda Mohamed Awad El-
Shishtawy**

Professor, Organic Chemistry,
Chemistry Department Faculty of
Science - King Abdulaziz
University, Saudi Arabia

Basem R. Alamri

Associate Professor of Electrical Power
Engineering, Taif University

Shamsuddin Ahmed

Professor, Industrial Engineering, The
Faculty of Computer and Information
Systems Islamic University of
Madinah

Editorial Secretary: **Ahmad Ziad Al-Zuhaily**

The Advisory Board

Hussein T. Mouftah
Professor, Electrical
Engineering and Computer
Science, University of Ottawa,
Ottawa, ON, Canada

Canada Research Chair in
Wireless Sensor Networks

Distinguished University
Professor, University of Ottawa

**Sultan T. Abu-Orabi
Aladwan**

Professor, Organic Chemistry,
Jordan

A. Ghafoor

Professor, Mechanical Engineering,
National University of Science and
Technology, Pakistan

Mahmoud Abdel-Aty

Professor, Applied
Mathematics, Egypt

Kamal Mansour Jambi

Professor, Computer and
Information Systems, King
Abdel-Aziz University, Jeddah,
Saudi Arabia

Claus Haetinger

Professor, Mathematics, Brazil

Diaa Khalil

Professor, Electrical Engineering,
and Vice-Dean, Ain-Shams
University, Cairo, Egypt

Ameen Farouq Fahmy

Professor, Chemistry,
Egypt

***The Islamic University Journal of Applied
Sciences***

Issued By

***Islamic University of Madinah, Madinah,
Saudi Arabia***

Table of Contents

Date-Palm Waste Usage for Low-cost Advanced Treatment for Domestic Wastewater in Arid regions	10
The Effect of Artificial Intelligence Applications on Quick Decision-Making in Government Hospitals in Al Madinah Al Munawarah	58
Design and Implementation of a Simulator of The Micro-Electromagnetic Generator Used to Power Medical Devices Implanted in The Human Body	77
Designing a Novel Algorithm for Drawing a Kappa Curve Using Bresenham's Approach	103
Geometry of Conformal Quasi Bi-Slant Submersions	120
Design and Fabrication of an Automatic Solar Tracking System & Comparative Analysis with Stationary Panel	156
Development of SMS Spam Filtering APP for Modern Mobile Devices	175
Utilisation of Risk Management, Project Management Tools and Teamwork for the Execution of Turnaround Maintenance Activities	189

Date-Palm Waste Usage for Low-cost Advanced Treatment for Domestic Wastewater in Arid regions

Abdelkader. T. Ahmed^{1&2} and Ayed E. Alluqmani ¹

¹Civil Engineering Department, Faculty of Engineering, Islamic University of Madinah,
Saudi Arabia
dratahmed@yahoo.com

² Civil Engineering Department, Faculty of Engineering, Aswan University, Aswan,
Egypt

ABSTRACT: Arid countries suffer from the water shortage especially, with the recent high-water demand. It is crucial for governmental sectors and researchers to find a solution to this critical problem. This study introduces a possible solution through the reuse of treated wastewater. The proposed solution provides the reuse of the treated wastewater for unrestricted irrigation purposes. This solution also solves the problem of wastewater discharge into the environment and saves natural water resources. The work adopted a low-cost and advanced treatment method by using natural materials such as date-palm wastes. These wastes are abundant in arid countries and may introduce a problem also for their landfill. The study explored the possibility of using the date-palm waste as an absorbent material for the pollutants from domestic wastewater effluents. The research methodology relied on the experimental work on a lab scale. Leaching batch tests for this waste were adopted initially to evaluate its ions' extraction into water. Then its ability for the purification of wastewater effluents was investigated through an absorption mechanism. Various parameters were examined in both processes such as the liquid to solid ratio (L/S), initial pH, and material size. In addition, different types of palm wastes were studied such as wastes from leaves, stems, and trunks. The results of leaching tests showed in general a high rate of release of many ions into distilled water at different

conditions. Treatment results also exhibited a notable increase of element release into wastewater effluents. Prewashing and drying the coarse wastes before using them with wastewater demonstrated a promising ability for these wastes to remove many elements from wastewater.

KEYWORDS: Wastewater, Treatment, Palm Waste, Absorption, Leaching

استخدام مخلفات النخيل في المعالجة المتقدمة منخفضة التكلفة لمياه الصرف الصحي المنزلية في المناطق القاحلة

المخلص: تعاني البلدان القاحلة من نقص المياه بشكل خاص، مع ارتفاع الطلب على المياه في الآونة الأخيرة. ومن الأهمية بمكان للقطاعات الحكومية والباحثين إيجاد حل لهذه المشكلة الحرجة. تقدم هذه الدراسة حلاً ممكناً من خلال إعادة استخدام مياه الصرف الصحي المعالجة. يوفر الحل المقترح إعادة استخدام مياه الصرف الصحي المعالجة لأغراض الري غير المقيدة. كما يعمل هذا الحل على حل مشكلة تصريف مياه الصرف الصحي إلى البيئة وتوفير موارد المياه الطبيعية. اعتمد العمل على أسلوب معالجة منخفض التكلفة ومتقدم باستخدام المواد الطبيعية مثل مخلفات النخيل. وتتوافر هذه النفايات بكثرة في البلدان القاحلة وقد تسبب مشكلة أيضاً لمدافن النفايات الخاصة بها. بحثت الدراسة في إمكانية استخدام مخلفات النخيل كمادة ماصة للملوثات الناتجة عن مياه الصرف الصحي المنزلية. اعتمدت منهجية البحث على العمل التجريبي على نطاق مختبري. تم اعتماد اختبارات الترشيح لهذه النفايات في البداية لتقييم استخلاص أيوناتها في الماء. ومن ثم تم دراسة قدرتها على تنقية مياه الصرف الصحي من خلال آلية الامتصاص. تم فحص معلمات مختلفة في كلتا العمليتين مثل نسبة السائل إلى المادة الصلبة (L/S) ، ودرجة الحموضة الأولية، وحجم المادة. بالإضافة إلى ذلك تمت دراسة أنواع مختلفة من مخلفات النخيل مثل مخلفات الأوراق والسيقان والجذوع. أظهرت نتائج اختبارات الترشيح بشكل عام ارتفاع نسبة إطلاق العديد من الأيونات في الماء المقطر عند ظروف مختلفة. أظهرت نتائج المعالجة أيضاً زيادة ملحوظة في إطلاق العناصر في مياه الصرف الصحي السائلة. وأظهر الغسيل المسبق للمخلفات الخشنة وتجفيفها قبل استخدامها مع مياه الصرف الصحي قدرة واعدة لهذه المخلفات على إزالة العديد من العناصر من مياه الصرف الصحي.

1.INTRODUCTION

The whole world in general, as well as the Arab region, suffers from a shortage of freshwater sources for drinking, irrigation, and industrial activities. There are many areas in the Arab regions, especially in the Gulf countries, suffering from a great shortage of freshwater sources due to the lack of surface water resources. It is essential for these regions to manage and save the current available resources of freshwater [1]. The most reliable option for providing renewable freshwater is the treatment and reuse of wastewater. A huge amount of wastewater is generated annually and causes a problem of disposal in a safe way. Reuse wastewater will have a double positive impact by providing fresh water and solving its problem of disposal [2].

Treating and reusing wastewater as a source of freshwater is a challenging process as it needs applying advanced treatment methods after the basic treatment stages. These advanced methods are regularly expensive and energy consumption. Thus, intensive research is required to find low-cost and affectable methods for the advanced treatment of wastewater effluents. One of these promising low-cost methods is adopting adsorbent and absorbent materials in the purification of wastewater effluents. Various materials were examined as potential adsorbents. The adsorbents in general are classified into two categories: conventional and non-conventional. Conventional adsorbents such as alumina and zeolite were adopted at a minimal level. For the non-conventional, the most frequently used is agro-wastes. These wastes may introduce a good bio-adsorbent for wastewater treatment and introduce a good reuse for these wastes before disposal [3]. Abundant of date-palm wastes are generated annually, especially in the Middle East area. 100 million date-palm trees exist approximately around the world. In the Middle East and North Africa, 62 % of these trees are implanted. In the Kingdom of Saudi Arabia, for an instant, date-palm trees generate 1500 tons of waste materials from tree leaves. These wastes cause a great problem for their disposal and landfilling. They usually are stored in agricultural lands, or burned, which causes health and environmental problems [4]–[6]. However, on the other hand, they have the potential to work as a bio-adsorbent for many elements dissolved in wastewater effluents.

Earlier studies investigated the possibility of using date-palm wastes as an adsorbent for pollutants. Ahmed et al. [7] addressed an overall review on date-palm trees and their uses

as adsorbents for removing pollutants, heavy-metals and dyes from water and wastewater. Some studies concluded that date-palm waste can be used as adsorbents for the removal of unwanted materials from wastewater. Nujic et al. [8] showed that the use of date-palms for adsorption purposes in removing pollutants such as heavy-metals, dyes and phosphates from aquatic has succeeded. They reported also that the research on the date-palm fibers and their uses as bio adsorbents for the removal of pollutants from wastewater are limited to date. Their conclusion showed that the fibers of date-palms can be employed as low-cost adsorbents in removing pollutants from wastewater. Jonoobi et al. [9] conducted a general review on the applications of date-palm tree in Middle East countries. They concluded, as proven by some researchers, that the date-palm is used for many applications including removing of heavy-metals and soil fertilizing. Mohamed *et al.*[10] studied using a powder of date seeds (PADS) as an adsorbent in removing heavy metal ions such as cadmium, lead, copper, chromium, cobalt, and manganese from water. A mass of 0.1 gram of PADS was added to a volume of 50 mL of the water sample. The maximum removal efficiency was 93.34%, 71.06%, 92.06%, 96.96%, 95.91% and 36.13% for Cd²⁺, Cr³⁺, Co²⁺, Cu²⁺, Pb²⁺ and Mn²⁺ ions respectively. They argued that the findings of this study can be taken as a solution and baseline information for heavy metal removal in different applications.

In this work, the date-palm wastes were evaluated as a treatment tool for removing contaminations from domestic wastewater effluents to be suitable for irrigation. The study investigated different types of date-palm waste components such as leaves, branch-stems, and trunk-fibers. The examination included the leaching and absorption properties of these wastes. The research was based on experimental work on a lab scale. Many parameters were examined such as the material size, different components of date-palm wastes, liquid to solid ratio (L/S), initial pH, and impact of the prewashing and drying process on the waste materials.

2. MATERIALS AND METHODS

2.1 Materials

The date-palm wastes used in this research are available in the western of the Kingdom of Saudi Arabia (KSA) in Madinah governorate. Samples from leaves, branch-stem and trunk were collected from three locations. Part of the samples was grinded into a powder with a size of less than 1 mm and others were cut into small pieces with sizes ranging between 10 to 300 mm. The main chemical compositions of these wastes are like all agricultural wastes, which include cellulose, hemicelluloses, and lignin. They are mainly carbohydrate polymers [11].

2.2 Leaching Tests

To examine the components released from date-palm waste into treated domestic wastewater, the leaching tests were adopted following to British Standard procedure [12]. The waste materials were soaked without shaking or mixing in distilled water for 24 hours. TDS, turbidity pH, and hardness were observed for 24 hours. Then a water sample was collected directly without filtrations and chemically analyzed to determine the released ions from waste materials into the water. Many cations, anions, and heavy metals were measured. Several parameters were investigated including the liquid-to-solid (L/S) as 10 and 20, and three values of pH namely 4, 6, and 10. Finally, the waste materials were used in two size sets namely, fine materials by grinding the waste to a particle size of less than 1 mm and coarse materials by cutting the waste to a size ranging from 10 to 300 mm. These sizes were chosen based on the available cutting and grinding tools to represent coarse and fine materials.

2.3 Absorption Tests (Treatment Tests)

In these experiments, the date-palm waste was examined as a bio-absorbent for the impurities in the wastewater. The waste was soaked in the domestic wastewater effluent for up to 24 hours. The effluent is collected from the wastewater treatment plant at Al Madinah city, KSA. The effluent has two types namely, secondary, or biologically treated with aeration tanks (WII); and tertiary treated with sand filters (WIII). Besides previously

mentioned measurements in the leaching tests, BOD and COD were observed after 24 hours. Studied parameters in these experiments included examining the wastes with both WII and WIII samples individually. Furthermore, another test investigated the waste treatment ability by soaking the waste in distilled water for 24 hours and drying before adding it to WII. This is to reduce the leached ions from the solid waste into the water sample. Table 1 presents a summary of the studied parameters.

3. RESULTS AND DISCUSSION

3.1 Leaching Properties

The leaching and absorption processes are the most important interactions between solid and liquid. The absorption process is the opposite of the leaching process as in the latter the particles are extracted from solid materials into water and in the former the particles were held by the solid materials from water. Therefore, it is crucial to investigate the leaching properties of any solid materials intended to be used as absorbent. Thus, in this work, the leaching properties of the date-palm waste were investigated by studying several influenced parameters as described above.

Table 1: Details of Studied Parameters with Date-Palm Waste Samples.

Sample	Material Size/Status	Water	Initial pH	Liquid to Solid (L/s)	Test Symbol
WII	--	Secondary treated wastewater	Natural	10	WII
WIII	--	Tertiary treated wastewater	Natural	10	WIII
P1	Fine materials (<1 mm) from branch stem and leaves	Distilled water	6.0	10	F-S&L/D
P2	Fine materials (<1 mm) from trunk	Distilled water	6.0	10	F-T/D

P3	Fine materials (<1 mm) Mixture from branch stem, leaves and trunk	Distilled water	6.0	10	Mix-F/D
P4	Coarse materials (10 to 300 mm) Mixture from branch stem, leaves and trunk.	Distilled water	6.0	10	Mix-C/D
P5	Coarse materials (10 to 300 mm) Mixture from branch stem, leaves and trunk.	Distilled water	4.0	10	Mix/C/D/ pH=4
P6	Coarse materials (10 to 300 mm) Mixture from branch stem, leaves and trunk.	Distilled water	10.0	10	Mix/C/D/ pH=10
P7	Coarse materials (10 to 300 mm) Mixture from branch stem, leaves and trunk.	Distilled water	6.0	20	Mix/C/D/ pH=6/L/s =20
P8	Fine materials (<1 mm) Mixture from branch stem, leaves and trunk	Secondary treated wastewater	Natural	10	Mix-F/WII
P9	Coarse materials (10 to 300 mm) Mixture from branch stem, leaves and trunk.	Secondary treated wastewater	Natural	10	Mix-C/WII
P10	Fine materials (<1 mm) Mixture from branch stem, leaves and trunk	Tertiary treated wastewater	Natural	10	Mix-F/WIII
P11	Coarse materials (10 to 300 mm) Mixture from branch stem, leaves and trunk.	Tertiary treated wastewater	Natural	10	Mix-C/WIII
P12	Coarse materials (10 to 300 mm) Mixture from branch stem, leaves and trunk. (Prewashed and dried)	Secondary treated wastewater	Natural	10	Mix-C/WII- prewashed

P (palm sample); F (fine materials); C (coarse materials); S (stem); L (leave); T (trunk);
D (distilled)

3.1.1 Physicochemical Characteristics

Figure 1 presents the results of TDS, hardness, turbidity, and pH measurements at 24 hours after adding date-palm waste to the distilled water for different parameters, P1 to P7. Samples from grinded branch stem and leaves, P1, showed less content of TDS and turbidity than those from grinded trunk, P2 or the mixture of all of them together as in P3. This perhaps due to ion exchange process. While P1 showed a slight increase in hardness and pH values. The coarse sample, P4 showed smaller values in general than fine the material samples. This confirms the fact that the release from waste as fine materials more than coarse sizes due to the increase in the surface area of the fine or grinded materials and consequently increase contact with liquid. The same results were reported by Altaher [11] who studied the impact of different particle sizes of agro-wastes on leaching properties. For initial pH values, results of TDS, hardness and pH showed an increase with increase initial pH values, samples P4 to P6, except for turbidity exhibited the highest value with a starting pH of 4. For the L/S ratio, comparing samples P7 to P4 having ratios of 20 and 10 respectively showed a decline in all properties with the increase in the ratio. This is perhaps due to reduce the mass of the solid waste in water. This agrees with results reported elsewhere [11].

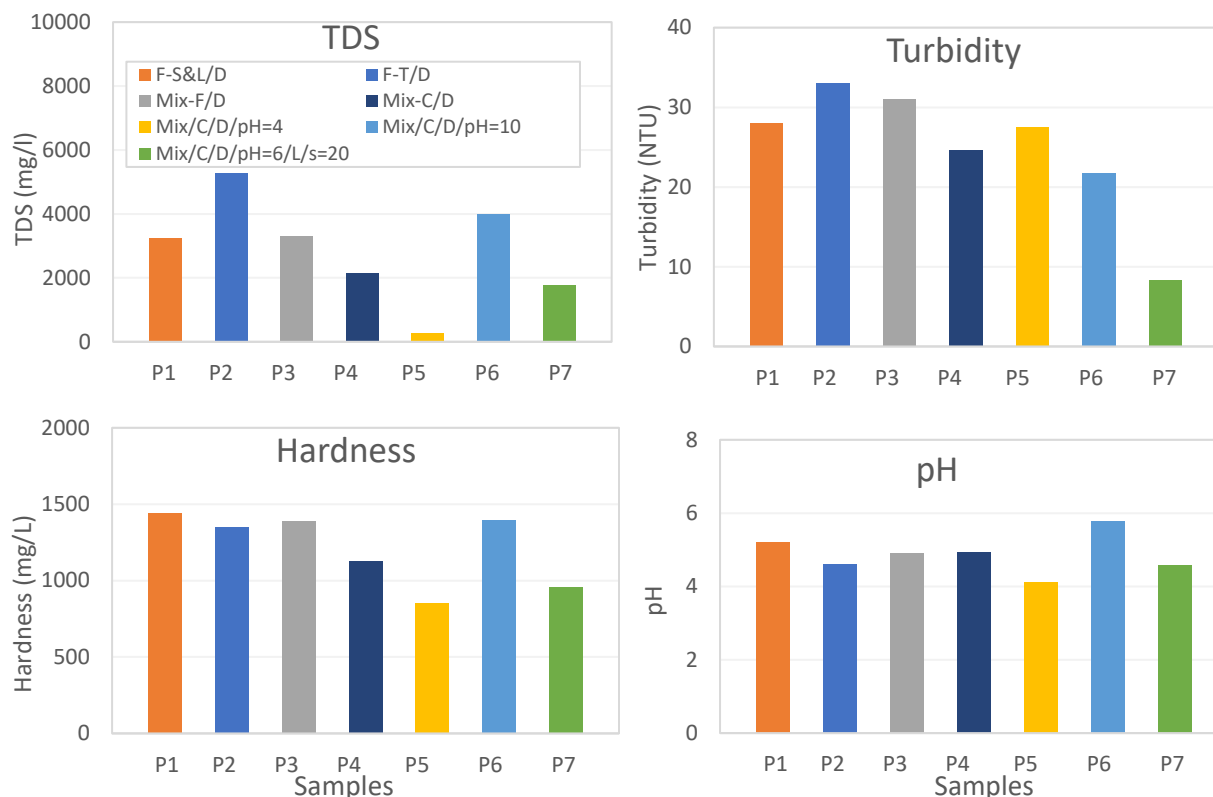


Figure 1: TDS, Hardness, Turbidity, and pH Results at 24 hours after Adding Date-Palm Waste to Distilled Water with Different Parameters.

3.1.2 Ions' Release

Many ions were investigated including cations such as K, Mg, Na, Ca, anions such as NO_3 and SO_4 , and heavy metals extracted from the date-palm waste due to contact with water. Selected elements are presented in Figure 2. The results in general showed a high rate of element extraction into water. Sample P2, i.e., fine materials from the trunk, showed the highest rate of element release except for heavy metals such as iron, Fe, and copper, Cu. It seems, that this part of the palm tree does not have abundant content of metals while P1 from leaves showed higher levels of metal extraction. Coarse materials exhibited a lower rate of extraction than fine ones as seen from P4 and P3 results. For initial pH values, results of the release such as K, Mg, Na, Ca, and Fe showed an approximately decline with an increase in initial pH values except for Cu showed a slight increase of the extraction in alkalinity conditions, which is considered as an odd result. Dortwegt and Maughan [13] concluded that the solubility of copper in water decreased with the increase of pH at different temperatures. The higher ratio of L/S demonstrated the less extraction as seen in sample P7 results. This is perhaps due to the dilution impact of increasing liquid

amount to solid. However, for Cu, the extraction of the element increased. Luo *et al.* [14] reported the same as they showed that the solubility of metals increases with the increase of liquid content.

3.2 Absorption Properties of the Date-Palm Waste

The absorption process is the treatment mechanism adopted in this work. The absorption ability of date-palm waste was examined with the wastewater effluents.

3.2.1 Physicochemical Characteristics

Results of TDS, hardness, turbidity, and pH measurements at 24 hours after adding date-palm waste to wastewater effluents with different parameters, i.e., samples WII, WIII and P8 to P12 are presented in Figure 3. All samples of the fine and coarse materials mixed from grinded branch-stems, leaves and trunk with secondary and tertiary treated wastewater, i.e., P8 to P11 demonstrated higher content of TDS, turbidity, and hardness than the reference samples of the secondary and tertiary treated wastewater, WII and WIII. Thus, still the prominent process here is leaching not absorption. The sample of the coarse materials mixed from cut branch-stems, leaves and trunk with the prewashing process, P12, revealed good improvement as it showed less content than all other samples. It demonstrates promising results for effective treatment as in this case, adding the waste into water

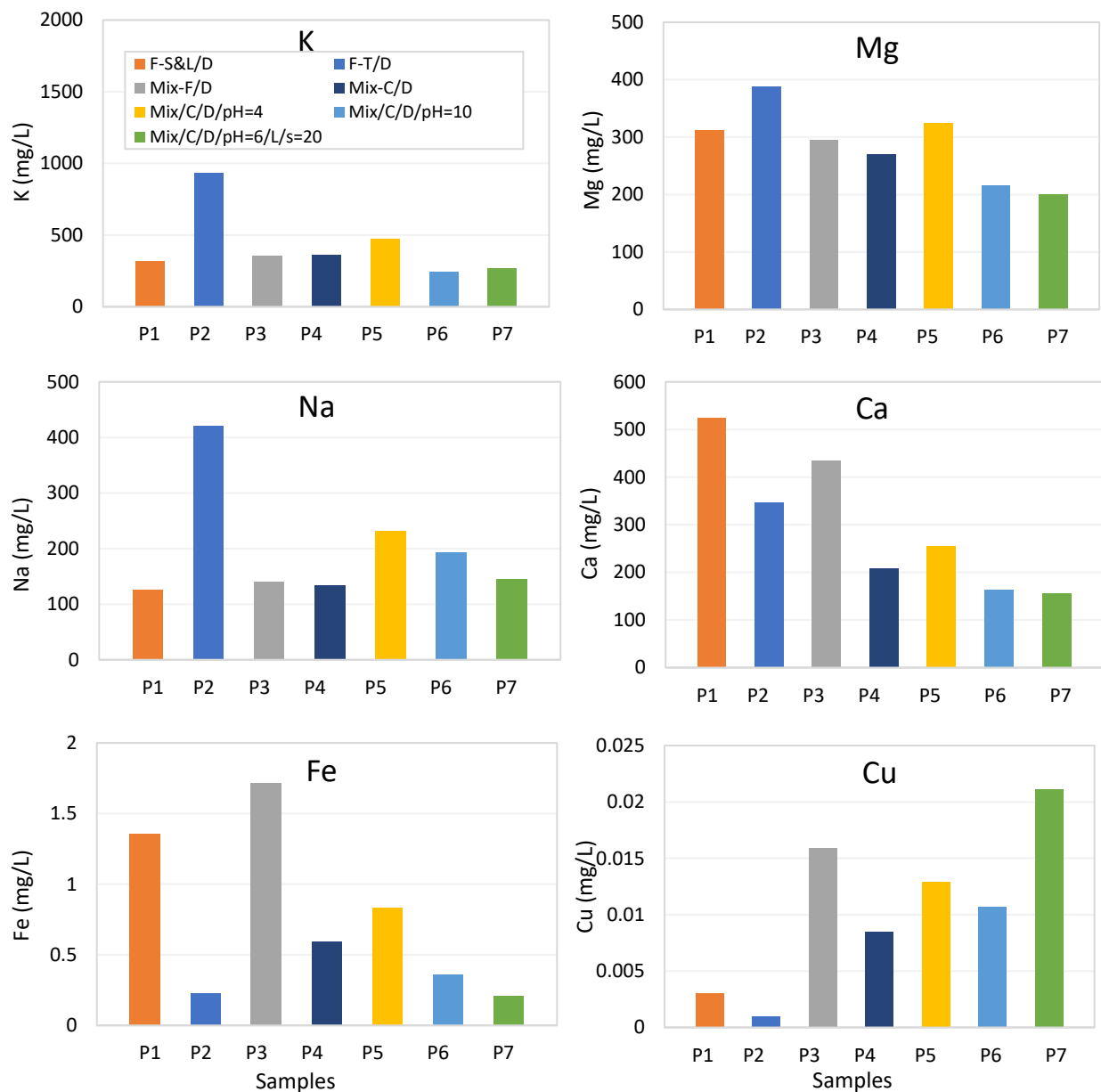


Figure 2: Ions' Release Results at 24 hours after Adding Date-Palm Waste to Distilled Water.

samples reduced the content of TDS, turbidity, and hardness of the reference samples as seen in Figure 3. Perhaps the prewashing and drying process reduced the extraction from the solid waste and

increased its absorbent ability. Samples with fine materials, i.e., P8 and P10, showed higher contents than their relevant samples with coarse materials, i.e. P9 and P11, due to the increase in the surface area of the fine materials, as reported also by Altaher [11].

3.2.2 Ions' Release

Figure 4 shows the results of ions' release at 24 hours after adding date-palm waste to wastewater effluents. In general, the results showed high rates of element extraction into water for samples P8 to P11 in comparison to the reference samples, WII and WIII. Samples P8 and P10 for the fine materials with secondary and tertiary treated wastewater, respectively, showed the highest rate of element release. This is due to the increase in the surface area of the grinded materials and consequently, the increase in the solubility.

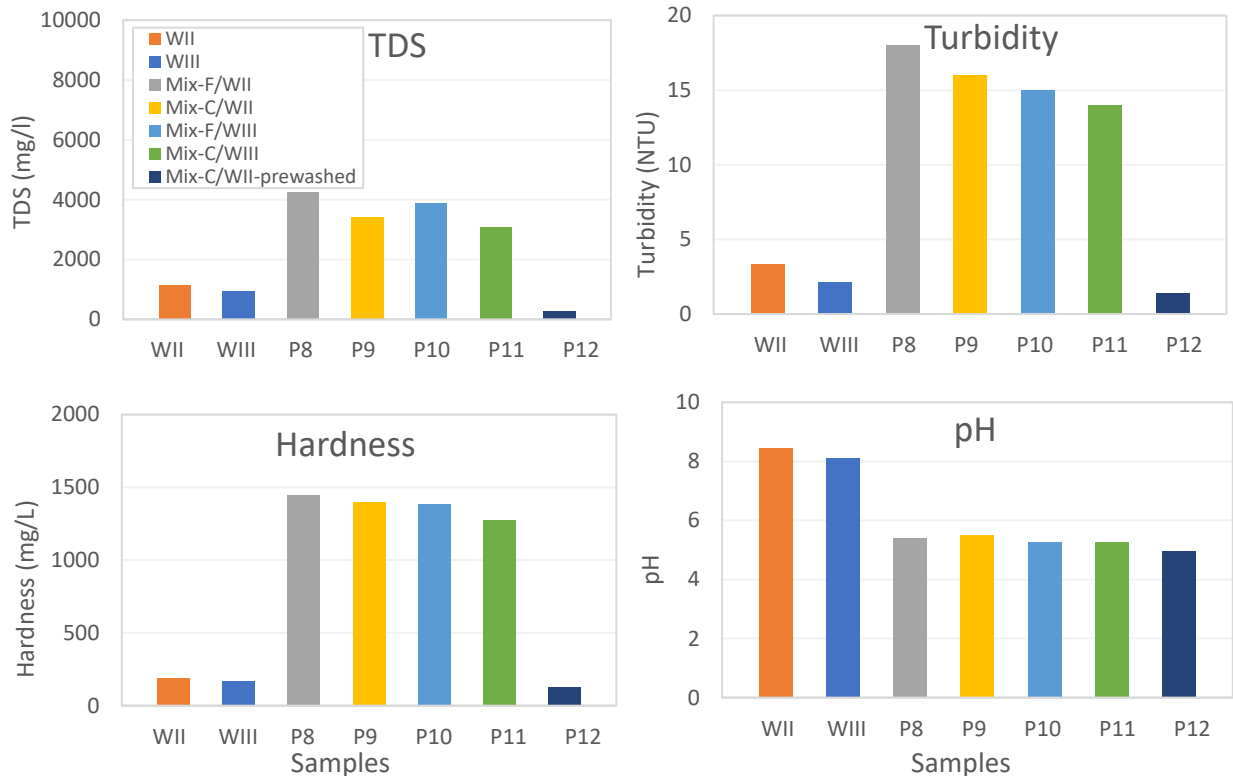


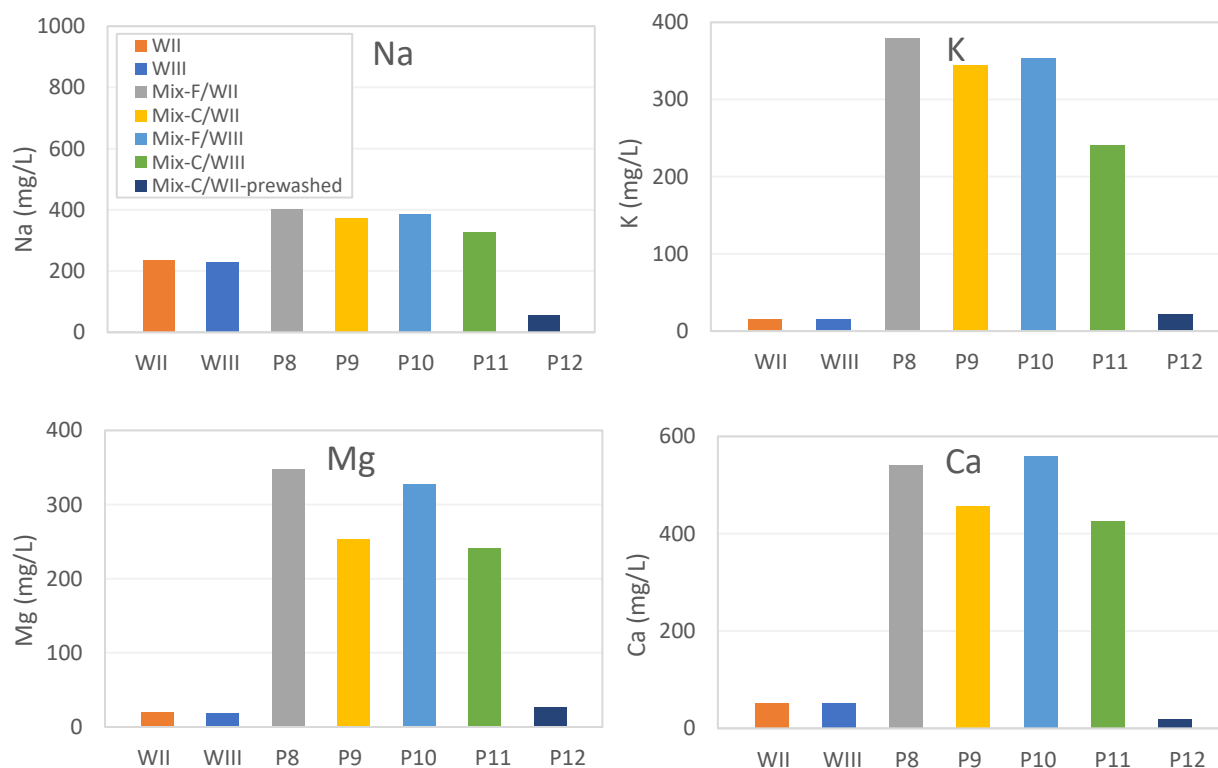
Figure 3: TDS, Hardness, Turbidity, and pH Results at 24 hours after Adding Date-Palm Waste to Wastewater Effluents with Different Parameters.

Sample P9 for the course materials with secondary treated wastewater showed lower levels of the extraction of iron and copper as compared to its relevant samples with the treated wastewater, i.e., P8, P10 and P11. For P12, the prewashed sample, results proved

that adding the waste into water samples reduced the content of most elements in comparison to the reference samples as seen in Figure 4. However, some elements such as K, Mg, and Cu showed a slight and negligible increase more than the original content of wastewater effluents. The result of the prewashed sample indicates the successful possibility of using such type of agro-waste in wastewater treatment after performing a kind of pretreatment for this waste before using it in wastewater treatment application.

3.2.3 BOD and COD

The results of BOD and COD after adding date-palm waste to wastewater effluents are presented in Figure 5. Results of samples P8 to P11 showed a notable increase in BOD and COD values in water samples in comparison to the original content of the reference samples, WII and WIII. A considerable increase was observed in COD. This is perhaps due to the high rate of element extraction into water samples. The case of mixed coarse materials with the prewashing process, i.e., P12, showed notable improvement in BOD and COD values comparing to the previous samples and the original content of



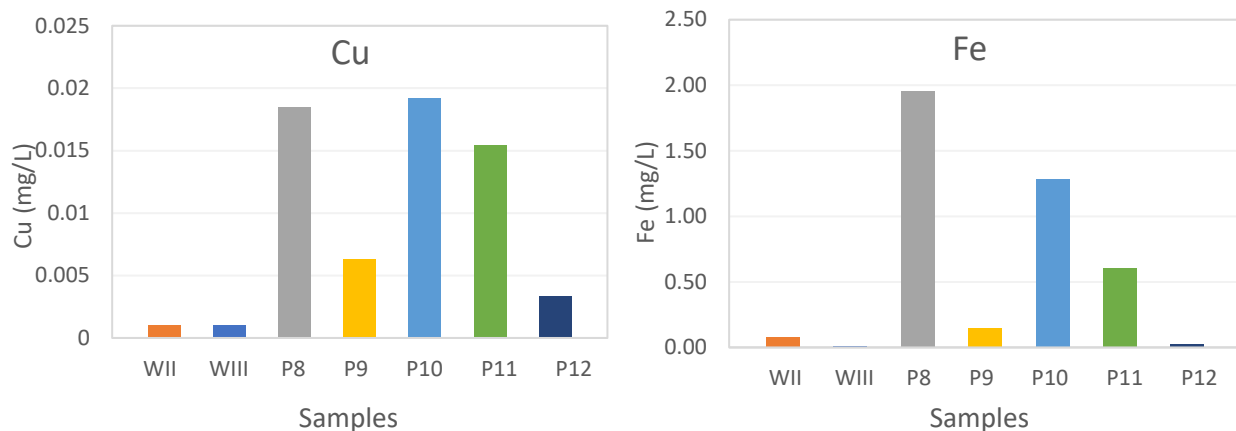


Figure 4: Ions' Release Results at 24 hours after Adding Date-Palm Waste to Wastewater Effluents.

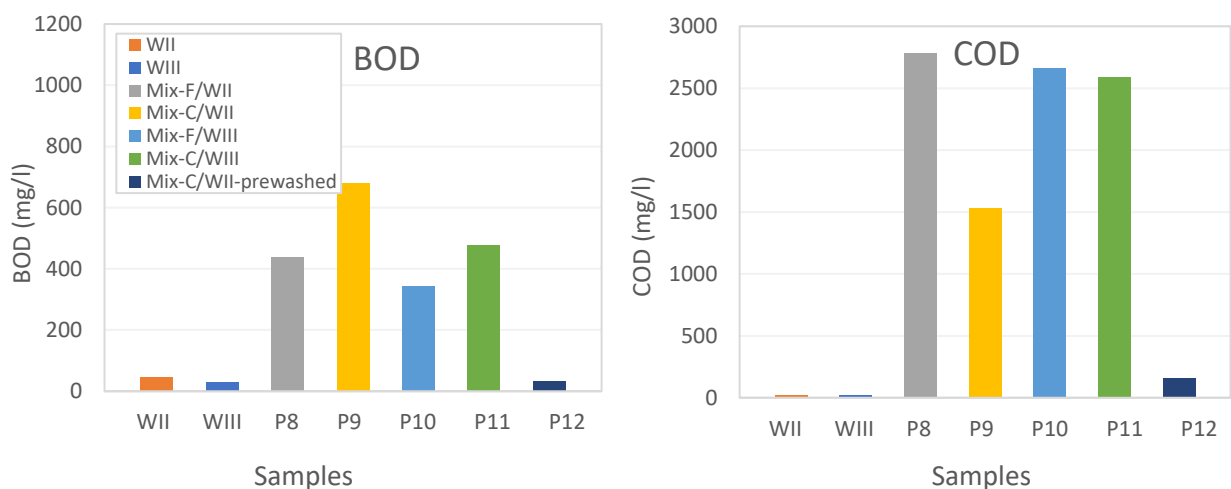


Figure 5: BOD and COD Results at 24 hours after Adding Date-Palm Waste to Wastewater Effluents.

wastewater effluents. BOD decreased by 27% less than original value of WII. This is perhaps of enhancing the empty ion sites and free electrons for improving adsorption process [15], [16]. This result is a promising finding for the treatment process by date-palm waste. Succeeding research is needed to investigate the suitable pretreatment process, which should be applied to this waste before being used as a treatment tool for wastewater effluents.

4. CONCLUSION:

This work studied the possibility of reusing date-palm wastes in the treatment of wastewater effluents relying on an experimental program. The experiments were conducted on a lab scale and various parameters were examined for leaching and absorption processes. The following findings were concluded from the study:

- The results of leaching tests showed, in general, a high rate of extraction of many ions into distilled water at different conditions. The coarse material samples of the waste exhibited less release than those from grinded materials. The conditions of initial pH and liquid to solid ratio have a notable impact on the leaching properties of the waste.
- Results of adding date-palm waste to wastewater exhibited a notable increase of element release into the effluents. BOD and COD values were also raised with the presence of waste in the water samples.
- The prewashing and drying process for the coarse waste before use with wastewater demonstrated a promising ability for this waste to remove many elements from wastewater and reduce BOD values.
- Succeeding research are needed to investigate the suitable pretreatment process, which should be applied to this waste before being used as a treatment tool for wastewater effluents.
- Prewashing plum waste with acid and alkali may enhance the morphological properties, potentially improving removal efficiency. This could be explored in future studies to optimize the recycling process.

ACKNOWLEDGEMENT:

The authors thank the Deputyship for Research and Innovation, Ministry of Education in Saudi Arabia for funding this research work through the project number (20/8). This work was also supported by Deanship of Research at the Islamic University of Madinah. The authors extend their appreciation to all the associated personnel that have

contributed to this study, especially Wastewater Treatment Plant of Al Madinah for providing wastewater samples.

REFERENCES

- [1] E. DeNicola, O. S. Aburizaiza, A. Siddique, H. Khwaja, and D. O. Carpenter, "Climate change and water scarcity: The case of Saudi Arabia," *Annals of Global Health*, vol. 81, no. 3. pp. 342–353, 2015, doi: 10.1016/j.aogh.2015.08.005.
- [2] B. Maryam and H. Büyükgüngör, "Wastewater reclamation and reuse trends in Turkey: Opportunities and challenges," *Journal of Water Process Engineering*, vol. 30. p. 100501, 2019, doi: 10.1016/j.jwpe.2017.10.001.
- [3] M. Shafiq, A. A. Alazba, and M. T. Amin, "Removal of heavy metals from wastewater using date palm as a biosorbent: A comparative review," *Sains Malaysiana*, vol. 47, no. 1. pp. 35–49, 2018, doi: 10.17576/jsm-2018-4701-05.
- [4] K. M. Alananbeh, N. A. Bouqellah, and N. S. Al Kaff, "Cultivation of oyster mushroom *Pleurotus ostreatus* on date-palm leaves mixed with other agro-wastes in Saudi Arabia," *Saudi J. Biol. Sci.*, vol. 21, no. 6, 2014, doi: 10.1016/j.sjbs.2014.08.001.
- [5] A. Faiad, M. Alsmari, M. M. Z. Ahmed, M. L. Bouazizi, B. Alzahrani, and H. Alrobei, "Date Palm Tree Waste Recycling: Treatment and Processing for Potential Engineering Applications," *Sustainability (Switzerland)*, vol. 14, no. 3. 2022, doi: 10.3390/su14031134.
- [6] K. Rambabu, G. Bharath, A. Avornyo, A. Thanigaivelan, A. Hai, and F. Banat, "Valorization of date palm leaves for adsorptive remediation of 2,4-dichlorophenoxyacetic acid herbicide polluted agricultural runoff," *Environ. Pollut.*, vol. 316, 2023, doi: 10.1016/j.envpol.2022.120612.
- [7] T. Ahmad *et al.*, "The use of date palm as a potential adsorbent for wastewater treatment: A review," *Environmental Science and Pollution Research*, vol. 19, no. 5. pp. 1464–1484, 2012, doi: 10.1007/s11356-011-0709-8.
- [8] M. Nujic, N. Velic, and M. Habuda-Stanić, "Application of Date-Palm Fibres for the Wastewater Treatment," 2019, pp. 179–191.
- [9] M. Jonoobi, M. Shafie, Y. Shirmohammadli, A. Ashori, H. Zarea-Hosseini, and T. Mekonnen, "A review on date palm tree: Properties, characterization and its

- potential applications,” *Journal of Renewable Materials*, vol. 7, no. 11. pp. 1055–1075, 2019, doi: 10.32604/jrm.2019.08188.
- [10] A. A. Juma Mohamed, L. A. Vuai, M. Kombo, and O. J. Chukwuma, “Removal of selected metal ions using powder of seeds of Ajwaa dates from aqueous solution,” *J. Anal. Pharm. Res.*, vol. 8, no. 6, pp. 228–232, 2019, doi: 10.15406/japlr.2019.08.00343.
- [11] H. Altaher, “Preliminary study of the effect of using biosorbents on the pollution of the treated water,” *Glob. Nest J.*, vol. 16, no. 4, pp. 707–716, 2014, doi: 10.30955/gnj.001385.
- [12] British Standards Institution, “British Standard: Characterisation of waste. Leaching. Compliance test for leaching of granular waste materials and sludges. One stage batch test at a liquid to solid ratio of 10 l/kg for materials with particle size below 4 mm (without or with size reduc,” *British Standard*. 2002.
- [13] R. Dortwegt and E. V. Maughan, “The chemistry of copper in water and related studies planned at the advanced photon source,” in *Proceedings of the IEEE Particle Accelerator Conference*, 2001, vol. 2, pp. 1456–1458, doi: 10.1109/pac.2001.986712.
- [14] H. Luo, Y. Cheng, D. He, and E. H. Yang, “Review of leaching behavior of municipal solid waste incineration (MSWI) ash,” *Science of the Total Environment*, vol. 668. pp. 90–103, 2019, doi: 10.1016/j.scitotenv.2019.03.004.
- [15] A. S. Mahmoud, R. S. Farag, and M. M. Elshfai, “Reduction of organic matter from municipal wastewater at low cost using green synthesis nano iron extracted from black tea: Artificial intelligence with regression analysis,” *Egypt. J. Pet.*, vol. 29, no. 1, 2020, doi: 10.1016/j.ejpe.2019.09.001.
- [16] M. Shafiquzzaman, M. M. Hasan, H. Haider, A. T. Ahmed, and S. A. Razzak, “Comparative evaluation of low-cost ceramic membrane and polymeric micro membrane in algal membrane photobioreactor for wastewater treatment,” *J. Environ. Manage.*, vol. 345, 2023, doi: 10.1016/j.jenvman.2023.118894.

The Effect of Artificial Intelligence Applications on Quick Decision-Making in Government Hospitals in Al Madinah Al Munawarah

Badr bin Abdul Rahman Al Matrafi

Specialist of Health Services and Hospitals Management

Assistant Executive Director of the University Medical Center for Administrative and Financial Affairs

Abstract: The study aims to identify the effect of artificial intelligence applications on quick decision-making in government hospitals in Al Madinah Al Munawarah. The researcher used the descriptive approach with the analytical method in order to achieve the objectives of the study. The study population consists of doctors, nursing staff, and technical and administrative staff in government hospitals in Al Madinah Al Munawarah in Kingdom of Saudi Arabia, who number (6897) according to the statistics of the year 1445 AH. The sample size was (364) of doctors, nursing staff, and technical and administrative staff in government hospitals in Al Madinah Al Munawarah in Kingdom of Saudi Arabia. As for the research results, it is clear that the total score for the first dimension, “Application of Fuzzy Logic Systems”, came at an average of (2.26), with a percentage of (50.5%), which is a low percentage according to the study tool. As for the second dimension, “Implementing expert systems”, the average was (2.64), with a percentage of (52.7%). The third dimension, “Application of neural network systems”, had an average of (2.33) and a percentage of (46.6%), which is a low percentage according to the study tool. The fourth dimension, “The role of artificial intelligence on quick decision-making”, came with an average of (4.31), and a percentage of (86.2%), which is a very high percentage according to the study tool. As for

the challenges dimension, the total score for the dimension “Challenges of applying artificial intelligence” was at an average of (3.51), with a percentage of (70.2%), which is a high percentage according to the study tool. The study recommended providing training and education, developing technological infrastructure, investing in cloud-based artificial intelligence solutions, and continuous evaluation and improvement.

Keywords: artificial intelligence - government hospitals - decision-making - government hospitals.

أثر تطبيقات الذكاء الاصطناعي على سرعة اتخاذ القرار في المستشفيات الحكومية بالمدينة المنورة

المخلص: تهدف الدراسة إلى التعرف على أثر تطبيقات الذكاء الاصطناعي على سرعة اتخاذ القرار في المستشفيات الحكومية بالمدينة المنورة. واستخدم الباحث المنهج الوصفي مع المنهج التحليلي لتحقيق أهداف الدراسة. يتكون مجتمع الدراسة من الأطباء وطواقم التمريض والطواقم الفني والإداري في المستشفيات الحكومية بالمدينة المنورة بالمملكة العربية السعودية والبالغ عددهم (6897) حسب إحصائيات عام 1445هـ. وبلغ حجم العينة (364) من الأطباء وطواقم التمريض والطواقم الفني والإداري في المستشفيات الحكومية بالمدينة المنورة في المملكة العربية السعودية. أما بالنسبة لنتائج البحث يتضح أن الدرجة الكلية للبعد الأول "تطبيق نظم المنطق المضرب" جاءت بمتوسط (2.26) وبنسبة مئوية (50.5%) وهي نسبة متدنية وفقاً لنتائج البحث. إلى أداة الدراسة. أما البعد الثاني "تطبيق النظم الخبيرة" فقد بلغ المتوسط (2.64) وبنسبة مئوية (52.7%). أما البعد الثالث وهو "تطبيق أنظمة الشبكات العصبية" فقد حصل على متوسط (2.33) وبنسبة مئوية (46.6%) وهي نسبة منخفضة حسب أداة الدراسة. أما البعد الرابع وهو "دور الذكاء الاصطناعي في سرعة اتخاذ القرار" فقد جاء بمتوسط (4.31)، وبنسبة مئوية (86.2%)، وهي نسبة عالية جداً بحسب أداة الدراسة. أما في بعد التحديات فقد جاءت الدرجة الكلية للبعد "تحديات تطبيق الذكاء الاصطناعي" بمتوسط (3.51)، وبنسبة مئوية (70.2%)، وهي نسبة عالية حسب أداة الدراسة. وأوصت الدراسة بتوفير التدريب والتعليم، وتطوير البنية التحتية التكنولوجية، والاستثمار في حلول الذكاء الاصطناعي السحابية، والتقييم والتحسين المستمر.

1.Introduction

The process of developing administrative and technical systems is one of the most important pillars of health care in Kingdom of Saudi Arabia. Hospitals in Kingdom of Saudi Arabia are considered an essential pillar for providing health care to citizens and residents. To ensure the quality and efficiency of this care, the development of administrative and technical systems plays a prominent and vital role. Effective administrative systems allow the hospital to be managed in a more organized and effective manner. Smooth internal operations are one of the main goals, and the introduction of advanced technologies can contribute to improving patient registration processes and medical file management, leading to reduced errors and improved patient experience (Al Alwan, 2020: 942). The role of technical development is not limited to administrative systems only, but also extends to advanced medical technology. Investing in modern medical equipment and devices enhances hospitals' ability to provide advanced medical services and accurate diagnosis, which leads to improving the level of health care provided. Another important aspect is that the development of administrative and technical systems can reduce administrative and operational costs. Thanks to automation and improvements in processes, resources can be saved and financial waste reduced, which contributes to enhancing the sustainability of hospitals and their ability to provide high-quality health services (Ajam, 2018: 96). The important technological developments that these hospitals are witnessing include the role of artificial intelligence is a key element in improving health services and developing medical care. Artificial intelligence is considered a powerful tool used to analyze huge medical data and has many applications in Saudi hospitals. There are many roles that artificial intelligence can play, such as helping doctors analyze medical images with high accuracy, which contributes to accelerating the diagnosis process and increasing accuracy in detecting diseases, analyzing patient data and providing personalized recommendations and personalized treatment based on that data, which enhances the effectiveness of treatment, as well as improving stock management and determining future needs for medicines and medical supplies. Patient experiences can also be customized using artificial intelligence, by improving appointment systems and providing accurate and smooth medical information. Artificial intelligence also has strong contributions to analyzing medical data to guide research and discover new and effective treatments.

Integrating smart technology such as artificial intelligence in Saudi hospitals contributes significantly to providing high-quality health services and enhances efficiency and effectiveness in health care provided to patients (Florea & Radu, 2019:381), since quick and effective decisions are one of the most important factors that determine the success of hospitals in providing excellent health services and meeting the needs of patients. In Kingdom of Saudi Arabia, the importance of this aspect is significantly increasing due to the quick development and great momentum in healthcare. Therefore, speed in decision-making represents an urgent challenge for Saudi hospitals in order to provide distinguished health services. But by using advanced technology and taking full advantage of big data, the decision-making processes can be improved and accelerated and overall healthcare enhanced.

2.The Study Problem

The Saudi health system is witnessing a noticeable increase in the number of cases and patients benefiting from health care, which places great pressure on hospitals to make quick and effective decisions. Health management also faces challenges in analyzing big data and using it to make strategic decisions that affect the efficiency of services, as technology is developing very quickly, including smart solutions that contribute to improving health care, but this requires quick decisions to be made regarding the adoption and integration of these technologies into the hospital environment.

Accordingly, the problem of the current study can be defined in the following question: “What is the effect of artificial intelligence applications on quick decision-making in government hospitals in Al Madinah Al Munawarah?”

3.Study Questions:

This study will seek to answer the following questions:

- What is the reality of applying fuzzy logic systems that affect quick decision-making in government hospitals in Kingdom of Saudi Arabia?
- What is the reality of implementing expert systems that affect quick decision-making in government hospitals in Kingdom of Saudi Arabia?

- What is the reality of applying neural network systems that affect quick decision-making in government hospitals in Kingdom of Saudi Arabia?
- What is the role of artificial intelligence on quick decision-making in government hospitals in Kingdom of Saudi Arabia?
- What are the challenges of applying artificial intelligence techniques that affect quick decision-making in government hospitals in Kingdom of Saudi Arabia?

4.Objectives of the Study:

- Determining the reality of applying fuzzy logic systems that affect quick decision-making in government hospitals in Kingdom of Saudi Arabia.
- Determining the reality of implementing expert systems that affect quick decision-making in government hospitals in Kingdom of Saudi Arabia.
- Determining the reality of applying neural network systems that affect quick decision-making in government hospitals in Kingdom of Saudi Arabia.
- Determining the role of artificial intelligence on speedy decision-making in government hospitals in Kingdom of Saudi Arabia.
- Determining the challenges that hinder the application of artificial intelligence technologies and that affect quick decision-making in government hospitals in Kingdom of Saudi Arabia.

5..Importance of the Study:

First: Theoretical Importance:

1. The study contributes to understanding how artificial intelligence technologies affect decision-making processes in hospitals, paving the way for improving health care and making it more effective.
2. The study contributes to analyzing the efficiency of applying artificial intelligence techniques in decision-making, which enables hospitals to identify the most effective tools and techniques in accelerating decision processes.
3. The study contributes to directing administrative and strategic decisions in hospitals to further adopt artificial intelligence technologies, which creates impactful changes in workflow and health care.

4. The study is an opportunity to expand scientific knowledge and development in the field of health care, which contributes to the production of new knowledge that benefits medical practices.
5. Providing the necessary support to make future decisions regarding investment in artificial intelligence technologies and directing efforts towards the most effective and sustainable aspects.

Second: Practical Importance:

1. Artificial Intelligence technologies enable massive amounts of medical data to be analyzed quickly and accurately, making it easier for decision-making based on accurate insights.
2. Artificial intelligence can help doctors analyze medical images and clinical data, speeding up diagnostic processes and increasing their accuracy.
3. Using AI analytics, personalized treatment plans can be provided to each patient based on their information and medical history.
4. Smart applications can create significant savings in the time and effort it takes for decision-making, which contributes to increasing work efficiency.
5. Speed of decision and appropriate intervention can improve the patient's experience within the hospital and increase his satisfaction.

6. Terminology of Study

Artificial Intelligence (AI)

The European Commission (2018:3) defines the term Artificial Intelligence (AI) to “systems that display intelligent behavior by analyzing their environment and taking actions – with a certain degree of autonomy – to achieve specific goals”. Laird (et al., 1987:6) defined artificial intelligence (AI) as “the ability of a digital computer or computer-controlled robot to perform tasks commonly associated with intelligent beings”. Russell and P. Norvig (2009: 16) defined artificial intelligence (AI) as “a branch of computer science that focuses on building and managing technology that can learn to independently make decisions and perform actions on behalf of humans”.

7. Decision-Making:

Qureshi (2020: 872) defined decision-making as “the process during which an individual or group identifies the options available to them and chooses one of them to take the final step or decision”. This work includes many steps such as collecting necessary information, analyzing data, and evaluating different options before making the final decision”.

8.Methodology:

The descriptive approach will be used using the analytical method to describe the phenomenon that is the subject of the study and analyze its data and the relationship between its components.

9.Study Population:

Nursing staff, doctors, technical and administrative staff in government hospitals in Al Madinah Al Munawarah

10.Study Sample:

A random sample of 6897 nurses, doctors, technical and administrative staff will be selected.

11.Limits of the Study:

Place Limits: The study will be conducted in government hospitals in Al Madinah Al Munawarah.

Time limits: The study will take place during the year 1445 AH - 2023 AD.

Human Limits: The study will be conducted on nursing staff, doctors, and technical and administrative staff.

12.Tool of the Study:

The questionnaire will be used to obtain the necessary primary data. The questionnaire was designed to find out the effect of artificial intelligence applications on quick decision-making in government hospitals in Al Madinah Al Munawarah.

13.Review of Literature:

Al Sardiya's study (2022) entitled: "The degree to which school principals in Mafraq Governorate use artificial intelligence applications and their relationship to the quality of administrative decision-making"

The study aimed to identify the degree to which school principals in Mafraq Governorate use artificial intelligence applications and their relationship to the quality of administrative decision-making, and to reveal the influence of the following variables: gender, years of experience, and academic qualification on that. To achieve the objectives of the study, the descriptive correlational survey method was used. The study sample consisted of (365) male and female teachers from Mafraq Governorate schools during the first semester of the 2021/2022 academic year. They were selected by a simple random method. To achieve the study objective, a questionnaire consisting of (43) items was developed, and the validity and reliability of the tool was confirmed. The study findings showed that the degree to which school principals in Mafraq Governorate used artificial intelligence applications from the point of view of teachers was moderate, and that the quality of administrative decision-making was moderate. The results also showed that there were no statistically significant differences at the level of significance ($\alpha = 0.05$) in the areas of the measure of the use of artificial intelligence applications by school principals in Mafraq Governorate and the areas of the measure of the quality of administrative decision-making due to the variables of the study (gender, practical experience, and academic qualification). The results also showed that there is a positive, statistically significant correlation between the degree to which school principals in Mafraq Governorate use artificial intelligence applications and its fields and the quality of administrative decision-making. In light of the study findings, the researcher recommended several recommendations, including training school principals on artificial intelligence applications in order to raise the quality of administrative decision-making in schools in Mafraq Governorate, the necessity of preparing effective plans to train and qualify all school principals and teachers to apply artificial intelligence applications.

Saleh's study (2022) entitled: "Proposed procedures for developing the decision-making process in educational departments using expert systems as an application of artificial intelligence"

The study aimed to develop the decision-making process in educational departments using expert systems as an application of artificial intelligence. To achieve this goal, the study relied on the descriptive approach, and also relied on the questionnaire as a data collection tool. The study consisted of three dimensions, in addition to the part related to defining the study's problem, questions, and methodology. The first dimension included the theoretical and intellectual foundations of expert systems as one of the applications of artificial intelligence in educational administration, while the second dimension included the role of expert systems in the decision-making process and the third dimension included proposed procedures to develop the decision-making process in educational departments in Minya Governorate using expert systems as an application of artificial intelligence.

Alwan's study (2020) entitled: "Artificial Intelligence and Crisis Management: A Case Study of the COVID-19 Pandemic Crisis"

This study aimed to identify the most prominent roles of artificial intelligence in crisis management, by applying it to Covid-19virus pandemic crisis in the pre-crisis phase, the crisis response phase, and the post-crisis phase. It also aimed to identify the most prominent challenges, including governance challenges, human and material challenges, technical challenges, and ethical challenges that artificial intelligence faces in managing Covid-19virus pandemic crisis. To achieve these goals, a case study methodology was adopted based on the sequence from the general framework to the specific framework, and information is extracted based on this sequence.

Accordingly, the analysis was based on a matrix consisting of a horizontal dimension and a vertical dimension. The horizontal dimension of the matrix consists of the three stages of the crisis, and the vertical dimension consists of three components: The role of crisis management, the role of artificial intelligence in crisis management, and the role of artificial intelligence in managing Covid-19 crisis.

The study found a set of roles for artificial intelligence in all stages of crisis management, including: predicting crises, activating teamwork, and generating knowledge. The study also found another set of roles for artificial intelligence to manage Covid-19 crisis, including: training, early diagnosis, and evaluating the impact of the epidemic. The study identified the most prominent challenges facing artificial intelligence in managing Covid-19 crisis,

classified into governance challenges, human and material challenges, technical challenges and ethical challenges. In conclusion, the study presented some recommendations drawn from the results.

Al Enezi's study (2020) entitled: "The Effect of artificial Intelligence on the Performance of Organizations: A Case Study of the Primary Health Care Corporation in the State of Qatar" This study aimed to identify the effect of artificial intelligence on the performance of organizations (internal operations, training and growth, auditor satisfaction), and the researcher followed the descriptive analytical approach to conduct this study. The study sample included (130) employees of the Primary Health Care Corporation in the State of Qatar, and the study used a tool developed for this purpose. The study findings showed that the arithmetic averages were very high, high, and medium for the independent dimension (artificial intelligence), and that the arithmetic average for the overall dimension (organizational performance) reached (4.00). The second dimension (training and growth) came in first place, followed in last place by the first dimension (internal processes). The results also showed that the independent variable (artificial intelligence) has a statistically significant effect on the dependent variable (task performance) with its combined dimensions (internal operations, training and growth, and auditors' satisfaction). Based on the study results, the researcher made several recommendations, as follows: It is necessary to pay attention to artificial intelligence applications related to the process of canceling customer electronic subscriptions, and to ensure that they are completed in a quick and easy manner, ensuring attention to the conduct of internal operations in the organization, improving relations between its employees and ensuring their commitment to regulations and laws.

Agam's study (2018) entitled: "Artificial Intelligence and its Implications for High-Performing Organizations: An Exploratory Study in the Ministry of Science and Technology" The study addressed the concept of artificial intelligence and its impact on high-performance organizations. The Ministry of Science and Technology was intentionally chosen to conduct the study and distribute the questionnaire. The study included mid-line managers because they were in direct contact with the topics covered by the study to know the impact of the four types of artificial intelligence that were studied, including: Expert systems, neural networks, genetic algorithms, and intelligent agents influence the ministry's work. To

determine the impact, two main hypotheses and eight sub-hypotheses were developed. A questionnaire was used to collect data. Forty questionnaires were distributed and retrieved in full. They were subjected to the Cronbach Alpha test to determine the validity and reliability of the tool. Arithmetic means, standard deviations, correlation and effect coefficients were used. A set of conclusions were reached, the most important of which is the existence of a significant correlation and the presence of a moral impact of the application of artificial intelligence within the departments investigated in the ministry. The results were consistent with the two hypotheses of the study. The researcher also presented a set of recommendations, the most important of which was the need to expand applications of artificial intelligence and according to the departments' need for each type of artificial intelligence in order to advance the ministry's reality to a better level.

14. Theoretical Framework and Literature of the Study

The Concept of Artificial Intelligence:

Laird et al (1987) defined artificial intelligence (AI) as a field in computer science concerned with creating technological systems and programs that have the ability to perform tasks that usually require human intelligence with the aim of developing systems capable of learning, thinking, making decisions and adapting to situations independently, based on data and analyses. The concept of artificial intelligence includes a wide range of technologies and concepts, including what the study (Pliakos, et.al, 2019) showed in the following:

1. **Machine Learning:** Machine learning allows computer systems to analyze data and gain experience by interacting with the environment and data, without the need for explicit programming.
2. **Artificial Neural Networks:** They depend on imitating the work of neural networks in the human brain to process information and analyze data.
3. **Natural Language Processing:** It allows the computer to understand and analyze human language and interact naturally with texts and commands.
4. **Smart Robotics and Autonomous Systems:** It allows robots and systems to carry out tasks independently without human intervention.
5. **Artificial Thinking:** Seeking to give artificial intelligence systems the ability to make independent decisions based on data and analyses.

6. **Narrow and General Artificial Intelligence AI:** Narrow artificial intelligence focuses on solving a specific task, while general intelligence aims to outperform systems in a wide range of tasks in a human-like manner.
7. **Self-adaptation and continuous improvement:** Artificial intelligence allows systems to adapt to the changing environment and continuously improve their performance.

Artificial Intelligence is a developing field that generates a lot of interest and is used in various industries such as medicine, business, industry, and technology.

15.Areas of Using Artificial Intelligence in Saudi Hospitals

Artificial intelligence is considered one of the modern tools that enhance innovation and improve health services in Saudi hospitals, and Alwan's study (2020) showed the areas of use of artificial intelligence in this context:

1. Diagnosis of diseases:

- **Medical image analysis:** Artificial intelligence is used to analyze medical images such as X-rays and MRI to diagnose diseases with high accuracy.
- **Clinical data analysis:** Artificial intelligence can be used to analyze patient data and medical records to identify factors associated with diseases and provide accurate treatment guidance.

2. Improving Health Care Services:

- **Personalize care:** Artificial intelligence helps direct medical care for each patient based on their health records and surrounding factors.
- **Improving reception and emergency operations:** It can be used for forecasting, early reporting of emergency situations and better prioritization.

3. Resource Management and Planning:

- **Providing administrative efficiency:** Artificial intelligence can be used to analyze performance data and effectively use resources such as medical beds and clinical beds.

- Forecasting needs: It helps in analyzing data to predict future needs for resources and medical devices.

4. Development of Treatments and Medicines:

- Research and development: Artificial intelligence can be used to analyze genetic data and clinical studies to develop effective treatments and medicines.
- Personalization of treatments: It can be used to customize medical treatments to the needs of specific patients.

5. Personal Care and Communication with Patients:

- **Healthcare applications:** Applications can be developed that facilitate communication between doctors and patients and provide personalized health advice.
- **Medical Robots:** Using robots to assist in medical care and provide assistance in certain medical procedures.

16. Requirements for Applying Artificial Intelligence in Saudi Hospitals

The application of artificial intelligence in Saudi hospitals requires consideration of several requirements to ensure the success and effectiveness of these technologies. Among these requirements are what Al Enezi's (2020) study explained in the following:

Data and Analysis:

- **Reliable and sufficient data:** Providing medical data of high quality and sufficient quantity to support artificial intelligence operations.
- **Data Analysis:** The ability to analyze and use data effectively to obtain accurate insights and guidance.

Technological Infrastructure:

- **Integrated and compatible systems:** The necessity of having a technological infrastructure capable of supporting artificial intelligence applications and integrating them with current hospital systems.

Training and Development:

- **Qualifying Cadres:** Providing training and education for doctors, nurses, and medical personnel on the use of new smart technologies.
- **Continuous Development:** the ability to keep pace with technological developments and continuous updates in the field of artificial intelligence.

Security and Privacy:

- **Data Protection:** Implement security measures and protect patient data and sensitive medical information from hacks and leaks.
- **Compliance with legislations:** Ensuring that the AI application complies with laws, health regulations, and privacy requirements.

Leadership Support and Funding:

- **Administrative support:** The presence of leadership support that encourages the application and investment in smart technologies.
- **Sustainable financing:** Allocate a sufficient budget to develop and maintain the hospital's artificial intelligence systems.

Communication and Transparency:

- **Exchange of knowledge and experiences:** Encouraging communication and exchange of knowledge with other hospitals and relevant parties for continuous learning and application of best practices.
- **Transparency:** Establishing artificial intelligence projects in a transparent manner that achieves trust and enhances the effective exchange of information.

Achieving the success of implementing artificial intelligence in hospitals requires considering these different aspects and focusing on meeting technical, operational, legal and human requirements.

17.Challenges Facing the Application of Artificial Intelligence in Saudi hospitals

The use of artificial intelligence in Saudi hospitals is witnessing remarkable progress in improving health care and making medical services more effective and accurate. However,

there are many challenges faced by the application of artificial intelligence, including what Ajam's study (2018) explained in the following:

1. Infrastructure and Technology:

- **Technology transformation:** Adopting the technology needed to implement AI can be expensive and require modernization of existing hospital infrastructure.

2. Data and Privacy:

- **Data quality:** Providing high-quality, reliable data is a challenge, as AI relies on accurate data to perform reliably.
- **Privacy and security:** Keeping medical data and personal information of patients requires following strict procedures to maintain privacy and security.

3. Interaction with Human Elements:

- **Acceptance of technology:** New technologies may face resistance from some medical or administrative personnel due to lack of confidence in the new system or fear of switching to the technology.

4. Training and Skills:

- **Training cadres:** The application of artificial intelligence requires training medical and technical personnel to use new technologies, and this requires investment in training and education.

5. Laws and Regulations:

- **Health legislation:** Hospitals may face legal or regulatory restrictions in using smart technologies in healthcare.

6. Challenges of Saving and Investing:

- **Costs and sustainability:** Implementing AI can be expensive and require ongoing investments, which can be a challenge for hospitals under financial pressures.

These challenges are part of the many factors that must be considered and addressed when applying smart technologies such as artificial intelligence in the medical field. The success of these technologies requires strategic thinking and good planning, in addition to cooperation between the public and private sectors and the adoption of solutions that meet the actual needs of patients and medical personnel.

To overcome these challenges, Saudi hospitals must invest in:

- **Smart decision-making technologies:** Adopting artificial intelligence systems and big data analysis to provide accurate and quick insights for decision-making.
- **Technical infrastructure development:** The necessity of updating systems and software and providing the necessary infrastructure for modern technology.
- **Strengthening organizational and leadership capabilities:** developing leadership skills in making quick and influential decisions.

Quick decision-making is a major challenge facing Saudi hospitals, but technology and improving administrative capabilities can contribute to meeting this challenge and achieving the provision of distinguished health services (Al Alwan, 2020: 974).

18.The role of artificial intelligence in speedy decision-making in Saudi hospitals:

Artificial intelligence plays an important and diverse role in improving health services within hospitals in Kingdom of Saudi Arabia. Al Anazi's (2020) study explained some of the main roles that artificial intelligence can play in this context:

1. **Assistant diagnosis and analysis of medical images:** Artificial intelligence can help doctors analyze and interpret medical images such as X-rays, CT scans, and MRI images. This can speed up the diagnostic process and help detect diseases and changes more accurately.
2. **Improving patient experience:** Artificial intelligence can be used to personalize patient experiences, such as improving appointment and scheduling systems, providing accurate information about health conditions, and providing immediate responses to patient inquiries.

3. **Improving inventory and resource management:** Artificial intelligence can improve inventory management in hospitals by anticipating needs, reducing waste, and ensuring the accurate and effective provision of medicines and medical supplies.
4. **Providing personalized healthcare:** Artificial intelligence can be used to analyze big data for patients and provide personalized recommendations and personalized treatment based on that data.
5. **Developing medical research:** Artificial intelligence can contribute to analyzing large medical data to identify new trends and treatments and guide medical research.
6. **Improving practical management:** Artificial intelligence can be used to improve medical management processes, analyze financial data, and provide guidance to improve efficiency and reduce costs.

Artificial intelligence applications contribute to improving the quality of health care and providing better medical services. They also contribute to providing health care more efficiently and effectively to patients in Kingdom of Saudi Arabia.

19. Methodological Procedures of the study

Field Study Procedures

This section deals with a detailed description of the procedures followed by the researcher in implementing the study, including a definition of the study methodology, a description of the study population and its sample, design and preparation of study tool used (the questionnaire) and ensuring its validity and reliability, as well as the procedures for using and applying the study tools, and the statistical treatments that the researcher relied on in analyzing the study findings.

First: The Aim of the Field Study:

The study aimed to identify the effect of artificial intelligence applications on quick decision-making in government hospitals in Al Madinah Al Munawarah.

Second: Methodology:

The researcher used the descriptive method using the analytical method in order to achieve the objectives of the study, which is defined as: "It deals with events, phenomena, and

practices that exist and are available for measurement, and the study as it is without interference from the researcher in its course, and the researcher can interact with them, describe them, and analyze them” (Darwish, 2017 AD).

Third: Population of the Study

The study population consists of doctors, nursing staff, and technical and administrative staff in government hospitals in Al Madinah Al Munawarah in Kingdom of Saudi Arabia, numbering (6897) according to the statistics of the year 1445 AH.

Fourth: Study Sample:

The study sample represents the original community, and contains its features and characteristics. It consists of doctors, nursing staff, and technical and administrative staff in the government hospitals of Al Madinah Al Munawarah in Kingdom of Saudi Arabia. The sample was determined based on the size of the original population (6897), according to the American Association’s approach to determining sample size, and calculating the equation. The sample size was (364) doctors, nursing staff, and technical and administrative staff in government hospitals in Al Madinah Al Munawarah in Kingdom of Saudi Arabia, and they represent the study population. The questionnaire tool was distributed to doctors, nursing staff, and technical and administrative staff in government hospitals in Al Madinah Al Munawarah in Kingdom of Saudi Arabia from the sample.

Characteristics of the Study Sample:

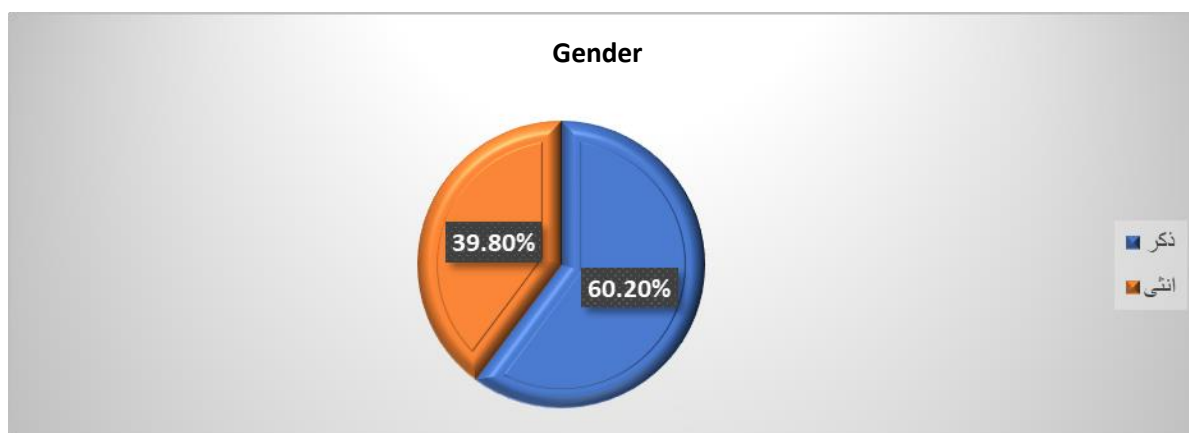
■ Gender

Table (1)
Distribution of sample members by gender

Gender	Frequency	%
Males	60.2	219
Females	39.8	145
Total	100.0	364

Table No. (1) shows that the percentage of males reaches 60.2% of the sample size and that the percentage of females reaches 39.8%.

Figure (1) shows the percentage of males and females in the study sample



■ **Academic Qualification**

Table (2)

Distribution of sample members according to academic qualification

Qualification	Total study sample	%
Less than the Bachelor	81	22.3
The Bachelor	230	63.2
Master's Degree	37	10.2
PhD	16	4.4
Total	364	100.0

It is clear from the previous table that the highest percentage is the number of holders of a bachelor's degree at a rate of (63.2%), followed by those who hold less than a bachelor's degree at a rate of (22.3%).

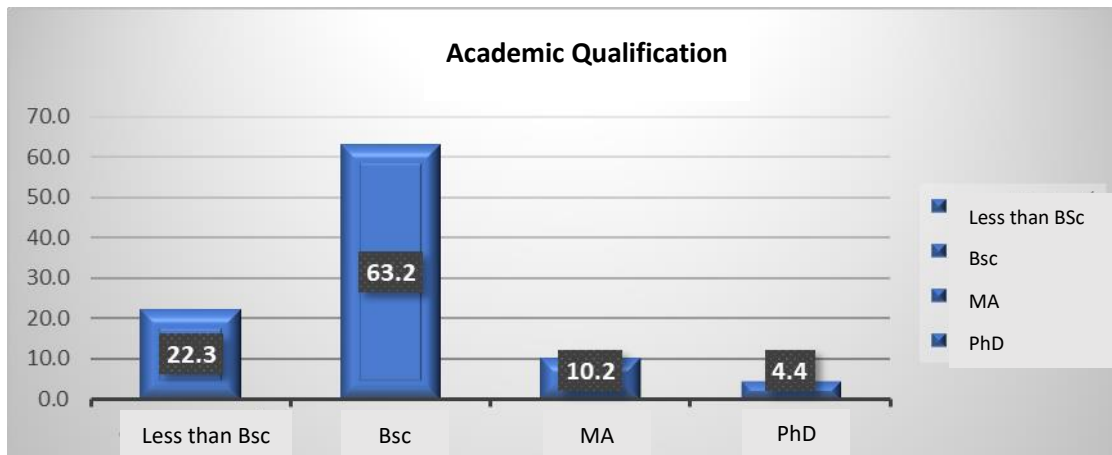


Figure (2): the percentage for the academic qualification variable

■ **Experience**

Table (4)

Distribute the research sample according to experience

Stage	Frequency	%
Less than 5 years	75	20.6
5 to 10 years	151	41.5
More than 10 years	138	37.9
Total	364	100.0

It is clear from the previous table that the highest percentage of those with less than 5 to 10 years of experience reached (41.5%), followed by those with more than 10 years of experience with a rate of (37.9).

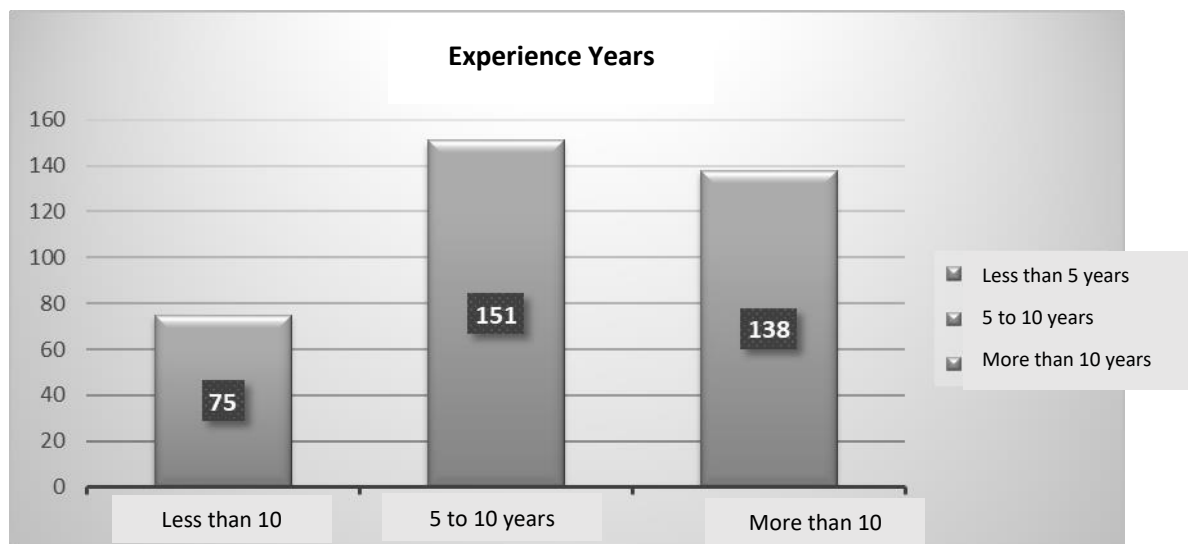


Figure (4): the percentage in relation to the experience variable

■ **Job**

Table (5)

Distribution of the study sample according to jobs

Stage	Frequency	%
Less than 5 years	75	20.6
5 to 10 years	151	41.5
More than 10 years	138	37.9
Total	364	100.0

It is clear from the previous table that the highest percentage is for the position of doctors, at a rate of (44.8%), followed by the position of nurses, at a rate of (28.3).

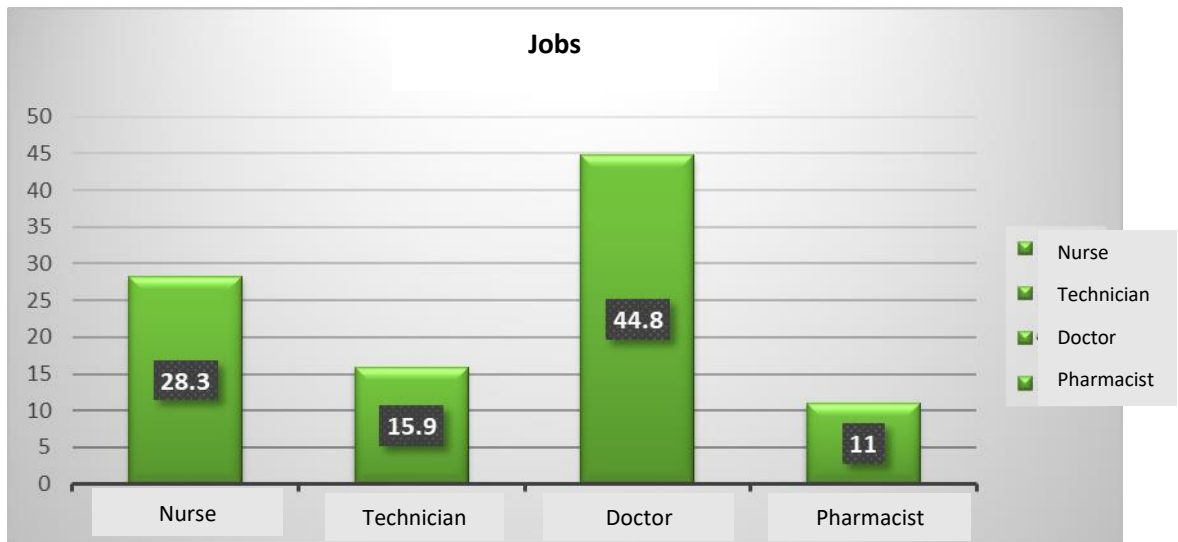


Figure (4): the percentage in relation to the function variable

20. Description of the design, preparation and control of the study tool:

Based on the nature of the data and the approach followed in the study, it was concluded that the most appropriate tool to achieve the objectives of the study is the questionnaire. The questionnaire was used to identify the effect of artificial intelligence applications on quick decision-making in government hospitals in Al Madinah Al Munawarah. The questionnaire was prepared by reviewing the literature related to the aim of the research, as well as after reviewing previous studies, Alwan's study (2020), Al Anazi's study (2020), and Ajam's study (2018), and its design is as follows:

- A. Questionnaire: The current study used a questionnaire consisting of two sections:
 - 1) The first section: data related to the study sample members, that is: personal data related to describing the study sample, which are:
 - i. Gender
 - ii. Qualification
 - iii. Job experience
 - iv. Job
 - 2) The second section: consists of (25) phrases, divided into five dimensions as follows:
 - i. First dimension: applying fuzzy logic systems. It consists of (5) phrases.

- ii. Second dimension: Application of expert systems and consists of (5) phrases.
- iii. Third dimension: Application of neural network systems and consists of (5) phrases.
- iv. Fourth dimension: The role of artificial intelligence in quick decision-making. It consists of (5) phrases.
- v. Fifth dimension: Challenges of applying artificial intelligence. It consists of (5) phrases.

21. Standardization of the study tool - Psychometric Properties

- Apparent validity (validity of arbitrators):

The tool was presented to a number of (9) faculty members to express their opinion on the validity of the tool and its relationship to the variables of the study, the extent to which the tool's items match what it measures, as well as the scientific validity of the terms and concepts used and linguistic validity. The items were presented to a number of faculty members in the Department of Administration, and some of them modified the wording of some phrases and deleted others. An agreement rate of no less than (80%) was relied upon.

- Content validity (logical validity):

This was verified by:

- Reviewing literature, books, previous studies and research, and theoretical frameworks that dealt with the variables of the study in general.
- Analyzing these references and studies; This is to reach the dimensions and expressions that are related to the problem of the study.

Internal Consistency:

First: Measuring Correlation Coefficients.

To measure the reliability of the tool, the researcher calculated the reliability coefficients for the tool by applying it to a survey sample consisting of (30) doctors, nursing staff, and technical and administrative staff in government hospitals in Al Madinah Al Munawarah in Kingdom of Saudi Arabia. It was chosen randomly by calculating the correlation coefficient between each statement and the total score of the dimension it follows, as follows:

The first dimension: applying fuzzy logic systems (5 phrases)

Table (6)

Values of correlation coefficients between each statement of the first dimension: applying fuzzy logic systems with the total score

Paragraph No.	first dimension: applying fuzzy logic systems	Correlation coefficient
1	Fuzzy logic systems are used within government hospitals for decision-making.	0.652**
2	Government hospitals use fuzzy logic systems to process data that cannot be processed through traditional computer programs.	0.632**
3	Fuzzy logic systems are used within government hospitals in several fields.	0.674**
4	Fuzzy logic systems are used in government hospitals in combination with artificial intelligence applications such as expert systems.	0.628**
5	Fuzzy logic systems are used within government hospitals as advanced information systems that help in decision-making.	0.696**

Significant at a significance level of 0.01 **

Significant at a significance level of 0.05*

It is clear from Table (6) that the correlation coefficients between the items in the first dimension and the total score for the dimension were all positive and statistically significant,

with medium and high values. It is also clear from the previous table that the (correlation) values between each of the first dimension’s phrases and the total score for the dimension ranged between (0.628) and (0.696), which are good correlation coefficients from which the researcher concludes that they are true to what they were designed to measure, and that they are significant at level (0.01), as well as being statistically significant. This indicates that the dimension of “applying fuzzy logic systems” has a high validity. Therefore, this result demonstrates the validity of the dimension items and its validity for field application.

The second dimension: application of expert systems.

Table (7)

Values of correlation coefficients between each statement of the second dimension: application of expert systems with the total score for the dimension

Paragraph No.	Second dimension: applying expert systems	Correlation coefficient
1	Government hospitals use expert computer systems to improve the decision-making process.	0.741**
2	Government hospitals rely on expert computer systems to solve various problems.	0.689**
3	Government hospitals rely on expert computer systems to acquire skills and knowledge in areas that help in decision-making.	0.617**
4	Government hospitals base their thinking processes on expert computer systems, and are not limited only to providing information.	0.614**
5	Expert systems contribute to modeling human experience in problem solving and decision-making.	0.639**

Significant at a significance level of 0.01 **

Significant at a significance level of 0.05*

It is clear from Table (8) that the correlation coefficients between the items in the second dimension and the total score of the dimension were all positive and statistically significant, with medium and high values. It is clear from the previous table that the (correlation) values

between each statement of the second dimension and the total score for the dimension ranged between (0.614) and (0.741), which are good correlation coefficients from which the researcher concludes that they are true to what they were designed to measure, and that they are significant at level (0.01).), as well as being statistically significant. This indicates that the “Application of Expert Systems” dimension has a high validity, and accordingly, this result demonstrates the validity of the dimension’ paragraphs and its validity for field application.

Table (8)

Values of correlation coefficients between each statement of the third dimension: applying neural network systems with the total score for the dimension

Paragraph No.	Third dimension: neural networks system application	Correlation coefficient
1	Neural networks help government hospitals upload enormous information.	0.661**
2	Government hospitals use neural networks to create workflows through which they process information.	0.687**
3	Government hospitals rely on neural networks for their ability to derive information from complex data.	0.617**
4	Government hospitals use neural network systems to excel in learning.	0.683**
5	Neural networks provide government hospitals with multiple options.	0.674**

Significant at a significance level of 0.01 **

Significant at a significance level of 0.05*

It is clear from Table (7) that the correlation coefficients between the items in the third dimension and the total score of the dimension were all positive and statistically significant, with medium and high values. It is also clear from the previous table that the (correlation) values between each of the third dimension's phrases and the total score for the dimension ranged between (0.617) and (0.687). These are good correlation coefficients from which the researcher concludes that they are true to what they were designed to measure, and that they are significant at level (0.01), in addition to being statistically significant, which indicates that the dimension of "Application of Neural Network Systems" has a high validity. Therefore, this result demonstrates the validity of the dimension items and its validity for field application.

Values of correlation coefficients between each of the phrases of the fourth dimension: The role of artificial intelligence in quick decision-making with the total score for the dimension

Paragraph No.	Fourth dimension: role of artificial intelligence in quick decision-making	Correlation coefficient
1	Artificial intelligence contributes to providing quick information that contributes to speedy decision-making.	0.624**
2	Artificial intelligence can be used to diagnose some medical conditions, which allows the appropriate action to be taken quickly for the patient.	0.643**
3	Artificial intelligence contributes to transferring sufficient realistic expertise, in cooperation with the largest international hospitals, to government hospitals in the Kingdom.	0.609**
4	Artificial intelligence allows government hospitals in the Kingdom to keep pace with medical developments and administrative work, which helps in determining the most appropriate decisions when providing services.	0.637**
5	Artificial intelligence allows the provision of all information about the history of various diseases and methods of treatment, and a quick answer to any information needed by the medical staff, which contributes to the speed of making the appropriate decision.	0.641**

Significant at a significance level of 0.01 **

Significant at a significance level of 0.05*

It is clear from Table (9) that the correlation coefficients between the items in the fourth dimension and the total score of the dimension were all positive and statistically significant, with medium and high values. It is clear from the previous table that the (correlation) values between each of the phrases of the third dimension and the total score of the dimension ranged between (0.609) and (0.643). These are good correlation coefficients from which the researcher concludes that they are true to what they were designed to measure, and that they

are significant at level (0.01), in addition to being statistically significant, which indicates that the dimension of “Application of genetic algorithm systems” has a high validity. Therefore, this result demonstrates the validity of the dimension items and its validity for field application.

Table (10)

Values of correlation coefficients between each statement of the fifth dimension: Challenges of applying artificial intelligence in Saudi hospitals with the total score for the dimension

Paragraph No.	Fifth dimension: Challenges of applying artificial intelligence in Saudi hospitals	Correlation coefficient
1	Infrastructure needs strong technological updates.	0.624**
2	New technologies face resistance from some medical or administrative staff due to lack of confidence in modern technological systems.	0.639**
3	Hospitals face legal or regulatory restrictions in using smart technologies in healthcare.	0.618**
4	Strict procedures are followed to maintain privacy and security to preserve medical data and personal information of patients.	0.698**

5	The application of artificial intelligence requires training medical and technical personnel to use new technologies.	0.634**
---	---	---------

Significant at a significance level of 0.01 **

Significant at a significance level of 0.05*

It is clear from Table (7) that the correlation coefficients between the items in the third dimension and the total score of the dimension were all positive and statistically significant, with medium and high values. It is also clear from the previous table that the (correlation) values between each of the third dimension's phrases and the total score for the dimension ranged between (0.618) and (0.698). These are good correlation coefficients from which the researcher concludes that they are true to what they were designed to measure, and that they are significant at level (0.01), in addition to being statistically significant, which indicates that the dimension of "Challenges of applying artificial intelligence in Saudi hospitals" has a high validity. Therefore, this result demonstrates the validity of the dimension items and its validity for field application.

22. Structural Validity of the Dimensions:

Table No. (11) shows the correlation values between the average of each dimension with the total average of all the dimension phrases, which shows that the correlation values have a good meaning and are significant at the significance level (0.01).

Table (11)

Values of correlation between each dimension of the questionnaire with the total score of the questionnaire phrases

S	Dimension	Correlation coefficient
1	Application of fuzzy logic systems	0.674**
2	Application of expert systems	0.682**
3	Application of neural network systems	0.649**
4	The role of artificial intelligence in speed of decision-making	0.693**
5	Challenges of applying artificial intelligence	0.678**

Significant at a significance level of 0.01 **

Significant at a significance level of 0.05*

It is clear from Table (11) that the correlation coefficients between the items in the first dimension and the total score for the dimension were all positive and statistically significant, with medium and high values. It is also clear from the previous table that the (correlation) values between all the scores of the first dimension, the second dimension, the third dimension, the fourth and fifth dimension, and the total score of the dimensions ranged between (0.649) and (0.693). These are good correlation coefficients from which the researcher concludes that they are true to what they were designed to measure, and that they are significant at level (0.01), in addition to being statistically significant, which indicates that the dimensions of the study have a high validity. Therefore, this result demonstrates the validity of the dimension items and its validity for field application.

Questionnaire Reliability:

The reliability of the study tool means that the tool will give the same results when applied multiple times to the same sample. This means to what degree the study tool will give close readings each time it is used, and it means ensuring that the response will be approximately the same if it is repeatedly applied to different people at different times.

Alpha Chronbach coefficient was used to verify the study tool, and Table (12) shows the values of the Cronbach Alpha reliability coefficients for each dimension of the questionnaire, which is shown in the following table:

Table (12)
Reliability coefficient (Cronbach's alpha) for the study dimensions

S	Dimension	No. of phrases	Cronbach's alpha
1	Application of fuzzy logic systems	5	0.889
2	Application of expert systems	5	0.878
3	Application of neural network systems	5	0.863
4	The role of artificial intelligence in speed of decision-making	5	0.891
5	Challenges of applying artificial intelligence	5	0.896

It is clear from the previous table that the reliability coefficients are high, ranging between (0.863) and (0.896), and from these values it is clear that the questionnaire is characterized by a high degree of reliability that the researcher is reassured about when applying it to the study sample.

Table (9)
Estimate of the average percentage of response for the two dimensions

Average	Average %	Estimate degree
From 1 to less than 1.8	20% to less than 36%	Very low
From 1.8 to less than 2.6	36% to less than 52%	Low
From 2.6 to less than 3.4	52% to less than 68%	Medium
From 3.4 to less than 4.2	68% to less than 84%	High
From 4.2 to less than 5	From 84 to 100%	20% to less than 36%

23. Study Results, Interpretation and Discussion

Introduction:

The researcher addresses the questions related to the study, with a review of the most important results that emerged through the application of the study tool (the questionnaire), especially from the analysis of its paragraphs. To identify the effect of artificial intelligence applications on quick decision-making in government hospitals in Al Madinah Al Munawarah, then verify the hypotheses of the study to know this role with the variables of the study, which are: -

- 1- Gender
- 2- Academic qualification
- 3- Experience
- 4- Jobs

24. Analysis and Interpretation of the Study Results:

1. What is the effect of artificial intelligence applications on quick decision-making in government hospitals in Al Madinah Al Munawarah?
2. What is the reality of applying fuzzy logic systems that affect quick decision-making in government hospitals in Kingdom of Saudi Arabia?
3. What is the reality of implementing expert systems that affect quick decision-making in government hospitals in Kingdom of Saudi Arabia?
4. What is the reality of applying neural network systems that affect quick decision-making in government hospitals in Kingdom of Saudi Arabia?
5. What is the role of artificial intelligence on quick decision-making in government hospitals in Kingdom of Saudi Arabia?
6. What are the challenges of applying artificial intelligence technologies that affect quick decision-making in government hospitals in Kingdom of Saudi Arabia?
7. Are there statistically significant differences at the level of significance ($\alpha = 0.05$) due to the variables (gender - academic qualification - years of experience - job)?

Therefore, the researcher here addresses the answer to the questions related to the field study, while reviewing the most important results that emerged through the application of the study tool (the questionnaire), especially from the analysis of its paragraphs. Therefore, statistical treatments were carried out on the data resulting from applying the questionnaire

to the study sample, where the researcher used the Statistical Packages for the Social Studies (SPSS) program to obtain the study findings. To interpret the study findings and estimate the level of responses, the researcher relied on a five-point Likert scale, considering that the maximum score corresponds to the relative weight (100%). He also used statistical treatments for arithmetic means, standard deviations, frequencies, and ratios

First: Displaying the Results

First: Results related to the first dimension, applying fuzzy logic systems

Table (13) Arithmetic means and standard deviations for the application of fuzzy logic systems dimension

Paragraph No.	Phrases	Weight average	SD	%	Degree	Rank
1	Fuzzy logic systems are used within government hospitals for decision-making.	2.05	0.578	%41.0	Low	5
2	Government hospitals use fuzzy logic systems to process data that cannot be processed through traditional computer programs.	2.91	0.288	%58.2	Medium	1
3	Fuzzy logic systems are used within government hospitals in several fields.	2.2	0.718	%44.0	Low	4
4	Fuzzy logic systems are used in government hospitals in combination with artificial intelligence applications such as expert systems.	2.73	0.66	%54.6	Medium	3

5	Fuzzy logic systems are used within government hospitals as advanced information systems that help in decision-making.	2.74	0.437	%54.8	Medium	2
Total degree		2.527	0.2669	50.5%	Low	

It is clear from the previous table that the total score for the dimension “Application of fuzzy logic systems” came with an average of (2.26), with a percentage of (50.5%), which is a low percentage according to the study tool. Phrase No. (2) states that “government hospitals use fuzzy logic systems to process data that cannot be processed through traditional computer programs”. This phrase came in ranked No. (1) as the highest ranking in the averages with an average percentage of (2.91) and a relative weight of (58.2%), while Phrase No. (1) came in the lowest ranking in the averages with a low percentage with an average of (2.05), and a relative weight of (41%), which stated, “Fuzzy logic systems are used within government hospitals for decision-making”. These results were consistent with the study of Al Anzi (2020), some of whose findings were that there is a deficiency in the application of artificial intelligence technologies in health care institutions.

Second: Results related to the second dimension:

Table (14) Arithmetic means and standard deviations for the expert systems application dimension

Paragraph No.	Phrases	Weight average	SD	%	Degree	Rank
1	Government hospitals use expert computer systems	2.93	1.155	%58.6	Medium	1

	to improve the decision-making process.					
2	Government hospitals rely on expert computer systems to solve various problems.	2.58	0.898	%51.5	Low	3
3	Government hospitals rely on expert computer systems to acquire skills and knowledge in areas that help in decision-making.	2.38	0.487	%47.6	Low	5
4	Government hospitals base their thinking processes on expert computer systems, and are not limited only to providing information.	2.52	0.572	%50.3	Low	4
5	Expert systems contribute to modeling human experience in problem solving and decision-making.	2.78	0.974	%55.6	Medium	2
Total degree		2.637	0.4779	52.7	Average	

It is clear from the previous table that the total score for the dimension “Implementing expert systems” came at an average of (2.64), with a rate of (52.7%), which is a very high percentage according to the study tool. Phrase No. (1), which states that “government hospitals use expert computer systems to improve the decision-making process”, was ranked No. (1) as the highest ranking in the averages, with an average percentage of (2.93), and a relative weight of (58.6%), while Phrase No. (3) was ranked lowest in the averages, with a low percentage with an average of (2.38), and a relative weight of (47.6%), which stated: “Government hospitals rely on expert computer systems to acquire skills and knowledge in

areas that help in decision-making”. These results were consistent with the study of Al Alwan (2020), Al Anazi (2020).

Third: Results related to the third dimension:

Table (15): Arithmetic means and standard deviations. Application of neural network systems

Paragraph No.	Phrases	Weight average	SD	%	Degree	Rank
1	Neural networks help government hospitals upload enormous information.	1.38	0.485	%27.5	Very low	5
2	Government hospitals use neural networks to create workflows through which they process information.	2.40	0.574	%48.0	Low	3
3	Government hospitals rely on neural networks for their ability to derive information from complex data.	2.37	0.483	%47.4	Low	4
4	Government hospitals use neural network systems to excel in learning.	2.82	0.485	%56.4	Medium	1
5	Neural networks provide government hospitals with multiple options.	2.67	0.470	%53.5	Medium	2
Total degree		2.328	0.2241	46.6%	Low	

It is clear from the previous table that the total score for the dimension “Application of Neural Network Systems” came with an average of (2.33), with a percentage of (46.6%), which is a low percentage according to the study tool. Phrase No. (4) stated that “government

hospitals use neural network systems to excel in learning”. Ranked No. (1) as the highest ranking in the averages with an average percentage of (2.82) and a relative weight of (56.4%), while Phrase No. (5) came in the lowest ranking in the averages with a very low percentage with an average of (1.38), and a relative weight of (27.5%), which stated: “Neural networks help government hospitals download enormous information”. These results were consistent with a study Alwan (2020).

Fourth: Results related to the fourth dimension: The role of artificial intelligence on quick decision-making

Table (15): Arithmetic means and standard deviations. The role of artificial intelligence on quick decision-making

Paragraph No.	Phrases	Weight average	SD	%	Degree	Rank
1	Artificial intelligence contributes to providing quick information that contributes to speedy decision-making.	4.2	0.601	84.0%	Very high	
2	Artificial intelligence can be used to diagnose some medical conditions, which allows the appropriate action to be taken quickly for the patient.	4.39	0.592	87.8%	Very high	
3	Artificial intelligence contributes to transferring sufficient realistic expertise, in cooperation with the largest international hospitals, to government hospitals in the Kingdom.	4.16	0.670	83.2%	High	

4	Artificial intelligence allows government hospitals in the Kingdom to keep pace with medical developments and administrative work, which helps in determining the most appropriate decisions when providing services.	4.32	0.751	86.4%	Very high
5	Artificial intelligence allows the provision of all information about the history of various diseases and methods of treatment, and a quick answer to any information needed by the medical staff, which contributes to the speed of making the appropriate decision.	4.48	0.419	89.6%	Very high
Total degree		4.31	0.2705	86.2%	Very high

It is clear from the previous table that the total score for the dimension “The role of artificial intelligence on quick decision-making” came at an average of (4.31), with a percentage of (86.2%), which is a very high percentage according to the study tool. Phrase No. (5), which states that “Artificial intelligence allows the provision of all information about the history of various diseases and methods of treating them, and a quick answer to any information needed by the medical staff, which contributes to the speed of making the appropriate decision”. It was ranked No. (1) as the highest ranking in the averages, with an average percentage (4.48), and a relative weight (89.6%), while Phrase No. (3) was ranked lowest in the averages, with a high percentage with an average of (4.16), and a relative weight of (83.2%), which stated: “Artificial intelligence contributes to transferring sufficient realistic expertise, in cooperation with the largest international hospitals, to government hospitals in

the Kingdom”. These results were consistent with Saleh’s study (2022), which included among its findings the importance of the role of artificial intelligence in quick decision-making.

Fifth: Results related to the fifth dimension: Challenges of applying artificial intelligence

Table (15): Arithmetic means and standard deviations. Challenges of applying artificial intelligence

Paragraph No.	Phrases	Weight average	SD	%	Degree	Rank
1	Infrastructure needs strong technological updates.	3.99	0.584	%79.8	High	1
2	New technologies face resistance from some medical or administrative staff due to lack of confidence in modern technological systems.	3.53	0.576	%70.7	High	3
3	Hospitals face legal or regulatory restrictions in using smart technologies in healthcare.	3.14	0.483	%62.9	Medium	5
4	Strict procedures are followed to maintain privacy and security to preserve medical data and personal information of patients.	3.33	0.511	%66.6	Medium	4
5	The application of artificial intelligence requires training medical and	3.55	0.551	%71.0	High	2

	technical personnel to use new technologies.					
Total degree		3.509	0.1605	70.2%	High	

It is clear from the previous table that the total score for the dimension “Challenges of applying artificial intelligence” came at an average of (3.51), with a percentage of (70.2%), which is a high percentage according to the study tool. Phrase No. (1), which states that “the infrastructure needs strong technological updates”, was ranked No. (1) as the highest ranking in the averages, with a very high percentage with an average of (3.99), and a relative weight of (79.8%), while Phrase No. (3) came in the lowest ranking in the averages with a high percentage with an average of (3.14), and a relative weight of (62.9%), which stated: “New technologies face resistance from some medical or administrative personnel due to a lack of confidence in modern technological systems”. These results were consistent with the study of Al Sardiya (2022) and the study (Florea, & Radu, 2019), where among their results was that there are many challenges faced by regular institutions, the most important of which are resistance to change, providing information security, and also providing the necessary infrastructure for applying artificial intelligence.

Sixth: The Answer to the question: “What is the effect of artificial intelligence applications on quick decision-making in government hospitals in Al Madinah Al Munawarah?”

The researcher extracted the frequencies for each of the phrases: “What is the effect of artificial intelligence applications on quick decision-making in government hospitals in Al Madinah Al Munawarah” as follows:

Table (16): Arithmetic means and standard deviations for each dimension: “Applications of artificial intelligence”

Paragraph No.	Phrases	Weight average	SD	%	Degree	Rank
1	Application of fuzzy logic systems	2.53	0.267	50.6%	Low	5
2	Application of expert systems	2.64	0.478	52.8%	Medium	3
3	Application of neural network systems	2.56	0.160	51.2%	Low	4
4	The role of artificial intelligence on quick decision-making	4.31	0.270	86.2%	Very high	1
5	Challenges of applying artificial intelligence	3.51	0.1605	70.2%	High	2
Total degree		3.110	0.2705	62.2%	Medium	

It is clear from the previous table that the total score for the dimension on artificial intelligence applications was at an average of (3.11), with a percentage of (62.2%), which is an average percentage according to the study tool. Dimension No. (4) came in the highest ranking in the averages with a very high percentage with an average of (4.16), and a relative weight of (86.2%), and its title was “The role of artificial intelligence on quick decision-making”. It was followed by Dimension No. (5) as the second highest in the averages, with a high percentage with an average of (3.51), and a relative weight of (70.2%), which was titled: “Challenges of applying artificial intelligence, followed by dimension No. (2) in the ranking of averages with a high percentage with an average of (2.64), and a relative weight of (52.7%), which was titled “Application of expert systems”. This was followed by Dimension No. (3), which stated that “application of neural network systems” had a high percentage with an average of (2.56), and a relative weight of (51.2%). Phrase No. (3) also came in the lowest ranking in the averages, with a low percentage with an average of (2.53), and a relative weight of (50.5%), where it stated “Applying fuzzy logic systems”.

25. Summary of Study Results:

Previously, the results of the field application of the study were presented in light of the responses of the research sample, and they were processed statistically using descriptive statistics and processed with specialized statistical programs, reaching the results, their analysis and interpretation. The study findings will be presented below, and recommendations and proposals will be presented.

26. Findings of the Study:

This includes presenting the most prominent findings of the study with regard to answering the questions and achieving its objectives, as follows:

- 1- The level of application of artificial intelligence systems is still weak in government hospitals in Al Madinah Al Munawarah due to many reasons, the most important of which is the lack of sufficient training among medical staff on the various artificial intelligence systems that can be applied within government hospitals.
- 2- It also became clear that there is a confusion between the concepts of artificial intelligence and its different types that can be applied within government hospitals.
- 3- It was also clear from the results that there are many challenges that prevent the application of artificial intelligence, the most important of which is providing infrastructure, as well as adequate training for medical staff to use artificial intelligence in diagnostic, therapeutic, technical or administrative aspects alike.
- 4- There is also a fear of data security and loss of information.
- 5- There is also a lack of good legislative and executive cover governing the process of applying artificial intelligence within government hospitals.
- 6- On the other hand, it was found that artificial intelligence, from the point of view of medical staff working in government hospitals, has a great impact on the decision-making process in government hospitals. It provides a huge amount of information that contributes to making appropriate decisions at the right time, its effective role in tracking the medical history of some patients, as well as its effective role in analyzing historical and current data on some endemic diseases and epidemics, which contributes to determining effective vaccines and treatments in a proactive manner.

27. Recommendations:

1. **Providing training and education:** Doctors, nurses and medical staff should be given opportunities to train in the use of smart technologies. This could include educational courses and workshops to understand how AI can be used to improve healthcare and streamline medical processes.
2. **Developing technological infrastructure:** Government hospitals must be equipped with the necessary infrastructure to accommodate artificial intelligence technologies, such as robust and secure computer systems and networks, and robust and secure data systems.
3. **Investing in cloud-based AI solutions:** Cloud computing can be beneficial for government hospitals that want to implement smart technology, as they can gain access to greater and more effective AI services without the need for large investments in infrastructure.
4. **Focus on security and privacy:** AI systems in hospitals must be highly protected and adhere to the highest standards of medical security and privacy.
5. **Continuous evaluation and improvement:** Continuous evaluation of AI applications is essential to ensure their efficiency and effectiveness. There must be mechanisms to measure the impact of the use of smart technologies on the quality of care and the efficiency of operations.
6. **Strengthening communication and partnerships:** Government hospitals can benefit from cooperation with technology companies and academic bodies to develop and improve artificial intelligence applications in health care. Implementing artificial intelligence in government hospitals requires a strategic vision and multifaceted efforts to ensure its effective integration within the healthcare environment.

28. Proposed Research

1. Studying the impact of applying artificial intelligence on improving the quality of health care within government hospitals.
2. Conducting studies on the financial and health costs and benefits of artificial intelligence applications in government hospitals.

3. Studying the effect of artificial intelligence on the experience of patients and patients, and its role in improving the patient experience within government hospitals.

29. References

-Arabic References

- [1] Ajam, Ibrahim Mohammad Hassan (2018), Artificial Intelligence and its Implications for High-Performing Organizations: An exploratory study in the Ministry of Science and Technology, Journal of Management and Economics, Al Mustansiriya University - College of Management and Economics, vol. 41, no. 115, 88-102.
- [2] Al Anazi, Saad Hamoud Saad Al Shamlani (2020), The Effect of artificial Intelligence on the Performance of Organizations: A Case Study of the Primary Health Care Corporation in the State of Qatar, Master's Thesis, Al Ahliyya Amman University - College of Business.
- [3] Al Sardiya, Heba Sobh Sadhan (2022), The degree to which school principals in Mafraq Governorate use artificial intelligence applications and their relationship to the quality of administrative decision-making, Master's thesis, Al Bayt University, College of Educational Sciences - Jordan.
- [4] Al Shaer, Adly Dawoud Mohammad (2007). Obstacles to implementing strategic planning among government school principals in the Gaza governorates. Gaza. College of Education. Islamic University.
- [5] Alwan, Jaafar Ahmed Abdul Karim (2020), Artificial Intelligence and Crisis Management: A Case Study of the COVID-19 Pandemic Crisis, Public Administration, Institute of Public Administration, S60, Special Issue, 931-979.
- [6] Qureshi, Ahmed (2020), Numerical Linear Programming as a tool to aid decision-making: A case study of Tablat Hospital - Medea, Journal of the Institute of Economic Sciences, Volume 23, No. 2, University of Algiers 3 - Faculty of Economic Sciences, Commercial Sciences and Management Sciences, 869 - 889.
- [7] Saleh, Osama Saleh Abdel Azim (2022), Proposed procedures for developing the decision-making process in educational departments using expert systems as one of the applications of artificial intelligence, Journal of Research in Education and Psychology, Minya University - Faculty of Education, vol. 37, no. 2, 425-454.

-Foreign References

- [1] Yeh, C., & Santagata, R. (2015). Preservice teachers' learning to generate evidence-based hypotheses about the impact of mathematics teaching on learning. *Journal of Teacher Education*, 66(1), 1-14.
- [2] Eguchi, A. (2016). RoboCupJunior for promoting STEM education, 21st century skills, and technological advancement through robotics competition. *Robotics and Autonomous Systems*, 75, 692–699.
- [3] Florea, A. M., & Radu, S. (2019). Artificial intelligence and education. In 2019 22nd international conference on control systems and computer science (CSCS) (pp. 381–382). IEEE.
- [4] Peters, M. A. (2018). *Deep learning, education and the final stage of automation*. Taylor & Francis.
- [5] Pliakos, K., Joo, S.-H., Park, J. Y., Cornillie, F., Vens, C., & Van den Noortgate, W. (2019). Integrating machine learning into item response theory for addressing the cold start problem in adaptive learning systems. *Computers & Education*, 137, 91–103
- [6] Star_ci_c, A. I. (2019). Human learning and learning analytics in the age of artificial intelligence. *British Journal of Educational Technology*, 50(6), 2974–2976.
- [7] Tang, K. Y., Chang, C. Y., & Hwang, G. J. (2021). Trends in artificial intelligencesupported e-learning: A systematic review and co-citation network analysis (1998- 2019). *Interactive Learning Environments*. <https://doi.org/10.1080/10494820.2021.1875001>
- [8] Tegmark, M. (2017). *Life 3.0: Being human in the age of artificial intelligence* (Knopf).
- [9] UNESCO. (2019). *Artificial Intelligence in education: Challenges and opportunities for sustainable development*. France: The United Nations Educational, Scientific and Cultural Organization (UNESCO) <https://en.unesco.org/news/challenges-andopportunities-artificiAl intelligence-education>.
- [10] Ayre, C., & Scally, A. J. (2013). Critical values for Lawshe's content validity ratio: Revisiting the original methods of calculation. *Measurement and Evaluation in Counseling and Development*, 47(1), 79-86. doi:10.1177/0748175613513808

- [11] S. Russell and P. Norvig (2009) “Artificial Intelligence: A Modern Approach”, Prentice Hall, 3rd edition.
- [12] Laird, J.E., Newell, A., & P.S. Rosenbloom. (1987). Soar: An architecture for general intelligence. *Artificial Intelligence*, 33, 1-64.
- [13] European Commission (2018). Communication from the Commission to the European Parliament, the European Council, the Council, the European Economic and Social Committee and the Committee of the Regions on Artificial Intelligence for Europe, Brussels, 25.4.2018 COM (2018) 237 final.

Design and Implementation of a Simulator of The Micro-Electromagnetic Generator Used to Power Medical Devices Implanted in The Human Body

Abdulkarim Almuhammad*, Mohanad Alrasheed*

*Computer Engineering Dept., Faculty of Informatic, Ittihad Private University, Aleppo, Syria.

Abstract: The issue of obtaining sustainable energy to power small electronic devices that are difficult to power with batteries is considered one of the important research topics, such as Biomedical Implants, as it depends on the nature of these devices in order to power them themselves, noting that most of these devices are located in a vibrating medium, and thus energy can be secured. It has a micro-generator that converts ambient energy into electrical energy that is used to charge a small battery installed on the device implanted within the human body. Micro-electromagnetic generators are considered one of the most important types that convert vibration energy into electrical energy used to charge a battery. In this research paper, we conducted a theoretical study of the micro-electromagnetic generator, and deduced its mathematical equations, leading to the final model that links the vibrations to the generated voltage. This model was later modeled and simulated using MATLAB/SIMULINK, and we designed and implemented an emulator circuit for the generator that uses a dsPIC digital signal processor through which parameters can be adjusted via an interactive GUI interface to obtain the output of the micro-generator similar to the real one, with the aim of using it later in research into developing collection systems. Energy for Biomedical Implants. Finally, we applied practical designs of micro-generators found in previous research to the simulator that we designed to ensure the accuracy of the results.

Keywords: Micro-electromagnetic, dsPIC, micro-generator, Biomedical Implants, MATLAB GUI.

تصميم وتنفيذ محاكي للمولد الكهرومغناطيسي المكروي المستخدم في تغذية الأجهزة الطبية المزروعة في جسم الانسان

الملخص: يعتبر موضوع الحصول على الطاقة المستدامة لتغذية الأجهزة الالكترونية الصغيرة التي يصعب تغذيتها بالبطاريات من المواضيع البحثية الهامة، مثل أجهزة الزرع الطبية Biomedical Implants بحيث يُعتمد على طبيعة هذه التجهيزات من أجل تغذيتها ذاتياً، بملاحظة أن معظم هذه التجهيزات موجودة في وسط اهتزازي، وبالتالي يمكن تأمين الطاقة لها من المولدات الميكروية Micro-generator التي تقوم بتحويل الطاقة المحيطة إلى طاقة كهربائية تستخدم في شحن بطارية صغيرة مركبة على الجهاز المزروع ضمن الجسم البشري.

تعتبر المولدات الكهرومغناطيسية الميكروية generatorMicro electromagnetic من أهم الأنواع التي تحول طاقة الاهتزاز إلى طاقة كهربائية تستخدم في شحن بطارية. قمنا في هذه الورقة البحثية بإجراء دراسة نظرية للمولد الكهرومغناطيسي الميكروي، واستنتاج معادلاته الرياضية وصولاً إلى الموديل النهائي الذي يربط الاهتزازات بالجهد المولد. تم فيما بعد نمذجة هذا الموديل ومحاكاته باستخدام MATLAB/SIMULINK وقمنا بتصميم وتنفيذ دارة محاكي Emulator للمولد يستخدم معالج الإشارة الرقمية dsPIC يمكن من خلاله ضبط البارامترات عن طريق واجهة تفاعلية GUI للحصول على خرج المولد الميكروي مشابه للحقيقي وذلك بهدف استخدامه فيما بعد في أبحاث تطوير أنظمة تحصيل الطاقة لأجهزة الزرع الطبية Biomedical Implants. وأخيراً قمنا بتطبيق تصاميم عملية لمولدات ميكروية موجودة في أبحاث سابقة على المحاكي الذي قمنا بتصميمه للتأكد من دقة النتائج.

1.Introduction:

Developing and improving the output of the direct rectifier lever switch requires providing an input voltage that practically simulates the output of the micro electromagnetic generator. Therefore, in this research paper, we studied the working principle of the micro electromagnetic generator, modeled and built a simulation model of the generator, and then we designed a simulator using a digital signal processor microcontroller. dsPIC based on the deduced mathematical model. We carried out the practical implementation of the simulator, and applied the designs of the micro electromagnetic generator to previous research, and we obtained results close to the results of the practical designs.

1. Micro electromagnetic generator:

The adopted micro electromagnetic generator can be represented by a permanent magnet, a damper element, a spring, and a coil, where the permanent magnet is fixed by the spring to the base of the generator body and has freedom of movement within the primary coil as shown in Figure (1) [1]. For ease of study, we considered that the vibrations occur in a plane applicable to Generator axis.

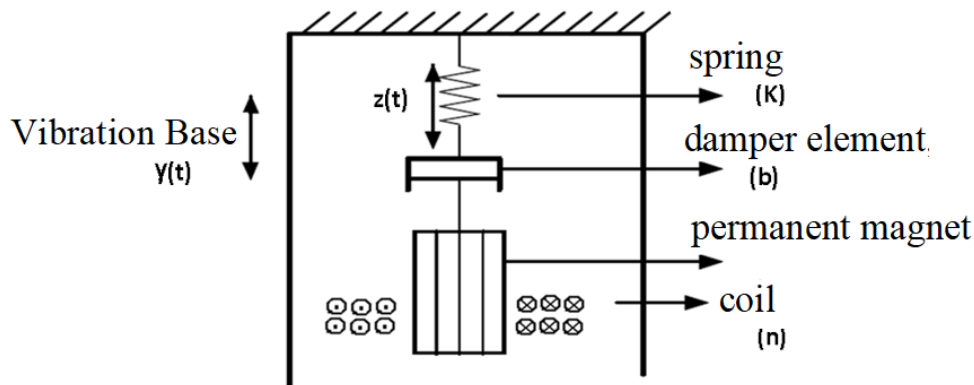


Figure 1. Micro electromagnetic generator

When the body of the generator is exposed to external mechanical vibration, the permanent magnet within the coil vibrates, and according to Faraday's law, an alternating voltage will be generated between the two ends of the coil. Its value depends on the

number of turns of the coil, the type of permanent magnet, and the strength of the vibration. The form of the generator's output voltage is sinusoidal and of the order of tens of millivolts [2][1].

2. Modeling of the micro electromagnetic generator:

The force F applied to the micro-generator causes external vibration $y(t)$, which in turn causes internal vibration $z(t)$ of the mechanical system (spring, damper element, permanent magnet). Then the mathematical model of the micro-generator can be expressed by the following differential equation (1): [3]

$$F = mz''(t) + bz'(t) + kz(t) \quad (1)$$

Where:

$m[\text{kg}]$ is the mass of the permanent magnet.

$b[(\text{N.S})/\text{m}]$ is the damping constant resulting from the sum of the mechanical damping b_m and the electrical damping b_e , i.e. $b=b_e+b_m$.

$K [\text{N/m}]$ Stiffness of spring constant. $F[\text{N}]$ The force applied to the mass and is given by the following relationship according to Newton's second law:

$$F = my''(t) \quad (2)$$

$$my''(t) = mz''(t) + bz'(t) + kz(t) \quad (3)$$

From equations (1), (2), (3) we get the following form for the generator model:

$$y''(t) = z''(t) + \left(\frac{b_m}{m} + \frac{b_e}{m}\right)z'(t) + \frac{k}{m}z(t) \quad (4)$$

For ease of modeling, we assume that the force F applied to the micro-generator generates a sinusoidal vibration $y(t)$, which is given by the following relationship:

$$y(t) = y_{\max} \sin \omega t \quad (5)$$

Where:

$y_{\max}[\text{m}]$: is the largest amplitude of vibration.

$\omega[\text{rad/s}]$: The angular frequency of vibration.

$$y''(t) = -\omega^2 y_{\max} \sin \omega t = -\omega^2 y(t) \quad (6)$$

By replacing equation (6) with equation (4), we get equation (7):

$$-\omega^2 y(t) = z''(t) + \left(\frac{b_m}{m} + \frac{b_e}{m}\right) z'(t) + \frac{k}{m} z(t) \quad (7)$$

We consider that $u(t)$ represents income and is given by equation (8):

$$u(t) = -\omega^2 y(t) \quad (8)$$

Therefore, the mathematical model of the generator becomes represented by Equation (7) according to Equation (9):

$$u(t) = z''(t) + \left(\frac{b_m}{m} + \frac{b_e}{m}\right) z'(t) + \frac{k}{m} z(t) \quad (9)$$

On the other hand, the vibration of the magnet produces an electrical force in the coil, which is given by the relationship (10):

$$e(t) = n \frac{\partial \phi}{\partial t} \quad (10)$$

Where:

ϕ [wb]: Magnetic flux resulting from the movement of a permanent magnet.

n : Number of turns of the primary coil.

By converting equation (10) to a partial derivative in terms of ∂z :

$$e(t) = n \frac{\partial \phi}{\partial z} \frac{\partial z}{\partial t} \quad (11)$$

Equation (11) can be written as follows Equation (12):

$$e(t) = C_E \frac{\partial z}{\partial t} = C_E Z' \quad (12)$$

where:

$$C_E = n \frac{\partial \phi}{\partial z} \quad (13)$$

It is a constant whose unit [SV/m] is related to the number of turns of the primary coil and the composition of the permanent magnet. The generated electrical power P_E is the result of converting the mechanical power P_m generated by work changes $w[(N.m)/S]$ during one time:

$$P_E = P_m = \frac{\partial w}{\partial t} = F_{eb} \vartheta = F_{eb} z' \quad (14)$$

Where:

$\vartheta[m/S]$: linear speed.

Note that the electrical damping force F_{eb} [N] is given by:

$$F_{eb} = b_e z' \quad (15)$$

Substituting (15) into (14):

$$P_E = b_e z' z' \quad (16)$$

On the other hand, the instantaneous electrical power is given by equation (17):

$$P_E = EI \quad (17)$$

Where:

$E[V]$ electric force generated at the output of the micro-generator.

$I[A]$ The current passing through the load connected to the output of the micro-generator.

From relations (12), (16) and (17) the electrical damping constant can be deduced:

$$b_e = \frac{C_E I}{z'} \quad (18)$$

$$I = \frac{E}{R_L} \quad (19)$$

Where:

R_L [Ω] is the resistance connected to the output of the micro-generator.

By replacing equation (19) with equation (18):

$$b_e = \frac{C_E E}{z' R_L} \quad (20)$$

Substituting E from equation (12) with equation (20):

$$b_e = \frac{C_E^2}{R_L} \quad (21)$$

By replacing equation (21) with equation (9):

$$u(t) = z''(t) + \left(\frac{b_m}{m} + \frac{C_E^2}{m R_L} \right) z'(t) + \frac{k}{m} z(t) \quad (22)$$

From equations (22) and (8), the mathematical model of the micro-generator can be represented with the diagram shown in Figure (2), where:

$$C1 = \frac{k}{m} \quad (23)$$

$$C2 = \frac{b_m}{m} + \frac{C_E^2}{m R_L} \quad (24)$$

$$A = -\omega^2 \quad (25)$$

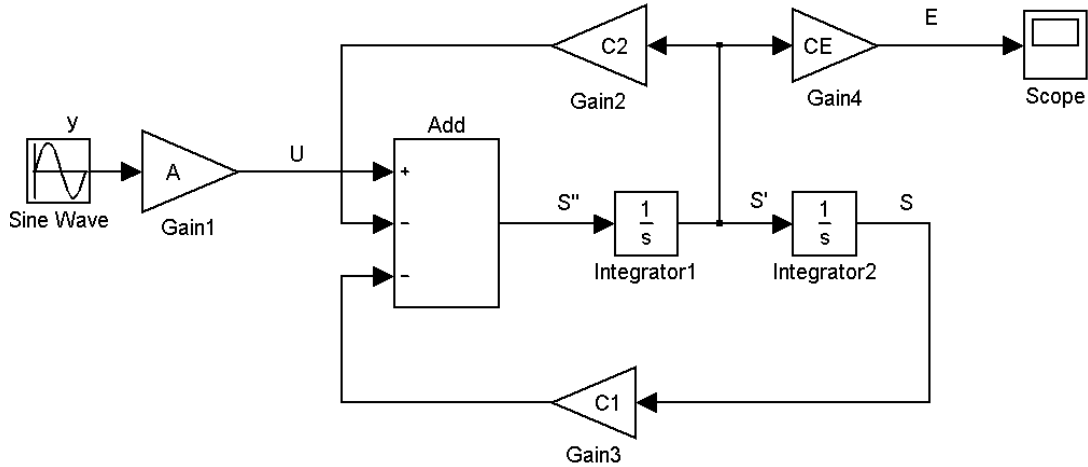


Figure 2. Box diagram of the mathematical model of the micro-generator

The transfer function can be obtained from the box diagram of the micro mathematical model shown in Figure (2) according to Equation (26):

$$H(s) = \frac{E(S)}{y(S)} = \frac{AC_E S}{S^2 + C1S + C2} \quad (26)$$

2. Frequency study of the transfer function of the micro electromagnetic generator:

In order to know the effect of the vibration provided to the generator on the gain, we will study the frequency response of the transfer function of the micro-generator, where the transfer function is given in standard form:

$$G(S) = \frac{aS}{S^2 + bS + c} \quad (27)$$

Figure (3) shows the frequency characteristic (Bode), from which the maximum value of the gain of the previous transfer function is given:

$$A_{Gmax} = \frac{a}{b} \quad (28)$$

Then the frequency is:

$$\omega_p = \sqrt{c} \quad (29)$$

Where ω_p is called the pole frequency, and it is the frequency at which the transfer function gain is maximum.

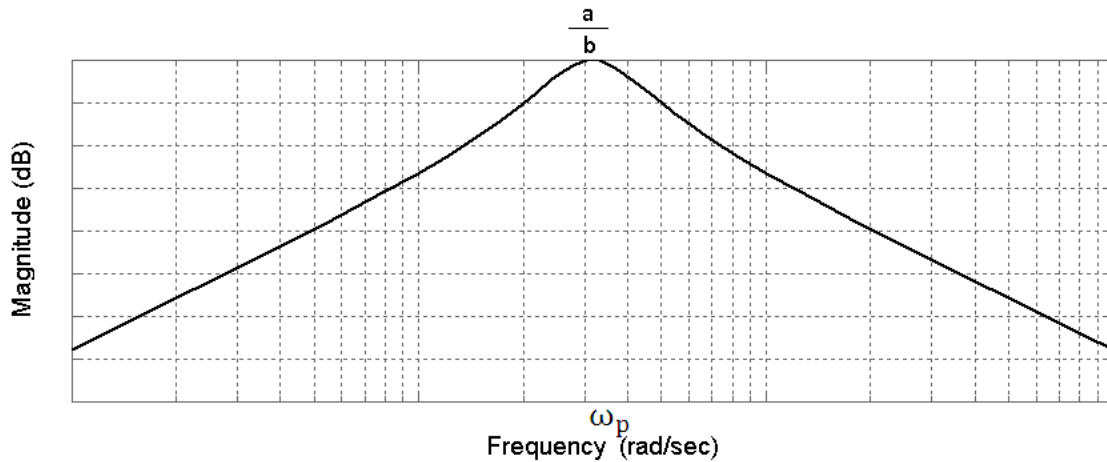


Figure 3. Bode frequency characteristic of the transmission function

By matching the transfer function of the generator given by equation (26) with the standard form equation (27), we find the values of:

$$a = AC_E \quad (30)$$

$$b = C1 \quad (31)$$

$$c = C2 \quad (32)$$

From this, the maximum value of the transfer function gain of the micro-generator is given:

$$A_{Hmax} = \frac{AC_E}{C1} \quad (33)$$

$$\omega_{Hp} = \sqrt{\frac{b_m}{m} + \frac{C_E^2}{mR_L}} \quad (34)$$

The generator output is given:

$$E = Hy \quad (35)$$

Therefore, from equations (5), (8), (33) and (35), the maximum output of the micro-generator when the vibration frequency ω_{Hp} is given by the relationship (36):

$$E_{\max} = \frac{AC_E}{C1} y_{\max} \quad (36)$$

From this, the maximum output power of the micro-generator is given:

$$P_{E\max} = \frac{E_{\max}^2}{R_L} = \frac{\left(\frac{AC_E}{C1} y_{\max}\right)^2}{R_L} \quad (37)$$

Through studying the frequency response of the transfer function, we conclude that the micro-generator has a maximum response at a certain vibration frequency. Therefore, the design values K , m , b_m , and CE must be chosen to determine the polar frequency ω_p according to the working environment of the micro-generator, based on the frequency range of mechanical vibration provided to the micro-generator.

3. Micro-electromagnetic generator simulation:

In order to simulate the mathematical model of the generator, the design values of the generator given in Table (1) were chosen [3] [4].

Table 1. Design practical values for simulating the mathematical model of the micro-generator

k	416[N/m]
m	0.005[kg]
b_m	0.00001[N.m/s]

R_L	100[Ω]
C_E	6.456[S.V/m]

By taking the practical design values of the generator from Table (1) and from equations (23) and (24), we calculate the values of the constants $C_1 = 83200$ and $C_2 = 83.3619$. For a vibration frequency of $\omega = 282.7433$ rad/sec for the input signal shown in Figure (4), the output of the micro-generator is E Shown in Figure (5) according to the simulation of the box diagram shown in Figure (2) in the Matlab environment.

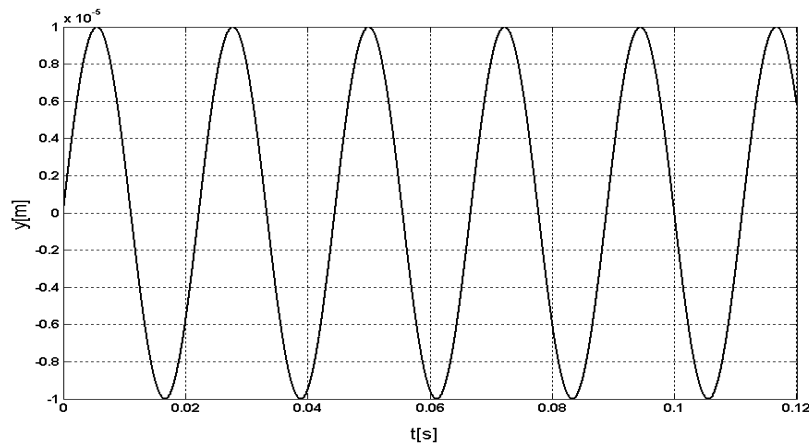


Figure 4. Microgenerator input signal

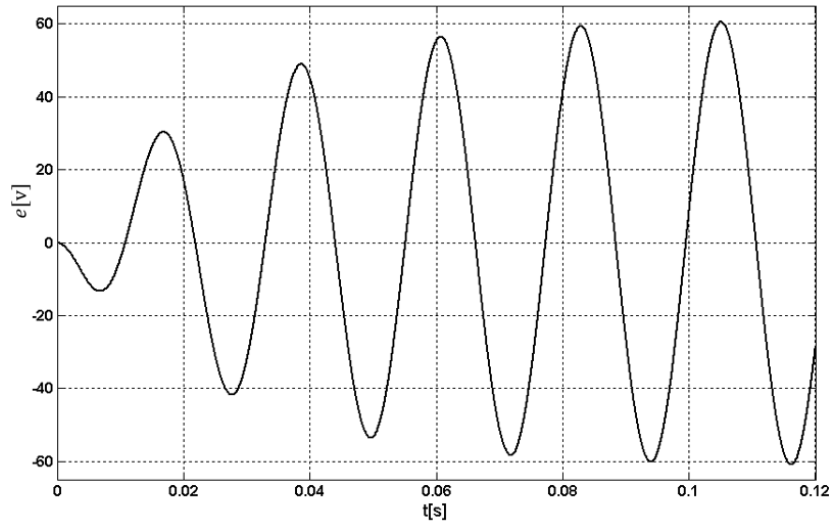


Figure 5. Microgenerator output signal

We notice from the simulation results that the amplitude of the generator output increases at the beginning of the vibration application and then stabilizes at a certain value as a result of mechanical inertia. Therefore, the energy harvesting system, the electronic part (switched), must be designed so that it tracks this change in the take-off phase to make the most of the energy provided to the micro-generator and increase the yield in particular. In an environment where the vibration provided is intermittent rather than continuous (the condition is more common).

3. Design a micro-generator simulator:

Designing a micro-generator simulator is one of the main steps in this research, as we designed a simulator circuit that uses a dsPIC digital signal processor to obtain the output of a micro-generator with certain design parameters that are entered through an interface available to the designer. The micro-generator simulator consists of the sections shown in Figure (6):[5]

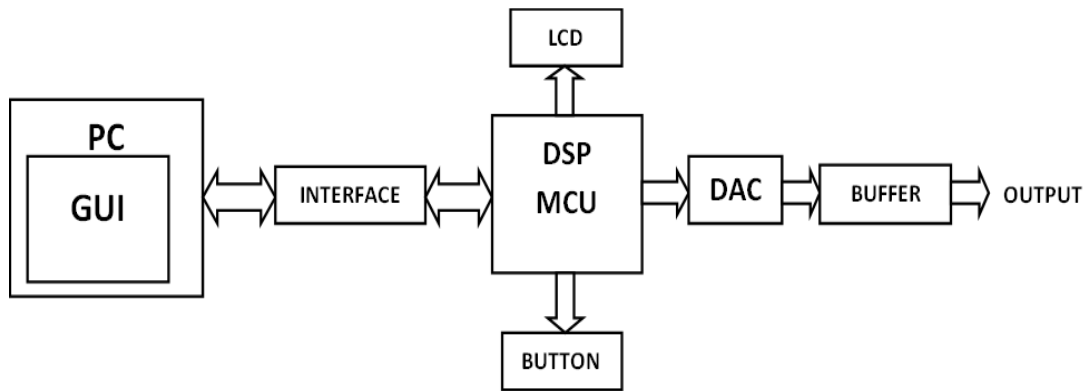


Figure 6. Block diagram of the microgenerator simulator

The work of this simulator is based on the mathematical model of the micro-generator shown in Figure (2) by mainly programming the dsPIC digital signal processor and the GUI program according to two modes of work:

- **Online mode:** In this mode, the mathematical model is simulated using dsPIC to obtain the output signal according to the requirements entered by the GUI interface. This mode is useful for studying the transient states of the micro-generator, but on the other hand, there is difficulty in changing the output parameters of the micro-generator directly.

- **Offline mode:** In this mode, the mathematical model is simulated using a GUI program according to the input parameters to obtain the parameters of the output signal, and this signal is generated by dsPIC. This mode is characterized by changing the output parameters of the micro-generator directly, but on the other hand, it is not possible to study cases through it. Trans.

The most important features of the simulator are:

- 1- It provides an easy design interface for choosing the values of the constants K, m, b_m , and CE for the micro-generator.
- 2- It allows the researcher and designer of the energy harvesting system to test and simulate his design using the MATLAB environment and practically using the simulator circuit.
- 3- It allows the vibration and amplitude to be changed in several ways, which provides a simulation of the natural environment in which the micro-generator may exist.
- 4- It provides the possibility of studying the efficiency of the energy harvesting system accurately.

The simulated system can be divided into two parts:

3.1 Hardware:

It consists of the following parts:

3.1.1 Interface connection circuit:

It is the circuit that connects the computer and a dsPIC digital signal processor in order to match the logical levels of the RS232 protocol between the COM port of the computer and the UART unit of the processor and Figure (7) the linking circuit.

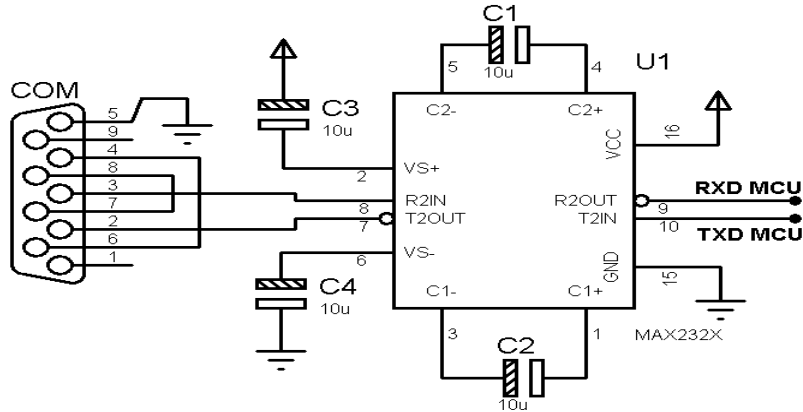


Figure 7. Interface circuit between the computer and the dsPIC digital signal processor

3.1.2 dsPIC digital signal processor circuit:

It is the main element in the simulator that generates the output signal in two modes, online or offline. The dsPIC30F3010 chip was chosen from the family of power inverters and motor control suitable for our research in terms of practical implementation because it has a high capacity in digital signal processing, as every instruction in the dsPIC digital signal processor is executed in One instruction cycle, which makes the dsPIC digital signal processor suitable for use in control systems that operate in real time, where the PWM motor control unit was used to build a digital-analogue converter (DAC) and a DSP core in order to perform mathematical operations. Figure (8) shows the digital signal processor circuit. dsPIC, where a screen is connected to show settings and working status.

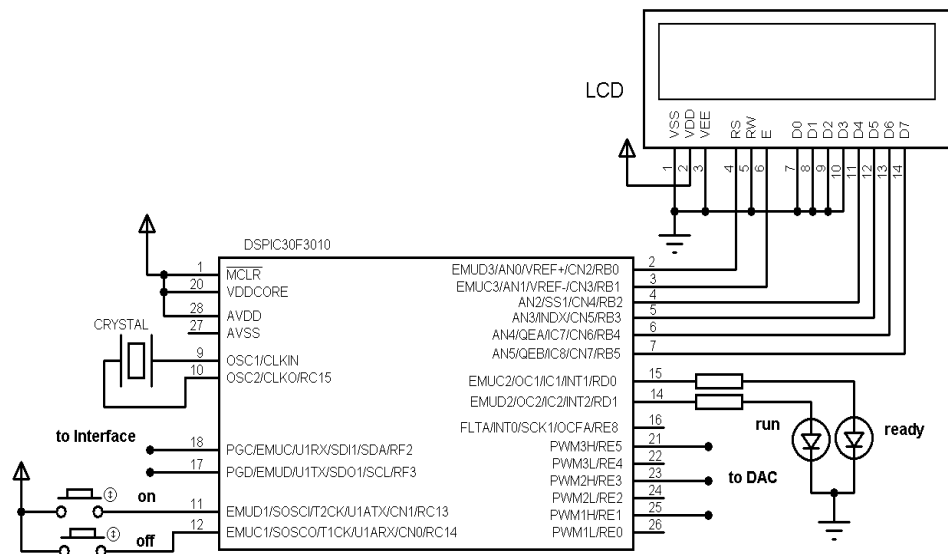


Figure 8. dsPIC digital signal processor circuit

3.1.3 DAC circuit:

Figure (9) shows the DAC circuit that we designed in order to convert the digital signal generated from the PWM ports into a signal expressing the output of the micro-generator. In this circuit, two RC low-frequency filters (PWM detector) were used with a cut-off frequency of $F_c=159\text{Hz}$, and the operational amplifier U2 combines the two part signals. The positive, negative, and U3 are for precise control of the amplitude. The transistors Q1, Q2, Q3, and Q4 are insulators on the one hand and a controller connecting the dsPIC digital signal processor and the filtering stage on the other hand.

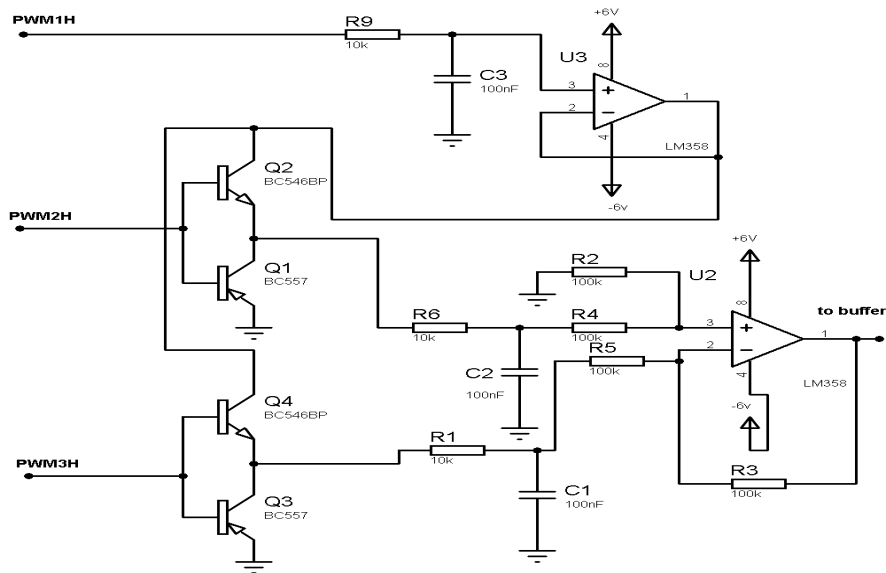


Figure 9. DAC circuit

3.1.4 Buffer circuit:

Figure (10) shows the Buffer circuit that we designed with the aim of eliminating the offset of the output voltage resulting from the inaccuracy of the elements, filters and operational amplifiers in the DAC circuit and obtaining the output voltage field of the order of millivolts, where the resistor RV1 is used to determine the output field and RV2 is used to cancel the offset of the output voltage.

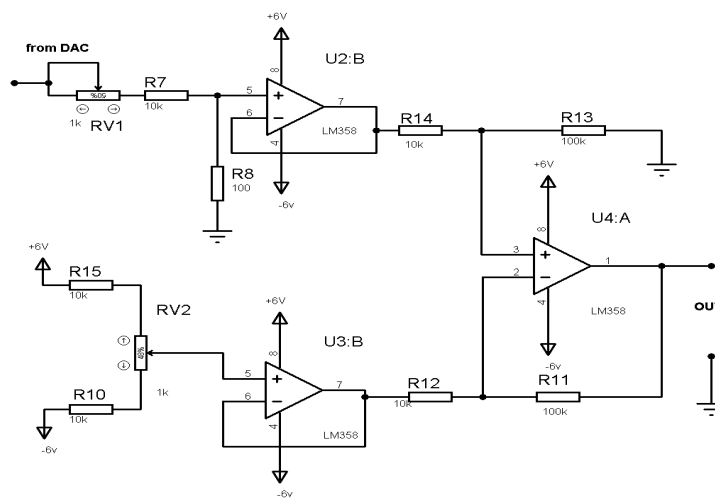


Figure 10. Buffer circuit

3.2 Software:

It consists of the following parts:

3.2.1 dsPIC digital signal processor software:

DSP instructions were used in two modes, online and offline, to achieve high speed of execution. We programmed the processor in C language using the mikroC PRO for dsPIC compiler. The program can be divided into the following parts:

- The first part: It receives parameters from the GUI program via the UART communication port at a speed of 138,000 Baud, according to the work mode and input parameters.
- The second part: It generates the micro-generator output in offline mode according to a fixed amplitude and frequency that are calculated by a GUI program according to a simulation in the MATLAB environment.
- The third part: It generates the micro-generator output in online mode based on the transfer function given in equation (27), where it is cut into a cut-off time T_s according to the backward difference method, so we get the following difference equation (38):

$$k1E(n) + k2E(n - 1) + k3E(n) = k4(y(n) - y(n - 1)) \quad (38)$$

Where: n is the sample number.

$$k1 = \frac{1}{T_s^2} + \frac{C1}{T_s} + C2 \quad (39)$$

$$k2 = \frac{-2}{T_s^2} - \frac{C1}{T_s} \quad (40)$$

$$k3 = \frac{-1}{T_s^2} \quad (41)$$

$$k4 = \frac{AKe}{T_s} \quad (42)$$

The previous constants are calculated by a GUI program through the input parameters and then sent to a dsPIC digital signal processor in order to obtain a fixed cutting time. Timer1 was used to generate an interrupt with a cutting time of $T_S=20\mu s$, which calls the interrupt service function, which calculates the output of the differential equation given by (38). We obtain the output voltage, which is converted to analog values by the PWM terminal and the DAC module.

3.2.2 GUI Program:

It is a program with a visual interface written in C language in the MATLAB environment through which the emulator is fully controlled, as it contains two visual interfaces:

- The main interface shown in Figure (11) through which the design values are entered, the results are simulated, the results are shown, and the simulated circuit is controlled.
- An interface for selecting and changing vibration parameters, shown in Figure (12), is used in offline mode only in two ways:
 - ❖ Linear, as in this method the amplitude and frequency of vibration within a field are changed linearly and with increasing value over a specific period of time.
 - ❖ Random: In this method, the amplitude and frequency of vibration within a field are changed randomly during a specific period of time.

The program performs the following tasks:

- Entering micro-generator parameters.
- Calculating the constants of the mathematical model from the microscopic input parameters according to equations (23), (24), and (25) and the discrete model according to equations (28), (29), (30), and (31).
- Simulating the micro-generator according to the mathematical model (Figure (2)) and showing the results.
- You can choose the online or offline work mode.
- Provides communication in order to transfer the constants of the mathematical model and the discrete model to the simulator circuit.

- Control the simulator circuit from turning it on and off.

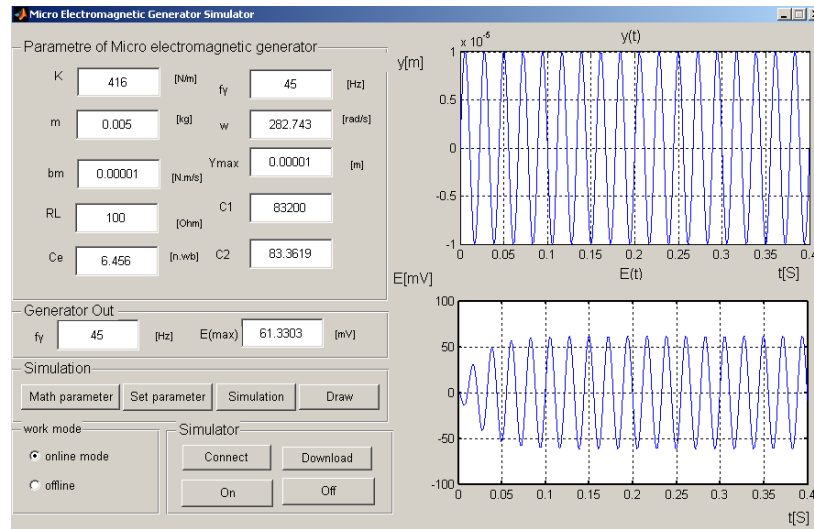


Figure 11. Main interface of the GUI program

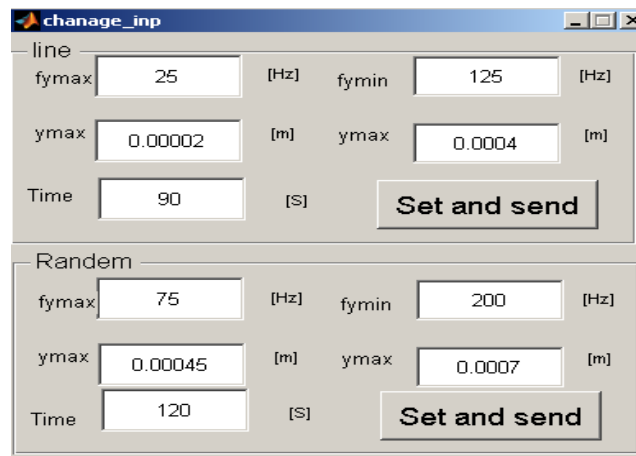


Figure 12. The interface for changing vibration parameters is used in offline mode

4. Testing and practical application of the simulator:

In order to test the simulator design, we applied two micro-electromagnetic generator designs that were implemented by previous research.

• **First design:** By applying the parameters shown in Figure (11) and practical values for the constants $c_1 = 83200$, $c_2 = 83.3619$, and $c_e = 6.456$ for the micro-electromagnetic generator (same simulation parameters for the mathematical model) that was designed by researchers Dwari, Dayal, Parsa, the practical laboratory picture of this generator is shown. Figure (13), where they applied a sinusoidal vibration with a frequency of 45 Hz from a controlled electric vibrator connected to the micro-generator with an amplitude $Y_{max} = 100\mu\text{m}$, so the maximum value of the microoutput voltage was $E_{max} = 55\text{mV}$, and using the analog signal analyzer connected to the output of the simulator circuit, we obtained the signal shown in Figure (14).) [6].

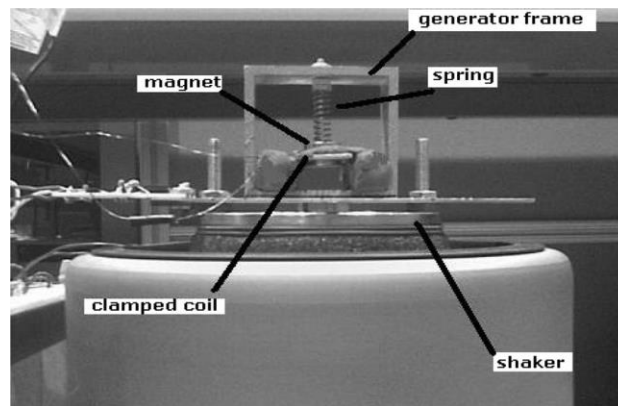


Figure 13. A practical picture of the micro-electromagnetic generator used in the simulator test

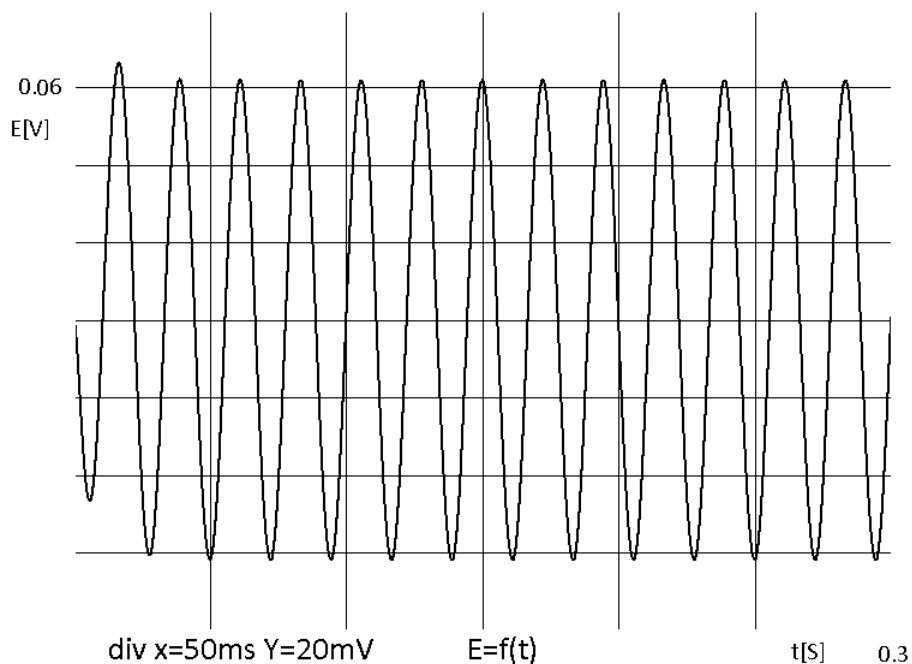


Figure 14. The output voltage of the circuit simulated for the first design of the micro-generator

We note from Figure (14) that the maximum value of the output voltage of the simulated circuit is $E_{max}=61\text{mV}$. It is close to the practical value of the designed generator.

• **The second design:** We applied the design of the micro-electromagnetic generator by researchers Cao, Chiang, Lee, with its parameters shown in Figure (15), to the simulator, where they obtained an output $E_{max}=108.89\text{mV}$ by applying a sinusoidal vibration with a frequency of 42Hz and an amplitude $Y_{max}=0.003\text{m}$. [7]

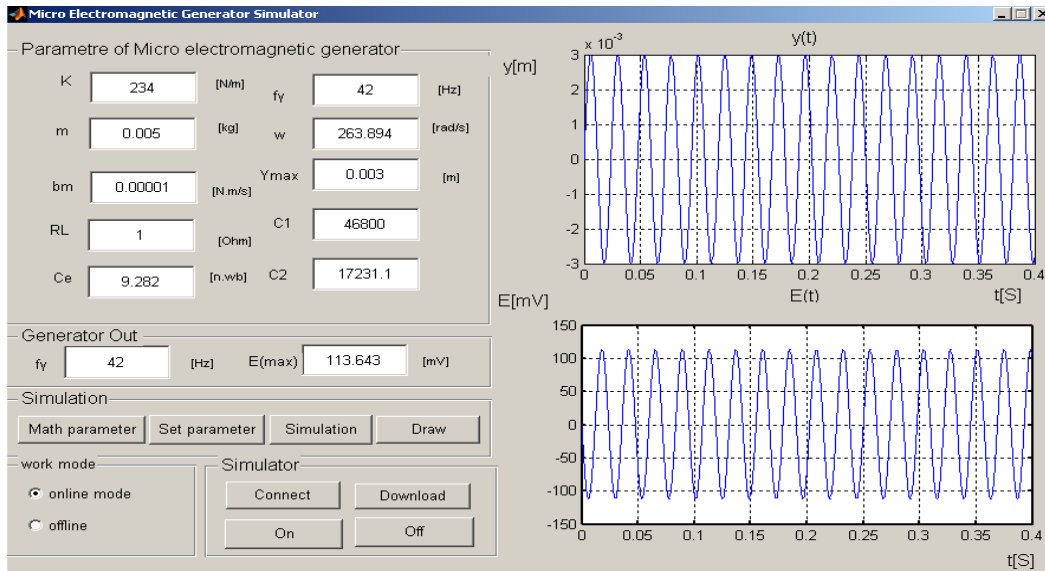


Figure 15. Parameters of the second design of the microgenerator

We note from Figure (16) the output of the simulator circuit that the maximum value of the output voltage of the simulator circuit is $E_{max}=113.6\text{mV}$, which is close to the practical value of the designed generator.

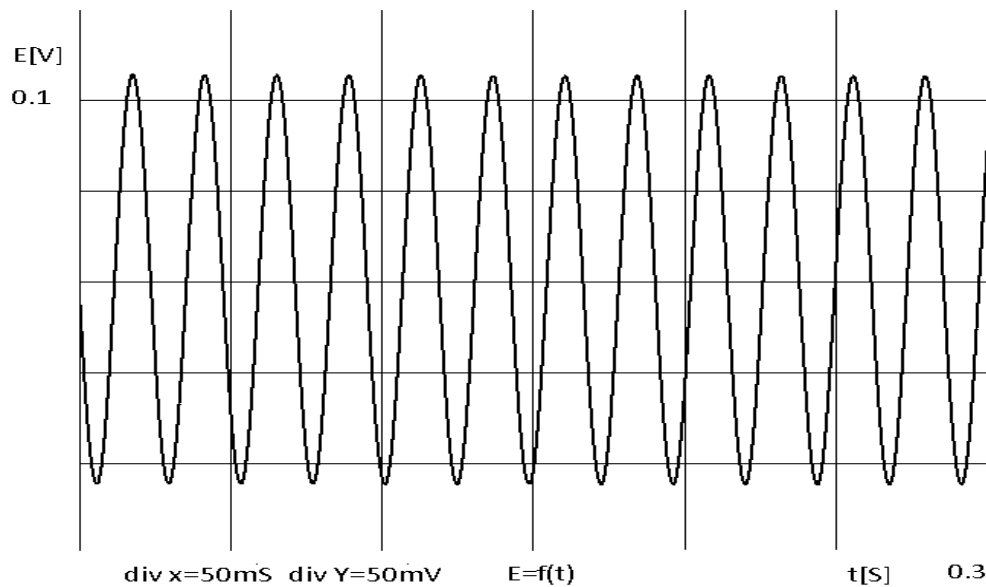


Figure 16. The output voltage of the simulated circuit for the second design of the micro-generator

5. Conclusion and discussion of results:

In this research paper, the micro-electromagnetic generator was studied, the main element in the microelectromechanical system for collecting energy from vibration. This study included the following:

- 1- Study the working principle of the micro-generator and its components.
- 2- Deducing the mathematical model of the micro-generator in several forms based on the basic mechanical and electrical equations.
- 3- Study the frequency response of the generator's transmission follower in order to know the effect of the vibration provided to the generator on the gain and output voltage and determine the best frequency for the generator to operate.
- 4- Building a simulation model in the MATLAB environment for the micro-generator.

A simulator was then designed based on the mathematical model derived using a dsPIC digital signal processor in online and offline modes (Figure 17), with the possibility of changing the amplitude and frequency of the vibration provided to the generator, which simulates the natural environments in which the microgenerator may exist.

In order to confirm the validity of the theoretical study and mathematical modeling, practical designs carried out by other researchers for the micro-generator were applied to the simulator that we designed. The practical results were close to the results of the researchers, which confirmed the validity of the theoretical study and the design of the micro-generator simulator.

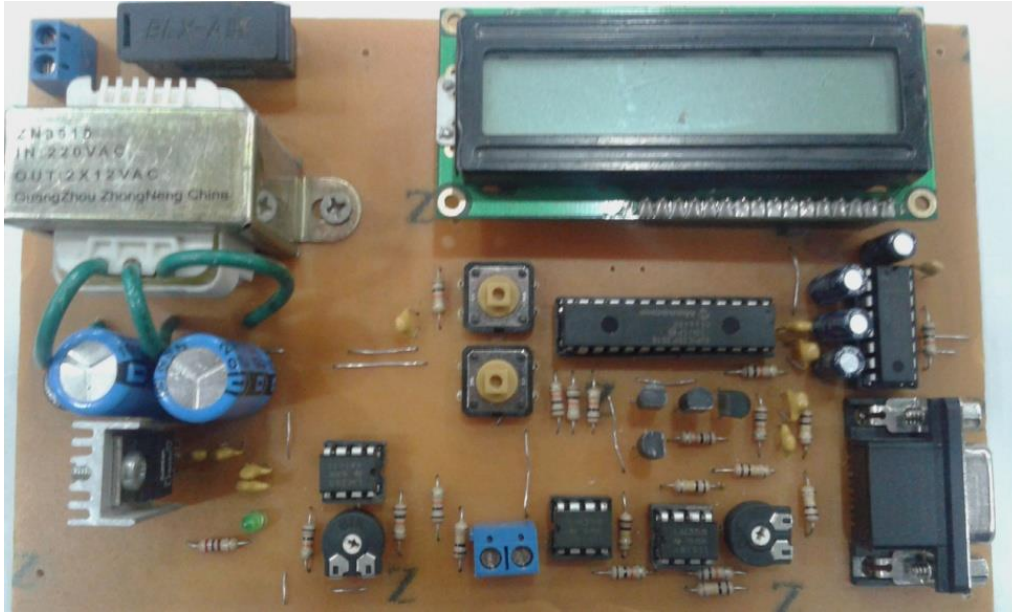


Figure 17. Practical circuit of the microgenerator simulator

References

- [1] R. Dayal, K. Modepalli and L. Parsa, “A new optimum power control scheme for low-power energy harvesting systems”, *IEEE Trans. Ind. Applic.*, vol. 49, pp. 2651-2661, 2013.
- [2] Vytautas Ostasevicius, Vytautas Markevicius , Cutting tool vibration energy harvesting for wireless sensors applications, *Sensors and Actuators A: Physical*, Volume 233, Pages 310–3181 ,September 2015.
- [3] Ji H, Qiu J, Zhu K, Badel A Two-mode vibration control of a beam using nonlinear synchronized switching damping based on the maximization of converted energy. *JSoundVib* 329(14):2751–2767 2010.
- [4] S. P. Beeby, R. N. Torah, M. J. Tudor, P. Glynn-Jones, T. O’Donnell, C. R. Saha, and S. Roy, “Micro electromagnetic generator for vibration energy harvesting,” *J. Micromech. Microeng.*, vol. 17, no. 7, pp. 1257–1265, Jul. 2007.
- [5] MICROCHIPcop.,dsPIC30FFamily Reference, 2022, <http://www.Microchip.com>.
- [6] Rohan, Dayal, Suman Dwari,, “A New Design for Vibration-Based Electromagnetic Energy Harvesting Systems Using Coil Inductance of Microgenerator” *IEEE Trans. Ind. Electron.*, vol. 56, no. 4, pp. 1101–1108, Apr. 2010.
- [7] Cao, Chiang, Lee, “Development of a Vibration-Base Electromagnetic Energy Harvester by a Conductive Direct-Write Process” *IEEE Trans. Ind. Electron*, vol. 56, no. 4, pp. 1101–1108, Apr. 2017.

Designing a Novel Algorithm for Drawing a Kappa Curve Using Bresenham's Approach

Abdulbasid Banga¹, Nadeem Iqbal², Khurram Ejaz³,

¹College of Computing and Informatics, Saudi Electronic University, Saudi Arabia

a.banga@seu.edu.sa

²Dept. of Computer Science & IT, The University of Lahore, Pakistan

nadeem.iqbal@cs.uol.edu.pk

³Dept. of Computer Science & IT, The University of Lahore, Pakistan

khurram.ejaz@cs.uol.edu.pk

Abstract: Bresenham's approach is a classical approach for developing different algorithms. It has already been applied to draw curves like lines, circles, ellipses, parabolas, and hyperbolas. Traditionally, the Kappa curve- Cartesian, parametric, and polar equations draw a mathematical curve. All these three approaches are plagued with some inherent problems. For instance, we can't isolate y from its Cartesian equation if we want to draw it on the display by using the Cartesian equation. Further, both the parametric and polar equations of the Kappa curve contain trigonometric functions which are time-consuming and, of course, run counter to the spirit of interactivity. The figure drawn through these approaches contains inter-pixel spacing. Our proposed algorithm using Bresenham's approach will avoid this spacing and hence the quality of the curve will improve.

Keywords: Kappa curve, Bresenham, pixel, algorithm.

تصميم خوارزمية جديدة لرسم منحنى كابا باستخدام طريقة بريسنهام

الملخص: يعد نهج بريسنهام بمثابة نهج كلاسيكي لتطوير خوارزميات مختلفة. لقد تم تطبيقه بالفعل لرسم منحنيات مثل الخطوط والدوائر والقطع الناقص والقطع المكافئ والقطع الزائد. تقليدياً، منحنى كابا - المعادلات الديكارتية والبارامترية والقطبية ترسم منحنى رياضياً. تعاني كل هذه الأساليب الثلاثة من بعض المشاكل المتأصلة. على سبيل المثال، لا يمكننا عزل y عن معادلتها الديكارتية إذا أردنا رسمها على الشاشة باستخدام المعادلة الديكارتية. علاوة على ذلك، تحتوي كل من المعادلات البارامترية والقطبية لمنحنى كابا على دوال مثلثية تستغرق وقتاً طويلاً، وبالطبع تتعارض مع روح التفاعل. يحتوي الشكل المرسوم من خلال هذه الأساليب على تباعد بين وحدات البكسل. سوف نتجنب الخوارزمية المقترحة لدينا باستخدام نهج بريسنهام هذا التباعد وبالتالي سنتحسن جودة المنحنى.

1. Introduction

Computer graphics lies at the intersection of computing and mathematics. Drawing different mathematical curves is a very important field of computer graphics. A lot more approaches exist to draw different curves with their pros and cons. Bresenham's approach is one of the best classical approaches to drawing different mathematical curves (Yi, Zeng et al. 2021). The main strength point of this approach is that it uses only integer arithmetic as far as calculations are concerned (Zhang, Zhang et al. 2022). It avoids the heavy calculations of finding the square roots, cube roots, trigonometric, and other transcendental functions. Of course, this avoidance is of great importance in the sense that the processing speed gets turbo-charged.

A host of mathematical curves exist, some important and some trivial. The Kappa curve is one of them (Popescu, Calbureanu et al. 2021). This curve is symmetrical about both the x-axis and y-axis. Figure 1 shows this curve. Moreover, below is its Cartesian equation:

$$y^2(x^2 + y^2) = a^2x^2 \text{-----}(1)$$

Normally, an equation is converted into explicit form by isolating the y value from the equation. But the problem inherent in this equation is that one can't separate the y value from this equation. This is the major problem to draw the curve of this equation in the computer graphics system. Our strategy will solve this problem. Other approaches also exist to draw this curve like the parametric and polar equations (Blazquez-Salcedo, Doneva et al. 2020). But they also suffer from other problems as well. First, there is an inter-pixel spacing among the different pixels drawn on the graphics system (Bhatnagar, Upadhyay et al. 2023). Further, both the parametric and polar equations contain trigonometric functions that are computationally very heavy consume a lot of precious time of the machine and run counter to the very spirit of interactivity (Mokry 2016). Our methodology will avoid all such kinds of problems.

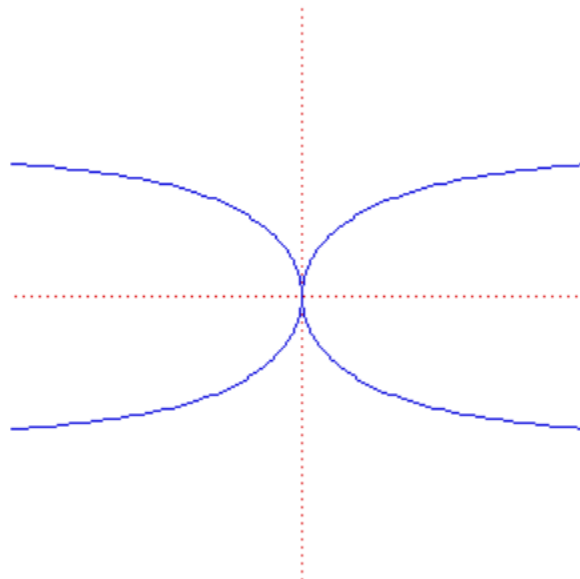


Figure 1. Kappa Curve.

2. Different Approaches for Drawing Kappa Curve

Normally there exist three equations for any curve. These are Cartesian, parametric, and polar equations. Normally, the Cartesian equation is manipulated in the way that y gets placed on the left side and all the other stuff is put on the right side. Once this has been done, the value of independent value is iterated for an arbitrary number of times and the corresponding value for the dependent value is calculated against this equation. This calculated point is drawn on the computer screen. But the problem with this equation is that we can't algebraically isolate the y value from the Cartesian equation. This is the major stumbling block to this equation. Of course, if we are willing to draw its graph on paper, the job will be done by using the symbolic manipulation of the variables but the same can't be done on the computer graphics system.

The second approach is by using the parametric equation. The parametric equations for the Kappa curve are described below:

$$\begin{cases} x = a \cos t \cot t \\ y = a \cos t \end{cases} \text{-----(2)}$$

Below is the algorithm to draw the Kappa curve by using the above equations:

Algorithm 1: Drawing of Kappa Curve Using Parametric Equations

for ($\theta \leftarrow 0$ to $\theta \leq \text{revolution}$)

$x \leftarrow a \times \cos \theta \cot \theta$

$y \leftarrow a \times \cos \theta$

drawpixel(x, y)

drawpixel($x, -y$)

end for

Figure 2 shows the output of this algorithm.

The third approach is by using the polar equation. In polar equation, there are usually two parameters, *i.e.*, r and θ . These correspondingly are called radius vector and angle.

$$r = a \cot \theta \text{ -----(3)}$$

Below is the algorithm to draw the Kappa curve by using the above equations:

Algorithm 2: Drawing of Kappa Curve Using Polar Equations

for ($\theta \leftarrow 0$ to $\theta \leq \text{revolution}$)

$r \leftarrow a \times \cot \theta$

$x \leftarrow r \times \cos \theta$

$y \leftarrow r \times \sin \theta$

drawpixel(x, y)

drawpixel($x, -y$)

end for

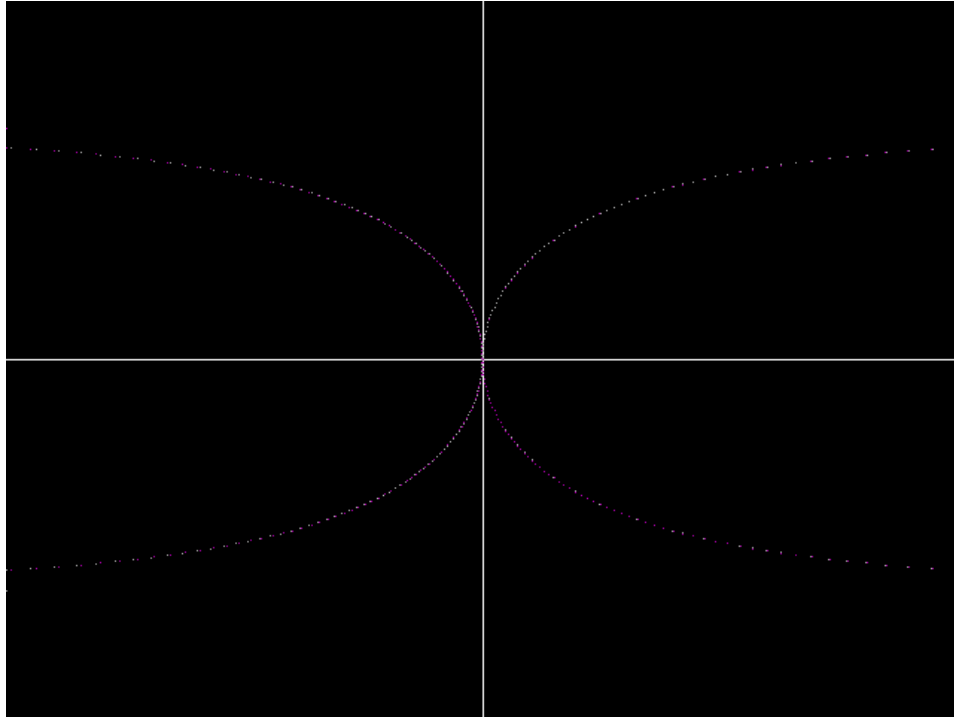


Figure 2. Kappa Curve is generated by using the Parametric Equations.

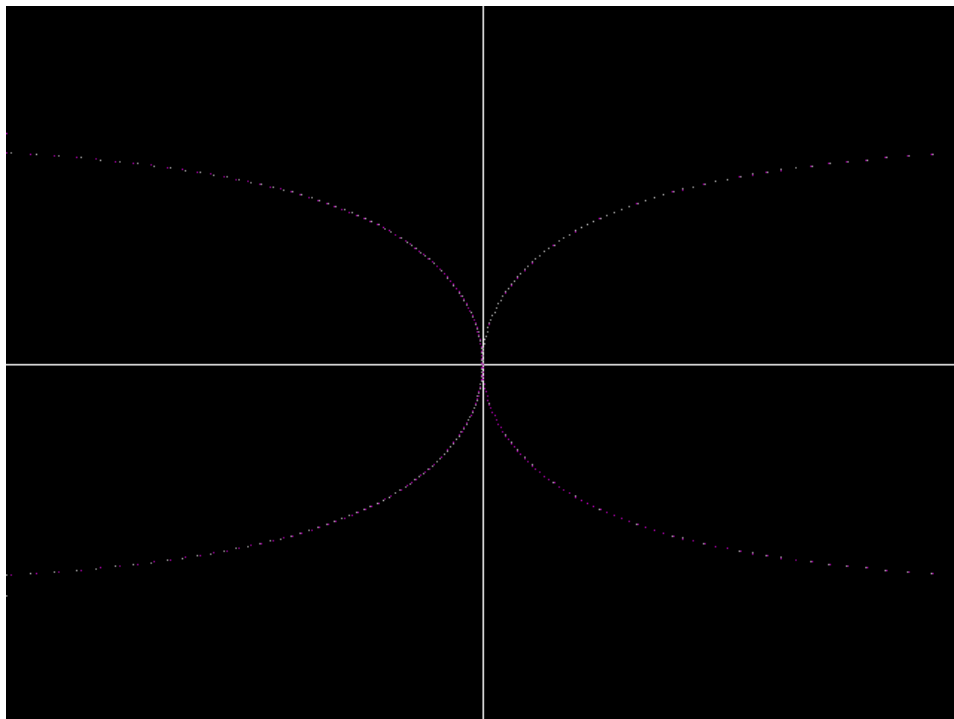


Figure 3. Kappa Curve is generated by using the Polar Equation.

3. Literature Review

In (Cao, Liu et al. 2020), four algorithms have been given namely line, circle, parabola and hyperbola. The later three are also sometimes called conic sections (Nienhaus, Smith et al. 2019). They have also incorporated antialiasing in it. One of the important features of these algorithms is that they have used only integer arithmetic. The problem with the previous approaches was that there was spacing among the pixels. Now with this new methodology, that space problem has been addressed. In yet another area, a 3D warping technique has been discussed at length in (Walia and Verma 2012). The main characteristic of this technique is that it requires small input data. Later, through the experimental results, they demonstrated that their new technique was computationally efficient. Parabola has been scan converted on hexagonal grid as well as discussed in (Prabukumar and Ray 2013). The main salient feature of their research work is that they have used the mid-point approach in their work. In this approach, a pixel closest to the real mathematical curve is chosen. The other benefit includes the visualization of the design ideas through simulation. In (Ray and Ray 2011), two new algorithms of a line have been designed using the parametric equations. The first one uses floating-point arithmetic and the second one uses integer arithmetic which is of course very efficient in the interactive settings. This work has been completed by borrowing the vector generation algorithm and that of Bresenham's. There is one serious drawback of the Bresenham's approach and that is the intersection of a curve with itself. Here that approach fails miserably. To address this problem, a method of deviation for the implicit curves has been devised in (Ray and Ray 2011). Their algorithm translates the implicit equation of analog curve into algorithm. For some curves, like Folium of Desecrate, integer arithmetic is sufficient whereas for other ones, floating point arithmetic is required. A hexagonal drawing grid has also been used for drawing the mid-point ellipse algorithm. For instance, in (Prabukumar and Ray 2012), they have done this task. Further, a comparison has been made between the conventional ellipse drawing algorithms and of their own contribution.

4. Proposed Methodology using the Mid-Point Strategy

Consider the Cartesian equation of the Kappa curve (Chang 2014):

$$y^2(x^2 + y^2) = a^2x^2 \text{-----(4)}$$

We define a Kappa curve function with parameter a as below:

$$f_{\text{kappa}}(x, y) = y^4 + x^2y^2 - a^2x^2 \text{-----(5)}$$

This function has the following properties:

$f_{\text{kappa}}(x, y) < 0$ if (x, y) is below the curve

$f_{\text{kappa}}(x, y) = 0$ if (x, y) is on the curve

$f_{\text{kappa}}(x, y) > 0$ if (x, y) is above the curve

Now obviously as we start from the origin, we will do sampling along y -axis and will determine whether we must increase the value of x or not.

This process will continue until we reach to the threshold where $\frac{dy}{dx} = 1$.

By taking derivative of the Kappa curve, we will equate $\frac{dy}{dx}$ to 1 which will lead us to the terminating condition for the sampling along y -axis. The moment we reach this point, the first region says R_1 will terminate. At that very point, the second region R_2 will start as can be seen in Figure 4.

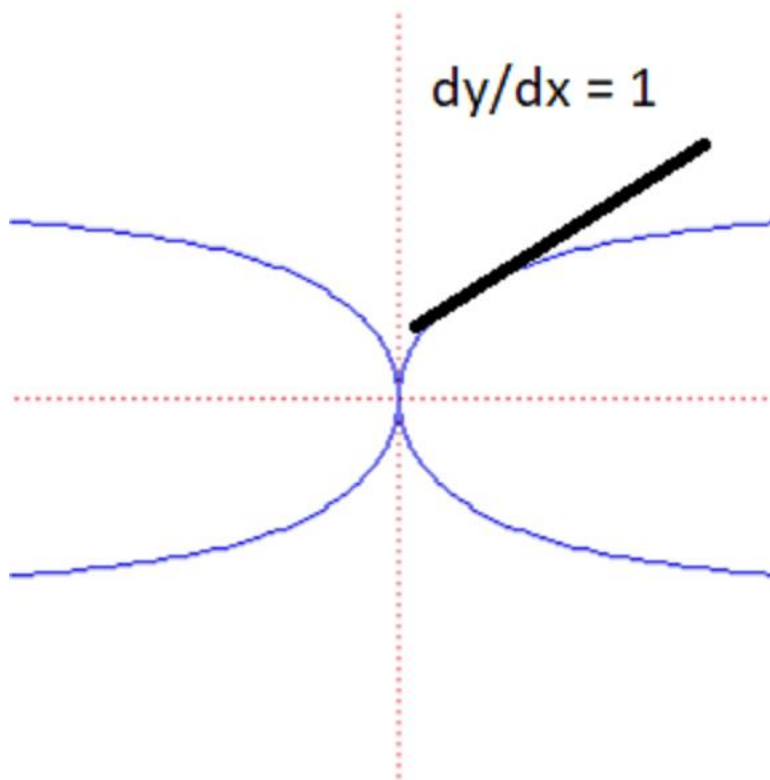


Figure 4. Demarcation of First Region.

The Kappa curve slope is calculated from equation 1 as:

$$\frac{dy}{dx} = \frac{a^2x - xy^2}{x^2y + 2y^3} \text{-----(6)}$$

At the boundary between R1 and R2,

$$\frac{dy}{dx} = 1 \text{-----(7)}$$

By equation these equations, we come up with the following terminating condition for the R₁:

$$x^2y + 2y^3 - a^2x + xy^2 \leq 0 \text{-----(8)}$$

We define the decision parameter for the R₁ as below:

$$p1_k = f_{kappa} (x_k + \frac{1}{2}, y_k + 1) \text{-----(9)}$$

$$= (y_k + 1)^4 + (x_k + \frac{1}{2})^2(y_k + 1)^2 - a^2(x_k + \frac{1}{2})^2$$

At the next sampling position ($y_{k+1} + 1 = y_k + 2$), the decision parameter for the R₁ will be evaluated as

$$p1_{k+1} = f_{kappa} (x_{k+1} + \frac{1}{2}, y_k + 2) \text{-----(10)}$$

$$= (y_k + 2)^4 + (x_{k+1} + \frac{1}{2})^2(y_k + 2)^2 - a^2(x_{k+1} + \frac{1}{2})^2$$

or

$$p1_{k+1} = p1_k + 4(y_k + 1)^3 + 6(y_k + 1)^2 + 4(y_k + 1) + 1 + (x_{k+1} + \frac{1}{2})^2 (y_k + 2)^2 - (x_k + \frac{1}{2})^2 (y_k + 1)^2 + a^2((x_k + \frac{1}{2})^2 - (x_{k+1} + \frac{1}{2})^2) \text{-----(11)}$$

Now if $p1_k < 0$ then $x_{k+1} = x_k$

and

$$p1_{k+1} = p1_k + 4(y_k + 1)^3 + 6(y_k + 1)^2 + 4(y_k + 1) + 1 + (x_k + \frac{1}{2})^2 (y_k + 2)^2 - (x_k + \frac{1}{2})^2 (y_k + 1)^2 \text{-----(12)}$$

If $p1_k \geq 0$ then $x_{k+1} = x_k + 1$

and

$$p1_{k+1} = p1_k + 4(y_k + 1)^3 + 6(y_k + 1)^2 + 4(y_k + 1) + 1 + \left(x_k + \frac{3}{2}\right)^2 (y_k + 2)^2 - \left(x_k + \frac{1}{2}\right)^2 (y_k + 1)^2 + a^2 \left(\left(x_k + \frac{1}{2}\right)^2 - \left(x_k + \frac{3}{2}\right)^2\right) \text{-----(13)}$$

Decision parameter is a very important concept for mid-point algorithm. In region R_1 , the value of the initial decision parameter is obtained by evaluating the kappa curve function for

$$(x_0, y_0) = (0, 0) \text{-----(14)}$$

$$p1_0 = \frac{1}{4}(5 - a^2) \text{-----(15)}$$

Over region R_2 , we sample along the x -axis and calculate the corresponding y values. The decision parameter for this region is calculated as:

$$p2_k = f_{\text{kappa}} \left(x_k + 1, y_k + \frac{1}{2}\right) \text{-----(16)}$$

$$= \left(y_k + \frac{1}{2}\right)^4 + (x_k + 1)^2 \left(y_k + \frac{1}{2}\right)^2 - a^2 (x_k + 1)^2$$

At the next sampling position ($x_{k+1} + 1 = x_k + 2$), the decision parameter for the second region R_2 will be evaluated as

$$p2_{k+1} = f_{\text{kappa}} \left(x_{k+1} + 1, y_{k+1} + \frac{1}{2}\right) \text{-----(17)}$$

$$= \left(y_{k+1} + \frac{1}{2}\right)^4 + (x_{k+1} + 1)^2 \left(y_{k+1} + \frac{1}{2}\right)^2 - a^2 (x_{k+1} + 1)^2$$

or

$$p2_{k+1} = p2_k + \left(y_{k+1} + \frac{1}{2}\right)^4 - \left(y_k + \frac{1}{2}\right)^4 + (x_{k+1} + 1)^2 \left(y_{k+1} + \frac{1}{2}\right)^2 - (x_k + 1)^2 \left(y_k + \frac{1}{2}\right)^2 + a^2 \left((x_k + 1)^2 - (x_{k+1} + 1)^2\right) \text{-----(18)}$$

If $p2_k \geq 0$ then $y_{k+1} = y_k$

and

$$p_{2_{k+1}} = p_{2_k} + \left(y_k + \frac{1}{2}\right)^2 \left((x_{k+1} + 1)^2 - (x_k + 1)^2 + a^2((x_k + 1)^2 - (x_{k+1} + 1)^2)\right) \text{-----}$$

(19)

If $p_{2_k} < 0$ then $y_{k+1} = y_{k+1}$

and

$$p_{2_{k+1}} = p_{2_k} + \left(y_k + \frac{3}{2}\right)^4 - \left(y_k + \frac{1}{2}\right)^4 + (x_k + 2)^2 \left(y_k + \frac{3}{2}\right)^2 - (x_k + 1)^2 \left(y_k + \frac{1}{2}\right)^2 + a^2((x_k + 1)^2 - (x_k + 2)^2) \text{-----(20)}$$

upon entering in the region R_2 , the initial value is taken as the last value calculated in the region 1 say (x_0, y_0) and the decision parameter for region R_2 is then calculated as

$$p_{2_0} = f_{kappa} \left(x_0 + 1, y_0 + \frac{1}{2}\right) \text{-----(21)}$$

$$= \left(y_0 + \frac{1}{2}\right)^4 + (x_0 + 1)^2 \left(y_0 + \frac{1}{2}\right)^2 - a^2(x_0 + 1)^2$$

5. Algorithms

1. Input a and obtain the first point on the kappa curve as

$$(x_0, y_0) = (0, 0)$$

2. Find the initial value of the decision parameter in region 1 as

$$p1_0 = \frac{1}{4}(5 - a^2)$$

3. In region R_1 , while the condition $x^2y + 2y^3 - a^2x + xy^2 \leq 0$ remains true do the following

if $p1_k < 0$, the next point on the kappa curve is $(x_k, y_k + 1)$ and

$$p1_{k+1} = p1_k + 4(y_k + 1)^3 + 6(y_k + 1)^2 + 4(y_k + 1) + 1 + \left(x_k + \frac{1}{2}\right)^2 (y_k + 2)^2 - \left(x_k + \frac{1}{2}\right)^2 (y_k + 1)^2$$

Otherwise, the next point on the kappa curve is $(x_k + 1, y_k + 1)$ and

$$p1_{k+1} = p1_k + 4(y_k + 1)^3 + 6(y_k + 1)^2 + 4(y_k + 1) + 1 + \left(x_k + \frac{3}{2}\right)^2 (y_k + 2)^2 - \left(x_k + \frac{1}{2}\right)^2 (y_k + 1)^2 + a^2\left(\left(x_k + \frac{1}{2}\right)^2 - \left(x_k + \frac{3}{2}\right)^2\right)$$

4. In region R_2 , do the following for an arbitrary number of times

If $p2_k > 0$, the next point of the kappa curve is $(x_k + 1, y_k)$ and

$$p2_{k+1} = p2_k + \left(y_k + \frac{1}{2}\right)^2 ((x_{k+1} + 1)^2 - (x_k + 1)^2 + a^2((x_k + 1)^2 - (x_{k+1} + 1)^2))$$

Otherwise, the next point on the kappa curve is $(x_k + 1, y_k + 1)$ and

$$p2_{k+1} = p2_k + \left(y_k + \frac{3}{2}\right)^4 - \left(y_k + \frac{1}{2}\right)^4 + (x_k + 2)^2 \left(y_k + \frac{3}{2}\right)^2 - (x_k + 1)^2 \left(y_k + \frac{1}{2}\right)^2 + a^2((x_k + 1)^2 - (x_k + 2)^2)$$

5. Find and draw the points in the other three quadrants by using symmetry.

6. Result and Discussion

Figure. 5 shows the Kappa curve drawn by using the proposed algorithm.

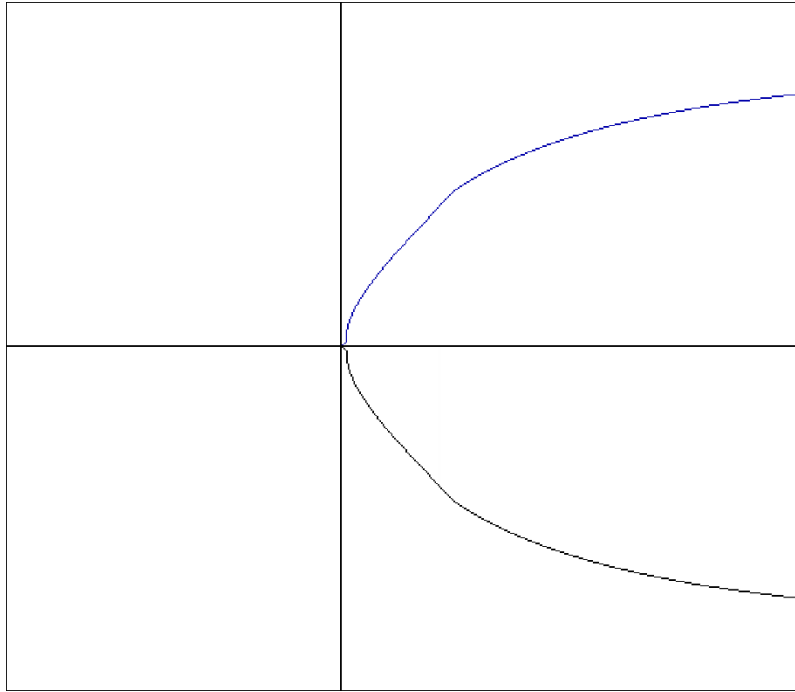


Figure 5. Kappa Curve Drawn through Our Approach.

One can observe a phenomenal difference in the quality of the curves drawn through the traditional approaches of parametric and polar equations and through the one we adopted. There is an inter pixel spacing of the Kappa curve drawn through the traditional approaches. One can clearly see that no such spacing exists in the curve we drawn by using the classical Bresenham approach. Since the Kappa curve is symmetrical about both the x -axis and y -axis, so we just calculated the points in a single quadrant only, i.e., the first quadrant. To draw the pixels for the remaining quadrants, we just exploited this inherent symmetry. Further, we applied calculus to demarcate the two regions. In the first region, there is sampling along y -axis and our algorithm calculates the corresponding x -value. As

we reach the threshold, a sampling along x -axis starts and our algorithm calculates the corresponding y -value. Now the questions arises, what will be its terminating condition? Actually, it will never end. Here exists the horizontal asymptote to this curve, so we have put a condition to draw the pixels for some arbitrary number of times.

7. Conclusion and Future Directions

Bresenham is a classical approach to drawing different curves. One of the salient features of this approach is that it uses only integer arithmetic. Further, it always selects the closest pixel along the real mathematical curve to glow a pixel on some calculated position. So, according to this methodology, a curve is drawn by combining different lines. As we have seen, the quality of the same curves drawn by using the parametric and polar equations is not good. A lot more curves exist on which the same methodology can be applied to get different curves with a better quality.

References

- [1] Bhatnagar, T., et al. (2023). Pixelated Interactions: Exploring Pixel Art for Graphical Primitives on a Pin Array Tactile Display. Proceedings of the 2023 ACM Designing Interactive Systems Conference.
- [2] Blázquez-Salcedo, J. L., et al. (2020). "Polar quasinormal modes of the scalarized Einstein-Gauss-Bonnet black holes." Physical Review D **102**(2): 024086.
- [3] Cao, M., et al. (2020). Midpoint distance circle generation algorithm based on midpoint circle algorithm and Bresenham circle algorithm. Journal of Physics: Conference Series, IOP Publishing.
- [4] Chang, C.-H. (2014). "Cohen's kappa for capturing discrimination." International Health **6**(2): 125-129.

- [5] Mokry, J. (2016). "Recalling prerequisite material in a calculus II course to improve student success." PRIMUS **26**(5): 453-465.
- [6] Nienhaus, V., et al. (2019). "Investigations on nozzle geometry in fused filament fabrication." Additive Manufacturing **28**: 711-718.
- [7] Popescu, I., et al. (2021). "'Kappa' and 'Kieroid' Curves Resulted as Loci." Problems of Locus Solved by Mechanisms Theory: 109-120.
- [8] Prabukumar, M. and B. K. Ray (2012). "A mid-point ellipse drawing algorithm on a hexagonal grid." International Journal of Computer Graphics **3**(1): 17-24.
- [9] Prabukumar, M. and B. K. Ray (2013). "An Efficient Scan Conversion of Parabola on Hexagonal Grid."
- [10] Ray, K. and B. Ray (2011). "An algorithm for Line Drawing Using Parametric Equation." International Journal of Computer Graphics, IJCG **2**(1): 9-16.
- [11] Ray, K. S. and B. K. Ray (2011). "A method of deviation for drawing implicit curves." International Journal of Computer Graphics **2**(2): 11-21.
- [12] Walia, E. and V. Verma (2012). "A computationally efficient framework for 3D warping technique." International Journal of Computer Graphics **3**(1): 1-10.
- [13] Yi, Z., et al. (2021). "A real-time touch control system design based on field-programmable gate array via optimizing Bresenham algorithm for electrowetting displays." Journal of the Society for Information Display **29**(7): 573-583.

- [14] Zhang, Y.-x., et al. (2022). "Comparative analysis of DDA algorithm and Bresenham algorithm." International Journal of Intelligent Internet of Things Computing **1**(4): 263-272.

Geometry of Conformal Quasi Bi-slant Submersions

Fahad Sikander¹ and Mohammad Shuaib²

¹College of Science and Theoretical Studies, Saudi Electronic University

(Jeddah Branch), Jeddah 23442, KSA

Email: f.sikander@seu.ed.sa

²Department of Mathematics, School of Chemical Engineering and Physical Sciences, Lovely Professional University, Jalandhar-144001, India

Email: shuaibyouf6@gmail.com

Abstract In this paper, we study conformal quasi bi-slant submersions from almost product Riemannian manifolds onto Riemannian manifolds as a generalization of bi-slant submersions and hemi-slant submersions. We discuss integrability conditions for distributions with the study of geometry of leaves of the distributions. Also, we discuss pluriharmonicity for conformal quasi bislant submersions.

Keywords: Almost Product Riemannian manifold, Riemannian submersions, bi-slant submersions, quasi bi-slant submersions.

2020 Mathematics Subject Classification: 53C15, 53C40, 53B20.

هندسة الغمرات شبه المائلة شبه المتماثلة

المخلص: في هذا البحث، قمنا بدراسة الغمر المطابق شبه ثنائي المائل من المشعبات الريمانية المنتجة تقريبا إلى المشعبات الريمانية كتعميم للغمرات ثنائية المائلة والغمرات نصف المائلة. نناقش شروط التكامل للتوزيعات مع دراسة هندسة أوراق التوزيعات. نناقش أيضًا تعدد التناغم في الغمرات شبه الثنائية المتطابقة.

1 Introduction

Both mathematics and physics employ immersions and submersions extensively. Yang-Mills theory ([6], [29]), Kaluza-Klein theory ([12], [15]) are the significant application of submersion. The characteristics of slant submersions have become a fascinating topic in differential geometry, as well as in complex and contact geometry. The concept of Riemannian submersion between Riemannian manifolds has been extensively studied by prominent mathematicians such as B. O'Neill [17] and A. Gray [8], who independently made significant contributions to this field. In 1976, B. Watson [28], introduced the notion of almost Hermitian submersions, which focuses on the submersion between almost Hermitian manifolds. Since then, they have been widely used in differential geometry to study Riemannian manifolds having differentiable structures [26].

D. Chinea [7] introduced the concept of almost contact Riemannian submersions between almost contact metric manifolds. In his work, Chinea extensively examined the differential geometric aspects of the fiber space, base space, and total space involved in these submersions. A step forward, R Prasad et. al. studied quasi bi-slant submersions from almost contact metric manifolds onto Riemannian manifolds [21], [19], [14]. As a generalization of Riemannian submersions, Fuglede [9] and Ishihara [13], separately studied horizontally conformal submersions. Later on, many authors investigated different kinds of conformal Riemannian submersions like conformal anti-invariant submersions ([4], conformal slant submersions [3], conformal semi-slant submersions ([2], [11], [18]) and conformal hemi-slant submersions ([27], [1]) etc. from almost Hermitian manifolds onto a Riemannian manifold. Most of these Riemannian submersions and conformal submersions are also studied from almost contact metric manifolds onto a Riemannian manifold.

In this paper, we study conformal quasi bi-slant submersions from locally product Riemannian manifold onto a Riemannian manifold. This paper is divided into six sections. Section 2 contains brief history of Riemannian and conformal

submersions. Also, we recall almost product Riemannian manifolds and, in particular, locally product Riemannian manifolds. In section 3, we investigate some fundamental results for conformal quasi bi-slant submersions from locally product Riemannian manifolds onto a Riemannian manifold those are required for our main sections. The results of integrability and totally geodesicness of distributions are presented in Section 4. In section 5, we discuss some decomposition theorems and also conditions under which locally product Riemannian manifold turns into locally twisted product manifold. While last section is devoted to the study of pluriharmonicity of conformal quasi bi-slant submersion.

Note: We will use some abbreviations throughout the paper as follows: locally product Riemannian manifold- *LPR* manifold, Conformal quasi bi-slant submersion- *CQBS* submersion,

2 Preliminaries

In this section, we will discuss the concept of almost product Riemannian manifold and also, Riemannian submersions and conformal submersions between two Riemannian manifolds with some basic facts and results. These concepts have been previously introduced in the earlier work in this field, so we mentioned them in quotation and proper references have been provided to acknowledge their contributions. Furthermore, the definitions have been restated here to ensure clarity and facilitate a comprehensive understanding of the concepts presented in this study.

"An n -dimensional manifold \bar{Q} with (1,1) type tensor field F such that

$$F^2 = I, (F \neq I), \tag{2.1}$$

is called an almost product manifold with almost structure F . There exists a Riemannian metric g on an almost product manifold which is compatible with the structure F in the sense that

$$g(FU, FV) = g(U, V),$$

(2.2)

for any $U, V \in \Gamma(TM)$, then (\bar{Q}, g, F) is called an almost product Riemannian manifold. The covariant derivative of F defined by

$$(\nabla_U FV) = \nabla_U FV - F\nabla_U V$$

(2.3)

for any vector fields $U, V \in \Gamma(\bar{T}Q)$. The manifold is called locally product Riemannian (LPR) manifold if F is parallel with respect to connection ∇ .e.,

$$(\nabla_U F)V = 0 \tag{2.4}$$

for any vector fields $U, V \in \Gamma(\bar{T}Q)$.

Let $\Psi: (\bar{Q}_1, g_1, F) \rightarrow (\bar{Q}_2, g_2)$ be a Riemannian submersion. A vector field \bar{X} on \bar{Q}_1 is called a basic vector field if $\bar{X} \in \Gamma(\ker \Psi_*)^\perp$ and Ψ -related with a vector field \bar{X} on \bar{Q}_2 i.e., $\Psi_*(\bar{X}(q)) = \bar{X}\Psi(q)$ for $q \in \bar{Q}_1$.

The formulae given by O'Neill [17] of two (1,2) tensor fields \mathcal{T} and \mathcal{A} , plays a crucial role in the theory of submersions

(2.5)

$$\mathcal{A}_{E_1} F_1 = \mathcal{H}\nabla_{\mathcal{H}E_1} \mathcal{V}F_1 + \mathcal{V}\nabla_{\mathcal{H}E_1} \mathcal{H}F_1, \tag{2.6}$$

$$\mathcal{T}_{E_1} F_1 = \mathcal{H}\nabla_{\mathcal{V}E_1} \mathcal{V}F_1 + \mathcal{V}\nabla_{\mathcal{V}E_1} \mathcal{H}F_1,$$

for any $E_1, F_1 \in \Gamma(T\bar{Q}_1)$ and ∇ is Levi-Civita connection of g_1 . Note that a Riemannian submersion $\Psi: (\bar{Q}_1, g_1, F) \rightarrow (\bar{Q}_2, g_2)$ has totally geodesic fibers if and only if \mathcal{T} vanishes identically. From (2.5) and (2.6), we can deduce

(2.7)

(2.8)

$$\nabla_{\tilde{U}_1} \tilde{V}_1 = \mathcal{T}_{\tilde{U}_1} \tilde{V}_1 + \mathcal{V}\nabla_{\tilde{U}_1} \tilde{V}_1 \tag{2.9}$$

$$\nabla_{\tilde{U}_1} \tilde{X}_1 = \mathcal{T}_{\tilde{U}_1} \tilde{X}_1 + \mathcal{H}\nabla_{\tilde{U}_1} \tilde{X}_1 \tag{2.10}$$

$$\nabla_{\tilde{X}_1} \tilde{U}_1 = \mathcal{A}_{\tilde{X}_1} \tilde{U}_1 + \mathcal{V}_1 \nabla_{\tilde{X}_1} \tilde{U}_1$$

$$\nabla_{\tilde{X}_1} \tilde{Y}_1 = \mathcal{H}\nabla_{\tilde{X}_1} \tilde{Y}_1 + \mathcal{A}_{\tilde{X}_1} \tilde{Y}_1$$

for any vector fields $\tilde{U}_1, \tilde{V}_1 \in \Gamma(\ker \Psi_*)$ and $\tilde{X}_1, \tilde{Y}_1 \in \Gamma(\ker \Psi_*)^\perp$.

It is observe that \mathcal{T} and \mathcal{A} are skew-symmetric, that is,

$$g(\mathcal{A}_{\tilde{X}}E_1, F_1) = -g(E_1, \mathcal{A}_{\tilde{X}}F_1), g(\mathcal{T}_{\tilde{V}}E_1, F_1) = -g(E_1, \mathcal{T}_{\tilde{V}}F_1), \quad (2.11)$$

for any vector fields $E_1, F_1 \in \Gamma(T_p\bar{Q}_1)$. It is also observed that the restriction of \mathcal{T} to the vertical distribution $\mathcal{T}|_{V \times V}$ is exactly the second fundamental form of the fibres of Ψ . Since $\mathcal{T}_{\tilde{V}}$ is skew-symmetric we say Ψ has totally geodesic fibres if and only if $\mathcal{T} = 0$. For the special case when Ψ is horizontally conformal submersion we have "

Proposition 2.1. [10] Let $\Psi: (\bar{Q}_1, g_1) \rightarrow (\bar{Q}_2, g_2)$ be a horizontally conformal submersion with dilation λ and X, Y be the horizontal vectors, then

$$\mathcal{A}_X Y = \frac{1}{2} \left[\mathcal{V}[X, Y] - \lambda^2 g_1(X, Y) \text{grad} \left(\frac{1}{\lambda^2} \right) \right] \quad (2.12)$$

We see that the skew-symmetric part of measures the obstruction integrability of the horizontal distribution $(\ker \Psi_*)^\perp$.

Definition 2.1. A horizontally conformally submersion $\Psi: \bar{Q}_1 \rightarrow \bar{Q}_2$ is called horizontally homothetic if the gradient of its dilation λ is vertical, i.e.,

$$\mathcal{H}(\text{grad } \lambda) = 0, \quad (2.13)$$

where \mathcal{H} is the orthogonal complementary distribution to $\nu = \ker \Psi_*$ in $\Gamma(T_p\bar{Q}_1)$.

The second fundamental form of smooth map Ψ is given by

$$(\nabla \Psi_*)(\tilde{U}_1, \tilde{V}_1) = \nabla_{\tilde{U}_1}^\Psi \Psi_* \tilde{V}_1 - \Psi_* \nabla_{\tilde{U}_1} \tilde{V}_1, \quad (2.14)$$

and the map be totally geodesic if $(\nabla \Psi_*)(\tilde{U}_1, \tilde{V}_1) = 0$ for all $\tilde{U}_1, \tilde{V}_1 \in \Gamma(T_p\bar{Q}_1)$, where ∇ and $\nabla \Psi_*$ are Levi-Civita and pullback connections."

Now, we recall the following lemma for our main section.

Lemma 2.1. Let $\Psi: \bar{Q}_1 \rightarrow \bar{Q}_2$ be a horizontal conformal submersion. Then, we have

$$(i) (\nabla\Psi_*)(\tilde{X}_1, \tilde{Y}_1) = \tilde{X}_1(\ln \lambda)\Psi_*(\tilde{Y}_1) + \tilde{Y}_1(\ln \lambda)\Psi_*(\tilde{X}_1) - g_1(\tilde{X}_1, \tilde{Y}_1)\Psi_*(\text{grad } \ln \lambda),$$

$$(ii) (\nabla\Psi_*)(\tilde{U}_1, \tilde{V}_1) = -\Psi_*(\mathcal{T}_{\tilde{U}_1}\tilde{V}_1),$$

$$(iii) (\nabla\Psi_*)(\tilde{X}_1, \tilde{U}_1) = -\Psi_*(\nabla_{\tilde{X}_1}\tilde{U}_1) = -\Psi_*(\mathcal{A}_{\tilde{X}_1}\tilde{U}_1),$$

for any horizontal vector fields \tilde{X}_1, \tilde{Y}_1 and vertical vector fields \tilde{U}_1, \tilde{V}_1 [5].

3 Conformal quasi bi-slant submersions

First of all we are giving in this sections some definitions that will useful throughtout the text.

Definition 3.1. [28] Let $\Psi: (\bar{Q}_1, g_{Q_1}) \rightarrow (\bar{Q}_2, g_{Q_2})$ be a smooth map between two Riemannian manifolds having dimensions m_1 and m_2 , respectively. Then Ψ is called horizontally weakly conformal or semi conformal at $x \in \bar{Q}_1$ if either

$$(i) \Psi_{*x} = 0, \text{ or}$$

$$(ii) \Psi_{*x} \text{ maps horizontal space } \mathcal{H}_x = (\ker(\Psi_{*x}))^\perp \text{ conformally onto } T_{\Psi(x)}(N) \text{ i} \quad (3.1)$$

is surjective and there exits a number $\Lambda(x) \neq 0$ such that

$$g_N(\Psi_{*x}X, \Psi_{*x}Y) = \Lambda(x)g(X, Y),$$

for any $X, Y \in \mathcal{H}_x$.

Equation (3.1) can be re-written as

$$(\Psi_*g_N)_x |_{\mathcal{H}_x \times \mathcal{H}_x} = \Lambda(x)g(x) |_{\mathcal{H}_x \times \mathcal{H}_x}.$$

A point x satisfies (i) in above definition if and only if it is a critical point of Ψ . A point, satisfying (ii) is called a regular point. At a critical point, Ψ_{*x} has rank 0 ; at a regular point, Ψ_{*x} has rank n and Ψ defines a submersion. The number $\lambda(x)$ is called the square dilation (of Ψ at x); it is necessarily nonnegative. Its square root $\lambda(x) = \sqrt{\Lambda(x)}$ is called the dilation of Ψ at x . The map Ψ is called horizontally weakly conformal or semi conformal on \bar{Q}_1 if it is horizontally weakly conformal at every point of M . It is clear that if Ψ has no critical points, then we call it a (horizontally) conformal submersion.

Definition 3.2

. Let us suppose that (\bar{Q}_1, g_1, F) be an almost product manifold and (\bar{Q}_2, g_2) be a Riemannian manifold. A Riemannian

submersion Ψ from \bar{Q}_1 onto \bar{Q}_2 is called a conformal quasi bi-slant (CQBS) submersion if there exists three mutually orthogonal distributions $\mathfrak{D}^{\mathfrak{I}}$, \mathfrak{D}^{θ_1} and \mathfrak{D}^{θ_2} such that

- (i) $\ker \Psi_* = \mathfrak{D}^{\mathfrak{I}} \oplus \mathfrak{D}^{\theta_1} \oplus \mathfrak{D}^{\theta_2}$,
- (ii) $\mathfrak{D}^{\mathfrak{I}}$ is invariant. i.e., $F\mathfrak{D}^{\mathfrak{I}} = \mathfrak{D}^{\mathfrak{I}}$,
- (iii) $F\mathfrak{D}^{\theta_1} \perp \mathfrak{D}^{\theta_2}$ and $F\mathfrak{D}^{\theta_2} \perp \mathfrak{D}^{\theta_1}$,
- (iv) for any non-zero vector field $\tilde{V}_1 \in (\mathfrak{D}^{\theta_1})_p, p \in \bar{Q}_1$ the angle θ_1 between $(\mathfrak{D}^{\theta_1})_p$ and $F\tilde{V}_1$ is constant and independent of the choice of the point p and $\tilde{V}_1 \in (\mathfrak{D}^{\theta_1})_p$,
- (v) for any non-zero vector field $\tilde{V}_1 \in (\mathfrak{D}^{\theta_2})_q, q \in \bar{Q}_1$ the angle θ_2 between $(\mathfrak{D}^{\theta_2})_q$ and $F\tilde{V}_1$ is constant and independent of the choice of the point q and $\tilde{V}_1 \in (\mathfrak{D}^{\theta_2})_q$.

If we denote the dimensions of $\mathfrak{D}^{\mathfrak{I}}, \mathfrak{D}^{\theta_1}$ and \mathfrak{D}^{θ_2} by m_1, m_2 and m_3 respectively, then we have the following observations:

- (i) If $m_1 \neq 0, m_2 = 0$ and $m_3 = 0$, then Ψ is an invariant submersion.
- (ii) If $m_1 \neq 0, m_2 \neq 0, 0 < \theta_1 < \frac{\pi}{2}$ and $m_3 = 0$, then Ψ is a proper semi-slant submersion.
- (iii) If $m_1 = 0, m_2 = 0$ and $m_3 \neq 0, 0 < \theta_2 < \frac{\pi}{2}$, then Ψ is a slant submersion with slant angle θ_2 .

(iv) If $m_1 = 0, m_2 \neq 0, 0 < \theta_1 < \frac{\pi}{2}$ and $m_3 \neq 0, \theta_2 = \frac{\pi}{2}$, then Ψ proper hemi-slant submersion.

(v) If $m_1 = 0, m_2 \neq 0, 0 < \theta_1 < \frac{\pi}{2}$ and $m_3 \neq 0, 0 < \theta_2 < \frac{\pi}{2}$, then Ψ is proper bi-slant submersion with slant angles θ_1 and θ_2 .

(vi) If $m_1 \neq 0, m_2 \neq 0, 0 < \theta_1 < \frac{\pi}{2}$ and $m_3 \neq 0, 0 < \theta_2 < \frac{\pi}{2}$, then Ψ is proper quasi bi-slant submersion with slant angles θ_1 and θ_2 .

Hence, it is clear that CQBS submersions are generalized version of conformal quasi hemi-slant submersions.

Let Ψ be a CQBS submersion from an almost product Riemannian manifold (\bar{Q}_1, g_1, F) onto a Riemannian manifold (\bar{Q}_2, g_2) . Then, for any $U \in (\ker \Psi_*)$, we have (3.2)

$$\tilde{U} = \mathfrak{A}\tilde{U} + \mathfrak{B}\tilde{U} + \mathfrak{C}\tilde{U},$$

where $\mathfrak{A}, \mathfrak{B}$ and \mathfrak{C} are the projections morphism onto $\mathcal{D}^{\mathfrak{A}}, \mathcal{D}^{\theta_1}$, and \mathcal{D}^{θ_2} , respectively. Now, for any $\tilde{U} \in (\ker \Psi_*)$, we have (3.3)

$$F\tilde{U} = \xi\tilde{U} + \eta\tilde{U}$$

where $\xi\tilde{U} \in \Gamma(\ker \Psi_*)$ and $\eta\tilde{U} \in \Gamma(\ker \Psi_*)^\perp$. From equations (3.2) and (3.3), we have

$$\begin{aligned} F\tilde{U} &= F(\mathfrak{A}\tilde{U}) + F(\mathfrak{B}\tilde{U}) + F(\mathfrak{C}\tilde{U}) \\ &= \xi(\mathfrak{A}\tilde{U}) + \eta(\mathfrak{A}\tilde{U}) + \xi(\mathfrak{B}\tilde{U}) + \eta(\mathfrak{B}\tilde{U}) + \xi(\mathfrak{C}\tilde{U}) + \eta(\mathfrak{C}\tilde{U}). \end{aligned}$$

Since $F\mathcal{D}^{\mathfrak{A}} = \mathcal{D}^{\mathfrak{A}}$ and $\eta(\mathfrak{A}\tilde{U}) = 0$, we have

$$F\tilde{U} = \xi(\mathfrak{A}\tilde{U}) + \xi(\mathfrak{B}\tilde{U}) + \eta(\mathfrak{B}\tilde{U}) + \xi(\mathfrak{C}\tilde{U}) + \eta(\mathfrak{C}\tilde{U}).$$

Hence, we have the decomposition as

$$F(\ker \Psi_*) = \xi\mathcal{D}^{\mathfrak{A}} \oplus \xi\mathcal{D}^{\theta_1} \oplus \xi\mathcal{D}^{\theta_2} \oplus \eta\mathcal{D}^{\theta_1} \oplus \eta\mathcal{D}^{\theta_2}.$$

From equations (3.4), we get

$$(\ker \Psi_*)^\perp = \eta \mathcal{D}^{\theta_1} \oplus \eta \mathcal{D}^{\theta_2} \oplus \mu, \quad (3.5)$$

where μ is the orthogonal complement to $\eta \mathcal{D}^{\theta_1} \oplus \eta \mathcal{D}^{\theta_2}$ in $(\ker \Psi_*)^\perp$ and μ is invariant with respect to F . Now, for any $\tilde{X} \in \Gamma(\ker \Psi_*)^\perp$, we have

$$L\tilde{X} = F\tilde{X} - P\tilde{X} \quad (3.6)$$

where $P\tilde{X} \in \Gamma(\ker \Psi_*)$ and $L\tilde{X} \in \Gamma(\mu)$.

Lemma 3.1. Let (\bar{Q}_1, g_1, F) be an almost product Riemannian manifold and (\bar{Q}_2, g_2) be a Riemannian manifold. If $\Psi: \bar{Q}_1 \rightarrow \bar{Q}_2$ is a CQBS submersion, then we have

$$\begin{aligned} \tilde{U} &= \xi^2 \tilde{U} + P\xi \tilde{U} + \eta \xi \tilde{U} + L\eta \tilde{U} = 0, \\ \tilde{X} &= \eta P\tilde{X} + L^2 \tilde{X} + \xi P\tilde{X} + PL\tilde{X} = 0, \end{aligned}$$

for $\tilde{U} \in \Gamma(\ker \Psi_*)$ and $\tilde{X} \in \Gamma(\ker \Psi_*)^\perp$.

Proof. By using equations (2.1), (3.3) and (3.6), we get the desired results.

Since $\Psi: \bar{Q}_1 \rightarrow \bar{Q}_2$ is a CQBS submersion, Here we give some useful results that will be used throughout the paper.

Lemma 3.2. [19] Let Ψ be a CQBS submersion from an almost product Riemannian manifold (\bar{Q}_1, g_1, F) onto a Riemannian manifold (\bar{Q}_2, g_2) , then we have

- (i) $\xi^2 \tilde{U} = \cos^2 \theta_1 \tilde{U}$,
 - (ii) $g_1(\xi \tilde{U}, \xi \tilde{V}) = \cos^2 \theta_1 g_1(\tilde{U}, \tilde{V})$,
 - (iii) $g(\eta \tilde{U}, \eta \tilde{V}) = \sin^2 \theta_1 g_1(\tilde{U}, \tilde{V})$,
- for any vector fields $\tilde{U}, \tilde{V} \in \Gamma(\mathcal{D}^{\theta_1})$.

Lemma 3.3. [19] Let Ψ be a CQBS submersion from an almost product Riemannian manifold (\bar{Q}_1, g_1, F) onto a Riemannian manifold (\bar{Q}_2, g_2) , then we have

- (i) $\xi^2 \tilde{Z} = \cos^2 \theta_2 \tilde{Z}$,
 - (ii) $g_1(\xi \tilde{Z}, \xi \tilde{W}) = \cos^2 \theta_2 g_1(\tilde{Z}, \tilde{W})$,
 - (iii) $g_1(\eta \tilde{Z}, \eta \tilde{W}) = \sin^2 \theta_2 g_1(\tilde{Z}, \tilde{W})$,
- for any vector fields $\tilde{Z}, \tilde{W} \in \Gamma(\mathfrak{D}^{\theta_2})$.

The proof of above Lemmas is similar to the proof of the Theorem 3.5 of [19]. Thus, we omit the proofs.

Let (\bar{Q}_2, g_2) be a Riemannian manifold and that (\bar{Q}_1, g_1, F) is a LPR manifold. We now observe how the tensor fields \mathcal{T} and \mathcal{A} of a CQBS submersion $\Psi: (\bar{Q}_1, g_1, F) \rightarrow (\bar{Q}_2, g_2)$ are affected by the LPR structure on \bar{Q}_1 .

Lemma 3.4. Let Ψ be a CQBS submersion from an almost product Riemannian manifold (\bar{Q}_1, g_1, F) onto a Riemannian manifold (\bar{Q}_2, g_2) , then we have

$$\mathcal{A}_{\tilde{X}} P \tilde{Y} + \mathcal{H} \nabla_{\tilde{X}} L \tilde{Y} = \xi \mathcal{H} \nabla_{\tilde{X}} \tilde{Y} + P \mathcal{A}_{\tilde{X}} \tilde{Y} \tag{3.7}$$

$$\mathcal{V} \nabla_{\tilde{X}} P \tilde{Y} + \mathcal{A}_{\tilde{X}} L \tilde{Y} = \eta \mathcal{H} \nabla_{\tilde{X}} \tilde{Y} + L \mathcal{A}_{\tilde{X}} \tilde{Y}. \tag{3.8}$$

$$\mathcal{V} \nabla_{\tilde{X}} \xi \tilde{V} + \mathcal{A}_{\tilde{X}} \eta \tilde{V} = P \mathcal{A}_{\tilde{X}} \tilde{V} + \xi \mathcal{V} \nabla_{\tilde{X}} \tilde{V} \tag{3.9}$$

$$\mathcal{A}_{\tilde{X}} \xi \tilde{V} + \mathcal{H} \nabla_{\tilde{X}} \eta \tilde{V} = \mathcal{C} \mathcal{A}_{\tilde{X}} \tilde{V} + \eta \mathcal{V} \nabla_{\tilde{X}} \tilde{V}. \tag{3.10}$$

$$\mathcal{V} \nabla_{\tilde{V}} P \tilde{X} + \mathcal{T}_{\tilde{V}} L \tilde{X} = \xi \mathcal{T}_{\tilde{V}} L \tilde{X} + P \mathcal{H} \nabla_{\tilde{V}} \tilde{X} \tag{3.11}$$

$$\mathcal{T}_{\tilde{V}} P \tilde{X} + \mathcal{H} \nabla_{\tilde{V}} L \tilde{X} = \eta \mathcal{T}_{\tilde{V}} \tilde{X} + L \mathcal{H} \nabla_{\tilde{V}} \tilde{X}. \tag{3.12}$$

$$\mathcal{V} \nabla_{\tilde{U}} \xi \tilde{V} + \mathcal{T}_{\tilde{U}} \eta \tilde{V} = \mathfrak{B} \mathcal{T}_{\tilde{U}} \tilde{V} + \xi \mathcal{V} \nabla_{\tilde{U}} \tilde{V} \tag{3.13}$$

$$\mathcal{T}_{\tilde{U}} \xi \tilde{V} + \mathcal{H} \nabla_{\tilde{U}} \eta \tilde{V} = L \mathcal{T}_{\tilde{U}} \tilde{V} + \eta \mathcal{V} \nabla_{\tilde{U}} \tilde{V}, \tag{3.14}$$

for any vector fields $\tilde{U}, \tilde{V} \in \Gamma(\ker \Psi_*)$ and $\tilde{X}, \tilde{Y} \in \Gamma(\ker \Psi_*)^\perp$.

Proof. By the direct calculation, using (3.6), (2.10) and (2.3), we can easily obtain relations given by (3.7) and (3.8). Remaining relations can be obtained similarly by using (3.3), (3.6), (2.7)-(2.10) and (2.3).

Now, we discuss some basic results which are useful to explore the geometry of CQBS submersion $\Psi: \bar{Q}_1 \rightarrow \bar{Q}_2$. For this, define the following :

(3.15)

$$(\nabla_{\tilde{U}}\xi)\tilde{V} = \mathcal{V}\nabla_{\tilde{U}}\xi\tilde{V} - \xi\mathcal{V}\nabla_{\tilde{U}}\tilde{V} \quad (3.16)$$

$$(\nabla_{\tilde{U}}\eta)\tilde{V} = \mathcal{H}\nabla_{\tilde{U}}\eta\tilde{V} - \eta\mathcal{V}\nabla_{\tilde{U}}\tilde{V} \quad (3.17)$$

$$(\nabla_{\tilde{X}}P)\tilde{Y} = \mathcal{V}\nabla_{\tilde{X}}P\tilde{Y} - P\mathcal{H}\nabla_{\tilde{X}}\tilde{Y} \quad (3.18)$$

$$(\nabla_{\tilde{X}}L)\tilde{Y} = \mathcal{H}\nabla_{\tilde{X}}L\tilde{Y} - L\mathcal{H}\nabla_{\tilde{X}}\tilde{Y}$$

for any vector fields $\tilde{U}, \tilde{V} \in \Gamma(\ker \Psi_*)$ and $\tilde{X}, \tilde{Y} \in \Gamma(\ker \Psi_*)^\perp$.

Lemma 3.5. Let (\bar{Q}_1, g_1, F) be LPR manifold and (\bar{Q}_2, g_2) be a Riemannian manifold. If $\Psi: \bar{Q}_1 \rightarrow \bar{Q}_2$ is a CQBS submersion, then we have

$$\begin{aligned} (\nabla_{\tilde{U}}\xi)\tilde{V} &= P\mathcal{J}_{\tilde{U}}\tilde{V} - \mathcal{J}_{\tilde{U}}\eta\tilde{V} \\ (\nabla_{\tilde{U}}\eta)\tilde{V} &= L\mathcal{J}_{\tilde{U}}\tilde{V} - \mathcal{J}_{\tilde{U}}\xi\tilde{V} \\ (\nabla_{\tilde{X}}P)\tilde{Y} &= \xi\mathcal{A}_{\tilde{X}}\tilde{Y} - \mathcal{A}_{\tilde{X}}L\tilde{Y} \\ (\nabla_{\tilde{X}}L)\tilde{Y} &= \eta\mathcal{A}_{\tilde{X}}\tilde{Y} - \mathcal{A}_{\tilde{X}}P\tilde{Y}, \end{aligned}$$

for all vector fields $\tilde{U}, \tilde{V} \in \Gamma(\ker \Psi_*)$ and $\tilde{X}, \tilde{Y} \in \Gamma(\ker \Psi_*)^\perp$.

Proof. By using equations (2.3), (2.7)- (2.10) and equations (3.15)-(3.18), we get the proof of the lemma.

If the tensors ξ and η are parallel with respect to the connection ∇ of \bar{Q}_1 then, we have

$$P\mathcal{J}_{\tilde{U}}\tilde{V} = \mathcal{J}_{\tilde{U}}\eta\tilde{V}, L\mathcal{J}_{\tilde{U}}\tilde{V} = \mathcal{J}_{\tilde{U}}\xi\tilde{V}$$

for any vector fields $\tilde{U}, \tilde{V} \in \Gamma(T\bar{Q}_1)$.

4 Integrability and totally geodesicness of distributions

Firstly, we are giving definition of Riemannian manifold.

A Riemannian metric on a smooth manifold M is a symmetric positive definite smooth 2-covariant tensor field g . A smooth manifold M equipped with a Riemannian metric g is called a Riemannian manifold and denoted by (M, g) .

Since, $\Psi: \bar{Q}_1 \rightarrow \bar{Q}_2$ is a CQBS submersion, where (\bar{Q}_1, g_1, F) representing a LPR manifold and (\bar{Q}_2, g_2) denoting a Riemannian manifold. The existence of three mutually orthogonal distributions, including an invariant distribution \mathfrak{D} , a pair of slant distributions \mathfrak{D}^{θ_1} and \mathfrak{D}^{θ_2} , is guaranteed by the definition of CQBS-submersion. We begin the subject of distributions integrability by determining the integrability of the slant distributions as follows:

Theorem 4.1. Let Ψ be a CQBS submersion from LPR manifold (\bar{Q}_1, g_1, F) onto a Riemannian manifold (\bar{Q}_2, g_2) . Then slant distribution \mathfrak{D}^{θ_1} is integrable if and only if

$$\begin{aligned} & \frac{1}{\lambda^2} \{g_2(\nabla_{\tilde{U}_1}^{\Psi} \Psi_* \eta \tilde{V}_1 + \nabla_{\tilde{V}_1}^{\Psi} \Psi_* \eta \tilde{U}_1, \Psi_* \eta \mathfrak{C}\tilde{Z})\} \\ & = \frac{1}{\lambda^2} \{g_2((\nabla \Psi_*)(\tilde{U}_1, \eta \tilde{V}_1) + (\nabla \Psi_*)(\tilde{V}_1, \eta \tilde{U}_1), \Psi_* \eta \mathfrak{C}\tilde{Z})\} \\ & \quad - g_1(\nabla_{\tilde{U}_1} \eta \xi \tilde{V}_1 - \nabla_{\tilde{V}_1} \eta \xi \tilde{U}_1, \tilde{Z}) - g_1(\mathcal{T}_{\tilde{U}_1} \eta \tilde{V}_1 - \mathcal{T}_{\tilde{V}_1} \eta \tilde{U}_1, F\mathfrak{A}\tilde{Z} + \xi \mathfrak{C}\tilde{Z}), \end{aligned} \tag{4.1}$$

for any $\tilde{U}_1, \tilde{V}_1 \in \Gamma(\mathfrak{D}^{\theta_1})$ and $\tilde{Z} \in \Gamma(\mathfrak{D}^{\mathfrak{x}} \oplus \mathfrak{D}^{\theta_2})$.

Proof. For $\tilde{U}_1, \tilde{V}_1 \in \Gamma(\mathfrak{D}^{\theta_1})$ and $\tilde{Z} \in \Gamma(\mathfrak{D}^{\mathfrak{x}} \oplus \mathfrak{D}^{\theta_2})$ with using equations (2.2), (2.3), (2.13) and (3.3), we get

$$\begin{aligned} g_1([\tilde{U}_1, \tilde{V}_1], \tilde{Z}) & = g_1(\nabla_{\tilde{U}_1} \xi \tilde{V}_1, F\tilde{Z}) + g_1(\nabla_{\tilde{U}_1} \eta \tilde{V}_1, F\tilde{Z}) \\ & \quad - g_1(\nabla_{\tilde{V}_1} \xi \tilde{U}_1, F\tilde{Z}) - g_1(\nabla_{\tilde{V}_1} \eta \tilde{U}_1, F\tilde{Z}). \end{aligned}$$

By using equations (2.3), (2.13) and (3.3), we have

$$g_1([\tilde{U}_1, \tilde{V}_1], \tilde{Z}) = g_1(\nabla_{\tilde{U}_1} \xi^2 \tilde{V}_1, \tilde{Z}) + g_1(\nabla_{\tilde{U}_1} \eta \xi \tilde{V}_1, \tilde{Z}) - g_1(\nabla_{\tilde{V}_1} \xi^2 \tilde{U}_1, \tilde{Z}) - g_1(\nabla_{\tilde{V}_1} \eta \xi \tilde{U}_1, \tilde{Z}) + g_1(\nabla_{\tilde{U}_1} \eta \tilde{V}_1, F\mathfrak{A}\tilde{Z} + \xi\mathfrak{C}\tilde{Z} + \eta\mathfrak{C}\tilde{Z}) - g_1(\nabla_{\tilde{V}_1} \eta \tilde{U}_1, F\mathfrak{A}\tilde{Z} + \xi\mathfrak{C}\tilde{Z} + \eta\mathfrak{C}\tilde{Z}).$$

Taking account the fact of Lemma 3.2 with using equation (2.8), we get

$$g_1([\tilde{U}_1, \tilde{V}_1], \tilde{Z}) = \cos^2 \theta_1 g_1([\tilde{U}_1, \tilde{V}_1], \tilde{Z}) + g_1(\nabla_{\tilde{U}_1} \eta \xi \tilde{V}_1 - \nabla_{\tilde{V}_1} \eta \xi \tilde{U}_1, \tilde{Z}) + g_1(\mathcal{T}_{\tilde{U}_1} \eta \tilde{V}_1 - \mathcal{T}_{\tilde{V}_1} \eta \tilde{U}_1, F\mathfrak{A}\tilde{Z} + \xi\mathfrak{C}\tilde{Z}) + g_1(\mathcal{H}\nabla_{\tilde{U}_1} \eta \tilde{V}_1 - \mathcal{H}\nabla_{\tilde{V}_1} \eta \tilde{U}_1, \eta\mathfrak{C}\tilde{Z}).$$

By using formula (2.14) with Lemma 2.1, we finally get

$$\begin{aligned} & \sin^2 \theta_1 g_1([\tilde{U}_1, \tilde{V}_1], \tilde{Z}) \\ &= \frac{1}{\lambda^2} \{g_2(\nabla_{\tilde{U}_1}^\Psi \Psi_* \eta \tilde{V}_1 - \nabla_{\tilde{V}_1}^\Psi \Psi_* \eta \tilde{U}_1, \Psi_* \eta \mathfrak{C}\tilde{Z})\} \\ &+ \frac{1}{\lambda^2} \{g_2((\nabla \Psi_*)(\tilde{U}_1, \eta \tilde{V}_1), \Psi_* \eta \mathfrak{C}\tilde{Z}) + g_2((\nabla \Psi_*)(\tilde{V}_1, \eta \tilde{U}_1), \Psi_* \eta \mathfrak{C}\tilde{Z})\} \\ &+ g_1(\mathcal{T}_{\tilde{U}_1} \eta \tilde{V}_1 - \mathcal{T}_{\tilde{V}_1} \eta \tilde{U}_1, F\mathfrak{A}\tilde{Z} + \xi\mathfrak{C}\tilde{Z}) + g_1(\nabla_{\tilde{U}_1} \eta \xi \tilde{V}_1 - \nabla_{\tilde{V}_1} \eta \xi \tilde{U}_1, \tilde{Z}). \end{aligned}$$

In a similar way, we can examine the condition of integrability for slant distribution as follows:

Theorem 4.2. Let $\Psi: (\bar{Q}_1, g_1, F) \rightarrow (\bar{Q}_2, g_2)$ be a CQBS submersion, where (\bar{Q}_1, g_1, F) a LPR manifold and (\bar{Q}_2, g_2) a Riemannian manifold. Then slant distribution \mathfrak{D}^{θ_2} is integrable if and only if

$$\begin{aligned} & - \frac{1}{\lambda^2} \{g_2((\nabla \Psi_*)(\tilde{U}_2, \eta \tilde{V}_2) - (\nabla \Psi_*)(\tilde{V}_2, \eta \tilde{U}_2), \Psi_* \eta \mathfrak{B}\tilde{Z})\} \\ &= g_1(\mathcal{T}_{\tilde{U}_2} \eta \xi \tilde{V}_2 - \mathcal{T}_{\tilde{V}_2} \eta \xi \tilde{U}_2, \tilde{Z}) + g_1(\mathcal{T}_{\tilde{U}_2} \eta \tilde{V}_2 - \mathcal{T}_{\tilde{V}_2} \eta \tilde{U}_2, F\mathfrak{A}\tilde{Z} + \xi\mathfrak{B}\tilde{Z}) \\ &+ \frac{1}{\lambda^2} \{g_2(\nabla_{\tilde{U}_2}^\Psi \Psi_* \eta \tilde{V}_2 - \nabla_{\tilde{V}_2}^\Psi \Psi_* \eta \tilde{U}_2, \Psi_* \eta \mathfrak{B}\tilde{Z})\}. \end{aligned}$$

for any $\tilde{U}_2, \tilde{V}_2 \in \Gamma(\mathfrak{D}^{\theta_2})$ and $\tilde{Z} \in \Gamma(\mathfrak{D}^{\mathfrak{x}} \oplus \mathfrak{D}^{\theta_\perp})$.

Proof. By using equations (2.2), (2.3), (2.13) and (3.3), we have

$$g_1([\tilde{U}_2, \tilde{V}_2], \tilde{Z}) = -g_1(\nabla_{\tilde{V}_2} \xi^2 \tilde{U}_2, \tilde{Z}) - g_1(\nabla_{\tilde{V}_2} \eta \xi \tilde{U}_2, \tilde{Z}) + g_1(\nabla_{\tilde{U}_2} \xi^2 \tilde{V}_2, \tilde{Z}) + g_1(\nabla_{\tilde{U}_2} \eta \xi \tilde{V}_2, \tilde{Z}) + g_1(\nabla_{\tilde{U}_2} \eta \tilde{V}_2 - \nabla_{\tilde{V}_2} \eta \tilde{U}_2, F\tilde{Z}),$$

for any $\tilde{U}_2, \tilde{V}_2 \in \Gamma(\mathfrak{D}^{\theta_2})$ and $\tilde{Z} \in \Gamma(\mathfrak{D}^{\mathfrak{X}} \oplus \mathfrak{D}^{\theta_1})$. From equations (2.8) and Lemma 3.3, we get

$$\begin{aligned} \sin^2 \theta_2 g_1([\tilde{U}_2, \tilde{V}_2], \tilde{Z}) = & g_1(\mathcal{T}_{\tilde{U}_2} \eta \tilde{V}_2 - \mathcal{T}_{\tilde{V}_2} \eta \tilde{U}_2, F\mathfrak{A}\tilde{Z} + \xi\mathfrak{B}\tilde{Z}) \\ & + g_1(\mathcal{H}\nabla_{\tilde{U}_2} \eta \tilde{V}_2 - \mathcal{H}\nabla_{\tilde{V}_2} \eta \tilde{U}_2, \eta\mathfrak{B}\tilde{Z}) \\ & + g_1(\mathcal{T}_{\tilde{U}_2} \eta \xi \tilde{V}_2 - \mathcal{T}_{\tilde{V}_2} \eta \xi \tilde{U}_2, \tilde{Z}). \end{aligned}$$

Since Ψ is CQBS submersion, using conformality condition with equation (2.14), we finally get

$$\begin{aligned} \sin^2 \theta_2 g_1([\tilde{U}_2, \tilde{V}_2], \tilde{Z}) = & \frac{1}{\lambda^2} \{g_2((\nabla\Psi_*)(\tilde{U}_2, \eta\tilde{V}_2) - (\nabla\Psi_*)(\tilde{V}_2, \eta\tilde{U}_2), \Psi_*\eta\mathfrak{B}\tilde{Z})\} \\ & + \frac{1}{\lambda^2} \{g_2(\nabla_{\tilde{U}_2}^{\Psi} \Psi_*\eta\tilde{V}_2 - \nabla_{\tilde{V}_2}^{\Psi} \Psi_*\eta\tilde{U}_2, \Psi_*\eta\mathfrak{B}\tilde{Z})\} \\ & + g_1(\mathcal{T}_{\tilde{U}_2} \eta \tilde{V}_2 - \mathcal{T}_{\tilde{V}_2} \eta \tilde{U}_2, F\mathfrak{A}\tilde{Z} + \xi\mathfrak{B}\tilde{Z}) \\ & + g_1(\mathcal{T}_{\tilde{U}_2} \eta \xi \tilde{V}_2 - \mathcal{T}_{\tilde{V}_2} \eta \xi \tilde{U}_2, \tilde{Z}) \end{aligned}$$

This completes the proof of the theorem.

Since, the invariant distribution is mutually orthogonal to the slant distributions in accordance with the concept of CQBS-submersion, this led us to investigate the necessary and sufficient condition for the invariant distribution to be integrable.

Theorem 4.3. Let $\Psi: (\bar{Q}_1, g_1, F) \rightarrow (\bar{Q}_2, g_2)$ be a CQBS submersion, where (\bar{Q}_1, g_1, F) a LPR manifold and (\bar{Q}_2, g_2) a Riemannian manifold. Then the invariant distribution $\mathfrak{D}^{\mathfrak{X}}$ is integrable if and only if

$$\begin{aligned} & g_1(\mathcal{T}_{\tilde{U}} \xi \mathfrak{A}\tilde{V} - \mathcal{T}_{\tilde{V}} \xi \mathfrak{A}\tilde{U}, \eta\mathfrak{B}\tilde{Z} + \eta\mathfrak{C}\tilde{W}) \\ & - g_1(\mathcal{V}\nabla_{\tilde{U}} \xi \mathfrak{A}\tilde{V} - \mathcal{V}\nabla_{\tilde{V}} \xi \mathfrak{A}\tilde{U}, \xi\mathfrak{B}\tilde{Z} + \xi\mathfrak{C}\tilde{Z}) = 0, \end{aligned} \tag{4.2}$$

for any $\tilde{U}, \tilde{V} \in \Gamma(\mathfrak{D}^{\mathfrak{X}})$ and $\tilde{Z} \in \Gamma(\mathfrak{D}^{\theta_1} \oplus \mathfrak{D}^{\theta_2})$.

Proof. For all $\tilde{U}, \tilde{V} \in \Gamma(\mathfrak{D}^{\mathfrak{X}})$ and $\tilde{Z} \in \Gamma(\mathfrak{D}^{\theta_1} \oplus \mathfrak{D}^{\theta_2})$ with using equations (2.2), (2.13), (2.7) and decomposition (3.2), we have

$$g_1([\tilde{U}, \tilde{V}], \tilde{Z}) = g_1(\nabla_{\tilde{U}} \xi \mathfrak{A}\tilde{V}, F\mathfrak{B}\tilde{Z} + F\mathfrak{C}\tilde{Z}) - g_1(\nabla_{\tilde{V}} \xi \mathfrak{A}\tilde{U}, F\mathfrak{B}\tilde{Z} + F\mathfrak{C}\tilde{Z}).$$

By using equation (3.3), we finally have

$$g_1([\tilde{U}, \tilde{V}], \tilde{Z}) = g_1(\mathcal{J}_{\tilde{U}}\xi\mathfrak{A}\tilde{V} - \mathcal{J}_{\tilde{V}}\xi\mathfrak{A}\tilde{U}, \eta\mathfrak{B}\tilde{Z} + \eta\mathfrak{C}\tilde{Z}) \\ + g_1(\mathcal{V}\nabla_{\tilde{U}}\xi\mathfrak{A}\tilde{V} - \mathcal{V}\mathcal{A}_{\tilde{V}}\xi\mathfrak{A}\tilde{U}, \xi\mathfrak{B}\tilde{Z} + \xi\mathfrak{C}\tilde{Z}).$$

This completes the proof of theorem.

After discussing the prerequisites for distribution's integrability, it is time to examine the necessary and sufficient conditions that must also exist in order for distributions to be totally geodesic. We begin by looking at the condition of totally geodesicness for invariant distribution.

Theorem 4.4. Let $\Psi: (\bar{Q}_1, g_1, F) \rightarrow (\bar{Q}_2, g_2)$ be a CQBS submersion, where (\bar{Q}_1, g_1, F) a LPR manifold and (\bar{Q}_2, g_2) a Riemannian manifold. Then invariant distribution $\mathfrak{D}^{\mathfrak{x}}$ defines totally geodesic foliation on \bar{Q}_1 if and only if

- (i) $\lambda^{-2}g_2\left((\nabla\Psi_*)(\tilde{U}, F\tilde{V}), \Psi_*\eta\tilde{Z}\right) = g_1(\mathcal{V}\nabla_{\tilde{U}}F\tilde{V}, \xi\tilde{Z})$
 - (ii) $\lambda^{-2}g_2\left((\nabla\Psi_*)(\tilde{U}, F\tilde{V}), \Psi_*L\tilde{X}\right) = g_1(\mathcal{V}\nabla_{\tilde{U}}F\tilde{V}, P\tilde{X}),$
- for any $\tilde{U}, \tilde{V} \in \Gamma(\mathfrak{D}^{\mathfrak{x}})$ and $\tilde{Z} \in \Gamma(\mathfrak{D}^{\theta_1} \oplus \mathfrak{D}^{\theta_2})$.

Proof. For any $\tilde{U}, \tilde{V} \in \Gamma(\mathfrak{D}^{\mathfrak{x}})$ and $\tilde{Z} \in \Gamma(\mathfrak{D}^{\theta_1} \oplus \mathfrak{D}^{\theta_2})$ with using equations (2.2), (2.3), (2.13) and (3.3), we may write

$$g_1(\nabla_{\tilde{U}}\tilde{V}, \tilde{Z}) = g_1(\mathcal{V}\nabla_{\tilde{U}}F\tilde{V}, \xi\tilde{Z}) + g_1(\mathcal{J}_{\tilde{U}}F\tilde{V}, \eta\tilde{Z}).$$

By using the conformality of Ψ with equation (2.14), we get

$$g_1(\nabla_{\tilde{U}}\tilde{V}, \tilde{Z}) = g_1(\mathcal{V}\nabla_{\tilde{U}}F\tilde{V}, \xi\tilde{Z}) - \lambda^{-2}g_2\left((\nabla\Psi_*)(\tilde{U}, F\tilde{V}), \Psi_*\eta\tilde{Z}\right).$$

On the other hand, using equations (2.2), (2.3) and (2.13) with conformality of Ψ , we finally have

$$g_1(\nabla_{\tilde{U}}\tilde{V}, \tilde{X}) = g_1(\mathcal{V}\nabla_{\tilde{U}}F\tilde{V}, P\tilde{X}) - \lambda^{-2}g_2\left((\nabla\Psi_*)(\tilde{U}, F\tilde{V}), \Psi_*L\tilde{X}\right).$$

This completes the proof of the theorem.

In similar way, we can discuss the geometry of leaves of slant distribution \mathfrak{D}^{θ_1} as follows:

Theorem 4.5. Let Ψ be a CQBS submersion from $LPR(\bar{Q}_1, g_1, F)$ onto a Riemannian manifold (\bar{Q}_2, g_2) . Then slant distribution \mathfrak{D}^{θ_1} defines totally geodesic foliation on \bar{Q}_1 if and only if

$$\begin{aligned} & \frac{1}{\lambda^2}g_2\left((\nabla\Psi_*)(\tilde{Z}, \eta\mathfrak{B}\tilde{W}), \Psi_*\eta\mathfrak{C}\tilde{U}\right) - \frac{1}{\lambda^2}g_2\left(\nabla_{\tilde{Z}}^{\Psi}\Psi_*\eta\mathfrak{B}\tilde{W}, \Psi_*\eta\mathfrak{C}\tilde{U}\right) \\ & = g_1(\mathcal{T}_{\tilde{Z}}\eta\xi\mathfrak{B}\tilde{W}, \tilde{U}) - g_1(\mathcal{T}_{\tilde{Z}}\eta\mathfrak{B}\tilde{W}, F\mathfrak{A}\tilde{U}) \\ & \quad - g_1(\mathcal{T}_{\tilde{Z}}\eta\mathfrak{B}\tilde{W}, \xi\mathfrak{C}\tilde{U}) - \cos^2\theta_1g_1(\mathcal{V}\nabla_{\tilde{Z}}\mathfrak{B}\tilde{W}, \tilde{U}) \end{aligned} \tag{4.3}$$

and

$$\begin{aligned} & \frac{1}{\lambda^2}g_2\left((\nabla\Psi_*)(\tilde{Z}, \eta\xi\mathfrak{B}\tilde{W}), \Psi_*\tilde{X}\right) + \frac{1}{\lambda^2}g_2\left((\nabla\Psi_*)(\tilde{Z}, \eta\xi\mathfrak{B}\tilde{W}), \Psi_*L\tilde{X}\right) \\ & = \frac{1}{\lambda^2}g_2\left((\nabla\Psi_*)(\tilde{Z}, \eta\xi\mathfrak{B}\tilde{W}), \Psi_*\tilde{X}\right) - \frac{1}{\lambda^2}g_2\left((\nabla\Psi_*)(\tilde{Z}, \eta\xi\mathfrak{B}\tilde{W}), \Psi_*L\tilde{X}\right) \\ & \quad + \cos^2\theta_1g_1(\nabla_{\tilde{Z}}\mathfrak{B}\tilde{W}, \tilde{X}) + g_1(\mathcal{T}_{\tilde{Z}}\eta\xi\mathfrak{B}\tilde{W}, P\tilde{X}), \end{aligned} \tag{4.4}$$

for any $\tilde{Z}, \tilde{W} \in \Gamma(\mathfrak{D}^{\theta_1})$, $\tilde{U} \in \Gamma(\mathfrak{D}^{\mathfrak{x}} \oplus \mathfrak{D}^{\theta_2})$ and $\tilde{X} \in \Gamma(\ker\Psi_*)^{\perp}$.

Proof. By using equations (2.2), (2.3), (2.13) and (3.3), we get

$$g_1(\nabla_{\tilde{Z}}\tilde{W}, \tilde{U}) = g_1(\nabla_{\tilde{Z}}\eta\mathfrak{B}\tilde{W}, F(\mathfrak{A}\tilde{U} + \mathfrak{C}\tilde{U})) + g_1(F\nabla_{\tilde{Z}}\xi\mathfrak{B}\tilde{W}, \tilde{U}),$$

for $\tilde{Z}, \tilde{W} \in \Gamma(\mathfrak{D}^{\theta_1})$ and $\tilde{U} \in \Gamma(\mathfrak{D}^{\mathfrak{x}} \oplus \mathfrak{D}^{\theta_2})$. Again using equations (2.2), (2.3), (2.13), (3.3), (2.8) with Lemma 3.2, we may write

$$\begin{aligned} g_1(\nabla_{\tilde{Z}}\tilde{W}, \tilde{U}) = & \cos^2\theta_1g_1(\nabla_{\tilde{Z}}\mathfrak{B}\tilde{W}, \tilde{U}) + g_1(\mathcal{T}_{\tilde{Z}}\eta\xi\mathfrak{B}\tilde{W}, \tilde{U}) + g_1(\mathcal{T}_{\tilde{Z}}\eta\mathfrak{B}\tilde{W}, F\mathfrak{A}\tilde{U}) \\ & + g_1(\mathcal{T}_{\tilde{Z}}\eta\mathfrak{B}\tilde{W}, \xi\mathfrak{C}\tilde{U}) + g_1(\mathcal{H}\nabla_{\tilde{Z}}\eta\mathfrak{B}\tilde{W}, \eta\mathfrak{C}\tilde{U}). \end{aligned}$$

Since, Ψ is conformal, using Lemma 2.1 with equation (2.14), we have

$$\begin{aligned}
 g_1(\nabla_{\tilde{Z}}\tilde{W}, \tilde{U}) = & \cos^2 \theta_1 g_1(\nabla_{\tilde{Z}}\mathfrak{B}\tilde{W}, \tilde{U}) + g_1(\mathcal{T}_{\tilde{Z}}\eta\xi\mathfrak{B}\tilde{W}, \tilde{U}) + g_1(\mathcal{T}_{\tilde{Z}}\eta\mathfrak{B}\tilde{W}, F\mathfrak{U}\tilde{U}) \\
 & + g_1(\mathcal{T}_{\tilde{Z}}\eta\mathfrak{B}\tilde{W}, \xi\mathfrak{C}\tilde{U}) + \frac{1}{\lambda^2} g_2(\nabla_{\tilde{Z}}^\Psi\Psi_*\eta\mathfrak{B}\tilde{W}, \Psi_*\eta\mathfrak{C}\tilde{U}) \\
 & - \frac{1}{\lambda^2} g_2\left((\nabla\Psi_*)(\tilde{Z}, \eta\mathfrak{B}\tilde{W}), \Psi_*\eta\mathfrak{C}\tilde{U}\right).
 \end{aligned}$$

On the other hand, for $\tilde{Z}, \tilde{W} \in \Gamma(\mathfrak{D}^{\theta_1})$ and $\tilde{X} \in \Gamma(\ker \Psi_*)^\perp$, with using equations (2.2), (2.3), (2.13) and (3.3), we get

$$g_1(\nabla_{\tilde{Z}}\tilde{W}, \tilde{X}) = g_1(\nabla_{\tilde{Z}}\xi\mathfrak{B}\tilde{W}, F\tilde{X}) + g_1(\nabla_{\tilde{Z}}\eta\mathfrak{B}\tilde{W}, F\tilde{X}).$$

From Lemma 3.2 with equations (2.8) and (3.6), the above equation takes the form

$$\begin{aligned}
 g_1(\nabla_{\tilde{Z}}\tilde{W}, \tilde{X}) = & \cos^2 \theta_1 g_1(\nabla_{\tilde{Z}}\tilde{B}\tilde{W}, \tilde{X}) + g_1(\mathcal{H}\nabla_{\tilde{Z}}\eta\xi\mathfrak{B}\tilde{W}, \tilde{X}) \\
 & + g_1(\mathcal{T}_{\tilde{Z}}\eta\xi\mathfrak{B}\tilde{W}, P\tilde{X}) + g_1(\mathcal{H}\nabla_{\tilde{Z}}\eta\xi\mathfrak{B}\tilde{W}, L\tilde{X}).
 \end{aligned}$$

Since Ψ is conformal and from equation (2.14), we have

$$\begin{aligned}
 g_1(\nabla_{\tilde{Z}}\tilde{W}, \tilde{X}) = & -\frac{1}{\lambda^2} g_2\left((\nabla\Psi_*)(\tilde{Z}, \eta\xi\mathfrak{B}\tilde{W}), \Psi_*\tilde{X}\right) + \frac{1}{\lambda^2} g_2(\nabla_{\tilde{Z}}^\Psi\Psi_*\eta\xi\mathfrak{B}\tilde{W}, \Psi_*\tilde{X}) \\
 & - \frac{1}{\lambda^2} g_2\left((\nabla\Psi_*)(\tilde{Z}, \eta\xi\mathfrak{B}\tilde{W}), \Psi_*L\tilde{X}\right) + \frac{1}{\lambda^2} g_2(\nabla_{\tilde{Z}}^\Psi\Psi_*\eta\xi\mathfrak{B}\tilde{W}, \Psi_*L\tilde{X}) \\
 & + \cos^2 \theta_1 g_1(\nabla_{\tilde{Z}}\tilde{W}, \tilde{X}) + g_1(\mathcal{T}_{\tilde{Z}}\eta\xi\mathfrak{B}\tilde{W}, P\tilde{X}).
 \end{aligned}$$

This completes the proof of theorem.

Theorem 4.6. Let $\Psi: (\bar{Q}_1, g_1, F) \rightarrow (\bar{Q}_2, g_2)$ be a CQBS submersion, where (\bar{Q}_1, g_1, F) a LPR manifold and (\bar{Q}_2, g_2) a Riemannian manifold. Then slant distribution \mathfrak{D}^{θ_2} defines totally geodesic foliation on \bar{Q}_1 if and only if

$$\begin{aligned}
 & \frac{1}{\lambda^2} g_2\left((\nabla\Psi_*)(\tilde{Z}, \eta\mathfrak{B}\tilde{W}), \Psi_*\eta\mathfrak{C}\tilde{V}\right) - \frac{1}{\lambda^2} g_2(\nabla_{\tilde{Z}}^\Psi\Psi_*\eta\mathfrak{B}\tilde{W}, \Psi_*\eta\mathfrak{C}\tilde{V}) \\
 & = g_1(\mathcal{T}_{\tilde{Z}}\eta\xi\mathfrak{B}\tilde{W}, \tilde{V}) - g_1(\mathcal{T}_{\tilde{Z}}\eta\mathfrak{B}\tilde{W}, F\mathfrak{U}\tilde{V}) \\
 & - g_1(\mathcal{T}_{\tilde{Z}}\eta\mathfrak{B}\tilde{W}, \xi\mathfrak{C}\tilde{V}) - \cos^2 \theta_1 g_1(\mathcal{V}\nabla_{\tilde{Z}}\mathfrak{B}\tilde{W}, \tilde{V}),
 \end{aligned} \tag{4.6}$$

and

$$\begin{aligned} & \frac{1}{\lambda^2} g_2 \left((\nabla \Psi_*) (\tilde{Z}, \eta \xi \mathfrak{B} \tilde{W}), \Psi_* \tilde{Y} \right) + \frac{1}{\lambda^2} g_2 \left((\nabla \Psi_*) (\tilde{Z}, \eta \xi \mathfrak{B} \tilde{W}), \Psi_* L \tilde{Y} \right) \\ &= \frac{1}{\lambda^2} g_2 \left((\nabla \Psi_*) (\tilde{Z}, \eta \xi \mathfrak{B} \tilde{W}), \Psi_* \tilde{Y} \right) - \frac{1}{\lambda^2} g_2 \left((\nabla \Psi_*) (\tilde{Z}, \eta \xi \mathfrak{B} \tilde{W}), \Psi_* L \tilde{Y} \right) \\ & \quad + \cos^2 \theta_2 g_1 (\nabla_{\tilde{Z}} \mathfrak{B} \tilde{W}, \tilde{Y}) + g_1 (T_{\tilde{Z}} \eta \xi \mathfrak{B} \tilde{W}, P \tilde{Y}), \end{aligned}$$

for any $\tilde{Z}, \tilde{W} \in \Gamma(\mathfrak{D}^{\theta_2}), \tilde{V} \in \Gamma(\mathfrak{D}^{\mathfrak{I}} \oplus \mathfrak{D}^{\theta_1})$ and $\tilde{Y} \in \Gamma(\ker \Psi_*)^\perp$.

Proof. The proof of above theorem is similar to the proof of Theorem 4.5.

Since, Ψ is CQBS-submersion, its vertical and horizontal distribution are $(\ker \Psi$ and $(\ker \Psi_*)^\perp$, respectively. Now, we examine the necessary and sufficient conditions under which distributions defines totally geodesic foliation on \bar{Q}_1 . With regards to the totally geodesicness of horizontal distribution, we have

Theorem 4.7. Let Ψ be a CQBS submersion from LPR manifold (\bar{Q}_1, g_1, F) onto a Riemannian manifold (\bar{Q}_2, g_2) . Then $(\ker \Psi_*)^\perp$ defines totally geodesic

foliation on \bar{Q}_1 if and only if

$$\begin{aligned} & \frac{1}{\lambda^2} \{ g_2 (\nabla_{\tilde{X}}^\Psi \Psi_* \eta \mathfrak{B} \tilde{Y} + \nabla_{\tilde{X}}^\Psi \Psi_* \eta \mathfrak{C} \tilde{Y}, \Psi_* \eta \tilde{Z}) \} \\ &= g_1 (\mathcal{A}_{\tilde{X}} \eta \xi \mathfrak{B} \tilde{Y} + \mathcal{A}_{\tilde{X}} \eta \xi \mathfrak{C} \tilde{Y} + \mathcal{A}_{\tilde{X}} \eta \xi \mathfrak{U} \tilde{Y} + \mathcal{V} \nabla_{\tilde{X}} \mathfrak{U} \tilde{Y}, \tilde{Z}) \\ & \quad + \cos^2 \theta_1 g_1 (\mathcal{V} \nabla_{\tilde{X}} \mathfrak{B} \tilde{Y}, \tilde{Z}) + \cos^2 \theta_2 g_1 (\mathcal{V} \nabla_{\tilde{X}} \mathfrak{C} \tilde{Y}, \tilde{Z}) \\ & \quad + g_1 (\eta \mathfrak{B} \tilde{Y}, \eta \tilde{Z}) g_1 (\tilde{X}, \text{grad ln } \lambda) + g_1 (\tilde{X}, \eta \tilde{Z}) g_1 (\eta \mathfrak{B} \tilde{Y}, \text{grad ln } \lambda) \\ & \quad - g_1 (\tilde{X}, \eta \mathfrak{B} \tilde{Y}) g_1 (\eta \tilde{Z}, \text{grad ln } \lambda) + g_1 (\eta \mathfrak{C} \tilde{Y}, \eta \tilde{Z}) g_1 (\tilde{X}, \text{grad ln } \lambda) \\ & \quad + g_1 (\tilde{X}, \eta \tilde{Z}) g_1 (\eta \mathfrak{C} \tilde{Y}, \text{grad ln } \lambda) - g_1 (\tilde{X}, \eta \mathfrak{C} \tilde{Y}) g_1 (\eta \tilde{Z}, \text{grad ln } \lambda), \end{aligned} \tag{4.8}$$

for any $\tilde{X}, \tilde{Y} \in \Gamma(\ker \Psi_*)^\perp$ and $\tilde{Z} \in \Gamma(\ker \Psi_*)$.

Proof. For any $\tilde{X}, \tilde{Y} \in \Gamma(\ker \Psi_*)^\perp$ and $\tilde{Z} \in \Gamma(\ker \Psi_*)$ with using equations (2.2), (2.3) and (2.13) with decomposition (3.2), we get

$$g_1(\nabla_{\tilde{X}}\tilde{Y}, \tilde{Z}) = g_1(\nabla_{\tilde{X}}F(\mathfrak{A}\tilde{Y}), F\tilde{Z}) + g_1(\nabla_{\tilde{X}}F(\mathfrak{B}\tilde{Y}), F\tilde{Z}) + g_1(\nabla_{\tilde{X}}F(\mathfrak{C}\tilde{Y}), F\tilde{Z}).$$

From equations (3.3) and (2.9) with Lemma 3.2, we have

$$\begin{aligned} g_1(\nabla_{\tilde{X}}\tilde{Y}, \tilde{Z}) = & g_1(\mathcal{V}\nabla_{\tilde{X}}\mathfrak{A}\tilde{Y}, \tilde{Z}) + \cos^2 \theta_1 g_1(\nabla_{\tilde{X}}\mathfrak{B}\tilde{Y}, \tilde{Z}) + \cos^2 \theta_2 g_1(\nabla_{\tilde{X}}\mathfrak{C}\tilde{Y}, \tilde{Z}) \\ & + g_1(\nabla_{\tilde{X}}\eta\xi\mathfrak{B}\tilde{Y}, \tilde{Z}) + g_1(\nabla_{\tilde{X}}\eta\mathfrak{B}\tilde{Y}, F\tilde{Z}) + g_1(\nabla_{\tilde{X}}\eta\xi\mathfrak{C}\tilde{Y}, \tilde{Z}) \\ & + g_1(\nabla_{\tilde{X}}\eta\mathfrak{C}\tilde{Y}, F\tilde{Z}) + g_1(\nabla_{\tilde{X}}\eta\xi\mathfrak{A}\tilde{Y}, \tilde{Z}) \end{aligned}$$

By using the equations (3.3) and (2.10), we get

$$\begin{aligned} g_1(\nabla_{\tilde{X}}\tilde{Y}, \tilde{Z}) = & g_1(\mathcal{V}\nabla_{\tilde{X}}\mathfrak{A}\tilde{Y} + \cos^2 \theta_1 \mathcal{V}\nabla_{\tilde{X}}\mathfrak{B}\tilde{Y} + \cos^2 \theta_2 \mathcal{V}\nabla_{\tilde{X}}\mathfrak{C}\tilde{Y}, \tilde{Z}) \\ & + g_1(\mathcal{A}_{\tilde{X}}\eta\xi\mathfrak{A}\tilde{Y} + \mathcal{A}_{\tilde{X}}\eta\xi\mathfrak{B}\tilde{Y} + \mathcal{A}_{\tilde{X}}\eta\xi\mathfrak{C}\tilde{Y}, \tilde{Z}) \\ & + g_1(\mathcal{H}\nabla_{\tilde{X}}\eta\mathfrak{B}\tilde{Y} + \mathcal{H}\nabla_{\tilde{X}}\eta\mathfrak{C}\tilde{Y}, \eta\tilde{Z}) \\ & + g_1(\mathcal{A}_{\tilde{X}}\eta\mathfrak{B}\tilde{Y} + \mathcal{A}_{\tilde{X}}\eta\mathfrak{C}\tilde{Y}, \xi\tilde{Z}). \end{aligned}$$

From formula (2.14), we yields that

$$\begin{aligned} g_1(\nabla_{\tilde{X}}\tilde{Y}, \tilde{Z}) = & g_1(\mathcal{V}\nabla_{\tilde{X}}\mathfrak{A}\tilde{Y} + \cos^2 \theta_1 \mathcal{V}\nabla_{\tilde{X}}\mathfrak{B}\tilde{Y} + \cos^2 \theta_2 \mathcal{V}\nabla_{\tilde{X}}\mathfrak{C}\tilde{Y}, \tilde{Z}) \\ & + g_1(\mathcal{A}_{\tilde{X}}\eta\xi\mathfrak{A}\tilde{Y} + \mathcal{A}_{\tilde{X}}\eta\xi\mathfrak{B}\tilde{Y} + \mathcal{A}_{\tilde{X}}\eta\xi\mathfrak{C}\tilde{Y}, \tilde{Z}) \\ & + \frac{1}{\lambda^2} \{g_2(\nabla_{\tilde{X}}^\Psi \Psi_*\eta\mathfrak{B}\tilde{Y} + \nabla_{\tilde{X}}^\Psi \Psi_*\eta\mathfrak{C}\tilde{Y}, \Psi_*\eta\tilde{Z})\} \\ & - \frac{1}{\lambda^2} \{g_2((\nabla\Psi_*)(\tilde{X}, \eta\mathfrak{B}\tilde{Y}) + (\nabla\Psi_*)(\tilde{X}, \eta\mathfrak{C}\tilde{Y}), \Psi_*\eta\tilde{Z})\} \end{aligned}$$

Since Ψ is conformal submersion, then we finally get

$$\begin{aligned}
 g_1(\nabla_{\tilde{X}}\tilde{Y}, \tilde{Z}) &= -g_1(\eta\mathfrak{B}\tilde{Y}, \eta\tilde{Z})g_1(\tilde{X}, \text{grad ln } \lambda) - g_1(\tilde{X}, \eta\tilde{Z})g_1(\eta\mathfrak{B}\tilde{Y}, \text{grad ln } \lambda) \\
 &+ g_1(\tilde{X}, \eta\mathfrak{B}\tilde{Y})g_1(\eta\tilde{Z}, \text{grad ln } \lambda) - g_1(\eta\mathfrak{C}\tilde{Y}, \eta\tilde{Z})g_1(\tilde{X}, \text{grad ln } \lambda) \\
 &- g_1(\tilde{X}, \eta\tilde{Z})g_1(\eta\mathfrak{C}\tilde{Y}, \text{grad ln } \lambda) + g_1(\tilde{X}, \eta\mathfrak{C}\tilde{Y})g_1(\eta\tilde{Z}, \text{grad ln } \lambda) \\
 &+ g_1(\mathcal{V}\nabla_{\tilde{X}}\mathfrak{A}\tilde{Y} + \cos^2 \theta_1 \mathcal{V}\nabla_{\tilde{X}}\mathfrak{B}\tilde{Y} + \cos^2 \theta_2 \mathcal{V}\nabla_{\tilde{X}}\mathfrak{C}\tilde{Y}, \tilde{Z}) \\
 &+ g_1(\mathcal{A}_{\tilde{X}}\eta\xi\mathfrak{A}\tilde{Y} + \mathcal{A}_{\tilde{X}}\eta\xi\mathfrak{B}\tilde{Y} + \mathcal{A}_{\tilde{X}}\eta\xi\mathfrak{C}\tilde{Y}, \tilde{Z}) \\
 &+ \frac{1}{\lambda^2} \{g_2(\nabla_{\tilde{X}}^{\Psi}\Psi_*\eta\mathfrak{B}\tilde{Y} + \nabla_{\tilde{X}}^{\Psi}\Psi_*\eta\mathfrak{C}\tilde{Y}, \Psi_*\eta\tilde{Z})\}.
 \end{aligned}$$

This completes the proof of theorem.

We can now talk about the geometry of leaves of horizontal distribution. The following theorem presents the necessary and sufficient condition under which vertical distribution defines totally geodesic foliation on \bar{Q}_1 .

Theorem 4.8. Let $\Psi: (\bar{Q}_1, g_1, F) \rightarrow (\bar{Q}_2, g_2)$ be a CQBS submersion, where (\bar{Q}_1, g_1, F) a LPR manifold and (\bar{Q}_2, g_2) a Riemannian manifold. Then $(\ker \Psi_*)$ defines totally geodesic foliation on \bar{Q}_1 if and only if

$$\begin{aligned}
 &\frac{1}{\lambda^2} \{g_2(\nabla_{\tilde{U}}^{\Psi}\Psi_*\eta\xi\mathfrak{B}\tilde{V} + \nabla_{\tilde{U}}^{\Psi}\Psi_*\eta\xi\mathfrak{C}\tilde{V}, \Psi_*\tilde{X})\} \\
 &= g_1(\mathcal{J}_{\tilde{U}}\mathfrak{A}\tilde{V} + \cos^2 \theta_1 \mathcal{J}_{\tilde{U}}\mathfrak{B}\tilde{V} + \cos^2 \theta_2 \mathcal{J}_{\tilde{U}}\mathfrak{C}\tilde{V}) + g_1(\mathcal{J}_{\tilde{U}}\eta\tilde{V}, P\tilde{X}) \\
 &\quad - \frac{1}{\lambda^2} \{g_2((\nabla\Psi_*)(\tilde{U}, \eta\xi\mathfrak{B}\tilde{V}) + (\nabla\Psi_*)(\tilde{U}, \eta\xi\mathfrak{C}\tilde{V}), \Psi_*\tilde{X})\} \\
 &\quad + \frac{1}{\lambda^2} \{g_2(\nabla_{\tilde{U}}^{\Psi}\Psi_*\eta\tilde{V} - (\nabla\Psi_*)(\tilde{U}, \eta\tilde{V}), \Psi_*L\tilde{X})\},
 \end{aligned} \tag{4.9}$$

for any $\tilde{U}, \tilde{V} \in \Gamma(\ker \Psi_*)$ and $\tilde{X} \in \Gamma(\ker \Psi_*)^\perp$.

Proof. For any $\tilde{U}, \tilde{V} \in \Gamma(\ker \Psi_*)$ and $\tilde{X} \in \Gamma(\ker \Psi_*)^\perp$ with using equations (2.2), (2.3), (2.13) with decomposition (3.2), we get

$$g_1(\nabla_{\tilde{U}}\tilde{V}, \tilde{X}) = g_1(\nabla_{\tilde{U}}F\mathfrak{A}\tilde{V}, F\tilde{X}) + g_1(\nabla_{\tilde{U}}F\mathfrak{B}\tilde{V}, F\tilde{X}) + g_1(\nabla_{\tilde{U}}F\mathfrak{C}\tilde{V}, F\tilde{X}).$$

By using equations (3.3) with Lemma 3.2 and Lemma 3.3, we have

$$g_1(\nabla_{\tilde{U}}\tilde{V}, \tilde{X}) = g_1(\nabla_{\tilde{U}}\mathfrak{A}\tilde{V}, \tilde{X}) + \cos^2 \theta_1 g_1(\nabla_{\tilde{U}}\mathfrak{B}\tilde{V}, \tilde{X}) + \cos^2 \theta_2 g_1(\nabla_{\tilde{U}}\mathfrak{C}\tilde{V}, \tilde{X}) \\ + g_1(\nabla_{\tilde{U}}\eta\mathfrak{B}\tilde{V}, F\tilde{X}) + g_1(\nabla_{\tilde{U}}\eta\xi\mathfrak{B}\tilde{V}, \tilde{X}) + g_1(\nabla_{\tilde{U}}\eta\xi\mathfrak{C}\tilde{V}, \tilde{X}) \\ + g_1(\nabla_{\tilde{U}}\eta\mathfrak{C}\tilde{V}, F\tilde{X}).$$

From equations (2.7), (2.8) and (3.6), we may yields

$$g_1(\nabla_{\tilde{U}}\tilde{V}, \tilde{X}) = g_1(\mathcal{J}_{\tilde{U}}\mathfrak{A}\tilde{V} + \cos^2 \theta_1 \mathcal{J}_{\tilde{U}}\mathfrak{B}\tilde{V} + \cos^2 \theta_2 \mathcal{J}_{\tilde{U}}\mathfrak{C}\tilde{V}, \tilde{X}) \\ + g_1(\mathcal{H}\nabla_{\tilde{U}}\eta\xi\mathfrak{B}\tilde{V} + \mathcal{H}\nabla_{\tilde{U}}\eta\xi\mathfrak{C}\tilde{V}, \tilde{X}) \\ + g_1(\mathcal{H}\nabla_{\tilde{U}}\eta\mathfrak{B}\tilde{V} + \mathcal{H}\nabla_{\tilde{U}}\eta\mathfrak{C}\tilde{V}, L\tilde{X}) \\ + g_1(\mathcal{J}_{\tilde{U}}\eta\mathfrak{B}\tilde{V} + \mathcal{J}_{\tilde{U}}\eta\mathfrak{C}\tilde{V}, P\tilde{X})$$

From decomposition (3.2), the above equation takes the form

$$g_1(\nabla_{\tilde{U}}\tilde{V}, \tilde{X}) = g_1(\mathcal{J}_{\tilde{U}}\mathfrak{A}\tilde{V} + \cos^2 \theta_1 \mathcal{J}_{\tilde{U}}\mathfrak{B}\tilde{V} + \cos^2 \theta_2 \mathcal{J}_{\tilde{U}}\mathfrak{C}\tilde{V}, \tilde{X}) + g_1(\mathcal{J}_{\tilde{U}}\eta\tilde{V}, P\tilde{X}) \\ + g_1(\mathcal{H}\nabla_{\tilde{U}}\eta\xi\mathfrak{B}\tilde{V} + \mathcal{H}\nabla_{\tilde{U}}\eta\xi\mathfrak{C}\tilde{V}, \tilde{X}) + g_1(\mathcal{H}\nabla_{\tilde{U}}\eta\tilde{V}, L\tilde{X}).$$

Using the conformality of Ψ with equation (2.14), we have

$$g_1(\nabla_{\tilde{U}}\tilde{V}, \tilde{X}) = g_1(\mathcal{J}_{\tilde{U}}\mathfrak{A}\tilde{V} + \cos^2 \theta_1 \mathcal{J}_{\tilde{U}}\mathfrak{B}\tilde{V} + \cos^2 \theta_2 \mathcal{J}_{\tilde{U}}\mathfrak{C}\tilde{V}, \tilde{X}) + g_1(\mathcal{J}_{\tilde{U}}\eta\tilde{V}, P\tilde{X}) \\ - \frac{1}{\lambda^2} \left\{ g_2 \left((\nabla\Psi_*)(\tilde{U}, \eta\xi\mathfrak{B}\tilde{V}) + (\nabla\Psi_*)(\tilde{U}, \eta\xi\mathfrak{C}\tilde{V}), \Psi_*\tilde{X} \right) \right\} \\ - \frac{1}{\lambda^2} \left\{ g_2 (\nabla_{\tilde{U}}^{\Psi}\Psi_*\eta\xi\mathfrak{B}\tilde{V} + \nabla_{\tilde{U}}^{\Psi}\Psi_*\eta\xi\mathfrak{C}\tilde{V}, \Psi_*\tilde{X}) \right\} \\ + \frac{1}{\lambda^2} \left\{ g_2 (\nabla_{\tilde{U}}^{\Psi}\Psi_*\eta\tilde{V} - (\nabla\Psi_*)(\tilde{U}, \eta\tilde{V}), \Psi_*L\tilde{X}) \right\}.$$

This completes the proof of the theorem.

We now have some necessary and sufficient conditions for a CQBS submersion $\Psi: \bar{Q}_1 \rightarrow \bar{Q}_2$ to be totally geodesic map. In this regard, we are presenting the following theorem.

Theorem 4.9. Let Ψ be a CQBS submersion from LPR manifold (\bar{Q}_1, g_1, F) onto a Riemannian manifold (\bar{Q}_2, g_2) . Then $\Psi: (\bar{Q}_1, g_1, F) \rightarrow (\bar{Q}_2, g_2)$ is totally geodesic map if and only if

(4.10)

$$\begin{aligned}
 & \Psi_* \{ \cos^2 \theta_1 \nabla_{\tilde{U}} \mathfrak{B} \tilde{V} + \cos^2 \theta_2 \nabla_{\tilde{U}} \mathfrak{C} \tilde{V} + \nabla_{\tilde{U}} \eta \xi \mathfrak{B} \tilde{V} + \nabla_{\tilde{U}} \eta \xi \mathfrak{C} \tilde{V} \} \\
 & = \Psi_* \{ L(-\mathcal{H} \nabla_{\tilde{U}} \eta \mathfrak{B} \tilde{V} - \mathcal{H} \nabla_{\tilde{U}} \eta \mathfrak{C} \tilde{V} - \mathcal{J}_{\tilde{U}} \xi \mathfrak{A} \tilde{V}) \} \\
 & \quad - \Psi_* \{ \eta (\mathcal{J}_{\tilde{U}} \eta \mathfrak{B} \tilde{V} + \mathcal{J}_{\tilde{U}} \eta \mathfrak{C} \tilde{V} + \mathcal{V} \nabla_{\tilde{U}} \xi \mathfrak{A} \tilde{V}) \}, \\
 & \Psi_* \{ \cos^2 \theta_1 \nabla_{\tilde{X}} \mathfrak{B} \tilde{U} + \cos^2 \theta_2 \nabla_{\tilde{X}} \mathfrak{C} \tilde{U} + \nabla_{\tilde{X}} \eta \xi \mathfrak{B} \tilde{U} + \nabla_{\tilde{X}} \eta \xi \mathfrak{C} \tilde{U} \} \\
 & = -\Psi_* \{ L(\mathcal{A}_{\tilde{X}} \xi \mathfrak{A} \tilde{U} + \mathcal{H} \nabla_{\tilde{X}} \eta \mathfrak{B} \tilde{U} + \mathcal{H} \nabla_{\tilde{X}} \eta \mathfrak{C} \tilde{U}) \} \\
 & \quad - \Psi_* \{ \eta (\mathcal{V} \nabla_{\tilde{X}} \xi \mathfrak{A} \tilde{U} + \mathcal{A}_{\tilde{X}} \eta \mathfrak{B} \tilde{U} + \mathcal{A}_{\tilde{X}} \eta \mathfrak{C} \tilde{U}) \}
 \end{aligned}$$

for any $\tilde{U}, \tilde{V} \in \Gamma(\ker \Psi_*)$ and $\tilde{X}, \tilde{Y} \in \Gamma(\ker \Psi_*)^\perp$.

Proof. Now, using equations (2.14), (2.3), (2.13) and (2.1).

$$(\nabla \Psi_*)(\tilde{U}, \tilde{V}) = -\Psi_*(F \nabla_{\tilde{U}} F \tilde{V}),$$

for any $\tilde{U}, \tilde{V} \in \Gamma(\ker \Psi_*)$. From decomposition (3.2) and equation (3.3), we may write

$$\begin{aligned}
 (\nabla \Psi_*)(\tilde{U}, \tilde{V}) = & \Psi_* \{ -F \nabla_{\tilde{U}} \xi \mathfrak{A} \tilde{V} - F \nabla_{\tilde{U}} \xi \mathfrak{B} \tilde{V} - F \nabla_{\tilde{U}} \eta \mathfrak{B} \tilde{V} \\
 & - F \nabla_{\tilde{U}} \xi \mathfrak{C} \tilde{V} - F \nabla_{\tilde{U}} \eta \mathfrak{C} \tilde{V} \}.
 \end{aligned}$$

By using equations (2.7) and (2.8), the above equation takes the form

$$\begin{aligned}
 (\nabla \Psi_*)(\tilde{U}, \tilde{V}) = & \Psi_* \{ -F \mathcal{J}_{\tilde{U}} \xi \mathfrak{A} \tilde{V} - F \mathcal{V} \nabla_{\tilde{U}} \xi \mathfrak{A} \tilde{V} \} - \Psi_*(\nabla_{\tilde{U}} F \xi \mathfrak{B} \tilde{V}) \\
 & - \Psi_* \{ F \mathcal{J}_{\tilde{U}} \eta \mathfrak{B} \tilde{V} + F \mathcal{H} \nabla_{\tilde{U}} \eta \mathfrak{B} \tilde{V} \} - \Psi_*(\nabla_{\tilde{U}} F \xi \mathfrak{C} \tilde{V}) \\
 & - \Psi_* \{ F \mathcal{J}_{\tilde{U}} \eta \mathfrak{C} \tilde{V} + F \mathcal{H} \nabla_{\tilde{U}} \eta \mathfrak{C} \tilde{V} \}.
 \end{aligned}$$

Since Ψ is conformal submersion, by using Lemma 3.2 and Lemma 3.3 with equation (3.3), we finally get

$$\begin{aligned}
 (\nabla \Psi_*)(\tilde{U}, \tilde{V}) = & \Psi_* \{ L(-\mathcal{H} \nabla_{\tilde{U}} \eta \mathfrak{B} \tilde{V} - \mathcal{H} \nabla_{\tilde{U}} \eta \mathfrak{C} \tilde{V} - \mathcal{J}_{\tilde{U}} \xi \mathfrak{A} \tilde{V}) \\
 & + \eta (-\mathcal{V} \nabla_{\tilde{U}} \xi \mathfrak{A} \tilde{V} - \mathcal{J}_{\tilde{U}} \xi \mathfrak{B} \tilde{V} - \mathcal{J}_{\tilde{U}} \xi \mathfrak{C} \tilde{V}) \} \\
 & - \Psi_* \{ \cos^2 \theta_1 \nabla_{\tilde{U}} \mathfrak{B} \tilde{V} + \cos^2 \theta_2 \nabla_{\tilde{U}} \mathfrak{C} \tilde{V} + \nabla_{\tilde{U}} \eta \xi \mathfrak{B} \tilde{V} + \nabla_{\tilde{U}} \eta \xi \mathfrak{C} \tilde{V} \}
 \end{aligned}$$

From this, the (i) part of theorem proved. On the other hand, for $\tilde{U} \in \Gamma(\ker \Psi_*)$ and $\tilde{X} \in \Gamma(\ker \Psi_*)^\perp$ with using equations (2.14), (2.3), (2.13) and (2.1), we can write

$$(\nabla \Psi_*)(\tilde{X}, \tilde{U}) = -\Psi_*(F\nabla_{\tilde{X}}F\tilde{U}).$$

By using decomposition (3.2) with equation (3.3), we have

$$(\nabla \Psi_*)(\tilde{X}, \tilde{U}) = -\Psi_*\{F(\nabla_{\tilde{X}}\xi\mathfrak{A}\tilde{U} + \nabla_{\tilde{X}}\xi\mathfrak{B}\tilde{U} + \nabla_{\tilde{X}}\eta\mathfrak{B}\tilde{U} + \nabla_{\tilde{X}}\xi\mathfrak{C}\tilde{U} + \nabla_{\tilde{X}}\eta\mathfrak{C}\tilde{U})\}.$$

By taking account the fact from equations (2.9) and (2.10), we get

$$\begin{aligned} (\nabla \Psi_*)(\tilde{X}, \tilde{U}) = & -\Psi_*\{F(\mathcal{A}_{\tilde{X}}\xi\mathfrak{A}\tilde{U} + \mathcal{V}\nabla_{\tilde{X}}\xi\mathfrak{A}\tilde{U} + \nabla_{\tilde{X}}F\xi\mathfrak{B}\tilde{U} \\ & + F(\mathcal{H}\nabla_{\tilde{X}}\eta\mathfrak{B}\tilde{U} + \mathcal{A}_{\tilde{X}}\eta\mathfrak{B}\tilde{U}) + \nabla_{\tilde{X}}F\xi\mathfrak{C}\tilde{U} \\ & + F(\mathcal{H}\nabla_{\tilde{X}}\eta\mathfrak{C}\tilde{U} + \mathcal{A}_{\tilde{X}}\eta\mathfrak{C}\tilde{U})\}. \end{aligned}$$

Finally, from conformality of Riemannian submersion Ψ and Lemma 3.2, Lemma 3.3, we can write

$$\begin{aligned} (\nabla \Psi_*)(\tilde{X}, \tilde{U}) = & -\Psi_*\{L(\mathcal{A}_{\tilde{X}}\xi\mathfrak{A}\tilde{U} + \mathcal{H}\nabla_{\tilde{X}}\eta\mathfrak{B}\tilde{U} + \mathcal{H}\nabla_{\tilde{X}}\eta\mathfrak{C}\tilde{U})\} \\ & -\Psi_*\{\eta(\mathcal{V}\nabla_{\tilde{X}}\xi\mathfrak{A}\tilde{U} + \mathcal{A}_{\tilde{X}}\eta\mathfrak{B}\tilde{U} + \mathfrak{A}_{\tilde{X}}\eta\mathfrak{C}\tilde{U})\} \\ & -\Psi_*(\cos^2 \theta_1 \nabla_{\tilde{X}}\mathfrak{B}\tilde{U} + \cos^2 \theta_2 \nabla_{\tilde{X}}\mathfrak{C}\tilde{U} + \nabla_{\tilde{X}}\eta\xi\mathfrak{B}\tilde{U} + \nabla_{\tilde{X}}\eta\xi\mathfrak{C}\tilde{U}). \end{aligned}$$

From which we obtain (ii) part of theorem. This completes the proof of theorem.

5 Decomposition Theorems

In this section, we recall the following result from [22] and discuss some decomposition theorems. Let g be a Riemannian metric tensor on the product manifold $M = \bar{Q}_1 \times \bar{Q}_2$ where \bar{Q}_1 and \bar{Q}_2 are two Riemannian manifold, then the from following conditions, it is easy to understand the concepts of locally product manifold and twisted product manifold.

- (i) $M = \bar{Q}_1 \times_\lambda \bar{Q}_2$ is a locally product if and only if \bar{Q}_1 and \bar{Q}_2 are totally geodesic foliations,
- (ii) a warped product $\bar{Q}_1 \times_f \bar{Q}_2$ if and only if \bar{Q}_1 is a totally geodesic foliation and \bar{Q}_2 is a spherics foliation, i.e., it is umbilic and its mean curvature vector field is parallel,
- (iii) $M = \bar{Q}_1 \times_\lambda \bar{Q}_2$ is a twisted product if and only if \bar{Q}_1 is a totally geodesic foliation and \bar{Q}_2 is a totally umbilic foliation.

The presence of three orthogonal complementary distributions $\mathfrak{D}^\mathfrak{X}$, \mathfrak{D}^{θ_1} , and \mathfrak{D}^{θ_2} , which are integrable and totally geodesic under the conditions that we have stated previously, is ensured by the fact that $\Psi: (\bar{Q}_1, g_1, F) \rightarrow (\bar{Q}_2, g_2)$ is CQBS submersion. It makes sense to now look for the conditions in which the total space \bar{Q}_1 converts into locally product manifolds or locally twisted product manifolds. In order to explore the geometry of conformal bi-slant submersion Ψ , we are providing here a few decomposition theorems that state that \bar{Q}_1 converts into locally product manifolds in a variety of situations.

Theorem 5.1. Let $\Psi: (\bar{Q}_1, g_1, F) \rightarrow (\bar{Q}_2, g_2)$ be a CQBS submersion, where (\bar{Q}_1, g_1, F) a LPR manifold and (\bar{Q}_2, g_2) a Riemannian manifold. Then \bar{Q}_1 is a locally product manifold if and only if

$$\begin{aligned}
 & \frac{1}{\lambda^2} \{g_2(\nabla_{\tilde{U}}^\Psi \Psi_* \eta \xi \mathfrak{B} \tilde{V} + \nabla_{\tilde{U}}^\Psi \Psi_* \eta \xi \mathfrak{C} \tilde{V}, \Psi_* \tilde{X})\} \\
 & = g_1(\mathcal{T}_{\tilde{U}} \mathfrak{A} \tilde{V} + \cos^2 \theta_1 \mathcal{T}_{\tilde{U}} \mathfrak{B} \tilde{V} + \cos^2 \theta_2 \mathcal{T}_{\tilde{U}} \mathfrak{C} \tilde{V}) + g_1(\mathcal{T}_{\tilde{U}} \eta \tilde{V}, P \tilde{X}) \\
 & \quad - \frac{1}{\lambda^2} \{g_2((\nabla \Psi_*)(\tilde{U}, \eta \xi \mathfrak{B} \tilde{V}) + (\nabla \Psi_*)(\tilde{U}, \eta \xi \mathfrak{C} \tilde{V}), \Psi_* \tilde{X})\} \\
 & \quad + \frac{1}{\lambda^2} \{g_2(\nabla_{\tilde{U}}^\Psi \Psi_* \eta \tilde{V} - (\nabla \Psi_*)(\tilde{U}, \eta \tilde{V}), \Psi_* L \tilde{X})\}
 \end{aligned} \tag{5.1}$$

and

$$\begin{aligned} & \frac{1}{\lambda^2} \{g_2(\nabla_{\tilde{X}}^{\Psi} \Psi_* \eta \mathcal{B} \tilde{Y} + \nabla_{\tilde{X}}^{\Psi} \Psi_* \eta \tilde{C} \tilde{Y}, \Psi_* \eta \tilde{Z})\} \\ & = g_1(\mathcal{A}_{\tilde{X}} \eta \xi \mathcal{B} \tilde{Y} + \mathcal{A}_{\tilde{X}} \eta \xi \mathcal{C} \tilde{Y} + \mathcal{A}_{\tilde{X}} \eta \xi \mathcal{A} \tilde{Y}, \tilde{Z}) \\ & + g_1(\mathcal{V} \nabla_{\tilde{X}} \mathcal{A} \tilde{Y} + \cos^2 \theta_1 \mathcal{V} \nabla_{\tilde{X}} \mathcal{B} \tilde{Y} + \cos^2 \theta_2 \mathcal{V} \nabla_{\tilde{X}} \mathcal{C} \tilde{Y}, \tilde{Z}) \\ & + g_1(\eta \mathcal{B} \tilde{Y}, \eta \tilde{Z}) g_1(\tilde{X}, \text{grad } \ln \lambda) + g_1(\tilde{X}, \eta \tilde{Z}) g_1(\eta \mathcal{B} \tilde{Y}, \text{grad } \ln \lambda) \\ & - g_1(\tilde{X}, \eta \mathcal{B} \tilde{Y}) g_1(\eta \tilde{Z}, \text{grad } \ln \lambda) + g_1(\eta \mathcal{C} \tilde{Y}, \eta \tilde{Z}) g_1(\tilde{X}, \text{grad } \ln \lambda) \\ & + g_1(\tilde{X}, \eta \tilde{Z}) g_1(\eta \mathcal{C} \tilde{Y}, \text{grad } \ln \lambda) - g_1(\tilde{X}, \eta \mathcal{C} \tilde{Y}) g_1(\eta \tilde{Z}, \text{grad } \ln \lambda), \end{aligned}$$

for any $\tilde{U}, \tilde{V} \in \Gamma(\ker \Psi_*)$ and $\tilde{X}, \tilde{Y} \in \Gamma(\ker \Psi_*)^\perp$.

Proof. The proof of this theorem is directly from Theorem 4.7 and Theorem 4.8 .

Since we discussed in the previous theorem, given certain necessary and sufficient conditions, the total space \bar{Q}_1 transforms into a locally product manifold. Now, it's intriguing to investigate if there are any circumstances under which the total space \bar{Q}_1 could turn into a locally twisted product manifold. The conditions that turn total space \bar{Q}_1 into a locally twisted product manifold are found in the following result.

Theorem 5.2. Let Ψ be a CQBS submersion from LPR manifold (\bar{Q}_1, g_1, F) onto a Riemannian manifold (\bar{Q}_2, g_2) . Then \bar{Q}_1 is locally twisted product of the form $\bar{Q}_{1(\ker \Psi_*)} \times \bar{Q}_{1(\ker \Psi_*)^\perp}$ if and only if

$$\begin{aligned} \frac{1}{\lambda^2} g_2 \left((\nabla \Psi_*)(\tilde{U}, \eta \tilde{V}), \Psi_* L \tilde{X} \right) & = g_1(\nabla_{\tilde{U}} \xi \tilde{V}, F \tilde{X}) + g_1(\mathcal{J}_{\tilde{U}} \eta \tilde{V}, P \tilde{X}) \\ & + \frac{1}{\lambda^2} g_2(\nabla_{\tilde{U}}^{\Psi} \Psi_* \eta \tilde{V}, \Psi_* L \tilde{X}). \end{aligned} \tag{5.3}$$

and

$$\begin{aligned} g_1(\tilde{X}, \tilde{Y}) H & = -P \mathcal{A}_{\tilde{X}} P \tilde{Y} - \xi \nabla_{\tilde{X}} P \tilde{Y} - \xi \mathcal{A}_{\tilde{X}} L \tilde{Y} - F \Psi_*(\nabla_{\tilde{X}}^{\Psi} \Psi_* L \tilde{Y}) \\ & + \tilde{X}(\ln \lambda) P L \tilde{Y} + L \tilde{Y}(\ln \lambda) P \tilde{X} - P(\text{grad } \ln \lambda) g_1(\tilde{X}, L \tilde{Y}). \end{aligned} \tag{5.4}$$

where H is a mean curvature vector and for any $\tilde{U}, \tilde{V} \in \Gamma(\ker \Psi_*)$ and $\tilde{X}_1, \tilde{X}_2 \in \Gamma(\ker \Psi_*)^\perp$.

Proof. For any $\tilde{X} \in \Gamma(\ker \Psi_*)^\perp$ and $\tilde{U}, \tilde{V} \in \Gamma(\ker \Psi_*)$ and using equations (2.2), (2.3), (2.13), (2.7), (2.8) (3.3) and (3.6), we have

$$g_1(\nabla_{\tilde{U}}\tilde{V}, \tilde{X}) = g_1(\nabla_{\tilde{U}}\xi\tilde{V}, F\tilde{X}) + g_1(\mathcal{J}_{\tilde{U}}\eta\tilde{V}, P\tilde{X}) + g_1(\mathcal{H}\nabla_{\tilde{U}}\eta\tilde{V}, L\tilde{X}).$$

From using formula (2.14) and definition of conformality, the above equation takes place as

$$g_1(\nabla_{\tilde{U}}\tilde{V}, \tilde{X}) = g_1(\nabla_{\tilde{U}}\xi\tilde{V}, F\tilde{X}) + g_1(\mathcal{J}_{\tilde{U}}\eta\tilde{V}, P\tilde{X}) - \frac{1}{\lambda^2}g_2((\nabla\Psi_*)(\tilde{U}, \eta\tilde{V}), \Psi_*L\tilde{X}) + \frac{1}{\lambda^2}g_2(\nabla_{\tilde{U}}^\Psi\Psi_*\eta\tilde{V}, \Psi_*L\tilde{X}).$$

It follows that the equation (5.3) satisfies if and only if $\bar{Q}_{1(\ker \Psi_*)}$ is totally geodesic. On the other hand, for $\tilde{U} \in \Gamma(\ker \Psi_*)$ and $\tilde{X}, \tilde{Y} \in \Gamma(\ker \Psi_*)^\perp$ with using equations (2.2), (2.13), (2.3) (2.10), (3.3) and (3.6), we get

$$g_1(\nabla_{\tilde{X}}\tilde{Y}, \tilde{U}) = g_1(\nabla_{\tilde{X}}P\tilde{Y}, F\tilde{U}) + g_1(\mathcal{A}_{\tilde{X}}L\tilde{Y}, \xi\tilde{U}) + g_1(\mathcal{H}\nabla_{\tilde{X}}L\tilde{Y}, \eta\tilde{U}).$$

By using the equation (2.14) with definition of conformality of Ψ , we deduce that

$$g_1(\nabla_{\tilde{X}}\tilde{Y}, \tilde{U}) = -\frac{1}{\lambda^2}g_2((\nabla\Psi_*)(\tilde{X}, L\tilde{Y}), \Psi_*\eta\tilde{U}) + \frac{1}{\lambda^2}g_2(\nabla_{\tilde{X}}^\Psi\Psi_*L\tilde{Y}, \Psi_*\eta\tilde{U}) + g_1(\nabla_{\tilde{X}}P\tilde{Y}, F\tilde{U}) + g_1(\mathcal{A}_{\tilde{X}}L\tilde{Y}, \xi\tilde{U})$$

Considering the (i) part of Lemma 2.1, above equation turns in to

$$g_1(\nabla_{\tilde{X}}\tilde{Y}, \tilde{U}) = \frac{1}{\lambda^2}g_2(\nabla_{\tilde{X}}^\Psi\Psi_*L\tilde{Y}, \Psi_*\eta\tilde{U}) + g_1(\nabla_{\tilde{X}}P\tilde{Y}, F\tilde{U}) + g_1(\mathcal{A}_{\tilde{X}}L\tilde{Y}, \xi\tilde{U}) - g_1(\text{grad } \ln \lambda, \tilde{X})g_1(L\tilde{Y}, \eta\tilde{U}) - g_1(\text{grad } \ln \lambda, L\tilde{Y})g_1(\tilde{X}, \eta\tilde{U}) + g_1(\text{grad } \ln \lambda, \eta\tilde{U})g_1(\tilde{X}, L\tilde{Y}).$$

By direct calculation, finally we get

$$g_1(\tilde{X}, \tilde{Y})H = -P\mathcal{A}_{\tilde{X}}P\tilde{Y} - \xi\nabla_{\tilde{X}}P\tilde{Y} - \xi\mathcal{A}_{\tilde{X}}L\tilde{Y} - F\Psi_*(\nabla_{\tilde{X}}^\Psi\Psi_*L\tilde{Y}) + \tilde{X}(\ln \lambda)PL\tilde{Y} + L\tilde{Y}(\ln \lambda)P\tilde{X} - P(\text{grad } \ln \lambda)g_1(\tilde{X}, L\tilde{Y}).$$

From the above equation we conclude that $\bar{Q}_{1(\ker \Psi_*)^\perp}$ is totally umbilical if and only if equation (5.4) satisfied. This completes the proof of the theorem.

F

6 -Pluriharmonicity of Conformal Quasi Bi-slant Submersion

In this section, we extend the concept of F -pluriharmonicity to almost product Riemannian manifolds and definition of Hermitian manifold.

Definition 6.1. On a manifold M , a pair (J, g) consisting of a complex structure J on M and a Hermitian metric g in the tangent space TM , that is, a Riemannian metric g that is invariant under $J, g(JX, JY) = g(X, Y)$ for any vector fields X and Y on M . A Hermitian structure specifies in any tangent space T_pM the structure of a Hermitian vector space. A manifold with a Hermitian structure is called a Hermitian manifold.

Let Ψ be a CQBS Riemannian submersion from LPR manifold (\bar{Q}_1, g_1, F) onto a Riemannian manifold (\bar{Q}_2, g_2) with slant angles θ_1 and θ_2 . Then CQBS Riemannian submersion is $\mathfrak{D}^\mathfrak{X} - F$ -pluriharmonic, $\mathfrak{D}^{\theta_1} - F$ -pluriharmonic, $\mathfrak{D}^{\theta_2} - F$ -pluriharmonic, $(\mathfrak{D}^\mathfrak{X} - \mathfrak{D}^{\theta_1}) - F$ pluriharmonic, $(\mathfrak{D}^\mathfrak{X} - \mathfrak{D}^{\theta_2}) - F$ pluriharmonic, $(\ker \Psi_* - F$ -pluriharmonic, $(\ker \Psi_*)^\perp - F$ -pluriharmonic and $((\ker \Psi_*)^\perp - \ker \Psi_*) - F$ -pluriharmonic if

$$(\nabla \Psi_*)(U, V) + (\nabla \Psi_*)(FU, FV) = 0,$$

for any $U, V \in \Gamma(\mathfrak{D}^\mathfrak{X})$, for any $U, V \in \Gamma(\mathfrak{D}^{\theta_1})$, for any $U, V \in \Gamma(\mathfrak{D}^{\theta_2})$, for any $U \in \Gamma(\mathfrak{D}^\mathfrak{X}), V \in \Gamma(\mathfrak{D}^{\theta_1})$, for any $U \in \Gamma(\mathfrak{D}^\mathfrak{X}), V \in \Gamma(\mathfrak{D}^{\theta_2})$, for any $U, V \in \Gamma(\ker \Psi_*)$, for any $U, V \in \Gamma(\ker \Psi_*)^\perp$ and for any $U \in \Gamma(\ker \Psi_*)^\perp, V \in \Gamma(\ker \Psi_*)$, respectively.

Theorem 6.1. Let Ψ be a CQBS submersion from LPR manifold (\bar{Q}_1, g_1, F) onto a rm (\bar{Q}_2, g_2) with slant angles θ_1 and θ_2 . Suppose that Ψ is $\mathfrak{D}^{\theta_1} - F$ pluriharmonic. Then \mathfrak{D}^{θ_1} defines totally geodesic foliation on \bar{Q}_1 if and only if

$$\begin{aligned} & \Psi_*(\eta\mathcal{T}_{\xi\bar{U}}\eta\xi\tilde{V} + L\mathcal{H}\nabla_{\xi\bar{U}}\eta\xi\tilde{V}) - \Psi_*(\mathcal{A}_{\eta\bar{U}}\xi\tilde{V} + \mathcal{H}\nabla_{\xi\bar{U}}\eta\tilde{V}) \\ &= \cos^2 \theta_1 \Psi_*(L\mathcal{T}_{\xi\bar{U}}\tilde{V} + \eta\mathcal{V}\nabla_{\xi\bar{U}}\tilde{V}) + \nabla_{\xi\bar{U}}^{\Psi} \Psi_*F\tilde{V} \\ & - \eta\tilde{U}(\ln \lambda)\Psi_*\eta\tilde{V} - \eta\tilde{V}(\ln \lambda)\Psi_*\eta\tilde{U} + g_1(\eta\tilde{U}, \eta\tilde{V})\Psi_*(\text{grad } \ln \lambda) \end{aligned}$$

for any $\tilde{U}, \tilde{V} \in \Gamma(\mathfrak{D}^{\theta_1})$.

Proof. For any $\tilde{U}, \tilde{V} \in \Gamma(\mathfrak{D}^{\theta_1})$ and since, Ψ is $\mathfrak{D}^{\theta_1} - F$ -pluriharmonic, then by using equation (2.7) and (2.14), we have

$$\begin{aligned} 0 &= (\nabla\Psi_*)(\tilde{U}, \tilde{V}) + (\nabla\Psi_*)(F\tilde{U}, F\tilde{V}) \\ \Psi_*(\nabla_{\bar{U}}\tilde{V}) &= -\Psi_*(\nabla_{F\bar{U}}F\tilde{V}) + \nabla_{F\bar{U}}^{\Psi} \Psi_*(F\tilde{V}) \\ &= -\Psi_*(\mathcal{A}_{\eta\bar{U}}\xi\tilde{V} + \mathcal{V}\nabla_{\eta\bar{U}}\xi\tilde{V} + \mathcal{T}_{\xi\bar{U}}\eta\tilde{V} + \mathcal{H}\nabla_{\xi\bar{U}}\eta\tilde{V}) - \Psi_*(F\nabla_{\xi\bar{U}}F\xi\tilde{V}) \\ &+ (\nabla\Psi_*)(\eta\tilde{U}, \eta\tilde{V}) - \nabla_{\eta\bar{U}}^{\Psi} \Psi_*\eta\tilde{V} + \nabla_{F\bar{U}}^{\Psi} \Psi_*F\tilde{V}. \end{aligned}$$

By using equations (3.3), (3.6) with Lemma 2.1 and Lemma 3.2, the above equation finally takes the form

$$\begin{aligned} \Psi_*(\nabla_{\bar{U}}V) &= -\cos^2 \theta_1 \Psi_*(P\mathcal{T}_{\xi\bar{U}}\tilde{V} + L\mathcal{T}_{\xi\bar{U}}\tilde{V} + \xi\mathcal{V}\nabla_{\xi\bar{U}}\tilde{V} + \eta\mathcal{V}\nabla_{\xi\bar{U}}\tilde{V}) \\ &+ \Psi_*(\xi\mathcal{T}_{\xi\bar{U}}\eta\xi\tilde{V} + \eta\mathcal{T}_{\xi\bar{U}}\eta\xi\tilde{V} + P\mathcal{H}\nabla_{\xi\bar{U}}\eta\xi\tilde{V} + L\mathcal{H}\nabla_{\xi\bar{U}}\eta\xi\tilde{V}) \\ &- \Psi_*(\mathcal{A}_{\eta\bar{U}}\xi\tilde{V} + \mathcal{V}\nabla_{\eta\bar{U}}\xi\tilde{V} + \mathcal{T}_{\xi\bar{U}}\eta\tilde{V} + \mathcal{H}\nabla_{\xi\bar{U}}\eta\tilde{V}) \\ &+ \eta\tilde{U}(\ln \lambda)\Psi_*\eta\tilde{V} + \eta\tilde{V}(\ln \lambda)\Psi_*\eta\tilde{U} - g_1(\eta\tilde{U}, \eta\tilde{V})\Psi_*(\text{grad } \ln \lambda) \\ &- \nabla_{\eta\bar{U}}^{\Psi} \Psi_*\eta\tilde{V} + \nabla_{F\bar{U}}^{\Psi} \Psi_*F\tilde{V} \end{aligned}$$

from which we get the desired result.

Theorem 6.2. Let Ψ be a CQBS submersion from LPR manifold (\bar{Q}_1, g_1, F) onto a rm (\bar{Q}_2, g_2) with slant angles θ_1 and θ_2 . Suppose that Ψ is $\mathfrak{D}^{\theta_2} - F$ pluriharmonic. Then \mathfrak{D}^{θ_2} defines totally geodesic foliation on \bar{Q}_1 if and only if

$$\begin{aligned} & \Psi_*(\eta\mathcal{T}_{\xi Z}\eta\xi\tilde{W} + L\mathcal{H}\nabla_{\xi Z}\eta\xi\tilde{W}) - \Psi_*(\mathcal{A}_{\eta Z}\xi\tilde{W} + \mathcal{H}\nabla_{\xi Z}\eta\tilde{W}) \\ & = \cos^2 \theta_2 \Psi_*(L\mathcal{T}_{\xi Z}\tilde{W} + \eta\tilde{W}\nabla_{\xi Z}\tilde{W}) + \nabla_{\xi Z}^\Psi \Psi_*F\tilde{W} \\ & \quad - \eta\tilde{Z}(\ln \lambda)\Psi_*\eta\tilde{W} - \eta\tilde{W}(\ln \lambda)\Psi_*\eta\tilde{Z} + g_1(\eta\tilde{Z}, \eta\tilde{W})\Psi_*(\text{grad } \ln \lambda) \end{aligned}$$

for any $\tilde{Z}, \tilde{W} \in \Gamma(\mathfrak{D}^{\theta_2})$.

Proof. The proof of the theorem is similar to the proof of Theorem 6.1.

Theorem 6.3. Let Ψ be a CQBS submersion from LPR manifold (\bar{Q}_1, g_1, F) onto a rm (\bar{Q}_2, g_2) with slant angles θ_1 and θ_2 . Suppose that Ψ is $((\ker \Psi_*)^\perp - \ker \Psi_*) - F$ -pluriharmonic. Then the following assertion are equivalent.

(i) The horizontal distribution $(\ker \Psi_*)^\perp$ defines totally geodesic foliation on \bar{Q}_1 .

$$\begin{aligned} & (\cos^2 \theta_1 + \cos^2 \theta_2)\Psi_*\{L\mathcal{T}_{P\tilde{X}}\xi\mathfrak{A}\tilde{U} + \eta\mathcal{V}\nabla_{P\tilde{X}}\xi\mathfrak{A}\tilde{U} + L\mathcal{A}_{L\tilde{X}}\xi\mathfrak{A}\tilde{U} + \eta\mathcal{V}\nabla_{L\tilde{X}}\xi\mathfrak{A}\tilde{U}\} \\ & = \Psi_*\{L\mathcal{T}_{P\tilde{X}}\xi\mathfrak{A}\tilde{U} + \eta\mathcal{V}\nabla_{P\tilde{X}}\xi\mathfrak{A}\tilde{U} + L\mathcal{A}_{L\tilde{X}}\xi\mathfrak{A}\tilde{U} + \eta\mathcal{H}\nabla_{L\tilde{X}}\xi\mathfrak{A}\tilde{U}\} \\ & \quad - \Psi_*\{\eta\mathcal{T}_{P\tilde{X}}\eta\xi\mathfrak{B}\tilde{U} + L\mathcal{H}\nabla_{P\tilde{X}}\eta\xi\mathfrak{B}\tilde{U} + \eta\mathcal{T}_{P\tilde{X}}\eta\xi\mathfrak{C}\tilde{U} + L\mathcal{H}\nabla_{P\tilde{X}}\eta\xi\mathfrak{C}\tilde{U}\} \\ & \quad + L\tilde{X}(\ln \lambda)\Psi_*\eta\xi\mathfrak{B}\tilde{U} + \eta\xi\mathfrak{B}\tilde{U}(\ln \lambda)\Psi_*L\tilde{X} - g_1(L\tilde{X}, \eta\xi\mathfrak{B}\tilde{U})\Psi_*(\text{grad } \ln \lambda) \\ & \quad + L\tilde{X}(\ln \lambda)\Psi_*\eta\xi\mathfrak{C}\tilde{U} + \eta\xi\mathfrak{C}\tilde{U}(\ln \lambda)\Psi_*L\tilde{X} - g_1(L\tilde{X}, \eta\xi\mathfrak{C}\tilde{U})\Psi_*(\text{grad } \ln \lambda) \\ & \quad - \Psi_*\{\eta\mathcal{A}_{L\tilde{X}}\eta\xi\mathfrak{B}\tilde{U} + \eta\mathcal{A}_{L\tilde{X}}\eta\xi\mathfrak{C}\tilde{U} - \mathcal{H}\nabla_{P\tilde{X}}\eta\tilde{U}\} - \nabla_{L\tilde{X}}^\Psi \Psi_*\eta\xi\mathfrak{B}\tilde{U} \\ & \quad + \Psi_*(\nabla_{\tilde{X}}\tilde{U}) + \nabla_{F\tilde{X}}^\Psi \Psi_*\eta\tilde{U} - \nabla_{L\tilde{X}}^\Psi \Psi_*\eta\xi\tilde{C}\tilde{U}, \end{aligned}$$

(ii)

$$\begin{aligned} & + L\tilde{X}(\ln \lambda)\Psi_*\eta\xi\mathfrak{B}\tilde{U} + \eta\xi\mathfrak{B}\tilde{U}(\ln \lambda)\Psi_*L\tilde{X} - g_1(L\tilde{X}, \eta\xi\mathfrak{B}\tilde{U})\Psi_*(\text{grad } \ln \lambda) \\ & + L\tilde{X}(\ln \lambda)\Psi_*\eta\xi\mathfrak{C}\tilde{U} + \eta\xi\mathfrak{C}\tilde{U}(\ln \lambda)\Psi_*L\tilde{X} - g_1(L\tilde{X}, \eta\xi\mathfrak{C}\tilde{U})\Psi_*(\text{grad } \ln \lambda) \\ & \quad - \Psi_*\{\eta\mathcal{A}_{L\tilde{X}}\eta\xi\mathfrak{B}\tilde{U} + \eta\mathcal{A}_{L\tilde{X}}\eta\xi\mathfrak{C}\tilde{U} - \mathcal{H}\nabla_{P\tilde{X}}\eta\tilde{U}\} - \nabla_{L\tilde{X}}^\Psi \Psi_*\eta\xi\mathfrak{B}\tilde{U} \\ & \quad + \Psi_*(\nabla_{\tilde{X}}\tilde{U}) + \nabla_{F\tilde{X}}^\Psi \Psi_*\eta\tilde{U} - \nabla_{L\tilde{X}}^\Psi \Psi_*\eta\xi\tilde{C}\tilde{U} \end{aligned}$$

for any $\tilde{X} \in \Gamma(\ker \Psi_*)^\perp$ and $\tilde{U} \in \Gamma(\ker \Psi_*)$

Proof. For any $\tilde{X} \in \Gamma(\ker \Psi_*)^\perp$ and $\tilde{U} \in \Gamma(\ker \Psi_*)$, since Ψ is $((\ker \Psi_*)^\perp - \ker \Psi_*) - F$ -pluriharmonic, then by using (2.14), (3.3) and (3.6), we get

$$\Psi_*(\nabla_{L\tilde{X}}\eta\tilde{U}) = -\Psi_*(\nabla_{P\tilde{X}}\xi\tilde{U} + \nabla_{P\tilde{X}}\eta\tilde{U} + \nabla_{L\tilde{X}}\xi\tilde{U}) + \Psi_*(\nabla_{\tilde{X}}\tilde{U}) + \nabla_{F\tilde{X}}^\Psi\Psi_*\eta\tilde{U}.$$

Taking account the fact from (2.1) and (2.8), we have

$$\begin{aligned} \Psi_*(\nabla_{L\tilde{X}}\eta\tilde{U}) = & -\Psi_*(\mathcal{T}_{P\tilde{X}}\eta\tilde{U} + \mathcal{H}\nabla_{P\tilde{X}}\eta\tilde{U}) + \Psi_*(\nabla_{\tilde{X}}\tilde{U}) + \nabla_{F\tilde{X}}^\Psi\Psi_*\eta\tilde{U} \\ & -\Psi_*(F\nabla_{P\tilde{X}}F\xi\tilde{U}) - \Psi_*(F\nabla_{L\tilde{X}}F\xi\tilde{U}) \end{aligned}$$

Now on using decomposition (3.2), Lemma 3.2, Lemma 3.3 with equations (3.3), we may yields

$$\begin{aligned} \Psi_*(\nabla_{L\tilde{X}}\eta\tilde{U}) = & \Psi_*\{F\nabla_{P\tilde{X}}\eta\xi\mathfrak{B}\tilde{U} + F\nabla_{P\tilde{X}}\eta\xi\mathfrak{C}\tilde{U} + F\nabla_{L\tilde{X}}\eta\xi\mathfrak{B}\tilde{U} + F\nabla_{L\tilde{X}}\eta\xi\mathfrak{C}\tilde{U}\} \\ & \Psi_*\{F\nabla_{P\tilde{X}}\xi\mathfrak{A}\tilde{U} - \cos^2\theta_1F\nabla_{P\tilde{X}}\xi\tilde{U} - \cos^2\theta_2F\nabla_{P\tilde{X}}\xi\tilde{U}\} \\ & +\Psi_*\{F\nabla_{L\tilde{X}}\xi\mathfrak{A}\tilde{U} - \cos^2\theta_1F\nabla_{L\tilde{X}}\xi\tilde{U} - \cos^2\theta_2F\nabla_{L\tilde{X}}\xi\tilde{U}\} \\ & -\Psi_*(\mathcal{H}\nabla_{P\tilde{X}}\eta\tilde{U}) + \Psi_*(\nabla_{\tilde{X}}\tilde{U}) + \nabla_{F\tilde{X}}^\Psi\Psi_*\eta\tilde{U} \end{aligned}$$

From equations (2.7)-(2.10) and after simple calculation, we may write

$$\begin{aligned} \Psi_*(\nabla_{L\tilde{X}}\eta\tilde{U}) = & -(\cos^2\theta_1 + \cos^2\theta_2)\Psi_*\{L\mathcal{T}_{P\tilde{X}}\xi\mathfrak{A}\tilde{U} + \eta\nabla_{P\tilde{X}}\xi\mathfrak{A}\tilde{U} + L\mathcal{A}_{L\tilde{X}}\xi\mathfrak{A}\tilde{U} \\ & +\eta\nabla_{L\tilde{X}}\xi\mathfrak{A}\tilde{U}\} - \Psi_*\{\eta\mathcal{A}_{L\tilde{X}}\eta\xi\mathfrak{B}\tilde{U} + \eta\mathcal{A}_{L\tilde{X}}\eta\xi\mathfrak{C}\tilde{U} - \mathcal{H}\nabla_{P\tilde{X}}\eta\tilde{U}\} \\ & +\Psi_*\{L\mathcal{T}_{P\tilde{X}}\xi\mathfrak{A}\tilde{U} + \eta\nabla_{P\tilde{X}}\xi\mathfrak{A}\tilde{U} + L\mathcal{A}_{L\tilde{X}}\xi\mathfrak{A}\tilde{U} + \eta\mathcal{H}\nabla_{L\tilde{X}}\xi\mathfrak{A}\tilde{U}\} \\ & -\Psi_*\{\eta\mathcal{T}_{P\tilde{X}}\eta\xi\mathfrak{B}\tilde{U} + L\mathcal{H}\nabla_{P\tilde{X}}\eta\xi\mathfrak{B}\tilde{U} + \eta\mathcal{T}_{P\tilde{X}}\eta\xi\mathfrak{C}\tilde{U} + L\mathcal{H}\nabla_{P\tilde{X}}\eta\xi\mathfrak{C}\tilde{U}\} \\ & -\Psi_*(L\mathcal{H}\nabla_{L\tilde{X}}\eta\xi\mathfrak{B}\tilde{U} + L\mathcal{H}\nabla_{L\tilde{X}}\eta\xi\mathfrak{C}\tilde{U}) + \Psi_*(\nabla_{\tilde{X}}\tilde{U}) + \nabla_{F\tilde{X}}^\Psi\Psi_*\eta\tilde{U} \end{aligned}$$

Since Ψ is conformal Riemannian submersion, the by using equations (2.14) and from Lemma 2.1, we finally have

$$\begin{aligned} \Psi_*(\nabla_{L\tilde{X}}\eta\tilde{U}) = & -(\cos^2\theta_1 + \cos^2\theta_2)\Psi_*\{L\mathcal{T}_{P\tilde{X}}\xi\mathfrak{A}\tilde{U} + \eta\nabla_{P\tilde{X}}\xi\mathfrak{A}\tilde{U} + L\mathcal{A}_{L\tilde{X}}\xi\mathfrak{A}\tilde{U} \\ & +\eta\nabla_{L\tilde{X}}\xi\mathfrak{A}\tilde{U}\} - \Psi_*\{\eta\mathcal{A}_{L\tilde{X}}\eta\xi\mathfrak{B}\tilde{U} + \eta\mathcal{A}_{L\tilde{X}}\eta\xi\mathfrak{C}\tilde{U} - \mathcal{H}\nabla_{P\tilde{X}}\eta\tilde{U}\} \\ & +\Psi_*\{L\mathcal{T}_{P\tilde{X}}\xi\mathfrak{A}\tilde{U} + \eta\nabla_{P\tilde{X}}\xi\mathfrak{A}\tilde{U} + L\mathcal{A}_{L\tilde{X}}\xi\mathfrak{A}\tilde{U} + \eta\mathcal{H}\nabla_{L\tilde{X}}\xi\mathfrak{A}\tilde{U}\} \\ & -\Psi_*\{\eta\mathcal{T}_{P\tilde{X}}\eta\xi\mathfrak{B}\tilde{U} + L\mathcal{H}\nabla_{P\tilde{X}}\eta\xi\mathfrak{B}\tilde{U} + \eta\mathcal{T}_{P\tilde{X}}\eta\xi\mathfrak{C}\tilde{U} + L\mathcal{H}\nabla_{P\tilde{X}}\eta\xi\mathfrak{C}\tilde{U}\} \\ & +L\tilde{X}(\ln\lambda)\Psi_*\eta\xi\mathfrak{B}\tilde{U} + \eta\xi\mathfrak{B}\tilde{U}(\ln\lambda)\Psi_*L\tilde{X} - g_1(L\tilde{X},\eta\xi\mathfrak{B}\tilde{U})\Psi_*(\text{grad}\ln\lambda) \\ & +L\tilde{X}(\ln\lambda)\Psi_*\eta\xi\mathfrak{C}\tilde{U} + \eta\xi\mathfrak{C}\tilde{U}(\ln\lambda)\Psi_*L\tilde{X} - g_1(L\tilde{X},\eta\xi\mathfrak{C}\tilde{U})\Psi_*(\text{grad}\ln\lambda) \\ & +\Psi_*(\nabla_{\tilde{X}}\tilde{U}) + \nabla_{F\tilde{X}}^\Psi\Psi_*\eta\tilde{U} - \nabla_{L\tilde{X}}^\Psi\Psi_*\eta\xi\mathfrak{B}\tilde{U} - \nabla_{L\tilde{X}}^\Psi\Psi_*\eta\xi\mathfrak{C}\tilde{U}, \end{aligned}$$

which completes the proof of theorem.

Conflict of Interest The authors declare that there is no conflict of interest.

Acknowledgement: The authors are thankful to the referees for the careful reading of the manuscript and for the suggestions, which improve the quality of the paper.

References

- [1] M. A. Akyol and Y. Gunduzalp., Hemi-slant submersions from almost product Riemannian manifolds, *Gulf J. Math.*, 4(3) (2016), 15-27.
- [2] M. A. Akyol., Conformal semi-slant submersions, *International Journal of Geometric Methods in Modern Physics*, 14(7) (2017), 1750114.
- [3] M. A. Akyol and B. Sahin., Conformal slant submersions, *Hacettepe Journal of Mathematics and Statistics*, 48(1) (2019), 28-44.
- [4] M. A. Akyol and B. Sahin., Conformal anti-invariant submersions from almost Hermitian manifolds, *Turkish Journal of Mathematics*, 40 (2016), 43-70.
- [5] P. Baird and J. C. Wood., *Harmonic Morphisms Between Riemannian Manifolds*, London Mathematical Society Monographs, 29, Oxford University Press, The Clarendon Press. Oxford, (2003).
- [6] J.-P. Bourguignon and H. B. Lawson., Jr., Stability and isolation phenomena for YangMills fields, *Comm. Math. Phys.*, 79 (1981), no. 2, 189-230. <http://projecteuclid.org/euclid.cmp/1103908963>.
- [7] D. Chinea., Almost contact metric submersions, *Rend. Circ. Mat. Palermo*, 34(1) (1985), 89-104.

- [8] A. Gray., Pseudo-Riemannian almost product manifolds and submersions, *J. Math. Mech.*, 16 (1967), 715-737.
- [9] B. Fuglede., Harmonic morphisms between Riemannian manifolds, *Annales de l'institut Fourier (Grenoble)*, 28 (1978), 107-144.
- [10] S. Gudmundsson., The geometry of harmonic morphisms, Ph.D. thesis, University of Leeds, (1992).
- [11] Y. Gunduzalp., Semi-slant submersions from almost product Riemannian manifolds, *Demonstratio Mathematica*, 49(3) (2016), 345-356.
- [12] S. Ianu,s and M. Vissinescu., Space-time compaction and Riemannian submersions, In: Rassias, G.(ed.) *The Mathematical Heritage of C. F. Gauss*, World Scientific, River Edge (1991), 358-371.
- [13] T. Ishihara., A mapping of Riemannian manifolds which preserves harmonic functions, *Journal of Mathematics of Kyoto University*, 19 (1979), 215-229.
- [14] S. Kumar., A. T. Vanli., S. Kumar., and R. Prasad., Conformal quasi bi-slant submersions, *Analele Stiintifice ale Universitatii Al I Cuza din Iasi-Matematica* 68, no. 2 (2022).
- [15] M. T. Mustafa., Applications of harmonic morphisms to gravity, *J. Math. Phys.*, 41 (2000), 6918-6929.
- [16] Y. Ohnita., On pluriharmonicity of stable harmonic maps, *J. London Math. Soc. (2)* 2 (1987), 563-568. 2.2
- [17] B. O'Neill., The fundamental equations of a submersion, *Michigan Math. J.*, 13 (1966), 459-469.
<http://projecteuclid.org/euclid.mmj/1028999604>.

- [18] K. S. Park and R. Prasad., Semi-slant submersions, Bull. Korean Math. Soc. 50(3) (2013), 951-962.
- [19] R. Prasad, S. S. Shukla and S. Kumar., On Quasi bi-slant submersions, Mediterr. J. Math., 16 (2019), 155.
<https://doi.org/10.1007/s00009-0191434-7>.
- [20] R. Prasad, M. A. Akyol, S. Kumar and P. K. Singh., Quasi bi-slant submersions in contact geometry, CUBO, A Mathematical Journal, no. 124 (2022), 1-22.
- [21] R. Prasad, M. A. Akyol, P. K. Singh and S. Kumar., On Quasi bi-slant submersions from Kenmotsu manifolds onto any Riemannian manifolds, Journal of Mathematical Extension, 8(16) (2021).
- [22] R. Ponge and H. Reckziegel., Twisted products in pseudo-Riemannian geometry, Geom. Dedicata, (1993), 48(1):15-25.
- [23] B. Sahin., Anti-invariant Riemannian submersions from almost Hermitian manifolds, Central European J. Math., 3 (2010), 437-447.
- [24] B. Sahin., Semi-invariant Riemannian submersions from almost Hermitian manifolds, Canad. Math. Bull., 56 (2011), 173-183.
- [25] B. Sahin., Slant submersions from almost Hermitian manifolds, Bull. Math. Soc. Sci. Math. Roumanie. 1 (2011) 93-105.
- [26] B. Sahin., Riemannian Submersions, Riemannian Maps in Hermitian Geometry and their Applications, Elsevier, Academic Press, (2017).
- [27] Sumeet Kumar et al., Conformal hemi-slant submersions from almost hermitian manifolds, Commun. Korean Math. Soc., 35 (2020),

No. 3, pp. 999-1018 <https://doi.org/10.4134/CKMS.c190448> pISSN:
1225-1763 / eISSN: 2234-3024.

[28] B. Watson., Almost Hermitian submersions, *J. Differential Geometry*, vol. 11, no. 1, pp. (1976), 147-165.

[29] B. Watson., G, G' -Riemannian submersions and nonlinear gauge field equations of general relativity, In: Rassias, T. (ed.) *Global Analysis - Analysis on manifolds, dedicated M. Morse*. Teubner-Texte Math., 57 (1983), 324-349, Teubner, Leipzig.

Design and Fabrication of an Automatic Solar Tracking System & Comparative Analysis with Stationary Panel

Md. Raqibul Hasan,

Department of Mechanical Engineering, Chittagong University of Engineering & Technology, Chittagong, Bangladesh
raqib.cuet@gmail.com

Abstract: Solar energy is considered to be one of the most promising renewable energies. Energy generated from the sun transmitted in the form of light energy is converted into electrical energy using solar cells. This technology is widely used, the main use of solar panels is mostly in the static flat-plate scheme based on pre-determined angles. As a result, because of the variation of solar irradiation with the progress of daytime, the energy conversion is found to be decreased prominently. For serving the purpose of getting maximum power possible, this study represents a microcontroller-based energy-efficient automatic solar-tracking system. This system helps in the alignment of solar panels with the direction of the sunlight as per the changing position of the sun for maximizing power generation. The tracking system has been implemented using the necessary hardware setup and a program that controls the respective hardware. Light Dependent Resistor (LDR) sensor has been used as the input for the system to detect the brightness level of sunlight. The solar panel can rotate along with the horizontal (east-west) axis and the vertical axis depending on the intensity of the sunlight calculating input of LDR sensor. Two servo motors have been utilized for tracing the sun position. In this study, the designed tracking system has been compared to a stationary flat-plate system (30° south facing horizontal) for the comparative analysis of power generation. The experimental result shows that the designed tracking system increased the power generation efficiency by 44.38% compared with the stationary panel. The result also indicates that in the mostly cloudy region the stationary panel will be more convenient than the automatic tracking system as in that case sunlight remains defused. But on regular sunny days, this proposed system over-performs existing stationary panel systems.

Keywords: Solar cell, Automatic tracker, servo motor, Arduino UNO, LDR sensor.

تصميم وتصنيع نظام التتبع الشمسي الأتوماتيكي والتحليل المقارن باللوحة الثابتة

المخلص: تعتبر الطاقة الشمسية من أكثر الطاقات المتجددة الواعدة. يتم تحويل الطاقة المولدة من الشمس المنقولة على شكل طاقة ضوئية إلى طاقة كهربائية باستخدام الخلايا الشمسية. تُستخدم هذه التقنية على نطاق واسع، والاستخدام الرئيسي للألواح الشمسية يكون في الغالب في مخطط اللوحة المسطحة الثابتة بناءً على زوايا محددة مسبقاً. نتيجة لذلك، بسبب اختلاف الإشعاع الشمسي مع تقدم النهار، وجد أن تحويل الطاقة قد انخفض بشكل ملحوظ. لخدمة غرض الحصول على أقصى قدر ممكن من الطاقة، تمثل هذه الدراسة نظاماً آلياً لتتبع الطاقة الشمسية يعتمد على متحكم دقيق وموفر للطاقة. يساعد هذا النظام في محاذاة الألواح الشمسية مع اتجاه ضوء الشمس وفقاً لموضع الشمس المتغير لتحقيق أقصى قدر من توليد الطاقة. تم تنفيذ نظام التتبع باستخدام إعداد الأجهزة اللازمة وبرنامج يتحكم في الأجهزة المعنية. تم استخدام مستشعر المقاوم المعتمد على الضوء (*LDR*) كمداخل للنظام للكشف عن مستوى سطوع ضوء الشمس. يمكن أن تدور اللوحة الشمسية جنباً إلى جنب مع المحور الأفقي (الشرقي الغربي) والمحور الرأسي اعتماداً على شدة ضوء الشمس الذي يحسب مدخلات مستشعر *LDR*. تم استخدام محركين مؤازرين لتتبع موضع الشمس. في هذه الدراسة، تمت مقارنة نظام التتبع المصمم بنظام اللوحة المسطحة الثابتة (300 درجة جنوباً أفقيًا) للتحليل المقارن لتوليد الطاقة. أظهرت النتائج التجريبية أن نظام التتبع المصمم أدى إلى زيادة كفاءة توليد الطاقة بنسبة 44.38% مقارنة باللوحة الثابتة. وتشير النتيجة أيضاً إلى أنه في المنطقة الغائمة في الغالب، ستكون اللوحة الثابتة أكثر ملاءمة من نظام التتبع التلقائي، حيث يظل ضوء الشمس في هذه الحالة معطلاً. ولكن في الأيام المشمسة العادية، يفوق هذا النظام المقترح أداء أنظمة اللوحات الثابتة الموجودة.

1. Introduction

Directly or indirectly the main source of renewable energy is the sun. Among all the renewable sources, solar is one of the sources which has the massive chance to replace conventional energy sources. Sunlight is converted directly into electrical energy by solar cells. A solar cell is an electrical device used to convert and produce electrical energy directly from light energy. This effect is called the photovoltaic effect. It is the phenomenon of chemical and physical. The solar panel is mainly made from the semiconductor. Mostly Si is used in the solar cell. Which have the 25% of efficiency in energy transformation. [1] Until the invention of high efficient solar cells, the mere way to increase the performance of the solar cell is tracking the sun's movement. If the tracker moves along with the sun's motion path then the PV cell converts maximum light energy to electrical energy. A solar tracker is the best and most accurate and applicable & proven system to enhance the efficiency of PV cells through alignment with the sun position. [2] The location of the sun varies with both time and season, for that reason the sun passes across the sky. So that increase of electrical energy production by using PV cell must track the location of the sun. [3] So that, the solar panel has to directly face the maximum light intensity. For that purpose, solar panels have to track the sunlight to get maximum intensity. The author [4] designed a single-axis tracker based on maximum power point tracking system (MPPT) using a DC motor and microcontroller for operation. This tracker can rotate only along horizontal axis. The author [5] designed a dual-axis solar tracker which is based on pseudo-azimuthal system for rotating the tracker. It obtains 44.89% energy efficiency compare to fixed panel.

In this paper, an automatic solar tracker is presented which is microcontroller based and easily programmable.

1.1 Types of Solar Tracker

There are two forms of the tracking system. One is manually tracking & the other is an automatic tracking system.

1.1.1 Manually Tracking

The manually tracking system is operated by a specialist operator, who aligns the PV cell to the direct location of the sun manually. It maintains with the time and movement of

the sun, operator check the time and position of the sun then move the tracker by using wheel or hand. It is not an efficient system. Because the operator does not measure the appropriate angle for the tracker to track sun position. This system is costly.

1.1.2 Automatic Tracking

The automatic system is more efficient and accurate than the manual system. Automatic system controlled by computer programming. It is one of the smart tracking systems nowadays. By automatic system solar panel move along the position of the sun to get maximum light by measuring light intensity to produce maximum electrical energy. The automatic system is a cheap operating system. That is why nowadays it has become a popular using technology.

1.3 Objectives

The objectives of the reports were to:

- To design an automatic dual-axis solar tracking system.
- Fabricate and testing the design in laboratory conditions.
- Performance comparison with the stationary solar panel.

The goal of the work was to produce a locally made prototype automatic solar tracking system. Having a prototype provides clear knowledge in terms of automated dual-axis solar tracker operation.

2. Literature Review

J.V. Patil, J.K. Nayak, and V.P. Sundersingh [6] designed a computer-controlled two-axis solar tracker and testing. The designed tracker had a small error. This tracker leads to an increase in the output up to 30%. The tracker consumes the output power very small amount.

Jerin Kuriakose Tharamuttam and Andrew Keong ng [7] designed a hybrid algorithm for the automatic solar tracker. Which is not like the usual traditional active and chronological algorithm. This algorithm combine with both mathematical models and

sensor for determine the very accurate sun location. To maximize collection and manage the energy of solar.

Md, Tanvir Arafat khan, S.M. Shahrear Tanzil, Rifat Rahman, and S M Shafiul Alam [2] designed an automatic solar tracking system. The designed tracker has the proper control mechanism and three-way of controlling. Their ways were daylight conditions which controlled only one direction that is east-west direction, second is a bad day condition when the sky will cloudy. And the last is bidirectional rotation. When the sun getting set then the tracker move to a certain angle till the sunset. Then the tracker moves revers to the previous direction for the next day. This tracker provides a profitable solution for the non-developed country.

Asmarashid Ponniran, Ammar Hashim, and Ariffuddin Joret [8] are constructed a single axis solar tracker where motor speed is not considerable. It was designed for residential usage and low-powered appliance. They did not consider the motor speed because, in this project, DC geared motor was used which offers a low rated speed in the output. The project was able to follow and track the sunlight intensity to collect high solar energy. The process was controlled by a microcontroller and intensity measured by an LDR sensor. They recommended that any kind of DC motor can be used because motor speed is not considerable. It was for the home appliance.

Salah Abdallah and Salem Nijmeh [9] evaluated two axes sun tracker which was automatically controlled by PLC. For the control, the program method was the open-loop system. This project was compared with a stationary surface tilted at a 32° angle. The experimental result was significantly higher than the fixed panel. The system showed efficient performance with an increase in the energy collection up to 41.34% than the stationary surface. Further studies can evaluate more performance in the application of a two-axis solar tracker.

Nur Mohammad and Tarequl Karim [10] designed a hybrid solar tracking system controlled automatically. This project's goal was to increase efficiency. For reaching the

goal researcher implement a hybrid system combined with the dual and single-axis tracking system. And researcher made a comparison among hybrid, dual, single, and stationary tracking systems. The Dual-axis system showed 18% more gain energy than the single axis. On the other hand, the hybrid system performed and showed up to 54% efficiency than the stationary system which was situated 23.5° with horizontal.

Asmarashid Ponniran, Ammar Hashim and Handy Ali Munir [11] designed a single axis sun tracker. Which was controlled by an LDR sensor with the help of a microcontroller. It successfully tracked the sun by the measuring intensity of the sunbeam. And their goal was successfully obtained. It was applicable for the house appliance and non-critical low-powered device. It will make more efficient by further study.

P. Roth, A. Georgiev, and H. Boudinov [12] designed a sun tracker system. Which was operate automatically. For this operation, they used a pyrhelimeter and guided by a closed-loop servo motor. A four-quadrant photodetector creates an image of the sun's position and the DC motor moved the system into the sun location through the sun-centered photodetector. When the sun getting invisible the system continues to move until the detector gets the sun in the center of it and making the image of the sun and stop movement. It is just a model to track the sun which will be used in the solar panel to track the sun's position accurately commercially.

Tung-Sheng Zhan, Whei-Min Lin, Ming-Huang Tsai, and Guo-Shiang Wang [13] designed a dual-axis solar tracker which was operated automatically by the programmable logic controller (PLC). This system-oriented the setup to directly perpendicular to the sunbeam. They have compared the result with a fixed solar panel. This project was cost-effective, reliable, and efficient than stationary. They got the successful result which was more than 17-25% than stationary on a sunny day. On the other hand on a cloudy day, they got 8-11% more than output than stationary. The overall output gets 8-25% more efficient than a fixed angle solar panel.

3. Methodology

The design of the framework is done by following parts:

- Program design – which is implemented in a microcontroller that controls the tracker.
- Circuit design – all electrical appliances are includes.
- Physical structure design – all mechanical parts such as the frame of the system, motor, etc.

The system of the project is constructed utilizing a decent idea which is two signs from the various sensors are compared. Light Dependent resistor (LDR) is used as a light sensor. For the solar tracker control unit, the microcontroller is used with input as LDR sensor response. A block diagram of the system is shown in Figure 1 below:

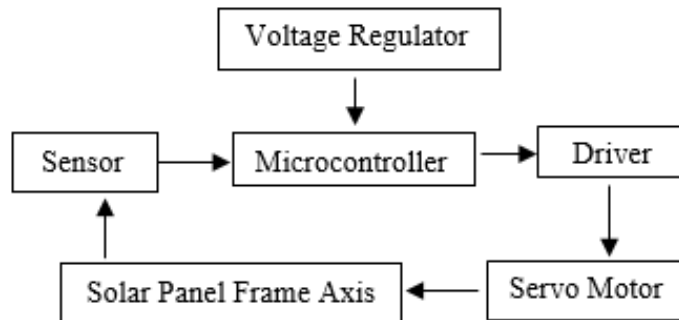


Figure 1. Block diagram of the project.

The methodology of the whole system is contracted as below in Figure 2:

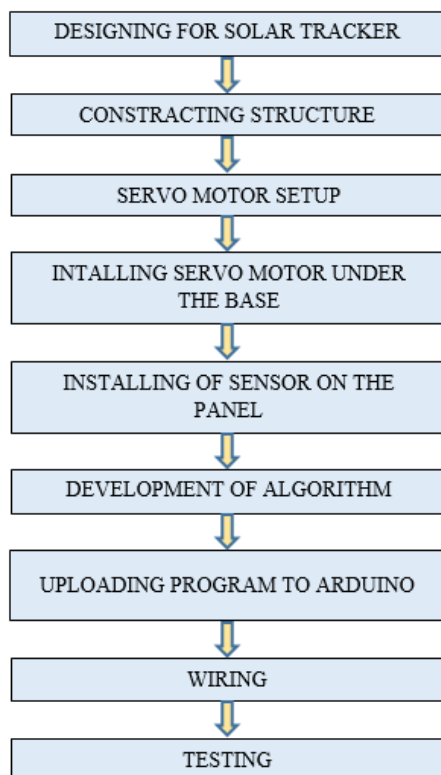


Figure 2. Flow chart of the project methodology

LDR changes resistance with a change in light intensity. Two servo motor was used for rotation of the panel. One servo motor rotates along the horizontal axis and the other rotate along with the vertical axis. Four LDR sensors are used in controlling servo rotation. Two sensors detect the sun's vertical position, while the other two detect the sun's horizontal position.

3.1 Microcontroller

Both the Arduino UNO and Nano have been used. The Arduino Nano board is identical to the Arduino UNO board in that it uses the same Atmega328p microprocessor. As a result, they can use the same program. The size difference is the most significant distinction between these two. Because the Arduino Uno board is double the size of the

Arduino Nano board. As a result, Uno boards take up more room on the system. UNO can be programmed using a USB cable, whereas Nano requires a small USB cable. Arduino Nano has 8 analog inputs and 14 digital outputs, while Arduino UNO has 14 digital outputs and 6 analog inputs. [14]

3.2 Servo motor

The servo motor is a type of rotary actuator that is widely used in a variety of applications. It's a self-contained electrical device that rotates machine parts with high efficiency and precision. The servo motor's output shaft can be rotated to a specific angle. Can perform well at low speeds and with the proper gear ratio, resulting in low heat production.[15]

3.3 Light Dependent Resistor

The light-dependent resistor (LDR) is made from the exposed semiconductor. Its resistor value changes exponentially with the change of intensity of light. It sensed the light intensity which is used as the analog input voltage to the microcontroller. [16]

3.4 Circuit Diagram

Figure 3 & Figure 4 showing the control circuit of the dual-axis solar tracker. Which is based on Arduino UNO & NANO.

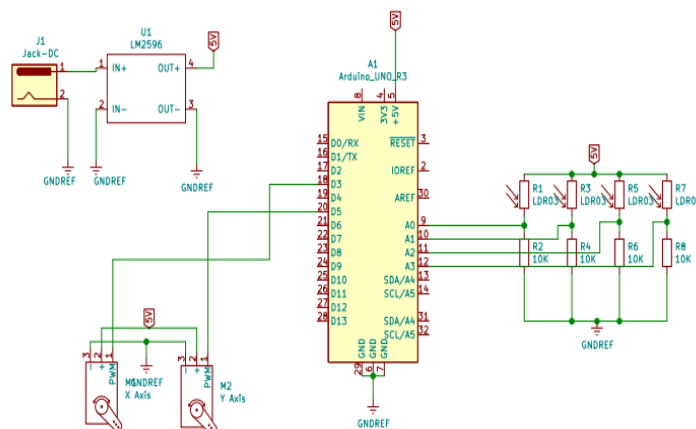


Figure 3. Circuit diagram for the dual-axis solar tracker

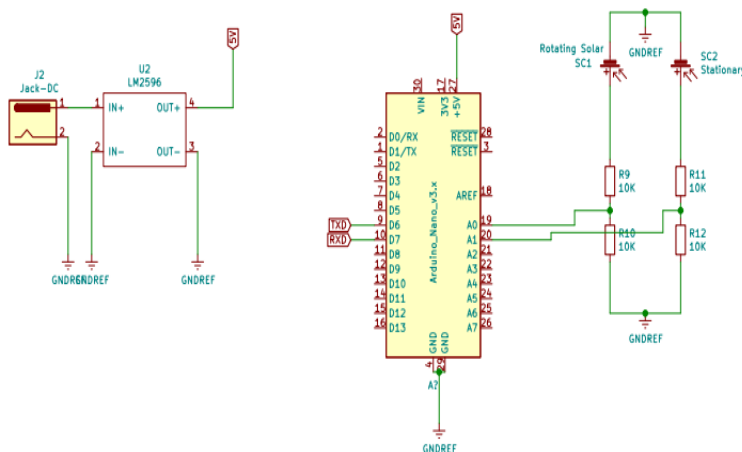


Figure 4. Circuit diagram for power logger.

3.5 Research Design

The structure of the automatic solar tracker consists of a solar panel, two servo motor, a wooden panel holding arm, and a wooden base. One servo motor is placed in the panel holding arm to rotate the panel at the horizontal axis about 65° horizontally in both side. Another servo motor is mounted on the wooden base so that the panel holding arm can rotate at the vertical axis about 165° vertically. Arduino UNO is used for this tracker which gets input from the LDR sensor and leads to rotate servo motors. Arduino Nano is used for logging the power output of the panel and send to the Bluetooth module. Panel holding arm mounted on servo motor which leads to rotate the arm in the vertical axis. Another servo motor mounting on the panel holding arm which leads to rotate the panel in the horizontal axis.

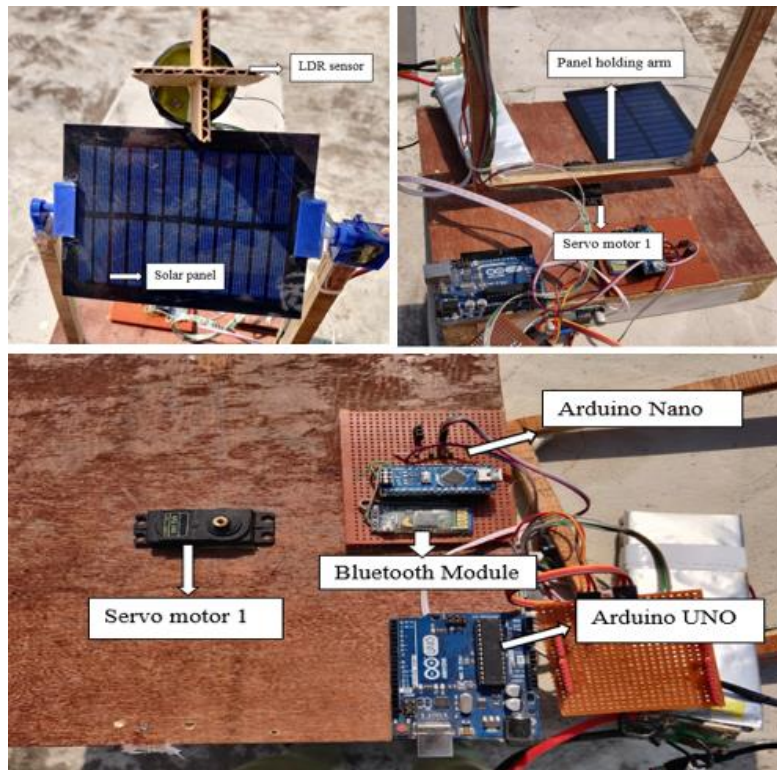


Figure 5. Construction of the system



Figure 6. Overall view of the tracker

The complete mechanical structure of the design of the automatic dual-axis solar tracker is shown in Figure 5 & Figure 6. Solar panels, Arduino UNO, Arduino Nano, LDR sensor, servo motor, motor driver, Bluetooth module, and power resistor are used to execute this project.

4. Result, Data Collection & Analysis

Table 1 shown a performance comparison of the Automatic dual axis solar tracker and stationary solar panel for day 1 (17/04/2021) which was a fully sunny and sun rises at 5.31 AM and sets at 6:14 PM on April 2021 in Raozan, Chittagong, Bangladesh.

Table 1. Performance of Automatic tracker & stationary solar panel (Day1)

Time Of the day(h)	Dual Axis Tracker			Stationary Panel(30°)			Condition
	Power (mW)	Current (mA)	Voltage (V)	Power (mW)	Current (mA)	Voltage (V)	
9.00	67.30	9.93	6.78	30.00	9.90	3.03	Sunny
9.20	65.20	9.97	6.54	33.10	9.97	3.32	Sunny
9.40	64.00	9.98	6.41	29.00	9.83	2.95	Sunny
10.00	66.90	9.99	6.70	33.30	9.97	3.34	Sunny
10.20	66.70	10.05	6.64	34.00	9.86	3.45	Sunny
10.40	66.30	10.03	6.61	34.80	9.94	3.50	Sunny
11.00	67.30	10.01	6.72	37.80	9.95	3.80	Sunny
11.20	67.40	10.00	6.74	34.40	9.94	3.46	Sunny
11.40	68.60	10.04	6.83	32.70	9.94	3.29	Sunny
12.00	71.20	10.06	7.08	46.40	9.87	4.70	Sunny
12.20	69.40	10.06	6.90	34.00	9.94	3.42	Sunny
12.40	68.50	10.07	6.80	34.70	9.89	3.51	Sunny
13.00	68.80	10.01	6.87	31.50	9.94	3.17	Sunny
13.20	67.40	10.00	6.74	30.70	9.90	3.10	Sunny
13.40	67.20	9.97	6.74	31.70	9.88	3.21	Sunny
14.00	66.70	10.06	6.63	33.00	9.88	3.34	Sunny
14.20	66.50	10.00	6.65	32.40	9.97	3.25	Sunny
14.40	66.30	10.02	6.62	32.00	9.88	3.24	Sunny
15.00	65.90	10.00	6.59	31.80	9.94	3.20	Sunny
Average	67.24	10.01	6.72	33.54	9.91	3.38	

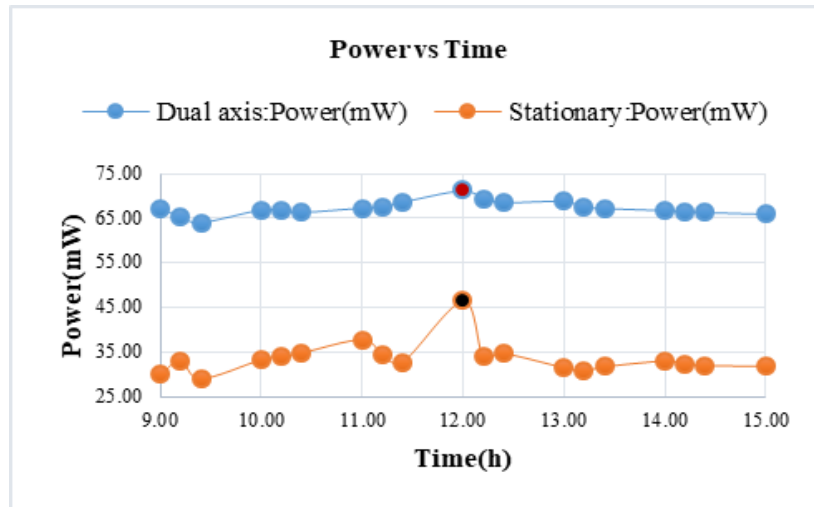


Figure 7. Power vs Time of automatic and stationary solar panels (Day1)

For day 1 the overall power for the automatic solar tracker is 67.24 mW, on the other hand for the stationary panel (30° south facing horizontally) the overall power is 33.34 mW. In Fig 7 (day1), the day was completely sunny all day. So that the power output for both panels has a huge difference. In the automatic tracker, overall performance was high all day than the stationary panel. From 9.00 AM to 12.00 PM output is increasing and after 12.00 PM output is decreasing for both panels. The peak value of power is obtained at sharp 12.00 PM for both panels is 71.20 mW for automatic tracker and 46.40 mW for the static panel.

Table 2 shown a performance comparison between the Automatic dual axis solar tracker and stationary solar panel for day 2 (18/04/2021) which was a partly cloudy.

Table 2. Performance of Automatic tracker & stationary solar panel (Day2)

Time Of the day(h)	Dual Axis Tracker			Stationary Panel(30°)			Condition
	Power (mW)	Current (mA)	Voltage (V)	Power (mW)	Current (mA)	Voltage (V)	
9.00	66.90	9.99	6.70	29.30	9.83	2.98	Sunny
9.20	66.60	10.05	6.63	33.80	10.03	3.37	Sunny
9.40	65.60	9.45	6.94	32.30	9.91	3.26	Sunny
10.00	68.90	10.06	6.85	36.70	10.11	3.63	Sunny
10.20	65.70	10.03	6.55	67.40	9.99	6.75	Cloudy
10.40	67.30	9.97	6.75	66.80	10.00	6.68	Cloudy

11.00	66.20	10.02	6.61	67.80	10.03	6.76	Cloudy
11.20	66.40	10.06	6.60	67.70	9.99	6.78	Cloudy
11.40	67.20	10.07	6.67	71.20	10.06	7.08	Cloudy
12.00	69.80	10.17	6.86	54.80	10.06	5.45	Cloudy
12.20	66.50	9.98	6.66	67.90	9.96	6.82	Cloudy
12.40	66.60	10.00	6.66	67.80	10.04	6.75	Cloudy
13.00	66.10	9.98	6.62	65.90	10.00	6.59	Cloudy
13.20	66.10	10.06	6.57	57.50	9.91	5.80	Sunny
13.40	66.50	9.97	6.67	54.30	9.96	5.45	Sunny
14.00	65.80	10.03	6.56	46.10	10.20	4.52	Sunny
14.20	65.30	10.02	6.52	43.20	9.69	4.46	Sunny
14.40	66.10	9.97	6.63	42.60	9.95	4.28	Sunny
15.00	66.30	10.03	6.61	45.10	10.07	4.48	Sunny
Average	66.63	10.00	6.67	53.59	9.99	5.36	

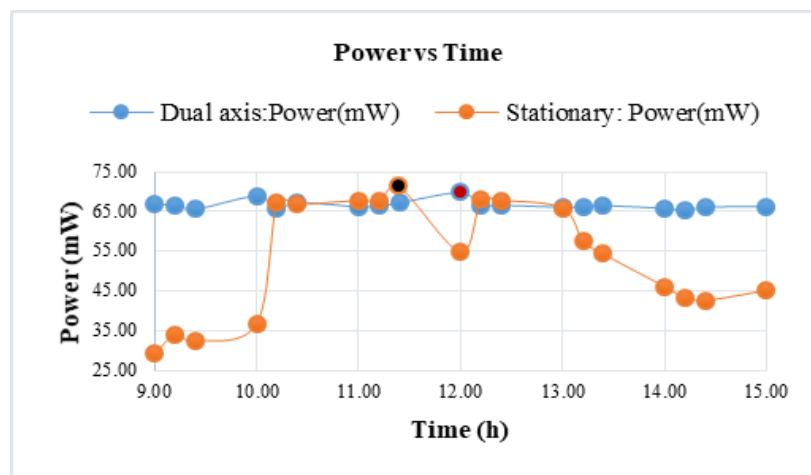


Figure 8. Power vs Time of automatic and stationary solar panels (Day2)

For day 2 the overall power for the automatic solar tracker is 66.63 mW on the other hand for the stationary panel (30° south facing horizontally) the overall power is 53.59 mW. In Fig 8 (day2), the day was cloudy from 10.20 AM to 1.00 PM. So that in this range the power output for both panels was near to same. 9.00 AM to 10.20 AM and 1.00 PM to rest of the day sky was sunny, in this range the output for dual-axis tracker is compared to high than the stationary panel. The peak value was achieved for the automatic tracker is 69.80 mW at 12.00 PM and the stationary panel is 71.20 mW at 11.40 AM.

It is observed that the dual-axis tracking system provides more power and voltage than the stationary panel. About 44.38% more power is produced by the automatic tracker than the stationary panel (30° south facing horizontally). And also shows that when the sky was sunny automatic tracker performed well than static. And when the sky was cloudy both panels performed too closed. So that for a sunny region, it is more efficient to use an automatic solar tracker for maximum output. For a partly cloudy or cloudy region, it will be efficient to use a usual or stationary solar panel.

4. Discussion on Result

The overall outcome for the dual-axis tracker is better than the stationary panel. The optimal power output for both of the panels is achieved from 11.40 AM to 12.20 PM. For day1 which was a sunny day, the average power output is 101.68% more for the automatic tracker than the stationary. For day2 which was cloudy, the average power output is 24.33% more for the automatic tracker than the stationary. Compared to the stationary panel, Overall performance increased by 44.38% for the dual-axis solar tracker than. The result demonstrate that for cloudy regions stationary solar panel would be more practical than an automatic tracker.

Table 3. Average performance comparison for both solar panels.

No. of day	Average Power (mW)		Average Voltage (V)	
	Automatic	Stationary	Automatic	Stationary
Day 1	67.24	33.34	6.72	3.38
Day 2	66.63	53.59	6.67	5.36

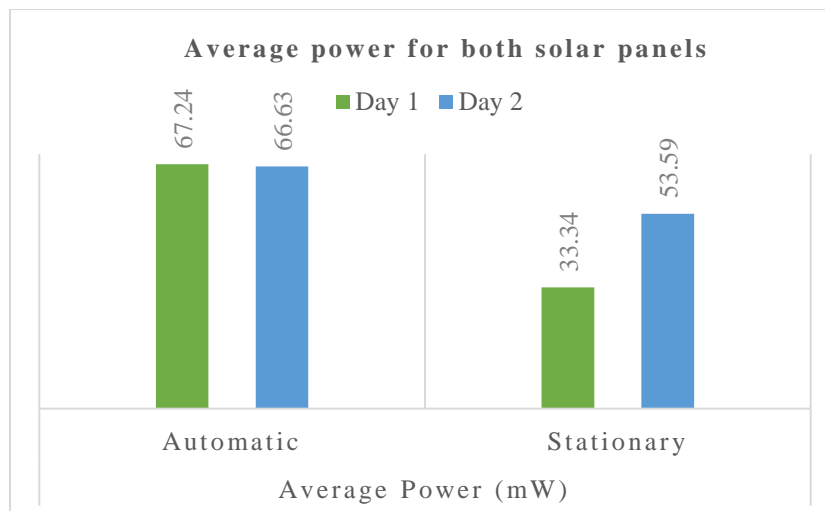


Figure 9: Average Power of the dual-axis solar tracker and stationary panel

For a sunny day, the result shows that the automatic tracker performed to compare to higher than the static solar panel. And for cloudy day stationary solar panel performed close to the automatic solar tracker. So it can be more effective to use a stationary panel instead of an automatic tracker in the cloudy region, which results in reducing maintenance costs. The structure and electrical circuit of the automatic solar tracker is a bit sensitive to strong wind conditions. It is the main disadvantage of this type of tracking system.

5. Conclusion

This paper describes a method of tracking sun position by using microcontroller. The designed tracker system is easy to operate under all circumstances. The automatic tracker is performed better overall. Recorded data and analysis represent that an automatic tracker is more convenient than stationary in the field of producing power in the sunny region. And in the cloudy condition since both are performed near to same so that, it will be wise to use stationary panel rather than automatic one. Which has an economic impact on operations. The solar tracker also provides a beneficial clue for third-world countries to accomplish it into their solar system. For a developing country, where the energy crisis is a big issue, these tracking systems may have an important aspect to make more power

and reduce power crises. Though the prototype has some limitations, still it provides a scope for the betterment of the design method in the future.

6. Acknowledgement

I would like to express my heartiest grateful to Almighty. I would also thankful to my thesis supervisor Prof. Md. Sanaul Rabbi, for his guidance and as well as his valuable advice during the work and the encouragement he has given me.

7. References

- [1] F. O. F. Engineering, I. Engineering, S. Tracker, F. O. R. Solar, and O. R. Otieno, "Faculty of Engineering Department of Electrical and Information Engineering Solar Tracker for Solar Panel," 2015.
- [2] M. T. A. Khan, S. M. S. Tanzil, R. Rahman, and S. M. S. Alam, "Design and construction of an automatic solar tracking system," *ICECE 2010 - 6th Int. Conf. Electr. Comput. Eng.*, no. December, pp. 326–329, 2010.
- [3] A. Z. Hafez, A. M. Yousef, and N. M. Harag, "Solar tracking systems: Technologies and trackers drive types – A review," *Renewable and Sustainable Energy Reviews*, vol. 91. Elsevier Ltd, pp. 754–782, 01-Aug-2018.
- [4] G. Mehdi, N. Ali, S. Hussain, A. A. Zaidi, A. Hussain Shah, and M. M. Azeem, "Design and fabrication of automatic single axis solar tracker for solar panel," *2019 2nd Int. Conf. Comput. Math. Eng. Technol. iCoMET 2019*, pp. 1–4, 2019.
- [5] C. Jamroen, P. Komkum, S. Kohsri, W. Himananto, S. Panupintu, and S. Unkat, "A low-cost dual-axis solar tracking system based on digital logic design: Design and implementation," *Sustain. Energy Technol. Assessments*, vol. 37, no. December 2019, p. 100618, 2020.
- [6] J. V. Patil, J. K. Nayak, and V. P. Sundersingh, "Design, fabrication and preliminary testing of a two-axes solar tracking system," *RERIC Int. Energy J.*, vol. 19, no. 1, 1997.
- [7] J. K. Tharamuttam and A. K. Ng, "Design and Development of an

- Automatic Solar Tracker,” *Energy Procedia*, vol. 143, pp. 629–634, 2017.
- [8] A. Ponniran, A. Hashim, and A. Joret, “A Design of Low Power Single Axis Solar Tracking System Regardless of Motor Speed,” *Int. J. Integr. Eng.*, vol. 3, no. 3, pp. 5–9, 2011.
- [9] S. Abdallah and S. Nijmeh, “Two axes sun tracking system with PLC control,” *Energy Convers. Manag.*, vol. 45, no. 11–12, pp. 1931–1939, 2004.
- [10] N. Mohammad and T. Karim, “Design and Implementation of Hybrid Automatic Solar-Tracking System,” *J. Sol. Energy Eng.*, vol. 135, no. 1, p. 011013, 2012.
- [11] A. Ponniran, A. Hashim, and H. Ali Munir, “A design of single axis sun tracking system,” *2011 5th Int. Power Eng. Optim. Conf. PEOCO 2011 - Progr. Abstr.*, no. June, pp. 107–110, 2011.
- [12] P. Roth, A. Georgiev, and H. Boudinov, “Design and construction of a system for sun-tracking,” *Renew. Energy*, vol. 29, no. 3, pp. 393–402, 2004.
- [13] T. S. Zhan, W. M. Lin, M. H. Tsai, and G. S. Wang, “Design and implementation of the dual-axis solar tracking system,” *Proc. - Int. Comput. Softw. Appl. Conf.*, vol. 2, pp. 276–277, 2013.
- [14] “Arduino.” [Online]. Available: <https://www.elprocus.com/an-overview-of-arduino-nano-board>. [Accessed: 20-Apr-2021].
- [15] A. Mansouri, F. Krim, and Z. Khouni, “Design of a prototypical dual-axis tracker solar panel controlled by geared dc servomotors,” *Sci. Iran.*, vol. 25, no. 6D, 2018.
- [16] C. M. Ojeda and J. C. Dela Cruz, “Analysis on the Optical Response of Ldr and Phototransistor in Photoplethysmography,” *Sens. Bio-Sensing Res.*, vol. 28, 2020.

Development of SMS Spam Filtering APP for Modern Mobile Devices

Musibau Adekunle IBRAHIM¹, Patrick OZOH¹

²Ayotunde Oladotun OJO

¹Department of Computer Science, Osun State University, Nigeria

²Department of Physics, Osun State University, Nigeria

[¹kunle_ibrahim2001@yahoo.com](mailto:kunle_ibrahim2001@yahoo.com)

[²dotun4realoj@gmail.com](mailto:dotun4realoj@gmail.com)

Abstract: Short Messaging Service (SMS) spam has been known to be the unwanted or unintended messages received on mobile phones. This paper has presented a review of current methods, existing problems, and future research directions on spam classification techniques of mobile SMS spams. The methodology involves collecting a large dataset of SMS messages, both legitimate and spam, to train and evaluate various machine learning algorithms. Feature extraction techniques have been employed to capture relevant information from SMS messages, such as the presence of specific keywords, the length of message, and the sender's identity. The experimental results on the proposed spam filtering system achieves a high level of accuracy with a low false-positive rate, thereby minimizing the chances of legitimate messages being classified as spam. The system effectively detects and blocks a significant portion of spam messages, providing mobile users with a reliable defense against unwanted SMS communications. The findings of this study reveal that machine learning algorithms, particularly ensemble methods like Random Forests, performed well in SMS spam filtering on mobile devices.

Keywords: SMS spam filtering, machine learning, mobile devices

تطوير تطبيق تصفية الرسائل غير المرغوب فيها عبر الرسائل النصية القصيرة للأجهزة المحمولة الحديثة

الملخص: من المعروف ان البريد العشوائي في خدمة الرسائل القصيرة هو الرسائل غير المرغوب فيها أو غير المقصودة التي يتم تلقيها على الهواتف المحمولة. قدمت هذه الورقة مراجعة للطرق الحالية، والمشاكل الحالية، واتجاهات البحث المستقبلية حول تقنيات تصنيف البريد العشوائي للرسائل النصية القصيرة المتقلة. تتضمن المنهجية جمع مجموعة كبيرة من البيانات من الرسائل النصية القصيرة، سواء الشرعية منها أو غير المرغوب فيها، لتدريب وتقييم خوارزميات التعلم الآلي المختلفة. تم استخدام تقنيات استخراج الميزات لالتقاط المعلومات ذات الصلة من رسائل SMS ، مثل وجود كلمات رئيسية محددة، وطول الرسالة، وهوية المرسل. تحقق النتائج التجريبية لنظام تصفية البريد العشوائي المقترح مستوى عالٍ من الدقة مع معدل إيجابي كاذب منخفض، مما يقلل من فرص تصنيف الرسائل المشروعة على أنها بريد عشوائي. يكتشف النظام بشكل فعال ويحظر جزءًا كبيرًا من رسائل البريد العشوائي، مما يوفر لمستخدمي الهاتف المحمول دفاعًا موثوقًا به ضد اتصالات الرسائل النصية القصيرة غير المرغوب فيها. تكشف نتائج هذه الدراسة أن خوارزميات التعلم الآلي، وخاصة طرق التجميع مثل Random Forests، كان أداءها جيدًا في تصفية الرسائل غير المرغوب فيها عبر الرسائل النصية القصيرة على الأجهزة المحمولة.

1.Introduction

This paper presents a detailed description of SMS Spamming Filtering Application (Android based app), which is to be used by most Android smartphone users to protect their Android devices from any harmful spams messages. The SMS Spamming Application will be a mobile based app exclusively for devices built with Android operating system. SMS is one of the popular communication services in which a message is sent electronically. The reduction in the cost of SMS services by telecom companies has led to the increased use of SMS. However, mobile users have become increasingly concerned regarding the security of their client confidentiality. This is mainly due to the fact that mobile marketing remains intrusive to the personal freedom of the subscribers, which has attracted and resulted into SMS Spam problem. A spam message is generally any unwanted message that is sent to a user's mobile phone. Spam messages include advertisements, free services, promotions, awards, etc. People are using SMS messages to communicate rather than emails because while sending SMS messages there is no need for an internet connection, and it is simple and efficient, which has led to a lot of spam messages (Gómez-Adorno, 2017).

Spam has been a large problem on the internet for as long as e-mail and personal computers have been ubiquitous. As a result, numerous methods have been proposed to reduce the ease at which spammers can retrieve messages on the internet. Previous efforts to fight spam on the internet have not totally eradicated it but rather increasing difficulty for those in the business of email spamming (Yadav et al., 2020). Various studies have been conducted by different researchers to resolve these problems, for instance, Li et al. (2020) presented a machine learning-based SMS spam filtering system that utilized features such as sender reputation, message length, and frequency of specific keywords to determine whether an SMS is a spam or not. The system achieved a high accuracy rate of 95% in detection and classification of spam messages.

Similarly, Santos et al. (2021) proposed a hybrid approach combining rule-based and machine learning techniques to effectively filter SMS spam with a precision of 97% and a

recall of 95%. Moreover, advancements in machine learning algorithms have demonstrated promising results in SMS spam filtering. Pham et al. (2018) explored the application of Support Vector Machines (SVM) and Naive Bayes classifiers for SMS spam detection on mobile devices.

Their study achieved an accuracy of 94% with SVM and 91% with Naive Bayes. The problem at hand is the inadequate SMS spam filtering systems designed for mobile devices. The rising use of mobile devices and Short Message Service (SMS) have resulted in a surge of unsolicited and unwanted SMS spam messages. Findings in this research reveal that existing filtering techniques have not been able to effectively address these issues, allowing spam messages to infiltrate users' inboxes. This leads to privacy invasion, wastage of network resources, and potential security risks for mobile users. The consequences include user frustration, decreased productivity, network congestion, and susceptibility to fraudulent activities. Therefore, there is a pressing need to develop robust and accurate SMS spam filtering solutions specifically tailored for mobile devices to alleviate these problems and provide users with a spam-free messaging experience.

On this note, this paper therefore aims at developing an Android smartphone users with a mobile-based security App using Python programming language. The proposed App would be developed in such a way that when the App is installed on the mobile phone, the entire system would have the capability to filter out unwanted messages through its various interfaces.

2.Literature Review

In this section, related publications on SMS spam detection and classification papers would be reviewed in order to determine their strength and weaknesses. Zainal et al. (2022) developed a spam detection model using Rapid Miner and Weka tools; they applied two malware tools to perform their experiments on the UCI repository dataset.

The research outputs demonstrated that both tools can produce almost a similar result on the same dataset with the same classification algorithms. El-Alfy (2019) has recently suggested a new method to identify spam messages on both email and SMS platforms. They tested many methods and features to achieve the best set of features with low level

of model complexity. In their research, they applied Support Vector Machine (SVM) and Naïve Bayes techniques with eleven different features due to the nature of their datasets. It was finally discovered that the model complexity of the developed system was very high and hence could not be used for detecting big datasets. Zainal et al. (2022) introduced a model for spam messages filtering to remove background noise and unwanted materials from bulk messages. The developed model was evaluated in terms of performance in spam messages detection using text classification algorithms on mobile phones. Filtering, training, and updating features could be performed on any Android mobile phones. It was discovered that the research outputs of their experiments revealed that the developed model could be used to filter out spam messages even with small memory usage and good classification accuracy. In another research, Chan et al. (2019) proposed two approaches for classifying and eliminating SMS spam messages, their approach was focused on the weight and length of the message; series of experiments were performed on the selected database and they achieved a remarkable result in terms spam detection and classifications. Uysal et al. (2019) developed a new approach for filtering SMS spam messages. In their approach, a hybrid method comprises of chi-square and information gain algorithm for spam messages was applied. Moreover, the authors also presented an android-based SMS spam filtering method using Bayesian approach. Based on their outputs, their method is efficient and can classify both ham and spam messages even with high degree of classification accuracy. In Serrano et al. (2019), a technique for detecting spam messages using extrinsic information was investigated. All experimental tests were performed in Weka environment using 10-fold cross validation approach. The authors achieved good classification and detection accuracy with a low memory usage.

Junaid (2019) proposed a system to detect and classify SMS spam messages on a mobile phone by applying different classifiers. In their results, it was concluded that supervised learning algorithms could be used to build original model. At the end, the developed model achieved a classification accuracy of over 80%. Choudhary (2017) investigated a system for detection and classification of spam messages. The authors extracted ten unique features and applied them for detecting unwanted messages. The techniques

adopted in their approach were True Positive (TP) rate, False Positive (FP) rate, precision, and F-measure. In their research, the authors compared various classification algorithms, and among them, the Random Forest algorithm achieved the best results with a classification accuracy of 96.1% TP rate.

In a similar research, Suleiman (2017) proposed a technique for removing SMS spam messages using hybrid technique. They applied the hybrid method for feature selection, and extracted some spam messages features. Selected features were then compared on various algorithms in order to determine the best.

This section has so far reviewed the advantages of recent developed approaches in detecting and filtering SMS spam messages while also noting their weaknesses and limitations. According to the literature, it has been discovered that most of the SMS spam detection techniques are not accurate enough in terms of detection of unwanted messages and classification. Therefore, this current study would propose a machine learning technique to identify SMS spam messages with high performance and acceptable classification accuracy.

3.Methodology

The public dataset of SMS labelled messages were obtained from UCI Machine Learning Repository. This study finds that there are only 5,574 labelled messages in the dataset, with 4827 of the messages belong to real messages while the other 747 messages belong to spam messages as shown in Table 1. Nonetheless, this dataset consists of two named columns starting with the message labels (ham or spam) followed by strings of text messages and three unnamed columns.

Table 1: Type of Features of Dataset

Data Set	Legitimate	Spam	Total
SMS spam	4827	747	5574
DIT SMS spam	0	1353	142
British English SMS	450	425	875

Total	5,277 (67.6%)	2,525(32.4%)	7802
-------	---------------	--------------	------

As shown in Table 1, the dataset has 67.6% of Ham message and 32.4% of Spam message. It has been discovered that this dataset contains some unwanted features and therefore requires preprocessing. The purpose of preprocessing is to convert a raw data into a form that can fit into a machine learning. The process of data preprocessing involves background noise removal, sampling and formatting. This paper uses a combination of content-based and user-based features for developing a robust system for efficient detection and classification of spam messages. Content-based features include the words, phrases, and patterns that are commonly found in spam messages, while user-based features include the sender's phone number, frequency of messages, and time of day the message was sent. The system design of SMS spam filtering typically involves several components, including data preprocessing, feature extraction, detection and classification algorithms. Feature extraction includes transformation of SMS messages into a set of features that can be used by the machine learning algorithm. This paper employed Naïve Bayes classifier for data classification to classify the dataset as spam or ham. In Figure 1, the flow chart diagram shows the steps of an SMS spam filtering, which start from the components and messages in raw data followed by preprocessing stage through various stages of algorithmic steps to detect the spam messages on mobile devices as either spam or non-spam.

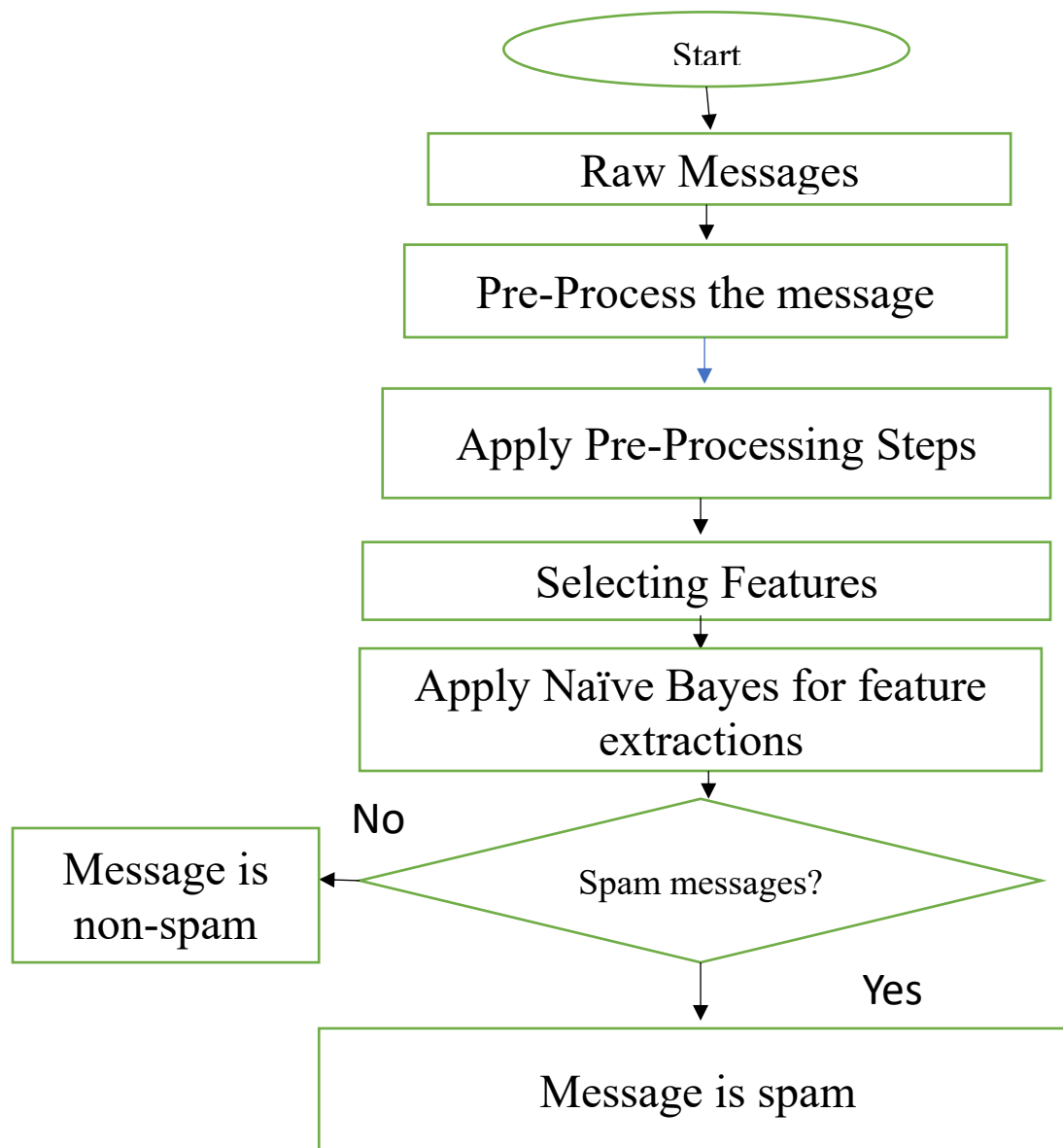


Figure 1: Flowchart Diagram of the System

The implementation of an SMS spam filtering system typically involves using a programming language or tool to develop the components described in the system design. There are many programming languages and tools available for implementing SMS spam filtering systems, including Python, Java, and MATLAB. In this paper, several Python libraries, including scikit-learn and NLTK have been used to implement the data preprocessing, feature extraction, and detection algorithm. This paper employed Naive

Bayes on a classification task involving spam SMS messages and the model was able to classify over 97 percent of all the SMS messages correctly as spam or non-spam.

4.Results and Discussion

The proposed system was successfully tested to detect spam messages on mobile phones. It basically detect spam messages by the developed app that includes normal messages, spam messages and filtered spam messages. Based on the above, the application is user friendly and meets all the requirements usability and security of personal data. This application contains an additional features, which includes some security measures to protect and guide our data against cybercriminals on mobile devices. This additional feature incorporated in the system is our major contribution to knowledge in this paper since in literature, most researchers did not security capability in their systems and they are mostly on desktop not on mobile device like our system.

Figure 2 displays the SMS spam filtering app using a splash-screen that boots to the main app. This icon was displayed for over 10 seconds before launching to the main app on a mobile device or on enumerator.

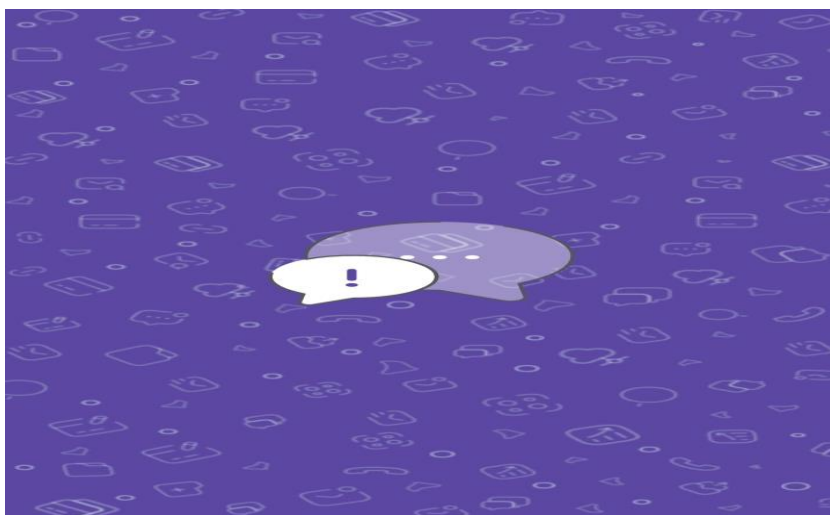


Figure 2:
Page for

Front
Spam

Filtering System

In Figure 3, it shows the front page for the filtering technique where all the images from the phone are stored. This was achieved by the work permission handler, which allows the developed mobile app to accept and store information. In the second tab, there is a feature for detection and classification of spam messages on mobile phone.

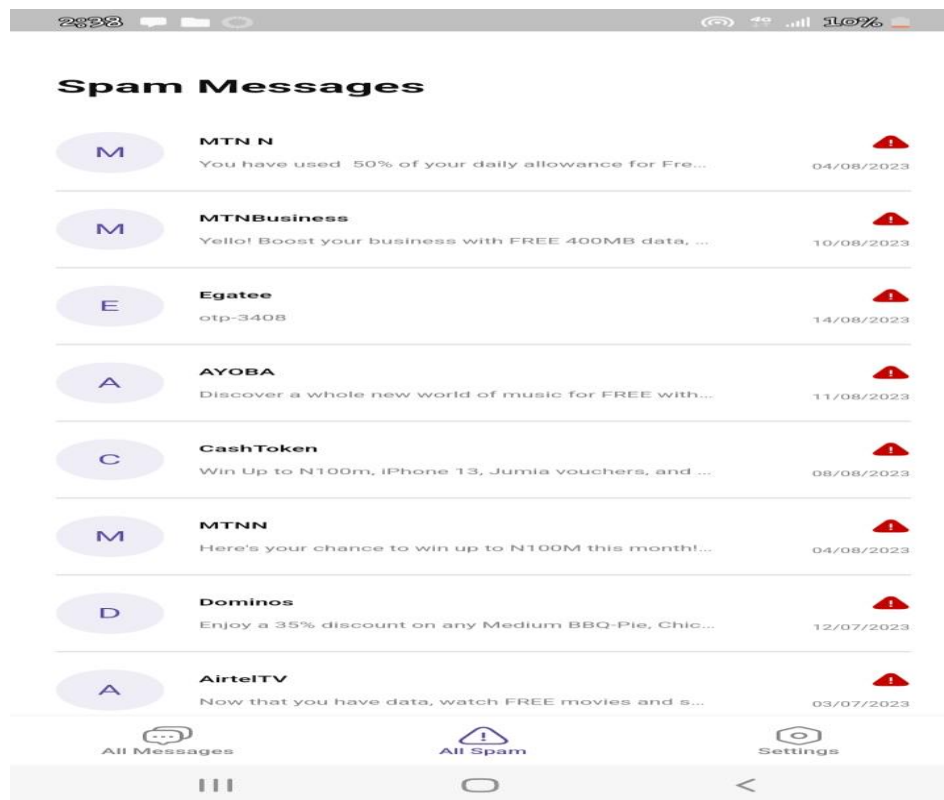


Figure 3: Front Page of SMS Spam filtering System

As presented in Figure 4, the developed app shows the message details of the SMS spam filtering app. It detects all messages that enter into your mobile phones with the help of the permission handler that was previously installed in the flutter. It runs on android version 10.2.0 to grant access to the mobile phones

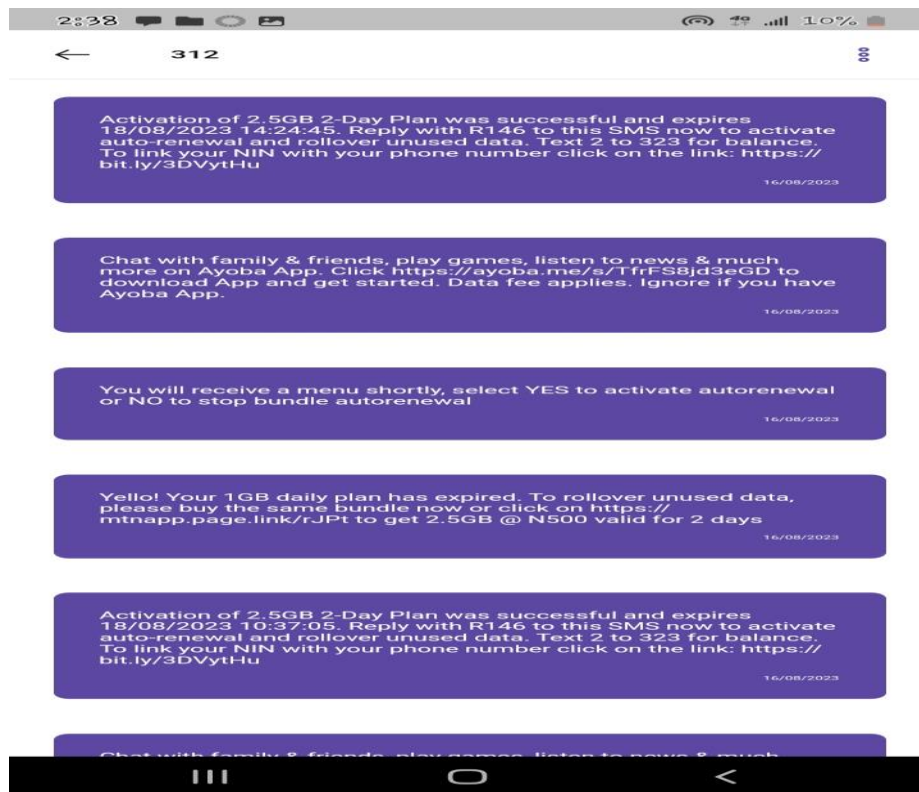


Figure 4: Examples of SMS Spam Messages

Figure 5 is the screenshot of the SMS spam filtering search icon, which grant permission for searching any messages on the app and checking the spam filtering commands within the system. The search icon help can help to detect and classify any message to determine if it belongs to spam or not.

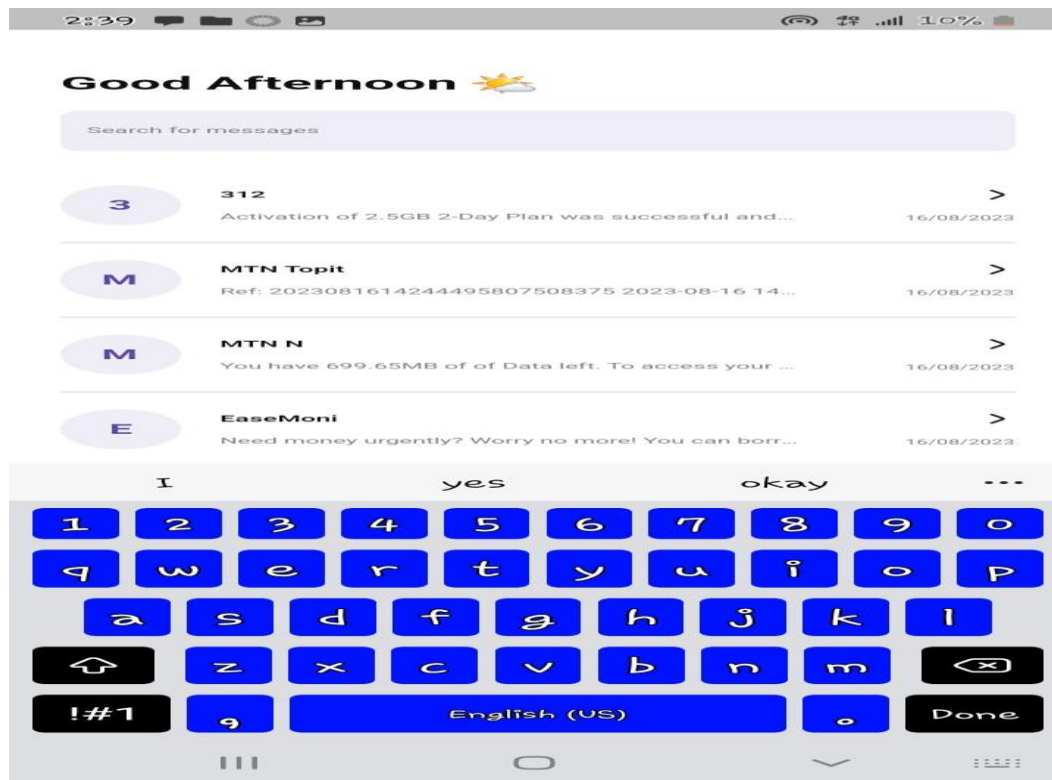


Figure 5: Search Icon on SMS spam app

Overall, the developed system was able to detect and classify messages received by mobile devices as either spams or non-spams using different experimental results as presented in this paper.

5. Conclusions

This paper studied some related research papers in the field of spam messages detection and classification with a view to developing a new approach for alleviating existing problems in this research area. About seventeen research papers have been selected and reviewed in order to understand the existing techniques in this field of study. The knowledge acquired in the literature review in this paper has been put together to propose a new method for addressing common challenges facing SMS spam filtering system. The proposed system contains some additional features that could be used to eliminate problems or limitations in spam detection and classification.

This paper has contributed to knowledge in the area of security by denying unauthorized access to SMS spam filtering model and the developed app is currently running on mobile

devices. This is a robust system that is portable, secured and efficient in terms of separating unwanted messages from useful ones. Generally, the developed system has been compared and evaluated with the existing techniques, the proposed system achieved higher classification and detection accuracy when compared with the state-of-art method in this research field. Future research direction in this field could be achieved by applying the proposed system for preventing hackers or unknown users from gaining access to detection systems.

6.References

- [1] Al-Hasan A.A., El-Alfy E.-S.M. (2019) Dendritic cell algorithm for mobile phone spam filtering, *Procedia Computer Science* 52244-251.
- [2] Chan, P.P., Yang, C., Yeung, D.S. and Ng, W.W. (2019) "Spam filtering for short messages in adversarial environment", *Neurocomputing*, Vol. 155, 167-176.
- [3] Choudhary, N. and Jain, A.K. (2019) "Towards filtering of SMS spam messages using machine learning based technique", in *International Conference on Advanced Informatics for Computing Research*, Springer., 18-30.
- [4] El-Alfy, E.-S.M. and AlHasan, A.A. (2019) "Spam filtering framework for multimodal mobile communication based on dendritic cell algorithm", *Future Generation Computer Systems*, Vol. 64, 98-107.
- [5] Gómez-Adorno, H., Pinto, D., Sidorov, G., & Villaseñor-Pineda, L. (2017). A linguistic approach and ensemble methods for SMS spam detection. *Expert Systems with Applications*, 68, 96-109.
- [6] Junaid, M.B. and Farooq, M. (2019) "Using evolutionary learning classifiers to do mobiles spam (SMS) filtering", in *Proceedings of the 13th annual conference on Genetic and evolutionary computation*, 1795-1802.
- [7] Li, B., Zhang, B., & Lee, W. C. (2020). SMS spam filtering based on keywords and spammers: A multi-view classification approach. *Expert Systems with Applications*, 39(10), 9229-9236.

- [8] Pham, D. T., Dang, T. D., & Nguyen, L. H. (2018). SMS spam filtering on mobile devices using machine learning techniques. In Proceedings of the International Conference on Advanced Computational Intelligence (ICACI) (pp. 435-440).
- [9] Santos, M. F., Cardoso, J. S., & Oliveira, H. P. (2021). Combining rule-based and machine learning classifiers for SMS spam filtering. *Expert Systems with Applications*, 41(4), 1933-1943.
- [10] Serrano, J.M.B., Palancar, J.H. and Cumplido, R. (2019) "The evaluation of ordered features for SMS spam filtering", in *Iberoamerican Congress on Pattern Recognition*, Springer., 383-390.
- [11] Suleiman, D. and Al-Naymat, G. (2017) "SMS spam detection using h2o framework", *Procedia Computer Science*, Vol. 113, 154-161.
- [12] Uysal, A.K., Gunal, S., Ergin, S. and Gunal, E.S., (2019) "A novel framework for SMS spam filtering", in *2012 International Symposium on Innovations in Intelligent Systems and Applications*, IEEE., 1-4.
- [13] Yadav, K., Saha, S., Kumaraguru, P., Kumra, R.. (2020) "Take control of your SMSes: Designing an usable spam SMS filtering system", *IEEE 13th International Conference on Mobile Data Management*, MDM.
- [14] Zainal, K., Sulaiman, N. and Jali, M., "An analysis of various algorithms for text spam classification and clustering using rapidminer and weka", *International Journal of Computer Science and Information Security*, Vol. 13, No. 3, (2022), 66-77.

Utilisation of Risk Management, Project Management Tools and Teamwork for the Execution of Turnaround Maintenance Activities

Abdullahi Mohammed¹, Umar Ali Umar^{1, *}, Ayodeji Nathaniel Oyedeji¹

¹Department of Mechanical Engineering, Ahmadu Bello University, Zaria, Nigeria

*Corresponding Author: umaraliumar@yahoo.co.uk

Abstract: This study is based on using management tools such as risk management, project management tools and teamwork in Turnaround Maintenance Activities (TMA) in a typical petrochemical and refinery industry in Nigeria, one of the notable oil-producing developing nations. To achieve the broad objective of the study, a structured questionnaire was developed based on three sub-hypotheses on the significance of the management tools under study in TMA in the petrochemical and refinery industry. The respondents consisted of carefully sampled 341 workers at a refining and petrochemical company, ranging from the Maintenance department, Engineering and Technical Services department, Health Services and Environment department, Supply Chain Management department, as well as contractors. Using inferential statistics and Pearson correlation analysis, the sub-hypotheses were analysed. The results of the study showed that the management tools considered have a significant relation with TMA with R-values of 0.617, 0.742, and 0.714 for the relationship of TMA with risk management, project management tools, and teamwork, respectively. Furthermore, the study's findings showed that most respondents strongly agree that the successful TMA implementation in the petrochemical and refinery industry is dependent on good risk management practices such as risk survey, quantification, mitigation, and leadership collaboration (p-value = 0.01), use of project management tools encompassing decomposition, critical path analysis, visualisation, accountability, and performance matrices (p-value = 0.002), and adequate integration of teamwork to ensure transparency, synchronisation, equity, and

collaboration (p-value = 0.002). The study concluded by recommending continuous application of these management tools and many more to ensure effective TMA in the industry.

Keywords: Turnaround Maintenance Activities (TMA), Petrochemical and refinery industry, Risk management, Project management, teamwork

الاستفادة من إدارة المخاطر وأدوات إدارة المشاريع والعمل الجماعي لتنفيذ أنشطة الصيانة الشاملة

المخلص: تعتمد هذه الدراسة على استخدام أدوات الإدارة مثل إدارة المخاطر وأدوات إدارة المشاريع والعمل الجماعي في أنشطة الصيانة الشاملة (TMA) في صناعة البتروكيماويات ومصافي التكرير النموذجية في نيجيريا، وهي إحدى الدول النامية البارزة المنتجة للنفط. ولتحقيق الهدف العام للدراسة، تم تطوير استبيان منظم يعتمد على ثلاث فرضيات فرعية حول أهمية أدوات الإدارة قيد الدراسة في TMA في صناعة البتروكيماويات والمصافي. تم اختيار المشاركين بعناية من 341 عاملاً في إحدى شركات التكرير والبتروكيماويات، بدءاً من قسم الصيانة، وقسم الخدمات الهندسية والفنية، وقسم الخدمات الصحية والبيئة، وقسم إدارة سلسلة التوريد، بالإضافة إلى المقاولين. وباستخدام الإحصاء الاستدلالي وتحليل ارتباط بيرسون، تم تحليل الفرضيات الفرعية. أظهرت نتائج الدراسة أن أدوات الإدارة المدروسة لها علاقة معنوية بـ TMA بقيم R تبلغ 0.617 و0.742 و0.714 لعلاقة TMA بإدارة المخاطر وأدوات إدارة المشاريع والعمل الجماعي على التوالي. علاوة على ذلك، أظهرت نتائج الدراسة أن معظم المشاركين يوافقون بشدة على أن التنفيذ الناجح للتحليل الحراري الميكانيكي (TMA) في صناعة البتروكيماويات ومصافي التكرير يعتمد على ممارسات إدارة المخاطر الجيدة مثل مسح المخاطر، والقياس الكمي، والتخفيف، وتعاون القيادة (القيمة الاحتمالية = 0.01)، والاستخدام لأدوات إدارة المشروع التي تشمل التحليل وتحليل المسار الحرج والتصوير والمساءلة ومصفوفات الأداء (القيمة الاحتمالية = 0.002)، والتكامل المناسب للعمل الجماعي لضمان الشفافية والتزام الإنصاف والتعاون (القيمة الاحتمالية = 0.002). واختتمت الدراسة بالتوصية بالتطبيق المستمر لأدوات الإدارة هذه وغيرها الكثير لضمان في الصناعة. TMA فعالية

1.Introduction

Maintenance activities (MA) are distinctive and complicated undertakings frequently carried out on constrained timeframes [1]. MA operations demand many personnel who carry out their duties in crowded spaces. However, MA initiatives are crucial to maintaining steady production levels because they increase process plant dependability, lower the cost of corrective maintenance, and boost resource management effectiveness [2]. The degree to which MA operations are correctly carried out affects the company's general performance [3]. Due to the complexity and intensity of MA projects, MA costs can reach millions of dollars, including lost income and maintenance expenses [1]. Such losses may significantly affect the profitability of petrochemical and refinery companies [4], [5].

Based on this fact, businesses must ensure that assets perform at their highest levels to achieve high corporate performance (such as increased earnings and sales). MA initiatives are among the most expensive and time-consuming projects in the process sector, according to Witteman et al. [1], due to cost overruns and scheduling delays, which are fairly common with MA projects. Numerous variables may be responsible for cost overruns, including deficient execution planning, productivity loss during MA execution, and scope modifications (caused by unforeseen mechanical issues) [6]. Defective execution planning, scope revisions, or low productivity—the latter brought on by a shortage of trained workers—are the main causes of schedule delays [4]. Organisations that do maintenance on time, on budget, and without surprises typically have a defined work process and follow it, according to Iheukwumere et al. [5]. A well-defined and standardised approach is essential for MA planning and administration. Managers may achieve this by adopting and putting into practice tried-and-true industry best practices.

The maintenance sub-sector now faces skilled worker attrition, which multiplies risks, raises the demand for best practices, and necessitates a new paradigm: process- and unit-specific knowledge transfer, according to research studies that have emphasised the rising need for adopting best practices [7], [8]. However, limited studies exist on the petrochemical and refinery industry's best practices for turnaround maintenance activity (TMA) planning and management. However, the building sector has produced several

planning best practices that TMA projects may use with some adjustments [9]–[12]. Specifically, the Nigerian petrochemical and refinery industries experience high and persistent production downtime, which usually results in completion extended scheduled time, costs above the budget and sometimes not conforming to the planned scope. The level of use of project management tools, risk management and teamwork in TMA is unknown in Nigeria and developing countries at large industries.

Hence, this study presents a case study that identifies and establishes the utilisation of risk management, project management tools and teamwork in executing TMA in the petrochemical and refinery industries. The study seeks to i) identify the level of usage of project management tools, risk management and teamwork in TMA and ii) determine the impacts of project management tools, risk management and teamwork on TMA success.

2.Literature Review

Petrochemical and refinery plants often perform major maintenance tasks during shutdowns and turnarounds. During a TMA, a routine maintenance event, plants are shut down to execute necessary maintenance work that must be carried out when the plant's facilities are offline [4]. Among these MAs are inspections, repairs, replacements, and overhauls. The business plan, conceptual development, work development, detailed planning, pre-turnaround work, turnaround execution, and post-turnaround stages are therefore included in the TMA phases [13]. Three different types of work are done during MA projects, and they include work on equipment that requires shutting down the entire plant, work that can be done while the plant or equipment is in operation, and work that fixes flaws that were discovered while operation but could not be fixed at the time [14].

MA operations support plant production consistency in the process sector, in which large-scale, intricate MA projects are the norm [15]. Petrochemical and refinery companies need to be able to perform MA tasks while adhering to the budget, deadline, and quality requirements [5]. Meeting those limits is challenging without solid and reliable methods for planning and managing MA initiatives.

To consider some related works on TMA of petrochemical industries, the study by AlHamouri et al. [6] researched the use of workforce planning for maintenance tasks, shutdowns, and turnarounds in petrochemical plants. The first section of the study focused on creating a customised version of Workforce Planning (WFP) that would suit MAs in the petrochemical sector using feedback from subject matter experts (SMEs). The study team was able to evaluate the current levels of MA execution planning and management and identify ineffective areas by monitoring its implementation. This research provides suggestions on how to execute MA while maximising planning procedures. Ghaithan [13] studied the optimisation model for TMA scheduling and operational planning of the oil and gas supply chain. The model integrated the hydrocarbon supply chain plants and jointly developed operation and maintenance schedules. A model with and without integration between operating and maintenance tasks was investigated. The obtained results demonstrated the significance of the suggested model, and the model's outcomes were encouraging. The model mandated that all hydrocarbon supply chain plants be kept operational during periods of low demand to prevent significant production losses, meet the majority of demand, and reduce lost sales as much as possible.

In similar industries, Zhicheng et al. [16] researched the assessment of TMA impacts in Indonesia's process sector. Plant availability and downtime loss were the important factors utilised to examine TMA's impact. The outcome revealed a link between TMA occurrences and rising availability of 0.315 and a correlation between growing downtime loss of -0.818. The correlation value demonstrates that TMA significantly affects plant availability and downtime loss in real-world process industry practice. Furthermore, Akbar and Ghazali [17] researched the impact of team alignment on the coordination performance of plant TMA in a Malaysian process-based sector. The study employed a survey technique to collect data from cement factories and electric power-producing facilities. The data were gathered using a straightforward random sampling approach.

A satisfactory response rate of 32 percent was obtained from the data gathered from 31 out of 96 firms. The empirical findings demonstrated that team alignment and coordination in plant turnaround maintenance improve performance. Also, Shou et al. [18] in Australia conducted a study on using 4D building information modelling to

enhance TMA in plants. The findings demonstrated that the use of building information modelling was able to ensure that TMA began on time, finished 9.6 hours ahead of schedule and 2.4 days ahead of the original schedule, as well as save a significant amount of maintenance costs in comparison to the actual cost with the initial budget.

Summarily, the extensive literature review on TMA in petrochemical and refinery plants highlights key phases, challenges, and critical considerations in managing large-scale maintenance projects. The TMA process, involving business planning, conceptual development, detailed planning, pre-turnaround work, execution, and post-turnaround stages, underscores the complexity of balancing budget, deadline, and quality requirements. Notable findings from related studies include custom workforce planning tailored for petrochemical MAs, an optimisation model for TMA scheduling in the oil and gas supply chain, an assessment of TMA impacts in Indonesia, an exploration of team alignment's impact on coordination in Malaysian plant TMAs, and successful use of 4D building information modelling to enhance TMA efficiency in Australian plants. These findings collectively contribute insights into workforce optimisation, planning procedures, and the coordination and performance aspects of plant TMA, forming a valuable foundation for the current research on risk management, project management tools, and teamwork in executing TMA activities. The research noted that there are only a few studies on the extent to which project management tools, risk management, and collaboration are used in increasing the efficacy of TMA, despite Africa and other developing countries' position in crude oil production. Hence, utilising the survey technique, this study seeks to fill this gap, using Nigeria as a case study.

3.Methodology

The current study used a survey research methodology. It is described as gathering information by delivering a questionnaire to pertinent individuals [19]–[25]. The employees of the refinery under study linked directly with maintenance activities are the pertinent parties in this situation. Using the formula provided in Eq. (1). by Taro Yamane [26], the sample size (SS) employed for this study with a total population of 2,312 components was established.

$$SS = \frac{N}{1+Ne^2} \quad \text{Eq. (1).}$$

Here, N is the population's known (limited) size, and e is the sampling error (taken as 5 percent). Applying Eq. (1), the sample size (SS) was obtained as 341 employees. Hence, 341 respondents were included in the sample size and received questionnaires using random sampling. They included 65 respondents from the Maintenance Planning Department, 150 from the Maintenance Department, 10 from the Engineering and Technical Services Department, 65 from the Health Services and Environment Department, 26 as Contractors, and 25 from the Supply Chain Management Department.

Due to the nature of this investigation, a combination of primary and secondary data-gathering methods were used. Primary data collected through physical copies of a specially developed questionnaire were given precedence. The main data sources were gathered by two authors directly from the organisation between December 2020 and January 2021.

The hypotheses (relationship between project management and TMA, risk management and TMA, and teamwork and TMA) were used to create the questionnaire.

H₀₁: There is no significant relationship between risk management and TMA

H₀₂: There is no significant connection between TMA and project management systems

H₀₃: There is no significant connection between TMA and teamwork

The questionnaire had two components: Section A provides demographic data such as qualification and years of experience (2 questions). Section B: Through direct questions, the responder evaluates the relationship between risk management, project management tools, and project teamwork as independent variables on project success as the dependent variable (14 questions). Strongly Agree to Strongly Disagree on a 5-point Likert scale was used to gather the responses. These inquiries came from earlier research by Ghaithan [13] and Zhicheng et al. [16].

The data was analysed using inferential statistics in Microsoft Excel (Version 2019), utilising frequency counts and percentages as the data collection methods. The mean

responses of the respondents were utilised to answer the research questions. However, the Pearson Correlation Coefficient Statistical (PPMC) tool was employed to investigate the study hypotheses utilising the SPSS (Version 26) Software. Based on the significance threshold, the level of each of the independent variable impact or correlation on the dependent variable is measured in correlation index r-value, which is compared with a correlation r critical obtained from a Pearson correlation table using the df (degree of freedom) values in each of the hypotheses, the decision to reject the null hypothesis or accept the alternate hypothesis is based on the 0.05 alpha level of significance.

4.Results And Discussion

Demographic Information of the Respondents

Information about the years of experience and qualifications of the respondents of the organisation that made up the sample size is shown in Table 1. The result shows the distribution of years of experience of the respondents in which the majority of the respondents (90.32%) have between 11 years to 30 years (sum of 46.04% and 44.28% for 11-20 years and 21-30 years, respectively) of experience in the petrochemical and refinery industry. This result denotes adequate knowledge from the sample size that made up this study, thereby rendering their findings from the place of experience and perspectives valid. Furthermore, the majority (43.99%) of the respondents have a BSc. /B.Eng. academic qualifications, followed by 21.41% with an HND degree, 19.65% with a Masters degree, 8.80% with a PGDE degree, and only 6.16% have a Diploma/ND degree. This result shows that all the respondents have adequate exposure and academic background that can render their perspectives on the utilisation of risk management, project management tools and teamwork for the execution of TMA in petrochemical and refinery companies.

Table 1. Demographic information of the respondents

Variable	Frequency	Percentage
Years of Experience		
0-10	16	4.69%
11-20	157	46.04%

21-30	151	44.28%
31-40	17	4.99%
Qualification		
Diploma/ND	21	6.16%
HND	73	21.41%
B.Sc./B.Eng.	150	43.99%
Masters	67	19.65%
PGDE	30	8.80%

Application of Risk Management, Project Management Tools and Team Work on TMA

Risk Management

From the result obtained in this study, shown in Table 2, it was observed that the majority of the respondents with a mean value of 4.20 agreed that for project success of the petrochemical and refinery industry understudy, the level of risk management has a significant effect. The respondents specifically believed that the appointment of a risk management team significantly contributes positively to TMA success, and this item had the highest mean of 4.28. Furthermore, the result showed that detailed risk control/reduction plans significantly contribute positively to TMA success, as this had the second-highest mean response of 4.22. Hence, to bring into context the findings of this result, it is important to consider the risk management team and detailed risk control/reduction plans to effectively apply risk management in ensuring project success. This result is supported by the findings of Mahamadi et al. [27].

Table 2. The perspective of the respondents on the application of risk management in TMA

S/N	Items	Response categories					Mean
		SA (5)	A (4)	UD (3)	D (2)	SD (1)	
1	Systematic risk identification will significantly contribute positively to turnaround maintenance success	158	117	50	12	4	4.21
2	Probabilistic/likelihood analysis of risk levels will significantly contribute positively to turnaround maintenance success	136	120	72	4	9	4.09
3	Detailed risk control/reduction plans will significantly contribute positively to turnaround maintenance success	148	135	50	2	6	4.22
4	The appointment of a risk manager will significantly contribute positively to turnaround maintenance success	151	126	56	2	6	4.21
5	Appointment of a risk management team will significantly contribute positively to turnaround maintenance success	159	130	44	4	4	4.28

SA: Strongly Agree, A: Agree, UD: Undecided, D: Disagree, SD: Strongly Disagree

Furthermore, the outcome of the PPMC statistics (Table 3) revealed that there is a significant relationship between risk management and TMA. From the analysis, the calculated p-value of 0.010 is lower than the 0.05 alpha significance level, and the computed R correlation value of 0.617 is higher than the critical r value of 0.113 at df 339. Hence, the null hypothesis of no significant relationship between risk management and TMA is rejected.

Table 3. PPMC statistics on the relationship between risk management, project management tools and teamwork on TMA.

Variables	N	Mean	STD	df	Correlation Index r	r critical	p
TMA	341	21.0117	3.50544	339	0.617**	0.113	0.010
Risk Management	341	19.3959	4.31262				
TMA	341	21.3900	3.74131	339	0.742**	0.113	0.002
Project Management Tools	341	19.8592	4.39560				
TMA	341	17.5220	2.66408	339	0.714**	0.113	0.002
Team Work	341	16.5513	3.20126				

**Correlation is significant at the 0.05 level (2-tailed)

Project Management Tools

Additionally, it was noted from the findings of this study, which are presented in Table 4, that the majority of respondents, with a mean value of 4.28, agreed that the successful use of project management tools has a significant impact on the project success of the understudied petrochemical and refinery industry.

Particularly, the usage of the responsibility assignment matrix (RACI), which had the highest mean agreement level of 4.30, greatly adds to the success of TMA. Additionally, the respondents felt strongly that the effectiveness of TMA is highly influenced by the usage of network scheduling techniques (such as CPM, and PERT). The second-highest mean score of 4.28 confirms this. The obtained result is in line with the findings of Dwi et al. [28] and Bagshaw [29].

Table 4. The perspective of the respondents on the application of project management tools on TMA

S/N	Items	Response categories					Mean
		SA (5)	A (4)	UD (3)	D (2)	SD (1)	
1	The use of a work breakdown structure (WBS) significantly contributes positively to turnaround maintenance success	188	89	44	10	10	4.28
2	The use of network scheduling techniques (i.e., CPM, PERT) significantly contributes positively to turnaround maintenance success	169	118	38	12	4	4.28
3	The use of Gant chart significantly contributes positively to turnaround maintenance success	166	117	46	6	6	4.26
4	The use of a responsibility assignment matrix (RACI) significantly contributes positively to turnaround maintenance success	162	133	36	6	4	4.30
5	The use of earned value management (EVM) significantly	177	108	40	4	12	4.27

	contributes positively to turnaround maintenance success						
--	--	--	--	--	--	--	--

SA: Strongly Agree, A: Agree, UD: Undecided, D: Disagree, SD: Strongly Disagree

Additionally, the results of the PPMC data (Table 2) showed a substantial correlation between TMA and project management tools. According to the study, the computed p-value of 0.002 is less than the alpha level of 0.05, while the computed R correlation value of 0.742 is more than the crucial r value of 0.113 at df 339. Therefore, the null hypothesis of no significant connection between TMA and project management systems is rejected.

Team Work

The results of this survey, shown in Table 5, also revealed that most respondents, with a mean value of 4.38, agreed that good teamwork substantially impacted the project success of the under-researched petrochemical and refinery business. The success of TMA is particularly impacted by the balance of member contributions, as seen by the fact that this item had the highest mean response at 4.45. The second-highest mean response, 4.37, indicates that the respondents strongly agreed that the team members' mutual support is a key factor in the success of TMA. The outcome is consistent with those seen in the study of Rogers [30] and Gunduz and Yahya [31].

Table 5. The perspective of the respondents on the application of teamwork in TMA

S/N	Items	Response categories					Mean
		SA (5)	A (4)	UD (3)	D (2)	SD (1)	
1	Effective communication (meeting regularly and other mediums of information exchange) significantly contributes to turnaround maintenance success	183	116	28	8	6	4.35

2	Effective coordination of subtasks, schedules and deliverables significantly contributes to turnaround maintenance success	189	94	50	4	4	4.35
3	Balance of member contribution significantly contributes to turnaround maintenance success	193	118	24	2	4	4.45
4	Mutual support from your team members significantly contributes to turnaround maintenance success	196	91	44	4	6	4.37

SA: Strongly Agree, A: Agree, UD: Undecided, D: Disagree, SD: Strongly Disagree

Additionally, the results of the PPMC data (Table 2) showed that there is a substantial correlation between TMA and teamwork. According to the study, the computed p-value of 0.002 is less than the alpha level of 0.05, while the computed R correlation value of 0.714 is more than the crucial r value of 0.113 at df 339. Therefore, the null hypothesis of no significant connection between TMA and teamwork is rejected.

As identified from the survey findings, the key elements of risk management, project management tools, and teamwork play integral roles in the success of TMA activities in the petrochemical and refinery industry. The relationships between key elements and subfactors in maintenance activities are shown in Figure 1. In terms of risk management, systematic risk identification involves conducting thorough surveys to identify potential risks associated with TMA.

Probabilistic analysis, such as quantification, is crucial for assessing the likelihood of these risks, allowing for informed decision-making. Detailed risk control plans, or mitigation strategies, are essential for minimising the impact of identified risks. The appointment of a dedicated risk manager and forming a risk management team demonstrate leadership and collaboration, fostering a proactive approach to risk mitigation.

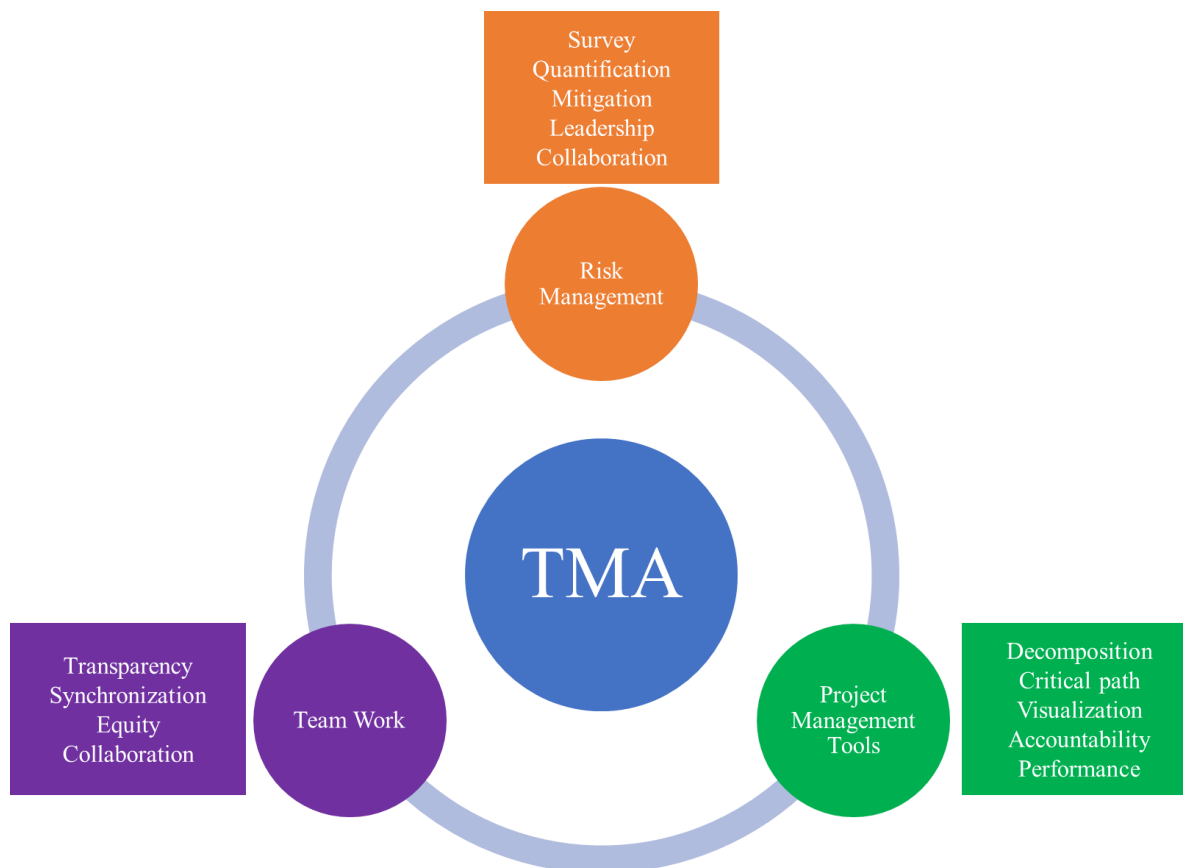


Figure 1. Relationships between key elements and subfactors in maintenance activities

Nevertheless, using risk management tools for TMA is not a novel concept in the chemical industry as stated by Muller [32]; however, restrictive approaches often hinder its effectiveness. Turnarounds and substantial capital projects, characterised by numerous variables and constant changes, demand a shift from viewing risk as a static obstacle to adopting a dynamic approach. In this context, continuous application of risk identification and mitigation tools throughout the planning and scheduling processes is imperative. Another challenge in integrating risk management into TMA in petrochemical industries lies in the common difficulty people face in comprehending probability concepts, leading to an inclination to overemphasise the likelihood of extraordinary events over more commonplace occurrences, as also confirmed in the study of AlHamouri et al. [6]. This bias can provide a false sense of security during execution, exposing projects and teams to significant dangers. A genuine understanding of risks' probability,

severity, and criticality demands experience and sound judgment, which can be obtained through leadership and collaboration, as identified in this study.

In the realm of project management tools, using WBS facilitates the decomposition of complex TMA projects into manageable tasks, ensuring a systematic approach to execution. Network scheduling techniques, including CPM and PERT, assist in identifying critical paths and scheduling, with visualisation through Gantt charts providing a comprehensive overview. A RACI ensures accountability, while EVM offers insights into project performance. Aside from these project management tools used in the understudy refinery for TMA, recent studies have highlighted the latest tools, such as Primavera, STO Planner, and iPlanSTO, as emerging technologies used in advanced refineries [33], [34]. Furthermore, drones now play a crucial role in inspecting hard-to-reach refinery equipment, particularly in remote or challenging environments [35]. Digital plant modelling has advanced, allowing the creation of digital replicas to monitor production and equipment under varying conditions in these refineries [34]. Leveraging data analytics and artificial intelligence on maintenance data provides valuable insights from historical information. Additionally, Industrial Internet of Things (IIoT) technologies enable real-time data collection and sharing, significantly improving the assessment of critical equipment's scope of work [36].

Teamwork is a cornerstone in TMA, and effective communication, exemplified by transparency, is crucial for conveying project goals, progress, and potential challenges. Coordination of subtasks, schedules, and deliverables through synchronisation enhances overall project efficiency. A balance of member contributions, emphasising equity, ensures that each team member plays a meaningful role, contributing to the success of the TMA. Mutual support among team members fosters collaboration, creating a positive and synergistic working environment essential for overcoming the complexities of TMA in the petrochemical and refinery industry. To align with these findings, previous studies showed the significance of aligning teams and groups involved in plant turnaround maintenance and established a strong correlation between teamwork and performance in plant turnaround maintenance [17], [37].

5. Conclusion

This study is based on project management tools, risk management techniques, and teamwork in a typical Nigerian petrochemical and refinery business, one of the world's major emerging oil producers. A structured questionnaire based on three sub-hypotheses on the importance of the management tools under research on TMA in the petrochemical and refinery industry was devised to fulfil the study's general purpose. The employees of the respondents that participated in the survey were 341 carefully chosen employees from several departments, including supply chain management, engineering and technical services, health services, and maintenance. The sub-hypotheses were examined using inferential statistics and Pearson correlation analysis. The study's findings demonstrated a substantial association between the management tools and TMA, with R-values for these relationships being 0.617, 0.742, and 0.714 for those with risk management, project management tools, and teamwork, respectively.

Moreover, the investigation results indicated a widespread consensus among the participants, expressing strong concurrence that the effective execution of TMA in the petrochemical and refinery sector relies significantly on sound risk management methodologies (p-value = 0.01). Similarly, project management tools were crucial for successful TMA implementation (p-value = 0.002). Additionally, the study highlighted the vital role of well-integrated teamwork in the TMA process, with the significance reflected in the p-value of 0.002. Therefore, these efficient management methods are recommended to be implemented with other effective tools from previous sectors to guarantee efficient TMA in the petrochemical and refinery industries.

Acknowledgement

The authors thank the staff of Kaduna Refining and Petrochemical Company and the Department of Mechanical Engineering, Ahmadu Bello University, Zaria, Nigeria.

Competing Interests

The authors declare that they have no competing interests.

Availability of Supporting Data

The data sets supporting the results of this article are available upon reasonable request.

Ethical Approval and Consent to Participate

Before conducting interviews, a verbal agreement was sought from each participant, and all respondents who took part in the field study were fully informed of the project's goals and their opportunity to opt out.

Funding

The study did not receive any external funding

6. References

- [1] M. Witteman, Q. Deng, and B. F. Santos, “A bin packing approach to solve the aircraft maintenance task allocation problem,” *Eur J Oper Res*, vol. 294, no. 1, pp. 365–376, 2021, doi: 10.1016/j.ejor.2021.01.027.
- [2] S. Antomarioni, O. Pisacane, D. Potena, M. Bevilacqua, F. E. Ciarapica, and C. Diamantini, “A predictive association rule-based maintenance policy to minimize the probability of breakages: application to an oil refinery,” *International Journal of Advanced Manufacturing Technology*, vol. 105, no. 9, pp. 3661–3675, Dec. 2019, doi: 10.1007/s00170-019-03822-y.
- [3] N. Serbulova, “Corporate survival in Industry 4.0 era: The enabling role of digital twin technologies,” *E3S Web of Conferences*, vol. 273, 2021, doi: 10.1051/e3sconf/202127308098.
- [4] L. O. Iheukwumere-Esotu and A. Yunusa-Kaltungo, “Knowledge management and experience transfer in major maintenance activities: A practitioner’s perspective,” *Sustainability (Switzerland)*, vol. 14, no. 1, 2022, doi: 10.3390/su14010052.
- [5] L. Iheukwumere-Esotu and A. Yunusa-Kaltungo, “A Systematic Analysis of Research Based Evidences of Major Overhauls, Outages, Shutdowns, Turnarounds (MoOSTs) Management,” *Mechanisms and Machine Science*, vol. 105, pp. 627–635, 2021, doi: 10.1007/978-3-030-75793-9_60.
- [6] K. AlHamouri, C. H. Caldas, B. G. Hwang, P. Krishnankutty, and D. P. de Oliveira, “Utilization of workforce planning for the execution of maintenance activities, shutdowns and turnarounds in petrochemical facilities—a case study,” *International Journal of Construction Management*, vol. 21, no. 11, pp. 1115–1129, 2021, doi: 10.1080/15623599.2019.1602807.
- [7] L. I. Kumajas, N. F. Wuryaningrat, and H. S. Lembong, “Profitability in The Automotive and Component Industry,” *Asia Pacific Journal of Management and Education*, vol. 4, no. 3, pp. 115–129, 2021, doi: 10.32535/apjme.v4i3.1273.

- [8] S. Majumder and S. Dey, "Light Engineering Industry Sector in Bangladesh: Challenges and Prospects," *The Cost and Management*, vol. 48, no. 1, pp. 46–57, 2020.
- [9] T. K. Leong, N. Zakuan, M. Z. Mat Saman, M. S. M. Ariff, and C. S. Tan, "Using project performance to measure effectiveness of quality management system maintenance and practices in construction industry," *The Scientific World Journal*, vol. 2014, 2014, doi: 10.1155/2014/591361.
- [10] A. O. R, E. O. D, and O. V. O., "Assessment of Project Monitoring and Control Techniques in Ondo State Agency for Road Maintenance and Construction (OSARMCO)," *International Journal of Engineering and Management Research*, vol. 8, no. 5, pp. 177–184, 2018, doi: 10.31033/ijemr.8.5.21.
- [11] P. B. Ahamed Mohideen and M. Ramachandran, "Strategic approach to breakdown maintenance on construction plant - UAE perspective," *Benchmarking*, vol. 21, no. 2, pp. 226–252, 2014, doi: 10.1108/BIJ-05-2012-0030.
- [12] A. Shehadeh, O. Alshboul, and O. Hamedat, "A Gaussian mixture model evaluation of construction companies' business acceptance capabilities in performing construction and maintenance activities during COVID-19 pandemic," *International Journal of Management Science and Engineering Management*, vol. 17, no. 2, pp. 112–122, 2022, doi: 10.1080/17509653.2021.1991851.
- [13] A. M. Ghaithan, "An optimization model for operational planning and turnaround maintenance scheduling of oil and gas supply chain," *Applied Sciences (Switzerland)*, vol. 10, no. 21, pp. 1–20, 2020, doi: 10.3390/app10217531.
- [14] U. Al-Turki, S. Duffuaa, and M. Bendaya, "Trends in turnaround maintenance planning: literature review," *J Qual Maint Eng*, vol. 25, no. 2, pp. 253–271, Apr. 2019, doi: 10.1108/JQME-10-2017-0074.
- [15] W. Shou, J. Wang, P. Wu, and X. Wang, "Value adding and non-value adding activities in turnaround maintenance process: classification, validation, and benefits," *Production Planning & Control*, vol. 31, no. 1, pp. 60–77, Jan. 2020, doi: 10.1080/09537287.2019.1629038.

- [16] Y. Zhicheng *et al.*, “Evaluation of turnaround maintenance practice effects in the process industry,” *IOP Conf Ser Mater Sci Eng*, vol. 673, no. 1, p. 012097, Dec. 2019, doi: 10.1088/1757-899X/673/1/012097.
- [17] J. Akbar and Z. Ghazali, “The influence of Coordination on the Performance of Plant Turnaround Maintenance through Team Alignment in Malaysian Process-Based Industry,” *SHS Web of Conferences*, vol. 56, p. 02007, 2018, doi: 10.1051/SHSCONF/20185602007.
- [18] W. C. Shou, J. Wang, and X. Y. Wang, “4D BIM for improving plant turnaround maintenance planning and execution: A case study,” *ISARC 2018 - 35th International Symposium on Automation and Robotics in Construction and International AEC/FM Hackathon: The Future of Building Things*, 2018, doi: 10.22260/ISARC2018/0165.
- [19] P. eLearning Programs, “Strengths and Weaknesses of Online Learning,” *University of Illinois*, vol. 24, no. 5, pp. 1–10, 2015, doi: 10.9790/0837-2405053138.
- [20] U. Bello, D. S. Yawas, and A. N. Oyedeji, “Assessment of Perceived Performance of Solar-Powered Borehole Projects in Nigeria.,” *Management Science and Business Decisions*, 2022, doi: <https://doi.org/10.52812/msbd.47>.
- [21] U. A. Umar, Y. O. Obadoba, and A. N. Oyedeji, “Risk Management Practices in Rice Production: A Case of Smallholder Farmers of Soba Community in Northern Nigeria,” *Nigerian Journal of Science and Engineering Infrastructure*, vol. 1, no. 1, pp. 174–182, Oct. 2023, doi: 10.61352/2023AT07.
- [22] H. Abubakar, U. Umar, and A. Oyedeji, “Comparative Analysis Of Ergonomic Knowledge And Implementation Among Sofa Producers In Kano State Nigeria,” *The Islamic University Journal of Applied Sciences (JESC)*, vol. V, no. 1, pp. 165–180, 2023, [Online]. Available: <https://jesc.iu.edu.sa/Main/Article/117>
- [23] B. S. Terab, U. A. Umar, and A. N. Oyedeji, “Information technology in supply chain management: Perspectives from key actors in the Nigerian petroleum sector,” <https://doi.org/10.1080/20421338.2023.2221876>, pp. 1–7, Jun. 2023, doi: 10.1080/20421338.2023.2221876.

- [24] L. S. Kuburi, U. Umar, and A. N. Oyedeji, "Risk Assessment of Petrol Filling Stations in a Metropolitan City of Kaduna State, Nigeria," *SINERGI*, vol. 27, no. 2, pp. 179–184, 2023, doi: 10.22441/SINERGI.2023.2.005.
- [25] P. Neminebor, A. U. Umar, and A. N. Oyedeji, "Feasibility Studies for a Biogas Powered Standalone Power Plant: A Case Study of Giwa Community, Kaduna State, Nigeria," *Nigerian Journal of Tropical Engineering*, vol. 16, no. 1, pp. 127–138, Dec. 2022, doi: 10.59081/NJTE.16.1.011.
- [26] T. Yamane, "Research Methods: Determination of Sample Size," *University of Florida, IFAS Extension*, 1967.
- [27] N. Mahamadi, H. Yan, L. Zhang, H. Li, and Y. Wang, "Identifying Key Risks of Private and Government Construction Project Failures in West Africa: Environmental and Social Performance," *ICCREM 2019: Innovative Construction Project Management and Construction Industrialization - Proceedings of the International Conference on Construction and Real Estate Management 2019*, pp. 498–508, 2019, doi: 10.1061/9780784482308.057.
- [28] R. Dwi, P. Suhandi, and D. Pratami, "RACI Matrix Design for Managing Stakeholders in Project Case Study of PT. XYZ," *International Journal of Innovation in Enterprise System*, vol. 5, no. 02, pp. 122–133, Jul. 2021, doi: 10.25124/IJIES.V5I02.134.
- [29] K. B. Bagshaw and K. B. Bagshaw, "PERT and CPM in Project Management with Practical Examples," *American Journal of Operations Research*, vol. 11, no. 4, pp. 215–226, Jul. 2021, doi: 10.4236/AJOR.2021.114013.
- [30] T. Rogers, "Project Success and Project Team Individuals," *European Project Management Journal*, vol. 9, no. 1, pp. 27–33, 2019.
- [31] M. Gunduz and A. M. A. Yahya, "Analysis of project success factors in construction industry," *Technological and Economic Development of Economy*, vol. 24, no. 1, pp. 67–80–67–80, Jan. 2018, doi: 10.3846/20294913.2015.1074129.
- [32] G Müller, "Managing risk during turnarounds and large capital projects: Experience from the chemical industry.," *Journal of Business Chemistry*, vol. 2015, no. October, 2015.

- [33] X. Han, “WBS-free scheduling method based on database relational model,” *International Journal of System Assurance Engineering and Management*, vol. 12, no. 3, pp. 509–519, Jun. 2021, doi: 10.1007/S13198-021-01106-X/FIGURES/8.
- [34] W. Shou, J. Wang, P. Wu, and X. Wang, “Lean management framework for improving maintenance operation: development and application in the oil and gas industry,” *Production Planning & Control*, vol. 32, no. 7, pp. 585–602, 2021, doi: 10.1080/09537287.2020.1744762.
- [35] P. Nooralishahi *et al.*, “Drone-Based Non-Destructive Inspection of Industrial Sites: A Review and Case Studies,” *Drones 2021, Vol. 5, Page 106*, vol. 5, no. 4, p. 106, Sep. 2021, doi: 10.3390/DRONES5040106.
- [36] H. A. Bramantyo, B. S. Utomo, and E. M. Khusna, “Data Processing for IoT in Oil and Gas Refineries,” *Journal of Telecommunication Network (Jurnal Jaringan Telekomunikasi)*, vol. 12, no. 1, pp. 48–54, Mar. 2022, doi: 10.33795/JARTEL.V12I1.300.
- [37] F. Masubelele and E. Mnkadla, “The identification of critical success factors for turnaround maintenance projects,” *IEEE AFRICON Conference*, vol. 2021-September, Sep. 2021, doi: 10.1109/AFRICON51333.2021.9570914.

هيئة التحرير

- أ.د. فضل نور
مدير التحرير
أستاذ علوم وهندسة الحاسب الآلي، بالجامعة
الإسلامية بالمدينة المنورة. المملكة العربية السعودية
- أ.د. فايز جبالي
أستاذ، الهندسة الكهربائية وهندسة الحاسبات،
جامعة فيكتوريا، فيكتوريا، كولومبيا البريطانية،
كندا
- أ.د. محمد معبد بيومي
أستاذ التحليل العددي، جامعة الإمام، الرياض.
المملكة العربية السعودية
- أ.د. سعد طلال الحربي
أستاذ علوم الحاسب -
التفاعل بين الإنسان والحاسب
كلية الحاسبات - جامعة طيبة
المملكة العربية السعودية
- أ.د. شمس الدين أحمد
أستاذ الهندسة الصناعية،
كلية الهندسة بالجامعة الإسلامية بالمنورة
- أ.د. احمد بدرالدين الخضر
رئيس التحرير
أستاذ علوم الحاسب، الجامعة الإسلامية بالمدينة
المنورة، المملكة العربية السعودية
- د. توميتا كنتارو
أستاذ مشارك، قسم علوم وهندسة الكم، كلية
الدراسات العليا للهندسة، جامعة هوكايدو، اليابان
- أ.د. رضا الششتاوي
أستاذ الكيمياء العضوية، قسم الكيمياء - كلية
العلوم - جامعة الملك عبد العزيز، المملكة العربية
السعودية
- أ.د. باسم راشد العمري
أستاذ هندسة القوى الكهربائية
جامعة الطائف
المملكة العربية السعودية
- أ.د. عصام شعبان حسانين
أستاذ الفيزياء، جامعة الأزهر، فرع أسبوط
مصر
- د. عبدالقادر رحيم بهاتي
أستاذ الهندسة المدنية، كلية الهندسة،
الجامعة الإسلامية بالمدينة المنورة. المملكة العربية
السعودية

سكرتير التحرير: أحمد زياد الزحيلي

الهيئة الاستشارية

- | | |
|---|---|
| أ.د. ضياء خليل
أستاذ الهندسة الكهربائية ، ووكيل الكلية ، جامعة
عين شمس ، القاهرة ، مصر | أ.د. حسين مفتاح
أستاذ ، الهندسة الكهربائية وعلوم الكمبيوتر ،
جامعة أوتاوا ، أوتاوا ، أونتاريو ، كندا
كرسي أبحاث كندا في شبكات الاستشعار اللاسلكية،
أستاذ جامعي ، جامعة أوتاوا |
| أ.د. كالوس هايتينجر
أستاذ رياضيات ، البرازيل | أ.د. سلطان العدوان
أستاذ الكيمياء العضوية ، الأردن |
| أ.د. أمين فاروق فهمي
أستاذ الكيمياء في جامعة عين شمس
القاهرة ، مصر | أ.د. كمال منصور جمبي
أستاذ الحاسب ونظم المعلومات ، جامعة الملك عبد
العزیز ، جدة ، المملكة العربية السعودية |
| أ.د. عبد الغفور ميمون
أستاذ الهندسة الميكانيكية ، الجامعة الوطنية
للعلوم والتكنولوجيا ، باكستان | أ.د. محمود عبدالعاطي
أستاذ دكتور الرياضيات وعلوم المعلومات في جامعة
العلوم والتكنولوجيا ، مصر |

قواعد النشر في المجلة

- أن يكون البحث جديداً، ولم يسبق نشره
- أن يتسم بالأصالة والجدة والابتكار والاضافة للمعرفة
- أن لا يكون مستلماً من بحوث سبق نشرها للباحث/ للباحثين
- أن تراعى فيه قواعد البحث العلمي الاصيل، ومنهجيته.
- أن يشتمل البحث على:
 - ✓ صفحة عنوان البحث باللغة الانجليزية.
 - ✓ مستخلص البحث باللغة الانجليزية.
 - ✓ صفحة عنوان البحث باللغة الانجليزية.
 - ✓ مستخلص البحث باللغة العربية.
 - ✓ مقدمة.
 - ✓ صلب البحث.
 - ✓ خاتمة تتضمن نتائج وتوصيات.
 - ✓ ثبت المصادر والمراجع.
 - ✓ الملاحق الملزمة (إن وجدت).
- في حال (نشر البحث ورقاً) يمنح الباحث نفسه نسخة من عدد المجلة الذي نشر بحثه بها و10 نسخ من بحثة بشكل مستقل
- في حال اعتماد نشر البحث تؤول حقوق نشره كافة للمجلة، ولها ان تعيد نشره ورقياً أو إلكترونياً، ويحق لها
- إدراجه في قواعد البيانات المحلية والعالمية- بمقابل أو بدون مقابل -وذلك دون حاجة للإذن الباحث.
- لا يحق للباحث إعادة نشر بحثه المقبول للنشر في المجلة- في أي وعاء من أوعية النشر- إلا بعد إذن
- كتابي من رئيس هيئة تحرير المجلة
- نمك التوثيق المعتمد في المجلة هو نمط IEEE

معلومات الإيداع

النسخة الورقية :

تم الإيداع في مكتبة الملك فهد الوطنية برقم 1439/8742 وتاريخ 1439/09/17 هـ

الرقم التسلسلي الدولي للدوريات (ردمد) 7936 – 1658

النسخة الإلكترونية:

تم الإيداع في مكتبة الملك فهد الوطنية برقم 1439/ 4287 تاريخ 1439/9/17 هـ

الرقم التسلسلي الدولي للدوريات (ردمد) 7944 -1658

الموقع الإلكتروني للمجلة:

<https://jesc.iu.edu.sa>

ترسل البحوث باسم رئيس تحرير المجلة إلى البريد الإلكتروني

jesc@iu.edu.sa

الآراء الواردة في البحوث المنشورة تعرب عن وجهة نظر الباحث فقط، ولا تعرب بالضرورة عن المجلة.





KINGDOM OF SAUDI ARABIA
MINISTRY OF EDUCATION
ISLAMIC UNIVERSITY OF MADINAH

Islamic University Journal of Applied Sciences (JESC)

Refereed periodical scientific journal

Volume: V

Issue: II

Year: 2023